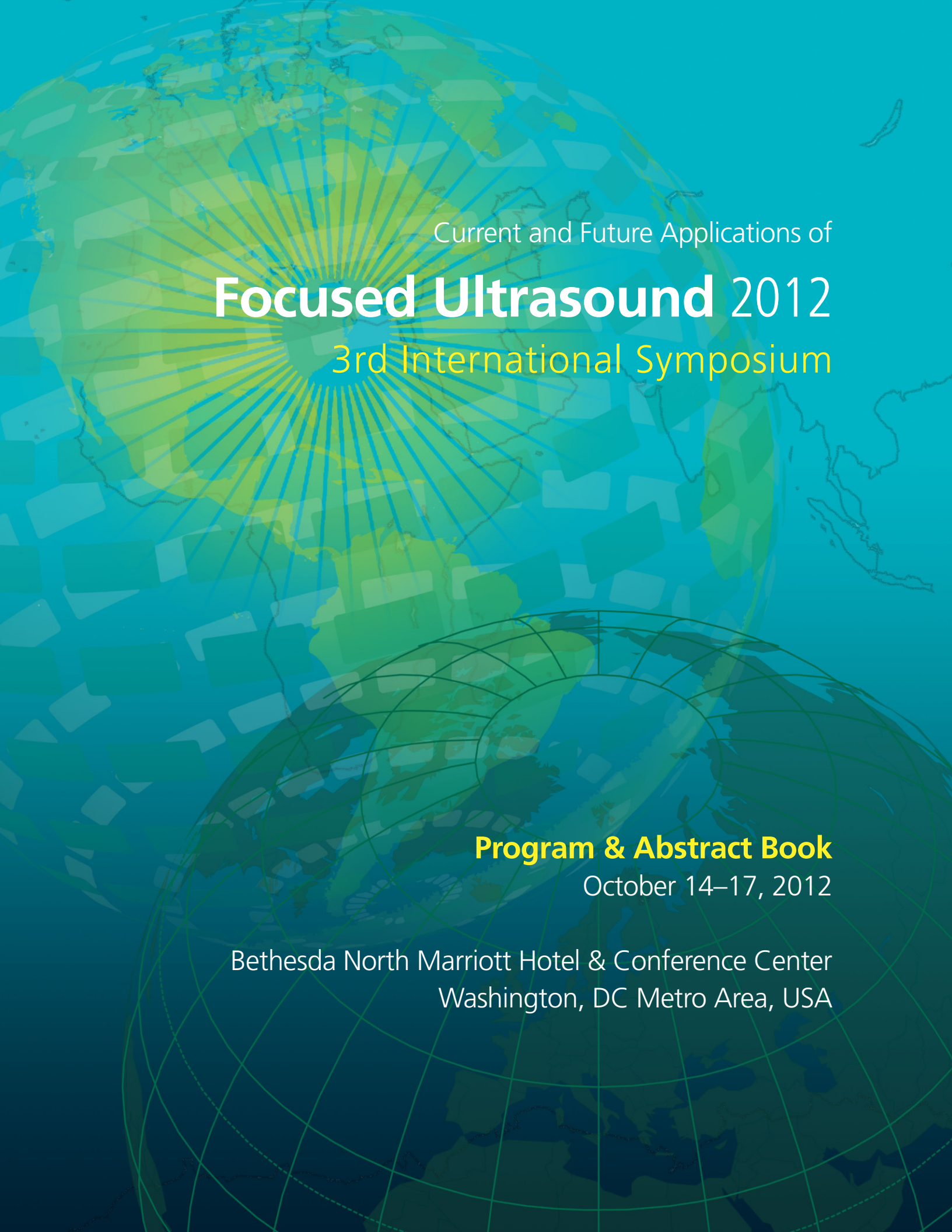

Current and Future Applications of

Focused Ultrasound 2012

3rd International Symposium

Program & Abstract Book

October 14–17, 2012

Bethesda North Marriott Hotel & Conference Center
Washington, DC Metro Area, USA

Sponsor Acknowledgements

GE Healthcare
Platinum

InSightec
Platinum

Philips
Platinum

Varian
Platinum

Elekta
Gold

FUS Instruments
Bronze

Supersonic Image
Bronze

Alpinion
Friend

EDAP
Friend

Image Guided Therapy
Friend

Imasonic
Friend

ISTU
Friend

Contents

Welcome Messages

From the Honorary President

Dear Colleagues:

Everyone working in the field of focused ultrasound has been intrigued and inspired by the therapeutic potential and promise of this exciting technology. While still at an early stage, our push to develop focused ultrasound applications is increasing in scope and intensity. To me, the best gauge of our progress is the 3rd International Symposium on Focused Ultrasound.

What makes this year's symposium different from its predecessors is the inclusion of more presentations, more indications and more advances in R&D and commercialization. All signal that the pace of progress in our field is escalating.

I hope that clinicians attending this year's symposium gain meaningful insight into the full range of applications that focused ultrasound can provide to them and, therefore, to their patients. After all, having patients live longer, healthier lives is the driving force in all of our work.

Sincerely,

Professor Wladyslaw M. Gedroyc
Director and Consultant Radiologist
St. Mary's Hospital, Imperial College
Honorary Symposium President

Welcome Messages (continued)

From the Foundation Chairman

Dear Colleagues:

Welcome to the 3rd International Symposium on Focused Ultrasound. You are participating in the most extensive program we have hosted to date featuring more than 170 oral and poster presentations spotlighting the latest developments in our field. This represents more than a 50% increase compared to the 2010 symposium and reflects the accelerating progress being achieved by the focused ultrasound community.

In keeping with the Foundation's intense patient-centric orientation, the program emphasizes the translational and clinical research that is moving focused ultrasound into the realm of patient care.

The potential focused ultrasound to improve the quality of life and longevity for millions of people around the world with serious medical disorders has never been more apparent. Effective therapies to decrease death, disability and suffering are now on the horizon, no longer beyond it. But we still need to shorten the distance. We will do that through capital – financial and, more importantly, human capital.

The number of focused ultrasound investigators is continuing to grow as evidenced by the applications received for the Young Investigator Travel Awards. In 2010, there were 11 applications; this year, there were 44. But in order to move focused ultrasound forward more rapidly, we need more human capital. The most expeditious way to achieve this is to leverage the people who are currently engaged.

The symposium is an important vehicle for disseminating knowledge and sharing ideas, the most important role is to serve as an incubator to foster collaboration – collaboration being the ultimate force multiplier for human capital. Please take advantage of the opportunities to establish new partnerships and collaborations, particularly during the Tuesday evening poster session.

Several special events are planned during the symposium, including keynote talks by Dean Kamen, one of the international leaders in medical device innovation and inventor of the Segway, at Sunday's opening reception and by John Grisham, best-selling author and Foundation board member, on Tuesday morning.

The Focused Ultrasound Foundation is proud to serve as the nexus for the global focused ultrasound ecosystem. We are deeply appreciative of your participation in the symposium and of your ongoing and steadfast commitment to advancing focused ultrasound. I am confident that this event will inspire and facilitate your continued contributions to the growing body of focused ultrasound research and knowledge.

In closing, I would like to acknowledge the generosity of our donors and the support of our sponsors – they have made this meeting possible. I thank both groups, and encourage all attendees to visit the exhibit area and meet with our sponsoring organizations.

Sincerely,

Neal F. Kassell, MD
Chairman, Focused Ultrasound Foundation

Symposium Organizer

FOCUSED ULTRASOUND FOUNDATION

About the Focused Ultrasound Foundation

The Focused Ultrasound Foundation is a medical technology research, education and advocacy organization dedicated to improving the lives of millions of people with serious medical disorders by accelerating the development and adoption of focused ultrasound. The Foundation is unique in that it supports development of improved treatment for a wide variety of diseases utilizing a platform technology that exerts multiple mechanisms of action.

Positioned at the nexus of the large, diverse group of stakeholders comprising the ultrasound community, the Foundation functions as an independent, trusted and unbiased third-party, aligning organizations into a cohesive ecosystem with a single goal: To make focused ultrasound technology available to patients in the shortest time possible. The Foundation works to establish a patient centric culture, instill a sense of urgency in all stakeholders, and alleviate barriers to progress.

The Foundation catalyzes collaboration and partnerships, organizes and funds research, spearheads advocacy and patient support initiatives, and sponsors meetings, symposia and workshops to create and disseminate knowledge and increase awareness of focused ultrasound. Early-stage research funded by the Foundation "de-risks" subsequent investment, thus encouraging other funding sources such as disease specific foundations, the National Institutes of Health (NIH), and industry to become more involved.

The Foundation is on the leading edge of the venture philanthropy and social entrepreneurship movements and is a model of how private philanthropy can work in concert with academia, industry and government to bridge the gap between research and commercialization of a high impact medical technology.

To learn more about focused ultrasound and the Focused Ultrasound Foundation, visit the Foundation's website: **www.fusfoundation.org**

Organizing Committee

Neal Kassell, MD, Chair
Focused Ultrasound Foundation;
University of Virginia

Arik Hananel, MD, MBA, Vice Chair
Focused Ultrasound Foundation

Robin Jones, Project Lead
Focused Ultrasound Foundation

Symposium Organizer (continued)

Board of Directors

Dorothy Batten
Former Director, Landmark Communications

S Morry Blumenfeld, PhD
Founding Partner, Meditech Advisors Management

Eugene V Fife
Founding Principle, Vawter Capital, LLC

John Grisham
Author

Daniel P Jordan, PhD
President Emeritus, Thomas Jefferson Foundation

Neal F Kassell, MD
Chairman, Focused Ultrasound Foundation;
Professor, Department of Neurosurgery,
University of Virginia

Edward D Miller, MD
Former CEO, Johns Hopkins Medicine

Frederic H Moll, MD
Co-founder and Executive Chairman,
Hansen Medical, Inc.

Steve Rusckowski
CEO, Quest Diagnostics
Former CEO, Philips Healthcare

Lodewijk JR de Vink
Founding Partner, Blackstone Health Care Partners

Andrew von Eschenbach, MD
President, Samaritan Health Initiatives

Kobi Vortman, PhD
Founder, President and CEO, InSightec Ltd.

Scientific Program Committee

Jean-Francois Aubry, PhD
University of Virginia

Kim Butts Pauly, PhD
Stanford University

Matthew Dreher, PhD
National Institute of Health

Keyvan Farahani, PhD
National Cancer Institute

Arik Hananel, MD
Focused Ultrasound Foundation

Joo Ha Hwang, MD, PhD
University of Washington

Kullervo Hynynen, PhD
Sunnybrook Health Sciences Centre

Young-Sun Kim, MD
Samsung Medical Center

Nathan McDannold, PhD
Harvard Medical School

Chrit Moonen, PhD
University Medical Center Utrecht

Dennis Parker, PhD
University of Utah

Richard Price, PhD
University of Virginia

Gail ter Haar, PhD (Chair)
Joint Department of Physics,
Institute of Cancer Research,
Royal Marsden Hospital

Map

Main Level — Grand Ballroom

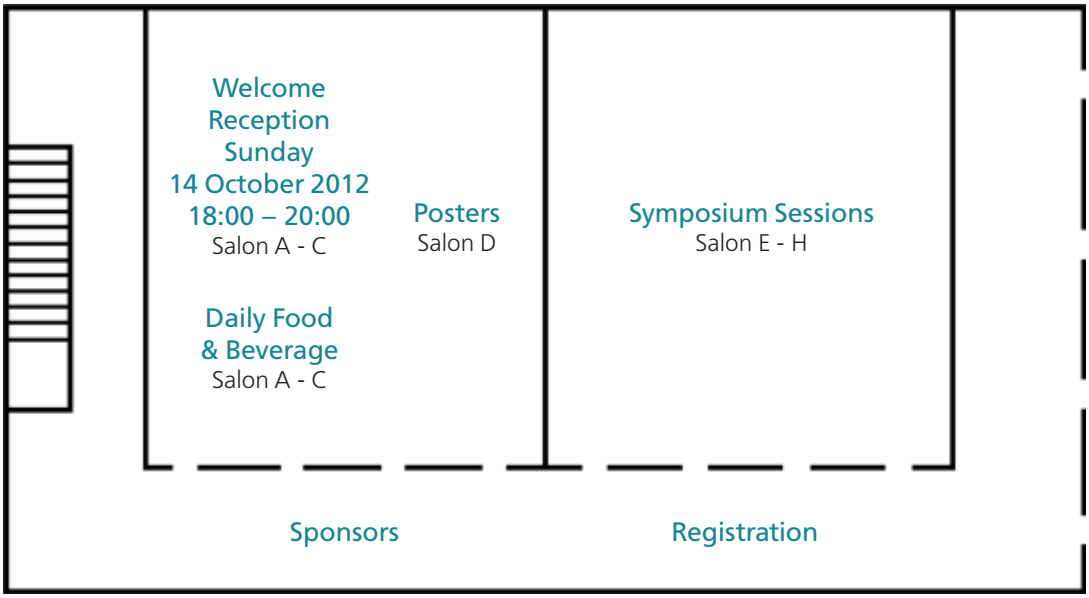

Lower Level

Lunch Discussion Sessions

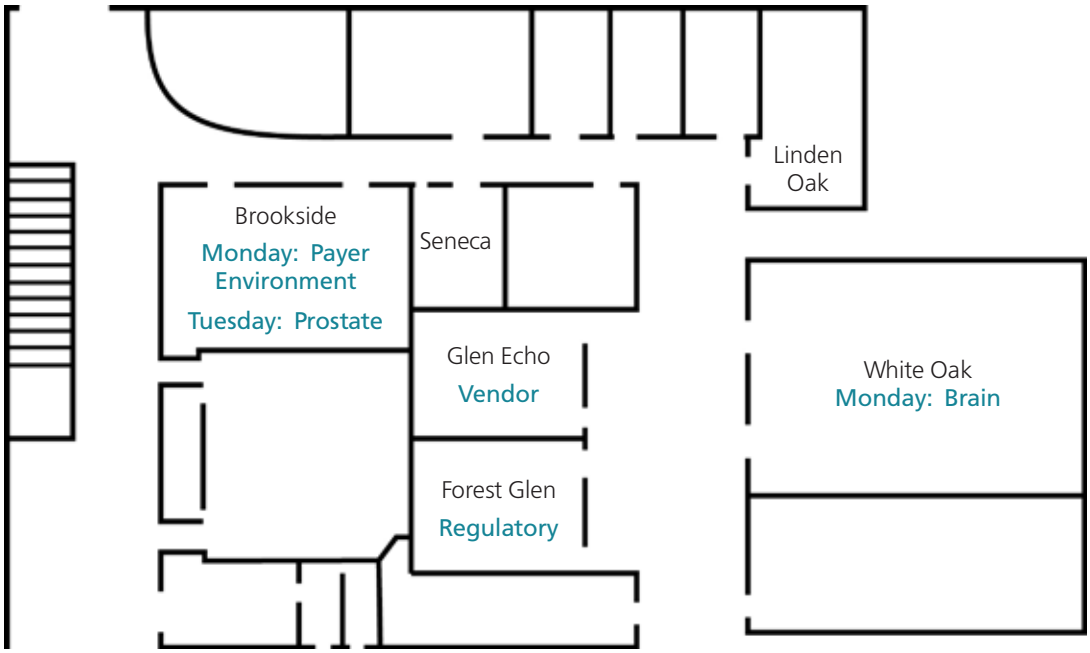

General Information

Registration & Information Hours

Sunday	16:00 – 20:00
Monday	7:00 – 18:00
Tuesday	7:00 – 18:00
Wednesday	7:00 – 18:00

Special Events

Sunday, 14 October 2012

Welcome Reception, 18:00 – 20:00, Salon A – C
Includes Drinks and hors d'oeuvres

Tuesday, 16 October 2012

Poster Session and Reception, 18:00 – 21:00, Salon D
Includes Drinks and hors d'oeuvres

Meals

Included in Symposium Registration

Registration includes continental breakfast, lunch and break refreshments in Salon A – C.

Dinner Options

Symposium registration does not include dinner. Meeting participants are welcome to dine at the Marriott Bethesda North or at a location of their choice. Information about nearby restaurants is available from the hotel Concierge Desk located in the lobby.

Local Transportation

Information about taxis and other local transportation options is available from the hotel Concierge Desk located in the lobby.

Internet Access

Wireless internet access is complimentary in the hotel lobby and in guest rooms that were reserved at the special conference rate.

Symposium Feedback Survey

To assist the Focused Ultrasound Foundation in evaluating the success of the symposium, attendees will be asked to complete a brief, anonymous survey before final adjournment.

Program

Program at a Glance

Monday
October 15

7:00
- Continental Breakfast — Salon A – C 7:00 – 8:00
- Registration — Foyer 7:00 – 8:00

8:00
- Welcome and Honorary President's Address — Salon E – H 8:00 – 8:20

9:00
- Brain — Salon E – H 8:20 – 10:15

10:00
- Break — Salon A – C 10:15 – 10:45

11:00
- Brain (continued) — Salon E – H 10:45 – 12:45

12:00
- Lunch — Salon A – C 12:45 – 13:15

13:00
- Lunch Discussion Sessions — Lower Level 13:15 – 14:15

14:00
- Uterine Fibroids — Salon E – H 14:15 – 15:45

15:00
- Break — Salon A – C 15:45 – 16:15

16:00
- Uterine Fibroids (continued) — Salon E – H 16:15 – 17:15

17:00
- Panel Discussion: UF Site Success — Salon E – H 17:15 – 18:00

18:00

19:00

20:00

Posters and Exhibits
Salon D and Foyer 7:00 – 18:00

Program at a Glance (continued)

Tuesday
October 16

7:00
- Continental Breakfast — Salon A – C 7:00 – 8:00
- Registration — Foyer 7:00 – 8:00

8:00
- Panel Discussion: Ultrasound vs. MRI Guidance — Salon E – H 8:00 – 8:45

9:00
- Emerging Applications — Salon E – H 8:45 – 10:30

10:00
- Break — Salon A – C 10:30 – 11:00

11:00
- Breast Tumors — Salon E – H 11:00 – 12:30

12:00
- Keynote Address — Diane and David Heller Lecture — Salon E – H 12:30 – 12:45

13:00
- Lunch — Salon A – C 12:45 – 13:15

14:00
- Lunch Discussion Sessions — Lower Level 13:15 – 14:15

15:00
- Prostate — Salon E – H 14:15 – 15:30

16:00
- Break — Salon A – C 15:30 – 16:00
- Panel Discussion: Prostate Controversies — Salon E – H 16:00 – 16:45

17:00
- Prostate (continued) — Salon E – H 16:45 – 17:30

18:00

19:00
- Poster Session and Reception — Salon D 18:00 – 21:00

20:00

21:00

Posters and Exhibits — Salon D and Foyer 7:00 – 21:00

Program at a Glance (continued)

Wednesday October 17

7:00
- Continental Breakfast — Salon A – C 7:00 – 8:00
- Registration — Foyer 7:00 – 8:00

8:00
- Bone Metastasis — Salon E – H 8:00 – 9:45

9:00

10:00
- Panel Discussion: Bone Metastasis — Salon E – H 9:45 – 10:30

Break — Salon A – C 10:30 – 11:00

11:00
- Bone Non-Metastasis — Salon E – H 11:00 – 12:00

12:00
- Foundation — Salon E – H 12:00 – 12:30

Lunch — Salon A – C 12:30 – 13:00

13:00
- Lunch Discussion Sessions — Lower Level 13:00 – 14:00

14:00
- Liver — Salon E – H 14:00 – 15:45

15:00

16:00
- Break — Salon A – C 15:45 – 16:15

17:00
- Liver (continued) — Salon E – H 16:15 – 17:45

Closing Remarks — Salon E – H 17:45 – 18:00

18:00

19:00

20:00

Posters and Exhibits — Salon D and Foyer 7:00 – 18:00

Detailed Program

Monday

October 15

Welcome; Honorary President's Address | 8:00 – 8:20 | Salon E – H

Welcome and Opening Remarks ..... *N. Kassell*

Honorary President's Address ..... *W. Gedroyc*

Brain Applications | 8:20 – 10:15; 10:45 – 12:45 | Salon E – H

Moderators: W.J. Elias, J.W. Chang

FUSF Strategic Focus: Brain Program ..... *N. Kassell*

1-BR Study on Incisionless Transcranial Magnetic Resonance-guided Focused Ultrasound Treatment of Neuropathic Pain: Safety, Accuracy and Clinical Outcomes ..... *D. Jeanmonod*

Discussion and Q&A - MRgFUS for Neuropathic Pain

2-BR Study on Incisionless Transcranial Magnetic Resonance-guided Focused Ultrasound Treatment of Parkinson's Disease: Safety, Accuracy and Initial Clinical Outcomes ..... *D. Jeanmonod*

3-BR Phase 1 Study of MRgFUS for Tremor Dominant Parkinson Disease ..... *W.J. Elias*

Discussion and Q&A - MRgFUS for Parkinson's disease

4-BR A phase 1 study of MR-guided focused ultrasound thalamotomy for the treatment of medication-refractory essential tremor ..... W.J. Elias

5-BR Preliminary report of MRI guided high intensity focused ultrasound surgery for the patient with essential tremor ..... *J.W. Chang*

6-BR Intra-procedural Assessment of Tremor and Neurological Status During Focused Ultrasound Surgery/Ablation in the Magnetic Resonance Environment ..... *D. Huss*

Discussion and Q&A - MRgFUS for Essential Tremor

7-BR "Non-thermal" ablation in the brain via focused ultrasound combined with an ultrasound contrast agent: long-term treatment effects and feasibility in a large animal model ..... *N. McDannold*

Discussion and Q&A - Non Thermal Ablation in the Brain

8-BR Ultrasonic Neuromodulation: in situ threshold for motor response in a rat model ..... *J. Aubry*

Discussion and Q&A - Neuro-modulation with Focused Ultrasound

9-BR Transcranial Sonothrombolysis In Ischemic Stroke Using the ExAblate® 4000 ..... *T. Hoelscher*

10-BR High Intensity Focused Ultrasound for the Treatment of Acute Ischemic Stroke ..... *D. Pajek*

11-BR Transcranial MR Guided Focused Ultrasound Treatment of ICH ..... *S. Monteith*

Discussion and Q&A - Sonothrombolysis for Stroke

12-BR Enhanced Delivery of Liposomal Doxorubicin via Permeabilization of the Blood-Brain/blood-tumor Barriers using Focused Ultrasound and Microbubbles Significantly Improves Survival in a Rat Glioma Model after Multiple Treatments ..... *M. Aryal*

13-BR Activation of Signaling Pathways Following Localized Delivery of Systemically-Administered Neurotrophic Factors across the Blood-Brain Barrier Using Focused Ultrasound and Microbubbles ..... *E. Konofagou*

14-BR Microbubble-Enhanced Focused Ultrasound Blood-Brain Barrier Opening in Non-Human Primates: Targeting Accuracy and Closing Timeline ..... *E. Konofagou*

Discussion and Q&A - Blood Brain Barrier Opening with Focused Ultrasound

Lunch Discussion Sessions | 13:15 – 14:15 | Lower Level

Vendor Profile | Glen Echo
Regulatory — Design considerations for technical and preclinical studies | Forest Glen
The Realities of a Payer Environment | Brookside
Brain | White Oak

Detailed Program (continued)

15-LD MRI as an Alternative to CT to Assess Skull Geometry and Plan Refocusing in MR-Guided Focused Ultrasound (MRgFUS) ..... *J. Snell*

16-LD Model Predictive Filtering for Large Coverage 3D Imaging of Transcranial MRgFUS procedures ..... *N. Todd*

17-LD Combined MRI and US guided Focused Ultrasound in the Brain ..... *C. Arvanitis*

18-LD Towards Experimental Validation of MR-ARFI Aberration Tomography ..... *W. Grissom*

Uterine Fibroids | 14:15 – 15:45; 16:15 – 17:15 | Salon E – H

Moderators: Y. Kim, E. Stewart

19-UF MRI-guided Focused Ultrasound Treatment of Symptomatic Uterine Fibroids: Impact of Technology Advancement on Ablation Volumes in 115 Patients ..... *M. Matzko*

20-UF Complete or Near-complete Ablation of Symptomatic Uterine Fibroids by Volumetric MR-guided High-intensity Focused Ultrasound Therapy: Assessments of Safety and Therapeutic Efficacy ..... *M.J. Park*

21-UF Follow up of 140 Patients Treated from 2005 to 2011 with MRgFUS for Symptomatic Uterine Fibroids ..... *G. Hesley*

22-UF MR Guided Focused Ultrasound for Uterine Fibroids: A Pilot Randomized, Placebo-Controlled Trial ..... *V. Jacoby*

23-UF Pregnancies after Magnetic Resonance-guided Focused Ultrasound Surgery (MRgFUS) for Conservative Treatment of Uterine Fibroids ..... *J. Rabinovici*

24-UF Predictive Value of Patient Screening for Successful MRgFUS Treatment of Uterine Fibroids ..... *G. Hesley*

25-UF Diffusion-weighted Magnetic Resonance Imaging (DWI) as a Predictor for Treatment Efficacy of Volumetric Magnetic Resonance(MR)-guided High-Intensity Focused Ultrasound (HIFU) Ablation of Symptomatic Uterine Fibroids ..... *M. Ikink*

26-UF Comparison of Overall Uterine Fibroid-related Health Care Costs between Magnetic-Resonance Focused Ultrasound, Myomectomy and Uterine Artery Embolization ..... *B. Borah*

27-UF African American Women are Uniquely Affected by Uterine Fibroids ..... *E. Stewart*

28-UF Cost-Effectiveness Analysis of Uterine-Preserving Procedural Treatments for Uterine Fibroids, Including Magnetic Resonance-Guided Focused Ultrasound (MRgFUS) ..... *A. Cain-Nielsen*

29-UF A Multidisciplinary Approach to Uterine Leiomyomas: Rationale, Design, Early Results and Predictors of Undergoing Uterine-Preserving Treatment ..... *N. Tan*

30-UF RELIEF - REgistry for Leiomyoma, International Efficacy of Focused Ultrasound ..... *J. Rabinovici*

Panel Discussion: UF Site Success | 17:15 – 18:00 | Salon E – H

Site Success in Uterine Fibroid Therapy
A. Dobrotwir, G. Hesley, Y. Kim, M. Matzko, J. Rabinovici, S. Raman, H. Rastogi, E. Stewart, S. Yoon

---

Tuesday October 16

Panel Discussion: Ultrasound vs. MRI | 8:00 – 8:45 | Salon E – H

Ultrasound vs. MRI as guidance for Focused Ultrasound Treatment
C. Chaussy, Y. Inbar, J. Souquet, C. Tempany, G. ter Haar

Emerging Applications | 8:45 – 10:30 | Salon E – H

Moderators: A. Melzer, B.Wood

31-EA Differences in Intratumoral Distribution of Doxorubicin Released from Temperature-sensitive Liposomes during Hyperthermia, Ablation and Combined Treatment ..... *E. Heijman*

Detailed Program (continued)

32-EA Ultrasound-triggered Release of Doxorubicin from Thermosensitive Liposomes Modified with Poly(N-Isopropylacrylamide-co-Propylacrylic Acid) Copolymers for Cancer Therapy ..... *T. Porter*

33-EA Mild Hyperthermia in Small Animals with a Sector-vortex Phased-array Transducer for Homogeneous Heating ..... *C. Burke*

34-EA Enhanced MR-guided HIFU Ablation of Rabbit VX2 Tumors In Vivo using Phase-Shift Nanoemulsions ..... *J. Kopechek*

35-EA Pulsed Focused Ultrasound (pFUS) Induces Targeted Homing of Therapeutic Mesenchymal Stem Cells (MSC) to Kidneys During Acute Tubular Necrosis and Leads to Improved Renal Function. ..... *S. Burks*

36-EA Boiling Histotripsy: A Method of Tissue Emulsification Using Millisecond-long Pulses of High Intensity Focused Ultrasound ..... *L. Crum*

37-EA Targeting Vascular Structures Noninvasively with Ultrasound Guidance ..... *J. Ballard*

Breast Tumors | 11:00 – 12:30 | Salon E – H

Moderators: W. Bartels, H. Furusawa

38-BT MRgFUS of Breast Cancer: It's Efficacy and Safety in the Clinical Studies ..... H. Furusawa

39-BT Clinical Study Design for the Evaluation of Volumetric MRI-guided High-Intensity Focused Ultrasound of Breast Cancer Using a Dedicated MR-HIFU Breast System ..... *L. Merckel*

40-BT Ultrasound-guided High-Intensity-Focused-Ultrasound (HIFU) Treatment of Breast Fibroadenoma ..... *R. Kovatcheva*

41-BT In Vivo Evaluation of a Breast-specific MRgFUS System in a Goat Udder Model ..... *A. Payne*

42-BT Optimizing MR Thermometry for Clinical Phase I Breast Tumor Ablation Study ..... *R. Deckers*

43-BT Internal Fiducial Tattoos Made with FUS For Surgical or Radiotherapy Image Guidance ..... *E. Hipp*

Keynote Address | 12:30 – 12:45 | Salon E – H

Diane and David Heller Lecture ..... *J. Grisham*

Lunch Discussion Sessions | 13:15 - 14:15 | Lower Level

Vendor Profile | Glen Echo
Regulatory — Tips for designing your first pilot study | Forest Glen
Prostate | Brookside

44-LD Near-Total Gland Ablation of Locally Confined Low and Intermediate Risk Prostate Cancer Using Magnetic Resonance Guided Focused Ultrasound Surgery (MRgFUS) ..... *S. Desai*

45-LD Preliminary Clinical Experience of Treatment Low-risk Prostate Cancer with the Use of the ExAblate® Magnetic Resonance Guided Focused Ultrasound Surgery (MRgFUS) ..... *V. Turkevich*

46-LD MR-guided Focused Ultrasound Treatment in Patient with Organ-Confined Prostate Cancer: An Initial Experience ..... *Y.T. Oh*

47-LD Feasibility Study to Evaluate the Safety and Preliminary Effectiveness of Focal MR-guided Focused Ultrasound Surgery (MRgFUS) for Locally Confined Low-Risk Prostate Cancer: The First North American Experience ..... *S. Ghai*

Detailed Program (continued)

Prostate | 14:15 – 15:30 | Salon E – H

Moderators: A. Blana, P. Scardino

48-PR Evolution and Outcomes of 3 MHz High-intensity Focused Ultrasound Therapy for Localized Prostate Cancer over 15 years ..... *C. Chaussy*

49-PR Medium Term Outcomes Following Primary Focal Therapy using HIFU for Localised Prostate Cancer ..... *L. Dickinson*

50-PR Non-invasive Treatment of Locally Non-advanced Prostate Cancer: Phase I Study Using Magnetic Resonance Guided High Intensity Focused Ultrasound Technology and Excision Pathology for Efficacy Assessment ..... *A. Napoli*

51-PR Hemi salvage HIFU in patients with radiorecurrent prostate cancer ..... *E. Baco*

Panel Discussion: Prostate Controversies | 16:00– 16:45 | Salon E – H

Focused Ultrasound Treatment for Prostate Cancer – Controversies
A. Blana, C. Chaussy, L. Dickinson, M. Hurwitz, P. Scardino

Prostate (continued) | 16:45 – 17:30 | Salon E – H

52-PR Clinical Evaluation of Transurethral MR-HIFU for the Treatment of Localized Prostate Cancer ..... *R. Chopra*

53-PR MR-guided Closed-loop Feedback Control of Transurethral Ultrasound Ablation for Treatment of Benign Prostatic Hyperplasia (BPH) ..... *P. Prakash*

54-PR Toward Real-Time Tissue Viability Mapping During MRgFUS in the Prostate ..... *K. Butts Pauly*

55-PR MRI Guided Prostate Cancer Focal Ablation using HIFU by Means of Image to Image Registration ..... *L. Dickinson*

Poster Session and Reception | 18:00 – 21:00 | Salon D

See Poster Overview on pages 16 – 19

Wednesday

October 17

Bone Metastasis | 8:00 – 9:45 | Salon E – H

Moderators: M. Hurwitz, V. Turkevich

56-BM Magnetic Resonance Guided Focused Ultrasound Surgery For Painful Bone Metastases is a Safe and Effective Treatment in Patients for Whom Radiation Therapy Is Contraindicated: Results of a Multi-Center Phase III Trial ..... *M. Hurwitz*

57-BM Clinical Results of Treatment Painful Bone Metastases with Magnetic Resonance Guided Focused Ultrasound ..... *V. Turkevich*

58-BM Primary Pain Palliation and Local Tumor Control in Bone Metastases Treated with Magnetic Resonance-guided Focused Ultrasound (MRgFUS) ..... *M. Anzidei*

59-BM A Comprehensive Quality Assurance Program for Bone Palliation Using MR Guided Focused Ultrasound: Fox Chase Experience ..... *L. Chen*

60-BM Volumetric MR-HIFU Ablation in a Patient with a Costal Metastasis and a Soft-tissue Mass ..... *M. Huisman*

61-BM Phase II Trial Design of MRI-Guided High Intensity Focused Ultrasound and Lyso-thermosensitive Liposomal Doxorubicin for Palliation of Painful Bone Metastases ..... *E.Smith*

62-BM Effects of HIFU Ablation on Bone Metastases: From MRI, SPECT/CT and MicroCT Point of View ..... *S.Y. Yeo*

Panel Discussion: Bone Metastasis | 9:45 – 10:30 | Salon E – H

Focused Ultrasound Treatment for Bone Metastasis
C. Catalano, P. Ghanouni, M. Hurwitz, J. Larner

Detailed Program (continued)

Bone Non-Metastasis | 11:00 – 12:00 | Salon E – H

Moderators: M. Kawasaki, A. Napoli

63-BN Osteoid Osteoma: Preliminary Results of a Non-invasive Treatment using Magnetic Resonance Guided Focused Ultrasound ..... *B. Cavallo Marincola*

64-BN Role of Magnetic Resonance Guided Focused Ultrasound Surgery (MRgFUS) in Treatment of Patients with Lumbar Facetal Arthropathy ..... *A. Patil*

65-BN Toward T1-Based Thermometry in Cortical Bone Using Ultrashort Echo-Time MRI ..... *W. Miller*

Foundation | 12:00 – 12:30 | Salon E – H

Moderators: A. Hananel, J. Snell

66-FD The Journal of Therapeutic Ultrasound ..... *A. Hananel*

67-FD Bio Mechanism ..... *J. Foley*

Lunch Discussion Sessions | 13:00 – 14:00 | Lower Level

Vendor Profile | Glen Echo

Regulatory Discussion — Advice for planning and running an FDA pivotal study | Forest Glen

Liver | 14:00 – 15:45; 16:15 –17:45 | Salon E – H

Moderators: W. Gedroyc, T. Leslie

FUSF Strategic Focus: Liver and Pancreas ..... *A. Hananel*

68-LV HIFU Ablation for Hepatocellular Carcinoma: Updated Clinical Applications ..... *F. Wu*

69-LV Magnetic Resonance guided Focused Ultrasound (MRgFUS) Treatment of Primary Pancreatic and Hepatic Cancer: Preliminary Experience in Tumor Control ..... *M. Anzidei*

70-LV MR-guided Focused Ultrasound Induced Hyperthermia for Enhancing Drug Delivery in a Pancreatic Cancer Mouse Model ..... *N. Farr*

71-LV Clinical Evaluation of a Toroidal High Intensity Focused Ultrasound Transducer Used Intra-operatively for the Treatment of Liver Metastases ..... *D. Melodelima*

72-LV FUSIMO - A European Project on Patient-specific Modeling and Simulation of FUS in Moving Organs ..... *S. Braunewell*

73-LV Ultrasound Thermography In Vivo: Tissue Property Measurements Using Subtherapeutic High Intensity Focused Ultrasound ..... *A. Haritonova*

74-LV In-vivo Evaluation of Acoustic Intensity Based Element Selection for Optimal Intercostal Firing ..... *M. de Greef*

75-LV T2-based MR Thermometry in Adipose Tissue Layers for HIFU Near-field Monitoring ..... *P. Baron*

76-LV Intrapleural Fluid Injection for MR-HIFU Ablation in the Subdiaphragmatic Liver ..... *J. Wijlemans*

77-LV Suitability of a Tumour-mimicking Material for the Evaluation of High Intensity Focused Ultrasound Ablation under Magnetic Resonance Guidance ..... *S. Pichardo*

78-LV MR-HIFU Drug Paintbrush: Large Volume, Conformal Mild Hyperthermia with MR-HIFU Used to Trigger and Monitor Release from Image-able, Temperature-sensitive Liposomes ..... *P. Yarmolenko*

79-LV Targeted Drug Delivery by Focused Ultrasound Mediated Hyperthermia Combined with Temperature Sensitive Liposomes ..... *D. Haemmerich*

Closing Remarks | 17:45 – 18:00 | Salon E – H

Closing Remarks ..... *N. Kassell*

Poster Overview

Bone

Brain

Poster Overview (continued)

Breast Tumors

Emerging Applications

Poster Overview (continued)

Liver and Pancreas

Prostate

Uterine Fibroids

Poster Overview (continued)

Young Investigator

Invited Panelists and Moderators

Wilbert Bartels, PhD
University Medical Center Utrecht
Utrecht, Netherlands

Andreas Blana, MD
Klinikum Fürth
Fürth, Germany

Carlo Catalano, MD
University of Rome — Sapienza
Rome, Italy

Jin Woo Chang, MD
Yonsei University College of Medicine
Seoul, Korea

Christian Chaussy, MD
University of Regensburg
Strasslach, Germany

Louise Dickinson, MD
University College Hospital
London, United Kingdom

Andrew Dobrotwir, MD
Royal Women's Hospital
Melbourne, Australia

W. Jeffrey Elias, MD
University of Virginia
Charlottesville, Virginia, United States

Hidemi Furusawa, MD
Breastopia Namba Hospital
Miyazaki, Japan

Wladyslaw Gedroyc, MD
Saint Mary's Hospital, Imperial College
London, United Kingdom

Pejman Ghanouni, MD
Stanford University
Stanford, California, United States

Arik Hananel, MD, MBA
Focused Ultrasound Foundation,
Charlottesville, Virginia, United States

Gina Hesley, MD
Mayo Clinic
Rochester, Minnesota, United States

Mark Hurwitz, MD
Brigham and Women's Hospital
Boston, Massachusetts, United States

Yael Inbar, MD
Sheba Medical Center
Qiryat Ono, Israel

Daniel Jeanmonod, MD
SoniModul AG, Center for Ultrasound
Functional Neurosurgery
Solothurn, Austria

Neal Kassell, MD
University of Virginia, Charlottesville,
Virginia, United States

Motohiro Kawasaki, MD
Kochi University
Kochi, Japan

Young-Sun Kim, MD
Samsung Medical Center
Seoul, Korea

James Larner, MD
University of Virginia
Charlottesville, Virginia, United States

Thomas Leslie, MD
University of Oxford, Churchill Hospital
Oxford, United Kingdom

Matthias Matzko, MD
Amper Kliniken AG
Dachau, Germany

Andreas Melzer, MD
University of Dundee, Institute for
Medical Science & Technology
Dundee, United Kingdom

Alessandro Napoli, MD
University of Rome — Sapienza
Rome, Italy

Jaron Rabinovici, MD
Chaim Sheba Medical Center
Ramat Gan, Israel

Steve Raman, MD
University of California at Los Angeles
Los Angeles, California, United States

Harsh Rastogi, MD
Indraprastha Apollo Hospitals
New Delhi, India

Peter Scardino, MD
Memorial Sloan-Kettering Cancer Center
New York, New York, United States

John Snell, PhD
Focused Ultrasound Foundation
Charlottesville, Virginia, United States

Jacques Souquet, PhD
Supersonic Imagine
Aix-en-Provence, France

Elizabeth Stewart, MD
Mayo Clinic
Rochester, Minnesota, United States

Clare Tempany, MD
Brigham and Women's Hospital /
Harvard Medical School
Boston, Massachusetts, United States

Gail ter Haar, PhD
The Institute of Cancer Research
Sutton, United Kingdom

Vladimir Turkevich, MD
N.N. Petrov Research Institute of Oncology
Saint Petersburg, Russian Federation

Bradford Wood, MD
National Institutes of Health (NIH)
Clinical Center
Bethesda, Maryland, United States

Sang-Wook Yoon, MD
CHA Bundang Medical Center
Gyunggi-do, Korea

Abstracts

Oral Presentations and Discussions

Monday

Tuesday

Wednesday

Posters

Author Index

1-BR

Monday
15 October 2012

Topic: Brain
Presentation type: Oral

Study on Incisionless Transcranial Magnetic Resonance-Guided Focused Ultrasound Treatment of Neuropathic Pain: Safety, Accuracy and Clinical Outcomes

Daniel Jeanmonod[1], David Moser[1], Anouk Magara[2], Milek Kowalski[3], Robert Bühler[4], Payam Pourtehrani[5], Tony Coray[5], Jörg Vogel[5]

[1]Center for Ultrasound Functional Neurosurgery, Solothurn, Switzerland
[2]Neurology Bern, Bern, Switzerland
[3]Privatklinki Obach, Solothurn, Switzerland
[4]Bürgerspital Solothurn, Solothurn, Switzerland
[5]Rodiag Diagnostic Centers, Solothurn, Switzerland

Background/Introduction: Recent technological developments in MR-guided focused ultrasound (MRgFUS) enable incisionless transcranial therapeutic interventions to the brain. The goal of this study is to establish the safety, targeting accuracy and efficiency of this technique in the treatment of neuropathic pain.

Methods: We present clinical, radiological and neurophysiological data on 3 month and 1 year follow-ups of 13 neuropathic pain patients. Medial thalamic (central lateral nucleus) FUS thermocoagulations were performed under real-time MR-imaging and MR-thermometry guidance, applying mean peak temperatures between 49° and 58°. Patients were evaluated at follow-up visits by two neurologists independent from the functional neurosurgical investigators. Comparison of quantitative EEG spectral activities between the patient group and a control group was performed. The method for targeting accuracy measurement was described in Moser et al. (Neurosurgical Focus 2012).

Results and Conclusions: The mean absolute targeting accuracy for 19 targets was 0.4 mm for the mediolateral dimension, 0.37 mm for the anteroposterior dimension and 0.71 mm for the dorsoventral dimension. There were no device- or procedure-related complications and no post-treatment neurological deficits. Currently, our patients present at 3 month or 1 year follow-ups (8 and 5 patients, respectively) a mean pain relief of 54.8%, a mean improvement of their visual analogue scale ratings of 36%, and 77% of them have a pain relief of or above 50%. There was a reduction of their quantitative EEG spectral overactivities particularly in the delta and theta frequency bands.

This study expands and confirms the already published evidence on MR-guided focused ultrasound in the treatment of neuropathic pain. This technology avoids the surgical risks related to brain penetration, and the real-time continuous MR-imaging and MR-thermometry allow an optimized lesioning safety and accuracy. Our experience has shown that the immediate thermal lesional effects could be used to enable a closed-loop control and optimization of target lesioning based on these two imaging modalities. In summary, MR-guided focused ultrasound offers a safe and precise option for the treatment of neuropathic pain.

Acknowledgements (Funding): This study was supported by InSightec Ltd (Haifa, Israel), Rodiag Diagnostic Centers AG (Olten, Switzerland), Privatklinik Obach (Solothurn, Switzerland) and GE Medical Systems (Switzerland)

2-BR

Monday
15 October 2012

Topic: Brain
Presentation type: Oral

Study on Incisionless Transcranial Magnetic Resonance-guided Focused Ultrasound Treatment of Parkinson's Disease: Safety, Accuracy and Initial Clinical Outcomes

Daniel Jeanmonod[1], David Moser[1], Anouk Magara[2], Milek Kowalski[3], Robert Bühler[4], Payam Pourtehrani[5], Tony Coray[5], Jörg Vogel[5]

[1]Center for Ultrasound Functional Neurosurgery, Solothurn, Switzerland
[2]Neurology Bern, Bern, Switzerland
[3]Privatklinki Obach, Solothurn, Switzerland
[4]Bürgerspital Solothurn, Solothurn, Switzerland
[5]Rodiag Diagnostic Centers, Solothurn, Switzerland

Background/Introduction: Recent technological developments in MR-guided focused ultrasound (MRgFUS) enable incisionless transcranial therapeutic interventions to the brain. The goal of this study is to establish the safety, targeting accuracy and efficiency of this technique in the treatment of Parkinson's disease.

Methods: We present clinical, radiological and neurophysiological data on 3 month follow-ups of 8 parkinsonian patients. Subthalamic FUS thermocoagulations (pallido-thalamic tractotomy, PTT) were performed under real-time MR-imaging and MR-thermometry guidance, applying mean peak temperatures between 52° and 59°. Patients were evaluated at follow-up visits by two neurologists independent from the functional neurosurgical investigators. Comparison of quantitative EEG spectral activities between the patient groups and a control group was performed. The method for targeting accuracy measurement was described in Moser et al. (Neurosurgical Focus 2012).

Results and Conclusions: The mean absolute targeting accuracy was 0.49 mm for the mediolateral dimension, 0.4 mm for the anteroposterior dimension and 0.56 mm for the dorsoventral dimension. There were no device- or procedure-related complications and no post-treatment neurological deficits. The first four patients presented at 3 month follow-up a mean improvement of their UPDRS of 7.6% and a mean global symptom relief of 22.5%. They maintained high dysrhythmic EEG spectral overactivities. No or minimal signs of their PTT lesion were seen on 3 month MR controls. The next four patients received the same treatment except that their final sonications were repeated 5-6 times. They enjoyed a 57.1% mean UPDRS improvement and a mean global symptom relief of 47.5%. Their spectral overactivities were reduced both in low and high frequencies, and their PTT lesions were clearly visible at the 3 month follow up MR control.

We present for the first time initial MRgFUS treatment results for Parkinson's disease. This technology avoids the surgical risks related to brain penetration, and the real-time continuous MR-imaging and MR-thermometry allow an optimized lesioning safety and accuracy. In view of the limited results of the first four patients, the assumption, confirmed by the presented data, was made that the PTT target placed in a dense fiber bundle is more resistant to heating than nuclear (thalamic) targets, and that it thus needs repeated end sonications to be completed. In summary, MR-guided focused ultrasound offers a safe and precise option for the treatment of Parkinson's disease.

3-BR

Monday
15 October 2012

Topic: Brain
Presentation type: Oral

Phase 1 Study of MRgFUS for Tremor Dominant Parkinson Disease

Jeff Elias

University of Virginia, Charlottesville, Virginia, United States

Background/Introduction: Researchers at UVA intend to investigate the safety and feasibility of transcranial MR-guided focused ultrasound for the treatment of tremor-dominant Parkinson's disease. 30 subjects will be enrolled in this FDA-approved clinical trial. Medication-refractory patients with tremor-dominant subtype as determined from UPDRS ratings are eligible. The subjects and raters will be blinded to the treatment as there is a 2:1 randomization to a control, sham-procedure arm with the possibility of crossover for all participants. The primary outcome is safety, but secondary measures include tremor improvement, quality of life, and higher cognitive function assessments. Study duration is 12 months following treatment.

4-BR

Monday
15 October 2012

Topic: Brain
Presentation type: Oral

A Phase 1 Study of MR-Guided Focused Ultrasound Thalamotomy for the Treatment of Medication-Refractory Essential Tremor

Jeff Elias, Diane Huss, Johanna Loomba, Mohamad Khaled, Robert Frysinger, Scott Sperling, Binit Shah, Madaline Harrison, Max Wintermark

University of Virginia, Charlottesville, Virginia, United States

Background/Introduction: Advances in ultrasound transducer technology have enabled for transcranial sonication with energy levels adequate to achieve tissue ablation. With MR-guidance and monitoring, precise lesioning is now possible of deep brain targets like the thalamus and basal ganglia so that stereotactic lesioning is being reconsidered for the treatment of movement disorders. In this phase 1 clinical trial, we investigate the feasibility and safety of MRgFUS for performing a unilateral thalamotomy for medication-refractory essential tremor (ET).

Methods: According to an FDA-approved protocol, fifteen patients with medication-resistant ET underwent unilateral MRgFUS lesioning of the ventralis intermedius nucleus of the thalamus for dominant limb tremor. Intraprocedural monitoring was conducted with each incremental sonication using MR thermometry and clinical examination. Neurological assessments, validated tremor ratings, MRI, and quality of life data were recorded preoperatively and during a year post treatment. Adverse events were recorded throughout the study duration.

Results and Conclusions: Accurate thalamic lesioning was achieved in all cases. Dominant limb tremor subscores improved by nearly 80% while ipsilateral limb tremor was unchanged. Functional activities and quality of life measures improved significantly. Refining of the thalamic target was possible in five cases where paresthesias where elicited, presumably from adjacent sensory thalamus. Serial MR imaging defined the evolution of the lesioning process with perilesional edema peaking at one week and resolving by one month.

Transcranial MRgFUS can be used to lesion Vim thalamus, and this results in clinical effects similar to radiofrequency halamotomy or thalamic DBS. Additional investigation of this procedure is warranted in ET and Parkinson's disease.

Acknowledgements (Funding): Focused Ultrasound Foundation

5-BR

Monday
15 October 2012

Topic: Brain
Presentation type: Oral

Preliminary Report of MRI Guided High Intensity Focused Ultrasound Surgery for the Patient with Essential Tremor

Jin Woo Chang

Yonsei University College of Medicine, Seoul, South Korea

Background/Introduction: The field of MRI guided high intensity focused ultrasound surgery (MRgFUS) is evolving and offers the new hope for the treatment of many neurological disorders through both ablative mechanism and non-ablative mechanisms such as drug delivery, neuromodulation and etc. Currently, Jeanmond et al demonstrated the beneficial effect of MRgFUS by performing noninvasive central lateral thalamotomies as a treatment for chronic neuropathic pain. And we believe that certain benefits of this MRgFUS are the elimination or the current surgical risk such as infection and hemorrhage by making a lesion with a noninvasive, precise method.

Methods: Thus, we also want to evaluate the role of MRgFUS for the management of essential tremor especially for those who are not good candidates for invasive surgery such as deep brain stimulation (DBS) or radiofrequency thalamotomy. And we had an approval of the feasibility study from the Korean FDA and the IRB of Yonsei University College of Medicine. As well, we had fully informed written consent for making unilateral thalamotomy to control the tremor of the dominant hand.

Results and Conclusions: The treatment was performed in a 3T MRI (Sgina, GE) using the ExAblate® 4000 device (Insightec), which features a 30 cm diameter hemispherical 1024 elements phased array transduced operating at 650 KHz. The patient's head was immobilized by fixation in an MRI compatible frame (Radionics). In this presentation, we will demonstrate the results of patient with essential tremor after MRgFUS with our imaging studies.

6-BR

Monday
15 October 2012

Topic: Brain
Presentation type: Oral

Intra-procedural Assessment of Tremor and Neurological Status during Focused Ultrasound Surgery/Ablation in the Magnetic Resonance Environment

Diane Huss, Max Wintermark, Mohamad Khaled, Madaline Harrison, Robert Frysinger, Jeff Elias

University of Virginia, Charlottesville, Virginia, United States

Background/Introduction: The brain applications for MR-guided FUS treatment provide a challenging physical environment for intra-procedure testing of clinical impact. The patient is awake for the procedure within the bore of the MRI with the head immobilized and eyes directed to the top of the bore. The upper limbs are restricted from free active movement by the size of the bore and the constraints of physiologic vital sign monitoring devices. Additionally, the metal free environment limits the selection of assessment tools.

Methods: Before entering the bore of the MRI, the patient was fit with a modified pair of mirrored glasses within the stereotactic frame. The glasses are adjusted to direct the patients gaze down the length of the body and out the bore of the MRI. Between each sonication, the patient was assessed for sensory, strength, speech and tremor changes. Tremor control was assessed by the clinical assessor during the sonications and immediately post. Visualization of postural tremor occurred during and after each sonication. Action tremor was assessed after each sonication. The patient was presented a metal free felt tip pen and a writing support was positioned to present prepared Archimedes spirals for targeted drawing within the spirals. These spirals are identical to those used for pre-procedure and post procedure testing out of the MRI. Sensory assessment was completed with plastic and wooden pins for pain, plastic monofilaments for pressure and fabric for light touch. Proprioceptive testing was conducted by identification of changed position of the distal phalanx of the index finger and great toe. Periodic repetition of a standardized phrase assessed for subtle dysarthria. Constant communication with the treating neurosurgeon provided immediate notification of adverse and beneficial change throughout the treatment.

Results and Conclusions: Progressive remediation of both the postural and action components of the patients' tremor was noted as the sonication intensity increased. Additionally, transient suppression of postural tremor was noted during the sonication at early temperatures with eventual obliteration of the postural tremor at the termination of treatment. The action tremor also followed a progressive suppression that was noted to occur later than the postural tremor component. Visualization of the terminal approach of the upper limb to the drawing target was informative of the modification in quality of tremor. Titration of the sonications to higher dosages resulted in progressive reduction of action tremor. Observed movement quality during terminal approach to target and accuracy of drawing within the target spirals was consistent and representative of tremor suppression during clinical assessments out of the MRI. Accuracy and quality of the final drawings within the MRI bore demonstrate consistency with the subjects' three-month assessment for each of the 15 individuals as well as for the patients that have reached their one-year follow-up assessments. The instantaneous impact on clinical status has obvious advantages over the delayed response that evolves over three months or more with Gamma Knife thalamotomy. Identification of slight sensory changes early in the sonications at low temperatures allowed for immediate target adjustment resulting in only minimal or no adverse neurologic effects.

Acknowledgements (Funding): Funding for this project was provided by the Focused Ultrasound Foundation.

Fitting with mirrored glasses before entering the MRI

Postural tremor testing within MRI bore

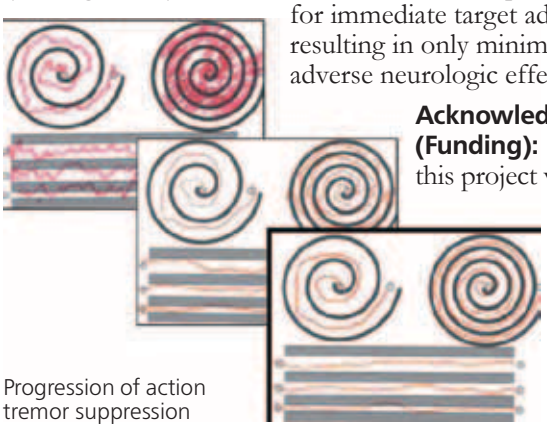

Progression of action tremor suppression

7-BR

Monday
15 October 2012

Topic: Brain
Presentation type: Oral

"Non-Thermal" Ablation in the Brain via Focused Ultrasound Combined with an Ultrasound Contrast Agent: Long-Term Treatment Effects and Feasibility in a Large Animal Model

Nathan McDannold[1], Margaret Livingstone[2], Costas Arvanitis[1], Yong-Zhi Zhang[1], Ferenc Jolesz[1], Natalia Vykhodtseva[1]

[1]Brigham and Women's Hospital/Harvard Medical School, Boston, Massachusetts, United States
[2]Harvard Medical School, Boston, Massachusetts, United States

Background/Introduction: After more than 50 years of interest, transcranial focused ultrasound (FUS) ablation in the brain has reached clinical trials. However, a major limitation of current FUS technology is the narrow central region in the brain where ablation can be applied without overheating the skull. A potential way to increase this "treatment envelope" is to combine the sonications with an ultrasound contrast agent. With such agents, ablation can be achieved at substantially lower pressure amplitudes. One can also dramatically reduce the duty cycle, leading to reductions in time-averaged powers by orders of magnitude. This method localizes the FUS-induced effects on the vasculature, leading to "non-thermal" ablation via mechanical effects.

Methods: Two studies were completed to evaluate this method. In the first, we sonicated at four overlapping locations in a 2×2 grid at in the rat brain with a 1.1 MHz FUS transducer within a 4.7T animal MRI (N: 15). The fate of the sonicated tissue was evaluated up to 9 weeks after sonication with serial MRI examinations. Next, we evaluated whether the method is feasible at deep targets in a large brain. In 4 macaques, we sonicated locations in the amygdala adjacent to the optic tract using a clinical transcranial MRI-guided FUS system (ExAblate®, 220 kHz, InSightec) developed for brain surgery. Here the acoustic power level, which ranged from 3.5-6.4 W, was set to be just above the threshold for inertial cavitation, which was measured at each target using passive cavitation detectors. The animals were sacrificed 2h or one week after sonication, and the tissue was evaluated in histology. In both experiments, burst sonications (10 ms bursts at 1 Hz) were applied for five min, and were combined with 20 μl/kg IV injections of Definity® microbubbles (2× the dose used for imaging).

Results and Conclusions: In the rats, the ablated volumes were initially enhancing in contrast-enhanced MRI and were hypointense in T2*-weighted MRI. Two weeks after FUS, the sonicated tissue mostly disappeared, and in most cases an empty volume filled with CSF was left behind which remained stable over time. In the macaques, we were able to ablate tissue volumes close to the skull base without evident thermal damage. The lesions were constrained to the focal region; however some blood-brain barrier disruption and petechaie were evident along the ultrasound beam path in front of the lesions. In histology, well-circumscribed lesions were found that were consistent with FUS-induced destruction of the vasculature. When the sonicated region included the optic tract, the damage to the nerve was substantially less than the adjacent gray matter.

Unlike thermal ablation, which produces thermally-coagulated tissue that can remain for extended periods in time, this sort of ablation is rapidly resolved, and an empty cavity remains that resembles surgical resection. This ablation can be achieved at deep brain locations using a clinical transcranial FUS system without overheating the skull base. If methods can be established to plan and monitor this type of ablation, it offers a potential way to greatly expand the "treatment envelop" for transcranial FUS and offer a noninvasive alternative to surgery to a greater number of patients.

Acknowledgements (Funding): This work was supported by the FUS Foundation and by NIH grant P41RR019703/P41EB015898.

8-BR

Monday
15 October 2012

Topic: Brain
Presentation type: Oral

Ultrasonic Neuromodulation: In Situ Threshold for Motor Response in a Rat Model

Youlian Younan[1], Thomas Deffieux[1], Benoit Larrat[1], Abdelhak Souilah[1], Mathias Fink[1], Jean-François Aubry [2], Mickael Tanter[1]

[1]Institut Langevin, Paris, France
[2]University of Virginia, Charlottesville, Virginia, United States

Background/Introduction: The recent discovery that low-intensity low frequency pulsed ultrasound could be used to stimulate the brain non-invasively without any noticeable tissue damage is expected to have a major impact in neuroscience in the coming years. Nevertheless, this emerging field also raises many questions. A controversy even rose on whether an intensity threshold exists for inducing a neurological response as such an effect has been observed with very low ultrasonic intensity. The existence of such an acoustic threshold is investigated here, both experimentally and numerically in order to take into account the head geometry for the estimation of the pressure level in the brain.

Methods: In this study, the motor responses of rats (N=10) were investigated as a function of the excitation pressure level with a 320kHZ focused transducer. Derived from typical parameters used for neuromodulation [Tufail et al, Nature Protocols 2011], sonication parameters were set to 75cycles burst duration, 50% duty cycle, 2kHz PRF, 476ms total stimulation time. Motor response was assessed by both visual inspection and electromyography measurements. Rats were anesthetized with a ketamine/xylazine cocktail. The transducer was calibrated in water with a heterodyne interferometer, with and without rat skull samples in order to determine the attenuation factor of the rat skull. Finally 3D finite differences simulations were performed based on rat skull CT scans, to evaluate the effect of reverberations in the closed skull cavity on the pressure amplitude at focus, compared to open space propagation. This 3D modeling of reverberations enables to avoid bias on the estimation of the pressure amplitude in the brain when providing experimental acoustic thresholds.

Results and Conclusions: A sharp threshold for these particular ultrasonic sonication parameters was observed for voltages corresponding to a peak negative pressure of 0.62 +- 0.04 MPa in water. Pressure measurements performed with and without a rat skull vault flap showed that the rat skull induced a mean 15% pressure loss. The derated in situ pressure threshold was thus 0.52 +- 0.03 MPa. Simulations exhibited the importance of the whole head cavity and not brain cavity as first expected: reverberations do not occur because of the skul bone itself but rather on the tissue/air reflections on the bottom of the head and on the transducter itself. Consequently, the maximum pressure in the brain is 1.3 times higher in the brain than in water, contrary to the 15% loss expected when taking into account the skull attenuation. It thus yields to a 60% error on the in situ Ispta values if such reverberations are not taken into account.

This study consolidates the hypothesis of a threshold for inducing significant motor response. The estimation of the acoustic threshold must be corrected to take into account the reverberations in the head since they significantly affect the in situ pressure field spatial distribution and amplitude especially when investigating multiple frequencies.

Acknowledgements (Funding): This work was supported by the Labex WIFI.

Transverse view of the simulate pressure in free field (left) and the rat head model (right)

9-BR

Monday
15 October 2012

Topic: Brain
Presentation type: Oral

Transcranial Sonothrombolysis in Ischemic Stroke Using the ExAblate® 4000

Thilo Hoelscher

University of California at San Diego, San Diego, California, United States

Background/Introduction: To test for transcranial sonothrombolysis using Focused Ultrasound (FUS) in vivo an appropriate animal model is needed. Current in vivo sonothrombolysis models for stroke are mainly established in rats and rabbits, using the middle cerebral artery (MCA) as the target vessel. The vast majority of this models aim to accomplish both efficacy and safety testing using the same approach. However, it is questionable whether this models are suitable due to the very different anatomy of the skulls as well as the intracranial vessel anatomy and vessel sizes compared to humans.

Methods: A rabbit carotid artery has been chosen because it is a bifurcational model and therefore comparable to the intracranial internal carotid artery bifurcation into middle/anterior cerebral artery or the bifurcation of the middle cerebral artery itself (M1/M2 segments). The rabbit carotid artery has average vessel diameters similar to human M1/M2 segments and allows the placement of human thrombus material under visual control as well as the real-time monitoring of flow and clot mechanics during the sonothrombolysis procedure. In this presentation, the model will be introduced and first results to show feasibility will be presented.

Results and Conclusions: To date, a total of N=48 in vivo sonothrombolysis studies using the rabbit carotid artery model have been performed. Anesthesia and monitoring, positioning of the animal using a customized rabbit holder as well as the surgical procedure itself could be performed in a timely fashion. Vessel occlusion using different thrombus preparation methods could be achieved with great confidence. In less than 10% of all interventions the initial thrombus dislocated further downstream after clamp release, which required a repetition of the clot formation procedure.

In conclusion, the use of a rabbit carotid artery model for sonothrombolysis research is feasible and provides features which might mimick an arterial thrombotic occlusive event in humans more closely. It has the potential to provide a more profound insight into the interplay between pro thrombolytic activities and counterbalancing platelet activation induced by ultrasound. The ability to study the flow mechanics during pre/post and during sonothrombolysis might be an additional option to study the impact of blood flow on sonothrombolysis. Further investigations are needed, and planned, to confirm reproducibility and reliability of this model.

Acknowledgements (Funding): This work was sponsored by InSightec, Inc.

10-BR

Monday
15 October 2012

Topic: Brain
Presentation type: Oral

High Intensity Focused Ultrasound for the Treatment of Acute Ischemic Stroke

Daniel Pajek, Alison Burgess, Yuexi Huang, Kullervo Hynynen

Sunnybrook Research Institute, Toronto, Canada

Background/Introduction: It is estimated that only 2–6% of patients receive thrombolytic therapy for acute ischemic stroke suggesting that alternative therapies are necessary. High intensity focused ultrasound (HIFU) is capable of mechanically disintegrating blood clots without the need for administered thrombolytics.

Methods: HIFU thrombolysis was initially characterized in vitro. At 1.5 MHz, pulses lengths of 0.1–10 ms and powers up to 300 W were investigated. In in vivo feasibility experiments, with clots formed in rabbit femoral arteries, it was found that 10 ms pulses were associated with bleeding, while 1 ms pulses were able to achieve partial flow restoration. Next, HIFU thrombolysis in an embolic model was investigated. Blood clots were injected into rabbit middle cerebral arteries and MRI was used to localize clots and target the HIFU sonications. Sonication parameters were based on the results of the initial feasibility studies. No evidence of reperfusion was seen at low powers (0/3), however reperfusion occurred in 5/7 animals when 550 W was applied. Histological analysis confirmed that the sonicated vessels remained intact after HIFU treatment. The human skull remains a barrier for the use of this technique clinically. So far, safe HIFU thrombolysis requires frequencies higher than those currently utilized by transcranial ultrasound arrays. Simulations have been conducted to evaluate the technical requirements needed to use this technique. Large aperture phased arrays in targeting clinically relevant vessel locations through an intact skull were simulated.

Results and Conclusions: These simulations suggest that transcranial phased arrays with transducer element counts about an order of magnitude higher than what currently exist would be required, so new arrays and multi-channel driver technology need to be developed to realize this as a treatment modality for stroke. HIFU thrombolysis is feasible as a means of restoring blood flow in occluded arteries in the absence of thrombolytic agents and could dramatically reduce the time to achieve flow restoration in patients.

11-BR

Monday
15 October 2012

Topic: Brain
Presentation type: Oral

Transcranial MR Guided Focused Ultrasound Treatment of ICH

Stephen Monteith[1], Sagi Harnof[2], Neal Kassell[1], Max Wintermark[1], Eyal Zadicario[3], Beatriz Lopes[1], John Snell[4], Matthew Eames[4], Jason Sheehan[1]

[1]University of Virginia, Charlottesville, Virginia, United States
[2]Sheba Medical Center, Tel Hashomer, Israel
[3]InSightec, Tirat Carmel, Israel
[4]Focused Ultrasound Foundation, Charlottesville, Virginia, United States

Background/Introduction: ICH is a major cause of death and disability throughout the world. Surgical techniques are complicated by their highly invasive nature, and the associated disability caused in the process ICH removal. Preliminary data have shown promise for the feasibility of transcranial MR guided Focused Ultrasound sonothrombolysis to liquefy the clotted blood in ICH, thereby facilitating minimally invasive evacuation with a small drainage tube.

Methods: In an in-vitro model, we have demonstrated feasibility of transcranial MR guided Focused Ultrasound sonothrombolysis. 40mL of human blood was injected into latex balloons. After incubation clots were weighed and imaged with MRI to confirm adequate clot formation and allow for clot retraction. Clot lysis through an explanted human calvarium using the ExAblate® Neuro 230KHz phased array transducer system (InSightec) under real time MRI guidance was performed. Up to 100% of solid clot was liquefied. In a swine model of ICH (Figure 1), transcranial sonothrombolysis has been performed. 3-4mL of autologous arterial blood was infused into the frontal lobe. The ICH was lysed through the pig skull and MRI was utilized to confirm lysis. Following sonothrombolysis the liquid clot was aspirated under MRI guidance with a 16G angio-catheter. Post evacuation MRI images demonstrate the evacuation of the majority of clot. Histological examination did not reveal brain injury due to the sonothrombolysis treatment. Biochemical analysis of the lysate was benign. In addition, preliminary results demonstrate feasibility in a cadaveric model of ICH and IVH (Figure 2).

Results and Conclusions: Feasibility of transcranial MR guided Focused Ultrasound sonothrombolysis has been demonstrated with in-vitro, cadaveric, and swine models of ICH. Initial in-vivo safety data suggests the process to be safe.

Acknowledgements (Funding): Focused Ultrasound Foundation. The study was supported by Insightec.

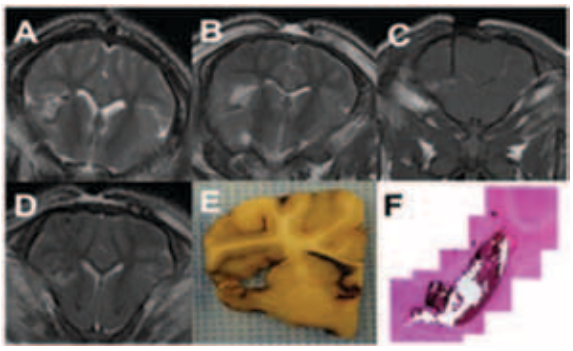

Figure 1. A: Swine model of ICH Pre-treatment. B: Post MRgFUS clot lysis with increased T2 signal indicating liquefication of clot. C: MRI guided aspiration of liquefied clot by 16G catheter. D: Post aspiration shows minimal residual liquid clot. E, F: Pathology shows no additional brain injury or blood brain barrier breakdown from MRgFUS.

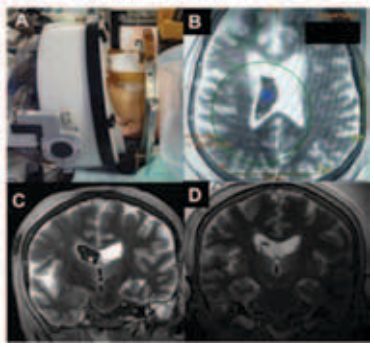

Fig 2: A: Following ICH/IVH placement and 3 hours dwell time, the cadaver is shaved, placed in the stereotactic frame, and the transducer filled with degassed water. A diaphragm holds the cooled circulating degassed water around the scalp. The system is moved into the bore of the MRI scanner. B: The blue circle represents the treatment plan for the first sonication to be made in the middle of the IVH. The green circle in (B) represents the treatment envelope which can be moved by moving the transducer. C: Pre and D: Post sagittal T2 weighted MR imaging demonstrating lysis of the intraventricular hemorrhage after the sonication process.

12-BR

Monday
15 October 2012

Topic: Brain
Presentation type: Oral

Enhanced Delivery of Liposomal Doxorubicin via Permeabilization of the Blood-Brain/Blood-Tumor Barriers Using Focused Ultrasound and Microbubbles Significantly Improves Survival in a Rat Glioma Model after Multiple Treatments

Muna Aryal[1], Yong-Zhi Zhang[2], Natalia Vykhodtseva[2], Juyoung Park[2], Nathan McDannold[2]

[1]Brigham & Women's Hospital, Boston, Massachusetts, United States
[2]Brigham & Women's Hospital/Harvard Medical School, Boston, Massachusetts, United States

Background/Introduction: The blood-brain barrier (BBB) prevents effective drug delivery to infiltrating tumor cells. Furthermore, although blood vessels in most brain tumors are leaky, heterogeneous permeability and other factors limit the effective delivery of drugs across the tumor vasculature. Focused ultrasound (FUS) combined with microbubbles can temporary disrupt the BBB and enhance the permeability of the "blood-tumor barrier" (BTB). Previous work by our group demonstrated that a single treatment with FUS and liposomal doxorubicin (DOX) can slow tumor growth and produce a modest improvement in survival in a rat glioma model. Here, we tested whether multiple sessions, like a patient might receive, can enhance the effectiveness of the treatment.

Methods: Tests were performed using the 9L rat gliosarcoma model. Seven days before treatment, 105 cells were injected into the right frontal lobe of the brain. Rats were randomly divided into four treatment groups: Control (no treatment; N=7), FUS-Only (N=8), DOX-Only (N=6) and FUS+DOX (N=8). The animals were treated in three weekly sessions. Sonications (0.69 MHz; 0.55-0.81MPa; 10ms bursts at 1Hz for 60s) were combined with Definity® (10µl/kg) and delivered in a grid to cover the tumor and a surrounding rim of brain tissue. The procedure was done under MRI guidance within a 3T MRI (GE). Contrast-enhanced T1-weighted images were taken before and after sonication to evaluate the BBB/BTB enhanced permeabilization. T2*-weighted imaging was used to detect vascular damage (petechaie), and T2-weighted imaging was used to evaluate tumor dimensions. Animals were monitored weekly with MRI after treatment. Animals were sacrificed when tumors dimensions exceeded 10-11 mm or when declining health was observed, based on pre-defined criteria

Results and Conclusions: In the animals in the Control and FUS-only groups, the tumors grew rapidly, reaching their maximum size at 15-21 days after implantation; animals were sacrificed shortly afterwards. No animal in these groups survived for the third treatment. The median survival time for these two groups was 18 days. Tumor growth in DOX-only animals was also rapid; only two animals received the third treatment. The median survival time was 21 days, a 17% improvement compared to the Control group. However, this improvement was not significant (p: 0.287). In contrast, tumor growth in the FUS+DOX group was slower than in the three other groups, and all animals received three treatments. Tumors were observed to shrink after the third treatment, and appeared to be completely resolved in histology in 5/8 animals. Median survival was 46 days, which was significantly ($P<0.001$) longer than the other groups. This was a 156% improvement compared to the controls. Depending on maximum tumor size, tissue scar, necrosis with macrophage infiltration, or fluid-filled regions were evident in the region where the tumors were previously. Adverse events in the FUS+DOX group included skin infection (3 animals), tissue loss or scarring at the tumor site, damage (infarct) in neighboring tissue, and in one animal, hemorrhage. However, we could not determine whether these effects were due to the FUS effects, the chemotherapy, or to the effects of the tumor itself, which in some cases reached a substantial volume before it began to resolve.

Conclusions: Overall, this work demonstrates that multiple DOX treatments enhanced by FUS-mediated BTB/BBB permeabilization can effectively inhibit tumor growth and significantly improve survival in this aggressive rat glioma model.

Acknowledgements (Funding): NIH: P41EB015898, P41RR019703, R01EB003268 , Gift from Brudnick family.

13-BR

Monday
15 October 2012

Topic: Brain
Presentation type: Oral

Activation of Signaling Pathways Following Localized Delivery of Systemically-Administered Neurotrophic Factors across the Blood-Brain Barrier Using Focused Ultrasound and Microbubbles

Babak Baseri, James Choi, Thomas Deffieux, Gesthimani Samiotaki, Yao-Sheng Tung, Scott Small, Barclay Morrison, Elisa Konofagou

Columbia University, New York, New York, United States

Background/Introduction: Neurotrophic factorshave been shown to have broad neuroprotective effects in addition to its therapeutic role in neurodegenerative disease. In this study, the efficacy of delivering exogenous BDNF, GDNF and NTN to the left hippocampus was assessed in wild-type mice through the noninvasively disrupted blood-brain barrier (BBB) using FUS and microbubbles.

Methods: A total of 20 C57Bl6 male mice were used for this study. A single-element spherical segment FUS transducer (center frequency: 1.525 MHz; focal depth: 90 mm) was driven by a function generator (Agilent Technologies) through a 50-dB power amplifier (ENI) to generate therapeutic ultrasound waves (Choi et al., 2007b). A pulse-echo transducer (center frequency: 7.5 MHz; focal length 60 mm) was positioned through a center hole of the FUS transducer so that the foci of the two transducers were aligned. It was driven by a pulser-receiver system (Panametrics) connected to a digitizer (Gage Applied Technologies) and was used for imaging. Definity® microbubbles were injected intravenously prior to sonication (peak-rarefactional pressure: 0.46 MPa; pulse repetition frequency: 10 Hz; pulse length: 20 ms). Each of the four target locations was sonicated twice, resulting in a total of 8 sets of 30s sonication with a 30s delay between each set. Three different neurotrophic factors, the Brain-Derived Neurotrophic Factor (BDNF) (40-90mg/kg in 0.15 ml PBS, n=8), the Glia-Derived Neurotrophic Factor (GDNF) (40-90mg/kg in 0.15 ml PBS, n=10) (20mg/kg in 0.2 ml PBS, n=2) and Neurturin (NTN) were conjugated to Alexa Fluor® 594 dye (Invitrogen Corp, Carlsbad, CA, USA) and injected intravenously prior to FUS. Upon sacrifice, fluorescence imaging and immunohistochemistry were performed to confirm molecular diffusion and triggered downstream effects, respectively.

Results and Conclusions: Both the BDNF and NTN were found to have significantly higher fluorescence in the sonicated hippocampus and putamen, respectively. The GDNF, however, was found not to cause any fluorescence in the sonicated region, as the GDNF was found to be rapidly broken down in circulation (within the first 45 s). The BDNF bioactivity was found to be preserved following delivery as assessed quantitatively by immunohistochemical detection of the pTrkB receptor and activated pAkt, pMAPK, and pCREB in the hippocampal neurons. Neurturin behaved similarly to BDNF permeating through the opened barrier and into the parenchyma); however, GDNF did not. It was therefore shown for the first time that systemically administered neurotrophic factors can cross the noninvasively disrupted BBB and trigger neuronal downstream signaling effects in a highly localized region in the brain but also that not all factors when administered systemically will successfully cross the opened BBB.

Acknowledgements (Funding): This study was supported in part by NIH R01EB009041, NIH R01AG038961 and the Kinetics foundation.

14-BR

Monday
15 October 2012

Topic: Brain
Presentation type: Oral

Microbubble-Enhanced Focused Ultrasound Blood-Brain Barrier Opening in Non-Human Primates: Targeting Accuracy and Closing Timeline

Fabrice Marquet, Yao-Sheng Tung, Tobias Teichert, Shih-Ying Wu, Shutao Wang, Matthew Downs, Vincent Ferrera, Elisa Konofagou

Columbia University, New York, New York, United States

Background/Introduction: The blood-brain barrier (BBB) is a selective barrier within the neurovascular unit formed by the endothelial cells that line the cerebral microvessels. The BBB hinders the effective systemic delivery to the brain of more than 98% of small molecule drugs and nearly all large molecule drugs. Previously, our group has shown initial feasibility of transcranial microbubble-enhanced focused ultrasound (FUS) BBB opening in non-human primates with a single-element transducer, operating at intermediate frequencies in order to solve the tradeoff between high aberrations (at higher frequencies) and low inertial cavitation threshold (at lower frequencies). In this study, the targeting precision and BBB recovery timeline were investigated.

Methods: A 500-kHz FUS transducer was used transcranially in Macaca Mulatta monkeys. This transducer was mounted on a stereotaxic frame enabling treatment planning using the brain atlas. In vivo experiments were conducted in 5 monkeys using Definity® or 4-5 μm, custom-made, lipid-shelled, microbubbles. The BBB opening was confirmed using T1-weighted, spoiled gradient pulse-echo MR sequence at 3T and gadodiamide IV injection. Damage was assessed using a T2 sequence with the same system. To obtain the BBB closing timeline, the T1-weighted MR sequence was repeated along with gadodiamide IV injection over four days. MR images were registered to a monkey brain atlas allowing targeting quality assessment. Post-processing was performed on combined pre and post-contrast agent T1 images to quantify BBB disruption at the targeted regions, i.e., caudate, hippocampus and visual cortex.

Results and Conclusions: BBB opening was achieved in six different animals using peak negative pressures ranging from 0.2 MPa to 0.6 MPa. No damage was detected at pressures below 0.45 MPa. The actual BBB-opened location was found to be in very good agreement with the targeted one under close to normal incidence angles with the absolute targeting error being less than 1 mm laterally and less than 6 mm axially. Initial findings on the closing timeline showed that the BBB was fully restored within two days after treatment at the pressures used.

This feasibility study demonstrated the capability of accurately targeting different brain regions with off-line MRI transdermally and transcranially in monkeys, i.e., without requiring simultaneous MRI. BBB closing occurred two days following treatment. This could prove as a major step in translating the FUS system developed to clinical applications.

Acknowledgements (Funding): This study was supported in part by NIH R01EB009041, NIH R01AG038961, NIH MH059244, and the Kavli Institute.

LD

Monday
15 October 2012

Topic: Uterine Fibroid
Presentation type:
Discussion

The Realities of a Payer Environment

Brent O'Connell

Argenta Advisors, Woodbury, Minnesota, United States

Background/Introduction: Dr. O'Connell will discuss the important role that payers play in making decisions that affect the reimbursement and adoption of new medical technologies. He will talk about the expectations payers have for evidence to support new treatments. He will share insights into the reimbursement challenges for focused ultrasound treatment of uterine fibroids, the impact of these challenges on future uses and what can be done to improve the outlook for broad reimbursement and access to focused ultrasound.

15-LD

Monday
15 October 2012

Topic: Brain
Presentation Type:
Discussion

MRI as an Alternative to CT to Assess Skull Geometry and Plan Refocusing in MR-Guided Focused Ultrasound (MRgFUS)

Max Wintermark[1], Alan Cupino[1], Ben Lau[1], Nick Demartini[1], John Snell[2], Neal Kassell[1], Nick Tustison[1]

[1]University of Virginia, Charlottesville, Virginia, United States
[2]Focused Ultrasound Foundation, Charlottesville, Virginia, United States

Background/Introduction: Presently, thin-slice CT of the skull is required to collect the information necessary to planning the transcranial MRgFUS refocusing. This information includes thickness of the skull, average CT density of the skull, and thickness of the inner and outer table and of the diploe. However, for a number of conditions that could benefit from MRgFUS treatment, such as stroke, the necessity of obtaining a CT of the skull prior to the MRgFUS represents a significant loss of time and a severe drawback, and being able not skip the CT and obtaining the information required for refocusing from an MRI scan would greatly benefit the patients. Also, more generally, patients may move during the course of a MRgFUS treatment, and it may be helpful to be able to rescan the patient and re-plan the refocusing during the course of the MRgFUS treatment (where registration with the skull CT may be less practical or less accurate).

The purpose of our study was to determine if there is an MRI sequence that matches CT in terms of measuring thickness of the skull, average density of the skull, and thickness of the inner and outer table and of the diploe; and to optimize this sequence.

Methods: In 15 patients prospectively enrolled in this study, we obtained T1, proton-density and T2-wieghted imaging, in addition to thin-slice CT. MRI datasets were registered to CT, and automated computer processing was used to calculate the parameters of interest for this study. Bland-Altman analysis was used to compare skull thickness derived from CT and MRI, and to compare the skull layer thicknesses derived from CT and MRI. The best MRI sequence was then analyzed to find the relationship between CT skull density and MRI skull intensity.

Results and Conclusions: The MRI sequence that yielded similar measurements to CT in terms of measuring skull thickness and skull layer thickness was T1-weighted imaging (Table 1). A formula could be developed that allowed to establish an equivalence between CT density and MRI T1 intensity measurements.

Table 1. Bland Altman measurement agreement summary.

Thickness	Mean Discrepancy			Mean – 2 SD			Mean + 2 SD		
Measure	Estimate	Lower 95% CL	Upper 95% CL	Estimate	Lower 95% CL	Upper 95% CL	Estimate	Lower 95% CL	Upper 95% CL
T1	0.025	-0.224	0.275	-2.685	-2.741	-2.631	2.735	2.681	2.791
T2	-0.049	-0.238	0.140	-3.249	-3.315	-3.185	3.151	3.087	3.217
PD	1.726	1.288	2.164	-2.716	-2.808	-2.628	6.168	6.080	6.260

In conclusion, MRI T1-weighted imaging can be used as a substitute to CT to measure skull thickness, skull layer thickness and skull intensity. Treatment simulations using CT and MRI is required to further validate this statement.

Acknowledgements (Funding): This project was supported by a grant from the Focused Ultrasound Foundation.

16-LD

Monday
15 October 2012

Topic: Brain
Presentation Type:
Discussion

Model Predictive Filtering for Large Coverage 3D Imaging of Transcranial MRgFUS Procedures

Nick Todd[1], Henrik Odeen[1], Joshua de Bever[1], Allison Payne[2], Scott Almquist[1], Douglas Christensen[1], Dennis Parker[1]

[1]University of Utah, Salt Lake City, Utah, United States
[2]Utah Center for Advanced Imaging Research at University of Utah, Salt Lake City, Utah, United States

Background/Introduction: Transcranial MR-guided focused ultrasound surgery (MRgFUS) procedures hold the potential to non-invasively treat a number of neurologic disorders. Full coverage monitoring over the entire acoustic window is desirable due to the critical nature of the tissue and the potential for inadvertent heating at tissue/bone interfaces. This work proposes to obtain MR temperature maps with the requisite spatial and temporal resolution and large 3D volume coverage using the model predictive filtering approach that combines thermal model predictions with acquired data in real time.

Methods: Model Predictive Filtering (MPF) algorithm. The MPF reconstruction algorithm uses a site-specific model of the tissue's thermal response based on the Pennes bioheat equation with parameters identified before the treatment using a low power sonication. The algorithm recursively combines the model predictions with the undersampled acquired data by: 1) forward predicting the temperature distribution from time n to n+1; 2) creating a complex image for time n+1 by transforming the predicted temperatures into phase and using magnitude from time n; 3) projecting this predicted image into k-space; 4) inserting the undersampled k-space data acquired at time n+1 and projecting back into image space to create an updated temperature map for time n+1.

HIFU heating experiments were carried out on a phantom with a plastic skull model embedded in an agar mold with an ex vivo pork muscle sample at the focus (Figure 1). Phase aberration correction was performed to improve focusing through the skull. Imaging was done with a 3D segmented EPI sequence with parameters: 1.25 x 1.25 x 4.0mm, 192 x 135 in-plane imaging matrix, TR/TE = 25/11 ms, EPI Factor = 9, bandwidth = 652 Hz/pixel. For model parameter determination, 10 slices of fully sampled data were acquired (4.5 s/scan) during HIFU sonication of 51W for 30 sec. For testing the MPF algorithm, 20 slices with 5.5X data undersampling were acquired (1.2 s/image) during HIFU sonication with a higher power of 75W for 30 sec.

Figure 1. Experimental set up showing the plastic skull embedded in an agar mold. The target is ex vivo pork muscle.

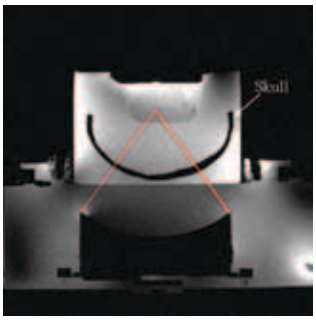

Results and Conclusions: Three orthogonal slices through the 3D volume of the MPF reconstructed temperatures for the higher power exposure are shown in Figure 2. The temperature evolution predicted by the model is shown in Figure 3A. The red curve in Figure 3B shows the MPF reconstruction of the undersampled data. The black curve shows a sliding window reconstruction of the same data, where temporal averaging effects can be seen.

The MPF algorithm is able to provide 3D temperature maps in real-time. The achieved parameters of 1.25 x 1.25 x 4.0mm spatial resolution and 1.2 s/image temporal resolution should be adequate for monitoring heating at the focus. The volume coverage of 240 x 169 x 80 mm, while a significant improvement over multi-slice 2D imaging, is not quite large enough to cover the entire region of interest in the brain and skull. Future work will validate and compare the MPF approach against fiber optic temperature measurements and other 3D imaging approaches.

Figure 2. Transverse, sagittal, and coronal slices through the 3D MPF temperature volume.

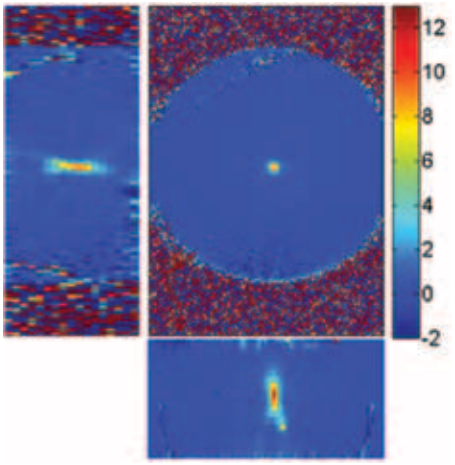

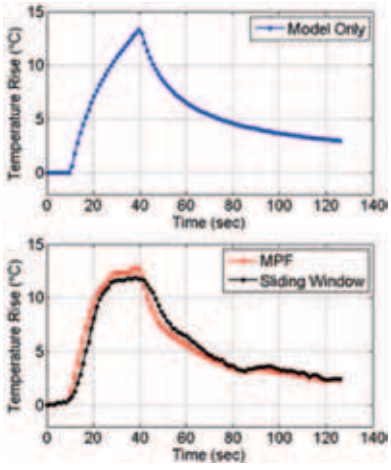

Acknowledgements (Funding): This work is supported by Siemens Medical Solutions, The Focused Ultrasound Foundation, The Ben B. and Iris M. Margolis Foundation, and NIH grants R01s CA87785, EB013433, and CA134599.

Figure 3. A) Temperature evolution predicted by the model only. B) MPF and sliding window reconstructions of the undersampled data.

17-LD

Monday
15 October 2012

Topic: Brain
Presentation Type:
Discussion

Combined MRI and US Guided Focused Ultrasound in the Brain

Costas Arvanitis[1], Margaret Livingstone[2], Nathan McDannold[1]

[1]Brigham and Women's Hospital/Harvard Medical School, Boston, Massachusetts, United States
[2]Harvard Medical School, Boston, Massachusetts, United States

Background/Introduction: Several promising therapeutic approaches harness thermal and/or mechanical effects of focused ultrasound (FUS), each of which have specific needs for monitoring and control. Here we present a dual modality approach (MRI and US), which allow us to assess FUS-induced effects with high spatiotemporal accuracy. The integrated system was tested in phantom and animal experiments during transcranial sonications.

Methods: The MRI and US imaging-guided FUS system (MR&USgFUS) utilized a 128-element (82 mm) linear US array (central frequency: 3.5 MHz) and a clinical 3T MRI (GE) to guide microbubble-enhanced sonications with an FUS system (ExAblate® 4000, InSightec) developed for brain surgery. This device is a 30 cm hemisphere 1024-channel, 220 kHz phased array. The linear US imaging array was connected to a research US imaging engine (Verasonics) through the MR penetration panel and operated in passive mode. Experiments were first performed in an ex vivo macaque skull filled with tissue-mimicking phantom that contained a vessel-mimicking tube (D=1.8 mm), where stabilized microbubbles (Definity®) could flow. The channel was sonicated at powers just above and below the inertial cavitation threshold of the microbubbles. The cavitation maps formed from the recorded acoustic emissions were co-registered with MR images acquired before sonication using fiducial markers. The experiments were repeated at different pressure amplitudes in two macaques. The reconstructed cavitation maps were co-registered with MRI (contrast-enhanced T1-weighted and T2* weighted images), acquired after the sonications, that depict blood brain barrier disruption and petechaie produced during inertial cavitation. Real-time assessment of the spectral content of the acoustic emissions was used to guide the procedure.

Results and Conclusions: Without microbubbles, no activity was observed in the cavitation maps. With the ex vivo skull, good co-localization between the microbubble-filled channel and the cavitation maps was observed in the presence of strong (SNR>20 at the 3rd harmonic of the FUS device) nonlinear terms (harmonic, ultraharmonic and broadband) in the acoustic emissions. These data indicated that aberration introduced by the thin monkey skull was minor. During the in vivo macaque experiments good co-localization between the MR contrast enhancement and cavitation activity was observed when strong harmonic emissions were recorded (SNR>20 at the 3rd harmonic) during sonication with microbubbles. At these sonications (N=3) higher harmonics (10th) and weak broadband emissions (SNR≈5) were also recorded. The localization precision in the transverse and axial direction of the US probe was 0.8±0.2 mm and 2.8±2.2 mm respectively. When broadband signal was recorded, cavitation activity was also co-localized with faint hypointense spots in T2* weighted images. When weak harmonics (SNR≈5 at the 3rd harmonic) were recorded, the origin of the emissions could not be established.

In conclusion, these preliminary data demonstrate that localization of cavitation activity can be achieved transcranially in vivo within an MRgFUS system. Strong nonlinear acoustic emissions at higher US frequencies improve the localization of cavitation activity. This is a very promising approach to improve guidance of cavitation-based therapies and provides a means to depict the mechanical effects of FUS simultaneously with MRI-derived information.

Acknowledgements (Funding): This work was supported by award numbers R25 CA089017 and RC2NS069413

18-LD

Monday
15 October 2012

Topic: Brain
Presentation Type:
Discussion

Towards Experimental Validation of MR-ARFI Aberration Tomography

William Grissom[1], Alexander Volovick[2], Elena Kaye[3], Kim Butts Pauly[3], Yuval Zur[4], Desmond Yeo[4], Yoav Medan[5], Cynthia Davis[4]

[1]Vanderbilt University, Nashville, Tennessee, United States
[2]InSightec, Tirat Carmel, Israel
[3]Stanford University, Stanford, California, United States
[4]GE Healthcare, Haifa, Israel
[5]Technion Isreal Institute of Technology, Haifa, Israel

Background/Introduction: Phase aberrations and attenuations caused by bone can prevent the application of HIFU in the brain. Using MR-ARFI1, the field can be refocused by measuring the relative tissue displacement that each transducer element produces2-4. We recently presented an autofocusing method called MR-ARFI Aberration Tomography, which uses the entire MR-ARFI image to determine the aberrations, dramatically reducing the number of image acquisitions required compared to other methods that use only the voxel at the center of the focus5. Here we present progress towards experimentally validating our method, in the form of simulations using MR-ARFI-measured HIFU pressure fields of a brain transducer.

Methods: It is assumed in our method that the pressure field in and around the focus is equal to the complex sum of the fields produced by the transducer elements, which are phase-shifted and attenuated by aberrations. A magnitude least-squares method6 is used to solve for the aberrations, given MR-ARFI images of the aberrated focus and a matrix of unaberrated complex fields for each transducer element. The matrix is constructed offline using MR-ARFI acquisitions or simulations of a phantom or tissue sample. Relative phases of the elements' pressure fields are measured using an interference method4.

To validate MR-ARFI Aberration Tomography, the pressure fields of 4 logical elements (each comprising 64 physical elements) synthesized from a 680 kHz Insightec ExAblate® Neuro HIFU transducer (Insightec Ltd., Haifa, Israel) were measured in a 1.5 T GE Scanner (GE Healthcare, Waukesha, WI) using EPI MR-ARFI in a plane parallel to the transducer face (1.2 x 1.2 mm res) (Figures 1 and 2). Random phases ([0, 3.10 2.33, -2.90] rad) were applied to the measured fields, and simulated aberrated MR-ARFI measurements were synthesized both for MR-ARFI Aberration Tomography (1 measurement) and the Conjugate Green's method4 (13 measurements). The two methods were then applied to refocus the array.

Results and Conclusions: Figure 3 shows that both methods refocused the array, but MR-ARFI Aberration Tomography enabled refocusing to within machine error, and required only one MR-ARFI acquisition, while 13 were required for the Conjugate Green's method.

We have demonstrated MR-ARFI Aberration Tomography in a simulation using pressure fields of an actual HIFU transducer measured using MR-ARFI. Full experimental validation is forthcoming, in which both known (programmed) aberrations, and unknown aberrations (from bone or other physical aberrators) will be applied and estimated by the method. In practice, MR-ARFI Aberration Tomography will require only a small number of image acquisitions, which will enable autofocusing in a clinically-feasible time.

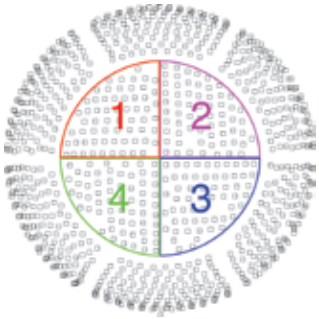

Logical element grouping, looking top-down at transducer.

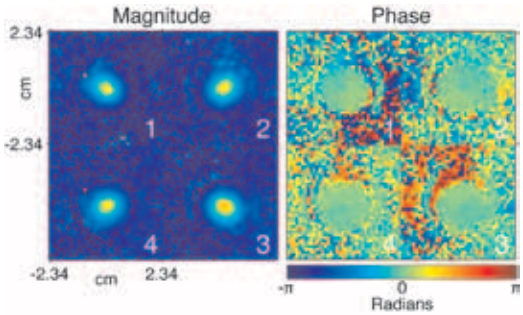

Measured (complex-valued) pressure fields for the logical elements.

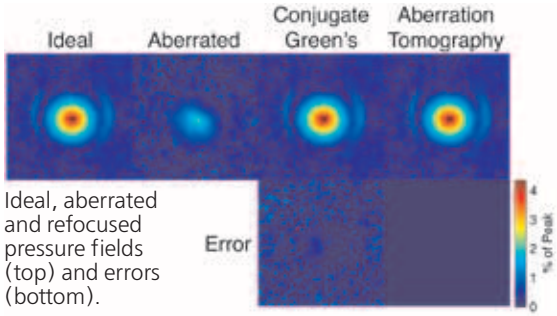

Ideal, aberrated and refocused pressure fields (top) and errors (bottom).

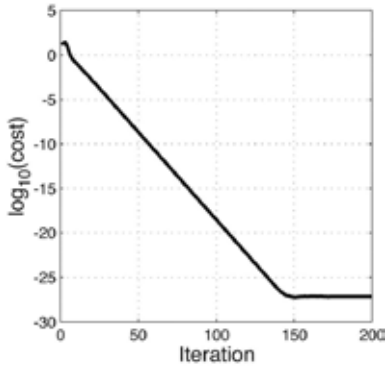

The MR-ARFI Aberration Tomography algorithm converges linearly.

References:

1. N McDannold et al. *Med Phys,* 2008.
2. M W Urban et al. *IEEE Trans UFFC,* 2007.
3. Y Hertzberg et al. *Med Phys*, 2010.
4. B Larrat et al. *IEEE Trans UFFC,* 2010.
5. W A Grissom et al. *ISTU* 2012.
6. P W Kassakian, PhD Thesis, UC Berkeley, 2006.

19-UF

Monday
15 October 2012

Topic: Uterine Fibroids
Presentation Type: Oral

Mri-Guided Focused Ultrasound Treatment of Symptomatic Uterine Fibroids: Impact of Technology Advancement on Ablation Volumes in 115 Patients

Christoph Trumm[1], Matthias Matzko[2], Maximilian Reiser[1]

[1]University of Munich, Munich, Germany
[2]Amper Kliniken AG, Dachau, Germany

Background/Introduction: To assess the impact of the advancement of MRI-guided focused ultrasound technology on treatment outcomes in patients with symptomatic uterine fibroids, as measured by the non-perfused volume ratio.

Methods: This is a retrospective analysis of 115 women (average age, 42 years; range 27 to 54 years) with symptomatic fibroids who consecutively underwent MRI-guided focused ultrasound treatment in a single center with the new generation ExAblate® 2100 system (Insightec Ltd., Haifa, Israel) from November 2010 to June 2011. Average total volume and number of the treated fibroids (per patient) were 89 ± 94 (SD) cm3 and 2.2 ± 1.7, respectively. Patient baseline characteristics were analyzed regarding their impact on the resulting non-perfused volume ratio.

Results: MRI-guided focused ultrasound treatment was technically successful in 115 of 123 patients (93.5%). In 8 patients treatment was not possible due to bowel loops in the beam pathway that could not be mitigated (n=6), patient movement (n=1) and system malfunction (n=1). Average non-perfused volume ratio was 88 ± 15% (range, 38 to 100). Mean applied energy level was 5400 ± 1200J, and mean number of sonications was 74 ± 27. No major complications occurred. Two cases of first degree skin burn resolved within one week after the intervention. Of the baseline characteristics analyzed, only the planned treatment volume had a statistically significant impact on the non-perfused volume ratio.

Conclusion: With technological advancement, outcome of MRI-guided focused ultrasound treatment in terms of the non-perfused volume ratio can be enhanced with a high safety profile, markedly exceeding results reported in previous clinical trials.

20-UF

Monday
15 October 2012

Topic: Uterine Fibroids
Presentation Type: Oral

Complete or Near-complete Ablation of Symptomatic Uterine Fibroids by Volumetric MR-guided High-intensity Focused Ultrasound Therapy: Assessments of Safety and Therapeutic Efficacy

Min Jung Park[1], Young-sun Kim[1], Bilgin Keserci[2], Hyunchul Rhim[1], Hyo Keun Lim[1]

[1]Samsung Medical Center, Seoul, South Korea
[2]Philips Healthcare, Seoul, South Korea

Background/Introduction: In the decision to treat the extent or intensity of MR-guided high-intensity focused ultrasound (MR-HIFU) ablation of uterine fibroids, the balance between therapeutic efficacy and safety is important. The current guideline, for instance, the FDA guideline which limits the treatment volume of fibroids to only 50% of the fibroid volume or 150cm^3, appears to lean more toward the safety aspect than therapeutic efficacy. On the other hand, therapeutic outcomes are known to be closely related to immediate non-perfused volume (NPV) ratio. Considering this, the current guideline may be too conservative, and consequently result in limited therapeutic efficacy. Therefore, the aim of this study was to evaluate the safety and therapeutic efficacy of cases with complete or near complete ablation (i.e., immediate NPV ratio≥80%) in MR-HIFU ablation of symptomatic uterine fibroids, as compared to cases with lower NPV ratios.

Methods: This study received institutional review board approval and we obtained informed consent for the procedure from all subjects. A total of 79 women (mean age, 43.4) with 117 uterine fibroids (volume, 396.6±316.3mL) were treated with volumetric MR-HIFU ablation (Sonalleve MR-HIFU Fibroid Therapy System, Philips Healthcare). We assessed immediate NPV, therapeutic efficacy (fibroid volume reduction ratio and symptom severity score [SSS] decrease at 3-month follow-up), and complications. Statistical comparisons of therapeutic efficacy and complication rate were performed between patients with an NPV ratio≥80% and patients with an NPV ratio<80% using chi-square test, Fisher exact test, or Mann-Whitney test.

Results and Conclusions: Technical success was achieved in 93.7%(74/79) of cases, and the immediate NPV ratio was 62.7±25.5%. Twenty-four patients showed NPV ratio≥80% (89.7±8.8%), and 50 patients showed NPV ratio<80% (49.8±20.7%). All complications were minor in severity and the incidences were not significantly different between the groups with NPV ratio≥80% (12.5%, 3/24) or <80% (22.0%, 11/50) (p=0.527). Among the 74 patients analyzed, 3-month follow-up data were available in 55 patients. At the 3-month follow-up MR, mean fibroid volume decreased significantly to 290.9±234.9mL (p<0.001), corresponding to a volume reduction ratio of 0.74±0.27. SSS was also significantly decreased to 26.9±12.8 (p<0.001). The 3-month volume reduction ratio was significantly superior in the patients with NPV ratio≥80% (0.58±0.18) as compared to those with NPV ratio<80% (0.80±0.27) (p=0.010), although SSS decreases were not significantly different (p=0.188).

In conclusion, in MR-HIFU ablation of symptomatic uterine fibroids, the achievement of immediate NPV ratio ≥80% is safe, and results in superior therapeutic efficacy compared to cases with a smaller NPV ratio. Therefore, as long as the safety is secured, we should try to achieve as large a NPV as possible to produce better therapeutic outcomes.

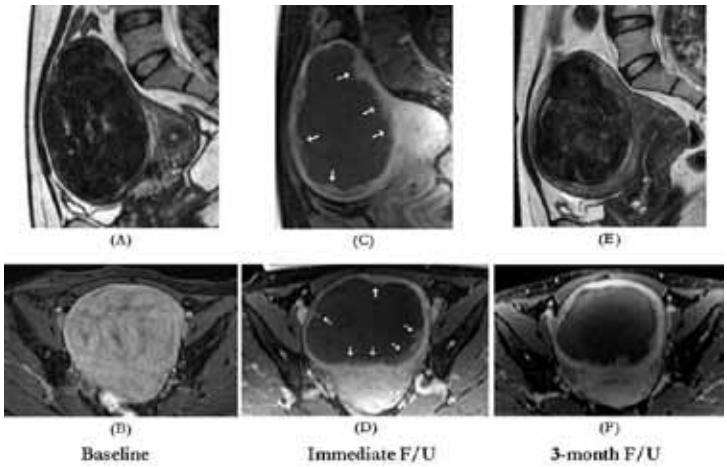

A 43-year-old woman with uterine fibroids who complained of urinary frequency was treated with volumetric MR-HIFU ablation. A, B. The baseline sagittal T2-weighted MR image (A) showed a large intramural uterine fibroid (maximal diameter, 13.0 cm; volume, 643.5 mL), and axial contrast-enhanced T1-weighted image (B) demonstrated diffuse enhancement. C, D. Sagittal (C) and axial (D) contrast-enhanced T1-weighted images taken immediately after MR-HIFU therapy, which demonstrated near complete ablation with minimal residual contrast enhancement in the periphery (arrows). NPV was quantified as 569.8 mL, therefore, NPV ratio was 88.5% of the fibroid volume. There was no procedure-related complication noted. E, F. Three-month follow-up MR images demonstrated obvious volume shrinkage of the fibroid.

	All patients (n=74)	NPV ratio ≥80% (n=24)	NPV ratio <80% (n=50)	*p-value**
Occurrence of complications	14 (19)	3 (13)	11 (22)	0.527
Thermal injury of the abdominal wall	9 (12)	1 (4)	8 (16)	0.256
First degree skin burn	2 (3)	1 (4)	1 (2)	0.546
Foley catheterization-related cystitis	2 (3)	1 (4)	1 (2)	0.546
Temporary sciatic nerve injury	1 (1)	0 (0)	1 (2)	1.000
	All patients (n=55)	**NPV ratio ≥80% (n=15)**	**NPV ratio <80% (n=40)**	***p-value†***
Fibroid volume, baseline (mL)	376.3±235.0 (32.6-1145.0)	375.3±213.5 (32.6-683.0)	376.6±244.4 (52.0-1145.0)	0.841
Fibroid volume, 3-month (mL)	290.9±234.9 (11.3-1130.0)	225.6±153.2 (11.3-529.6)	312.7±254.4 (27.4-1130.0)	0.416
Fibroid volume reduction ratio	0.74±0.27 (0.33-1.88)	0.58±0.18 (0.33-0.82)	0.80±0.27 (0.39-1.88)	0.010‡
SSS, baseline	43.2±15.7 (12.5-81.3)	42.8±20.9 (12.5-81.3)	43.4±13.3 (21.9-71.9)	0.975
SSS, 3-month	26.9±12.8 (6.3-53.1)	29.2±17.4 (6.3-53.1)	26.2±11.0 (6.3-50.0)	0.636
SSS decrease	13.2±9.8 (-6.3-34.4)	12.2±8.8 (-3.1-31.3)	13.6±10.4 (-6.3-34.4)	0.527

Table 1. Comparisons of Complication Incidences and Therapeutic Efficacies According to Immediate NPV Ratio of 80%. Note: Values represent number of patients, with percentages in parentheses (for complications) or meanÂ±standard deviation, with in ranges in parentheses (for fibroid volume and SSS); * Fisher's exact test; † Mann-Whitney test; ‡ Statistically significant; NPV: non-perfused volume, SSS: symptom severity score

21-UF

Monday
15 October 2012

Topic: Uterine Fibroids
Presentation Type: Oral

Follow Up of 140 Patients Treated from 2005 to 2011 with MRgFUS for Symptomatic Uterine Fibroids

Gina Hesley, Krzysztof Gorny, Bijan Borah, Elizabeth Stewart, David Woodrum, Douglas Brown

Mayo Clinic, Rochester, Minnesota, United States

Background/Introduction: ExAblate® 2000 was approved for use in the United States in October 2004 for the treatment of symptomatic uterine fibroids. Comparison of the outcomes of patients has been made to other uterine sparing procedures including uterine artery embolization and myomectomy. However, little data exists on outcomes of patients more than 2-years out from treatment.

Methods: This study describes the results of a retrospective review of patients treated with MRgFUS at a single institution for symptomatic fibroids. The treatments were performed between March, 2005 and June of 2011, and the follow-up ranged between one and seven years. The patient data and pre-treatment MR findings were reviewed and analyzed to identify factors that correlate with the need for subsequent further intervention due to lack of resolution of fibroid symptoms or recurrent symptoms.

Results: 140 patients with at least one year of follow up were evaluated. The range of the follow up varied between 1 and 7 years (median, 3 years; average, 2.7±1.7 years). During their follow up 105 patients did not seek further intervention for fibroid related symptoms; with the remaining 35 patients having further intervention (5 of these patients had uterine intervention unrelated to continued or recurrent symptoms).

We find statistically significant differences between groups of patients who did not need further intervention versus those who did. In the group of patients who did not require further intervention, age at time of treatment was higher (46+/-5 vs 43+/-6 years, $p=0.003$), ablated volume was more confluent ($p=0.004$), and the T2 signal intensity of the dominant fibroid was on average lower ($p=0.011$ for homogeneously dark and $p=0.006$ for mildly heterogeneous fibroids).

Conclusion: 22% of patients followed for 1 to 7 years after MRgFUS treatment had further intervention for persistent or recurrent fibroid symptoms. Older patient age, higher confluence of ablated area, and T2 signal intensity of dominant fibroid correlated with treatment success (defined as lack of further intervention).

Acknowledgements (Funding): Investigator time was funded by NIH HD RC1063312 and R01060503

22-UF

Monday
15 October 2012

Topic: Uterine Fibroids
Presentation Type: Oral

MR Guided Focused Ultrasound for Uterine Fibroids: A Pilot Randomized, Placebo-Controlled Trial

Vanessa Jacoby, Alison Jacoby, Maureen Kohi, Viola Rieke, Antonio Westphalen, Fergus Coakley

University of California at San Francisco, San Francisco, California, United States

Background/Introduction: MRgFUS is in limited use to treat symptomatic fibroids because third party payers are reluctant to reimburse without outcome data from randomized controlled trials. We undertook this pilot study to determine the feasibility of conducting a randomized, placebo-controlled trial of MRgFUS for women with symptomatic fibroids with the ultimate goal of completing a larger, definitive trial to demonstrate safety and efficacy.

Methods: Twenty premenopausal women with symptomatic fibroids were randomly assigned in a 2:1 ratio to undergo actual MRgFUS or a placebo MRgFUS. All participants were similarly prepared with abdominal shaving, intravenous sedation, Foley catheter placement, and preliminary MRI imaging and treatment planning. The treating radiologist then opened an envelope with the random group assignment and performed either actual MRg-FUS or a placebo procedure of matched duration with performance of intermittent MR thermometry only. Three months after the study procedure, participants were unblinded to their group assignment and women in the placebo group were invited to undergo an actual MRgFUS procedure. Study outcomes were change over 3 months in fibroid symptoms and quality of life using the UFS-QOL questionnaire, fibroid volume and nonperfused volume ratio at MRI, and hemoglobin/hematocrit level. With 20 participants, there is 80% power to detect at least a 18 point difference between groups in the UFS-QOL questionnaire 3 months after the intervention.

Results and Conclusions: Over one year of recruitment beginning in June 2011, 341 women were screened to participate in the trial; 297 (87%) were ineligible to participate, 6 (2%) declined to participate, and 35 (10%) were invited to attend a baseline screening visit to undergo a pelvic MRI and medical evaluation. Among women who completed this screening visit, 15 (43%) were excluded because they did not meet full enrollment criteria; 10 of these women had fibroids that were not amenable to MRgFUS. The 20 participants were racially and ethnically diverse (55% white, 25% black, 15% Asian, 5% Latina) with a mean age of 44+5 years. The mean uterine volume was 533 + 184cc and the mean volume of treatable fibroids was 198 + 113cc. One randomized participant could not be treated due to unfavorable bowel location on the day of treatment, despite a screening MRI with favorable anatomy. The other 19 participants completed the study treatment without complication. We will have complete study data with all 3 month follow-up outcomes by September 2012 to present at the FUS Foundation Symposium.

Conclusions: Women with symptomatic uterine fibroids, including women from under-represented minority groups, can be successfully recruited into a randomized, placebo-controlled trial of MRg-FUS.

Acknowledgements (Funding): This study was funded by the NIH K12 Women's Reproductive Health Research Career Development Program, the UCSF Resource Allocation Program, and the UCSF Radiology Seed Grant Program.

23-UF

Monday
15 October 2012

Topic: Uterine Fibroids
Presentation Type: Oral

Pregnancies after Magnetic Resonance-Guided Focused Ultrasound Surgery (MRgFUS) for Conservative Treatment of Uterine Fibroids

Jaron Rabinovici[1], Haywood Brown[2], Matthias David[3], Hidenobu Fukunishi[4], Yutaka Morita[5], Bobbie S Gostout[6], Sang-Wook Yoon[7], Helena Millan-Cantero[8], Andrew Dobrotwir[9], Matthias Matzko[10], Wladyslaw Gedroyc[11]

MRgFUS Study Group

[1]Chaim Sheba Medical Center, Ramat Gan, Israel
[2]Duke University, Durham, North Carolina, United States
[3]Humboldt University, Berlin, Germany
[4]Shinsuma General Hospital, Kobe, Japan
[5]Itabashi Chuo Medical Center, Tokyo, Japan
[6]Mayo Clinic, Rochester, Minnesota, United States
[7]Bundang CHA General Hospital, Gyunggi-do, Republic of Korea
[8]Instituto Cartuja de Tecnicas Ayanzadas en Medicina, Sevilla, Spain
[9]Future Medical Imaging Group, Victoria, Australia
[10]Amper Kliniken AG, Dachau, Germany
[11]St. Mary's Hospital, Imperial College, London, United Kingdom

Background/Introduction: The first MRgFUS treatments for uterine fibroids were performed only for women who declared that they were not interested in future pregnancies. After several unplanned pregnancies, data began to accumulate that demonstrated the relative safety of post- MRgFUS pregnancies and deliveries. Today, in most countries, MRgFUS can be performed for women who wish to retain the option of future fertility. The aim of this study was to report on all known pregnancies that occurred after MRgFUS treatments for uterine fibroids or adenomyosis.

Methods: We obtained the data of all known pregnancies occurring after ExAblate® treatments and reported by the treatment sites to InSightec.

Results and Conclusions: One hundred and seventeen pregnancies have occurred post MRgFUS treatment of uterine leiomyomas or adenomyosis (mean age: 36 years, range 27-49). The mean time to conception was 9 months after the treatment. Live births occurred in 64 of the pregnancies (55%) and 38 of those were vaginal deliveries (59% of all deliveries). The mean birth weight was 3.27 kg. Twenty-two pregnancies resulted in a spontaneous abortion (19%), and 10 pregnancies were electively terminated (9%). Nine pregnancies (8%) are still ongoing. The outcome of twelve pregnancies (10%) could not be ascertained.

Our results suggest that conceptions, on-going pregnancies and vaginal deliveries are possible after MRgFUS for uterine fibroids. The relatively high rate of uncomplicated pregnancies, vaginal deliveries and term births in women after MRgFUS compares very favorably with other treatment alternatives for uterine fibroids. Based on these data, MRgFUS might present a safe and cost-effective treatment option for women with uterine fibroids who are interested in future pregnancies.

24-UF

Monday
15 October 2012

Topic: Uterine Fibroids
Presentation Type: Oral

Predictive Value of Patient Screening for Successful MRgFUS Treatment of Uterine Fibroids

Gina Hesley, Krzysztof Gorny, Bijan Borah, Elizabeth Stewart, David Woodrum, Douglas Brown

Mayo Clinic, Rochester, Minnesota, United States

Background/Introduction: To aid in communicating with our patients and referring physicians, our practice routinely categorized prospective MRgFUS patients as: "good", "questionable", or "poor" treatment candidates. The categories were selected based on patient MR screening images and fibroid symptoms. The purpose of this study was to evaluate whether the categorization was accurate in predicting which patients would be successfully treated with focused ultrasound.

Methods: The following findings were considered during selection of patient category: number of fibroids and their size, correlation of fibroid location with patient symptoms, T2 signal intensity, and access for FUS beam (e.g. presence of abdominal scarring, proximity to sensitive tissues). Patients were labeled as "good" candidates if the number of their fibroids was low, the fibroids to be targeted were low signal intensity on T2 images, fibroids appeared to correlate with symptoms, and access for treatment was unobstructed by patient anatomy. Patients were labeled as "questionable" if they presented with multiple fibroids or additional significant adenomyosis, the T2 signal intensity of the fibroids presented was heterogeneous or brighter than the myometrium, access for FUS beam was difficult, or symptoms were difficult to correlate with the fibroids. Poor candidates included those with numerous fibroids, marked surgical abdominal scarring causing significant limitations in access, or symptoms that were unlikely attributed to fibroids. Success of patient's treatment was judged by patient's lack of need for further intervention due to fibroid symptoms. This study is based on a retrospective review of patients treated at a single institution for symptomatic fibroids with MRgFUS from March 2005 to June of 2011.

Results: 140 patients were evaluated. Within the group, the range of the follow up varied between 1 and 7 years (median, 3 years; average, 2.7±1.7 years). During their follow up 105 patients did not seek further intervention for their fibroid symptoms; with the remaining 35 patients having further intervention (5 patients had intervention unrelated to continued or recurrent symptoms and were not included in the analysis). 135 patients were included in the study, 64 patients were categorized as "good", 66 as "questionable", and 5 as "poor" candidates.

"Good" candidates were statistically less likely to require further intervention for their fibroid symptoms ($p=0.01$, 8 patients sought further treatment). Similarly, in the group of "questionable" candidates, the patients were also less likely to seek further intervention ($p=0.009$, 21 patients sought further treatment). Only 5 patients labeled as "poor" candidates were treated. However, 4 of the 5 patients required no further intervention.

Conclusion: The treatment candidate categories selected during the screening process are fairly accurate in predicting success of MRgFUS procedures. As the practice is cautious in offering patients treatment and attempt to ensure patients are counseled appropriately, it is not surprising that patients labeled as "questionable" also statistically are more likely to not need further intervention. This study demonstrates that the evaluation of MR screening findings correlated with patients symptoms can be a helpful predictor and serve as a useful form of communication with referring providers and patients.

Acknowledgements (Funding): Investigator time was funded by NIH HD EC1063312 and R01060503

25-UF

Monday
15 October 2012

Topic: Uterine Fibroids
Presentation Type: Oral

Diffusion-Weighted Magnetic Resonance Imaging (DWI) as a Predictor for Treatment Efficacy of Volumetric Magnetic Resonance(MR)-Guided High-Intensity Focused Ultrasound (HIFU) Ablation of Symptomatic Uterine Fibroids

Marlijne Ikink, Lambertus Bartels, Marianne Voogt, Koen Vincken, Maurice van den Bosch

University Medical Center Utrecht, Utrecht, Netherlands

Background/Introduction: To evaluate the value of DWI and apparent diffusion coefficient (ADC) mapping for prediction of treatment efficacy after volumetric MR-HIFU ablation of uterine fibroids. High cellularity and increased vascularity of uterine fibroids have been identified as predictors for poor therapeutic efficacy of MR-HIFU ablation. DWI can be used pre-treatment to provide information on the diffusivity of water molecules within the fibroids, which is expected to depend on cellularity and vascularity. We investigated if the ADC of water is a predictor for treatment efficacy of volumetric MR-HIFU in patients with symptomatic uterine fibroids.

Methods: A total of 30 symptomatic uterine fibroids (median fibroid volume 269 cm3, range 23-1028) in 25 premenopausal women (median age 45-years, BMI 23.1 kg/m2) were treated with volumetric MR-HIFU. Prior to the procedure, DWI was performed on a clinical 1.5-T MRI-system (Achieva, Philips Healthcare, Best, the Netherlands). ADC maps were generated for each fibroid using the two lowest b-values (0, 200 s/m2). This combination of b-values stresses the perfusion effects in ADC. ADC values were recorded by drawing a region of interest (ROI) over the untreated fibroid, as seen on the coronal image. Immediately after treatment T1-weighted contrast enhanced images were made to calculate non-perfused volume (NPV). Two types of treatment efficacy indices were used, ratio of NPV / fibroid volume and ratio of NPV / treatment-cell volume. The NPV / treatment-cell volume was calculated using the entire NPV and the sum of treatment-cell volumes. Therefore, ratios could be greater than 1.

Results and Conclusions: The median non-perfused volume was 97 cm3 (range 5–531), which corresponded to 35% (range 4–86) of the fibroid volume treated. An MR-HIFU treatment was classified successful with a NPV / fibroid volume ratio ≥ 0.35. Median pre-treatment ADC value of the successfully treated fibroids was 1.993x10-3 mm2/s (inter-quartile range 1.870-2.200x10-3), and for the unsuccessfully treated group 2.271x10-3 mm2/s (inter-quartile range 2.149-2.360x10-3). The pre-treatment ADC value of the successfully treated group (n=13) was significantly lower (p=0.006) than those treated unsuccessfully (n=17). HIFU ablation was classified technical successful with a NPV / treatment-cell volume ratio ≥ 1. Median ADC values were again significantly lower in the technically successful treated group (p=0.045). A scatter plot indicates a negative trend between the post-treatment NPV-ratio and pre-treatment ADC values, where a high ADC value tends to correlate with a low NPV-ratio. In conclusion, DWI with ADC mapping may serve as predictor for treatment efficacy of volumetric MR-HIFU of symptomatic uterine fibroids, since a higher ADC value pre-treatment suggested a lower NPV ratio after ablation.

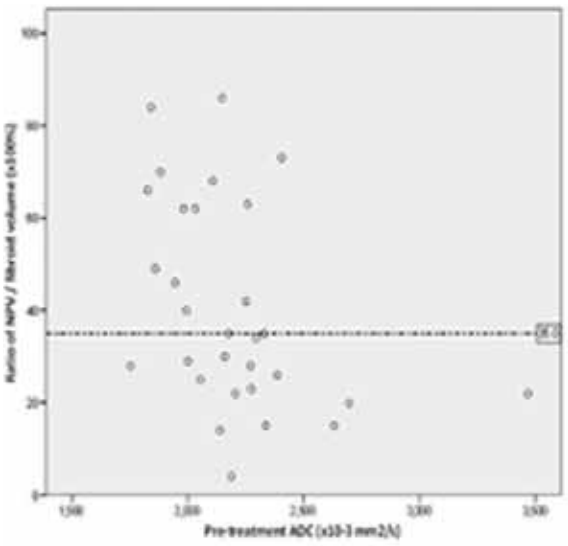

Scatter plot shows pre-treatment ADC values (b-values 0 and 200 s/m2) in relation to NPV / fibroid volume after volumetric MR-HIFU treatment, a higher ADC value suggests a lower NPV-ratio.

26-UF

Monday
15 October 2012

Topic: Uterine Fibroids
Presentation Type: Oral

Comparison of Overall Uterine Fibroid-Related Health Care Costs between Magnetic-Resonance Focused Ultrasound, Myomectomy and Uterine Artery Embolization

Bijan Borah[1], Ginger Carls[2], Teresa Gibson[3], Brian Moore[3], James Moriarty[1], Elizabeth Stewart[1]

[1]Mayo Clinic, Rochester, Minnesota, United States
[2]Truven Health Analytics (formerly Thomson Reuters), Bentonville, Arkansas, United States
[3]Truven Health Analytics (formerly Thomson Reuters), Ann Arbor, Michigan, United States

Background/Introduction: Uterine leiomyomas (fibroids) affect 20-40% of reproductive age women and are the major indication for hysterectomy in the US. Although benign, uterine fibroids (UF) often produce debilitating symptoms including prolonged and heavy menstrual bleeding, anemia, pelvic pain, bladder and bowel pressure, infertility and spontaneous abortion. Direct costs associated with UF range from $4,600 to $8,400, while the indirect costs reach $11,750. Magnetic resonance-guided focused ultrasound (FUS) is a new, potentially disruptive, non-invasive and uterine-sparing treatment option that has been shown to yield similar or better clinical outcomes than other uterine-sparing interventions. However, the costs of FUS and other minimally-invasive treatment options have not been compared using US practice data. The aims of this study were to compare one year costs for patients treated with FUS with those of uterine artery embolization (UAE) and myomectomy.

Methods: We use healthcare claims 2003-2010 from MarketScan® Commercial Claims and Encounters Database containing inpatient, outpatient and outpatient prescription drug experience of several million employees of self-insured employers. UF patients age 25-54 at the date of their first UF procedure were used in the study. The first procedure was defined as the index date (ID), with the one year operative period segmented as follows: pre-operative (2-weeks prior to ID), peri-operative (from ID until discharge) and post-operative (from discharge to 1 year after the start of the pre-operative period). A one year baseline period was measured during the year prior to the start of the pre-operative period. Continuous health plan enrollment with medical & pharmacy benefits across the entire study period and the absence of any procedures to treat UF (the study procedures plus hysterectomy and endometrial ablation) during baseline were required. Cost outcomes, measured by allowed charges, were reported for each of the above periods. Regression adjustment was used to minimize differences in baseline demographic and clinical characteristics of women receiving different treatments. Both binary (unadjusted) and adjusted costs are presented.

Results and Conclusions: The study sample comprised 14,566 subjects (FUS=14; UAE=4,143; myomectomy=10,409). Compared to FUS, UAE (46 vs. 44, P=0.182) and myomectomy (46 vs. 37, P<0.001) subjects were younger. Patients receiving FUS treatment lived in ZIP codes with fewer Blacks, measured as a percent of the population in the ZIP code (P<0.001). FUS patients appeared to be more complicated during baseline, with mean ER visits per patient of 0.50 compared to 0.21 for UAE (P=0.056) and 0.24 (P=0.088) for myomectomy. During the 1 year operative period, myomectomy patients cost the least ($19,313) compared with $24,241 for UAE and $25,840 for FUS (regression adjusted), although differences between FUS and the other treatments were not statistically significant due to the small sample of FUS patients. Peri-operative costs were lowest for FUS patients, but these patients also had higher post-operative costs. Regression adjustment decreased costs differences between each of the groups, but did not significantly alter conclusions (Table 1, next page).

Women undergoing FUS appear to be older, more medically complicated and to be from zip codes where there are fewer African American women than women undergoing other uterine sparing treatment options. Differences in costs between the three uterine-sparing procedures were not statistically significant.

Acknowledgements (Funding): This study was funded by a research grant from Focus Ultrasound Surgery Foundation and NIH/NICHD R01HD060503 and NIH/NCRR CTSA Grant Number UL1 RR024150.

Table 1. Comparison of Costs between Magnetic-Resonance Focused Ultrasound, Uterine Artery Embolization and Myomectomy

	Unadjusted Costs			Adjusted[1] Costs		
	FUS	UAE	Myomectomy	FUS	UAE	Myomectomy
Number of patients	14	4,143	10,409	14	4,143	10,409
Mean costs (95% Confidence intervals)						
Baseline	$14,483	$7,711	$7,511	$11,637	$9,038	$7,458
	($2,755, $26,211)	($7,407, $8,014)	($7,257, $7,765)	($7,235, $18,728)	($8,696, $9,390)	($7,176, $7,745)
Pre-operative	$718	$911	$670	$604	$923	$670
	($49, $1,387)	($828, $993)	($625, $715)	($117, $3,131)	($808, $1,053)	($587, $765)
Peri-operative	$9,495	$14,252	$12,110	$9,819	$14,620	$11,983
	($6,039, $12,951)	($13,811, $14,693)	($11,933, $12,287)	($6,555, $14,704)	($14,152, $15,111)	($11,594, $12,383)
Post-operative	$14,956	$7,599	$6,896	$15,417	$8,698	$6,659
	($3,027, $26,884)	($7,086, $8,113)	($6,643, $7,148)	($5,793, $41,013)	($8,051, $9,396)	($6,167, $7,193)
1-year[2]	$25,169	$22,762	$19,675	$25,840	$24,241	$19,313
	($14,233, $36,105)	($22,022, $23,502)	($19,349, $20,002)	($17,428, $38,618)	($23,458, $25,054)	($18,684, $19,957)

Notes:

1. Adjusted costs employed regression adjustment (generalized linear model with gamma distribution and logarithmic link) to control for baseline differences between women receiving each treatment. The regression included the following control variables, all measured on the index date or during the 1 year baseline period: age, region, type of health plan, year of procedure, demographics characteristics of the ZIP Code where the patient lived, indicators for any outpatient prescription drug fills of hormone therapies and NSAIDs, the Deyo Charlson Comorbidity Index, number of psychiatric diagnosis groups, indicators for UF related conditions, and indicators for any hospital stays and any emergency department visits during the baseline year. Demographics of the ZIP code included median family income, percent Black, percent Hispanic, and percent with a college education.
2. One year costs includes all operative costs (pre-, peri- and post- operative)

27-UF

Monday
15 October 2012

Topic: Uterine Fibroids
Presentation Type: Oral

African American Women Are Uniquely Affected by Uterine Fibroids

Elizabeth Stewart[1], Wanda Nicholson[2], Linda Bradley[3], Bijan Borah[1]

[1]Mayo Clinic, Rochester, Minnesota, United States
[2]University of North Carolina School of Medicine, Chapel Hill, North Carolina, United States
[3]Cleveland Clinic, Cleveland, Ohio, United States

Background/Introduction: The AHRQ evidence-based report for uterine fibroids identifies assessing the burden of disease and the way women acquire and process treatment strategies for uterine fibroids as prioritized research questions. While studies have documented increased rates of hospitalization, hysterectomy and myomectomy as well as greater incidence and prevalence for African American (AA) women, there is no data to compare racial differences in symptoms, quality of life, concerns, effect on employment and information-seeking behavior for this disease. The goal of the current project was to conduct a national survey of women with uterine fibroids and assess differences between AA and white women.

Methods: An online survey of 968 women aged 29-59 with uterine fibroids was conducted between 12/1/11-1/16/12 by Harris International based on questions designed b the investigators. Questions were based on a 5- or 4-point Likert scale and comparison were made between the two top categories and the remaining two or three categories using t-tests for continuous variables and Chi-squared tests for categorical variables.

Results and Conclusions: 271 AA women and 571 white women completed the survey. There were no differences between groups in education, employment status, gravidity or health status. AA women were significantly younger (43.5 vs. 46.0), had lower incomes and had differences in marital status (all $p<0.001$). AA women were significantly more likely to have severe or very severe symptoms including heavy or prolonged menses, (37 vs. 24%, $P=0.02$), menstrual cramps, (42 vs. 24%, $P<0.01$), abdominal bloating (37 vs. 15%, $P<0.01$) and anemia (22 vs. 6%, $P<0.01$). AA women more often reported fibroids interfered with physical activities (45 vs 26%, $P=0.01$) and. relationships with friends and family (22 vs. 11%, $P=0.01$). They were more likely to miss days from work (45 vs 23%, $P<0.01$) and to be afraid they would lose their job due to fibroids (21% vs.9%, $P=0.03$). AA women were more likely to consult friends and family (36 vs. 22 %) and health brochures (32 vs. 18%, $P<0.01$ for both) for health information. Concerns for future fertility (40 vs. 11 %) and the ability to have a healthy pregnancy (36 vs. 9%, $P<0.01$ for both) were key concerns for AA women contemplating fibroid therapy. Only 20% of AA and 13% of white women reported discussing focused ultrasound as a treatment option with a provider.

AA women with uterine fibroids have more severe symptoms and this has more impact on their employment. AA use different sources of information when deciding on a treatment and are significantly more likely to view future fertility and pregnancy as key concerns. Despite these differences, most women are not receiving information about focused ultrasound treatment of fibroids.

Acknowledgements (Funding): The survey was funded by Fibroid Relief, a program of the Focused Ultrasound Foundation (Charlottesville, Virginia,) Investigator time was funded by NIH HD RC1063312 and R01060503 (EAS &BJB).

28-UF

Monday
15 October 2012

Topic: Uterine Fibroids
Presentation Type: Oral

Cost-Effectiveness Analysis of Uterine-Preserving Procedural Treatments for Uterine Fibroids, Including Magnetic Resonance-Guided Focused Ultrasound (MRgFUS)

Anne Cain-Nielsen[1], James Moriarty[2], Elizabeth Stewart[2], Bijan Borah[2]

[1]University of Michigan School of Public Health, Ann Arbor, Michigan, United States
[2]Mayo Clinic, Rochester, Minnesota, United States

Background/Introduction: Uterine fibroids are highly prevalent in women of childbearing age, affecting an estimated 30% of premenopausal women in the U.S. Annual costs of uterine fibroids were at least $4.1 billion in 2010 and were estimated to accrue over twice the annual costs of cervical cancer or melanoma treatment. Despite high prevalence and high disease costs, the comparative effectiveness of available treatments for uterine fibroids remains understudied. Economic evaluations of MRgFUS are particularly rare, despite the technology's potential to provide effective and minimally invasive treatment. No existing economic analyses for procedural treatments specifically evaluate the population of reproductive-aged women who wish to preserve their uteri; to our knowledge this is the first evaluation of the cost-effectiveness of MRgFUS relative to the other uterine-preserving procedural treatments.

Methods: A decision analysis Markov model was constructed to evaluate the cost-effectiveness of three treatment strategies: uterine artery embolization (UAE) with myomectomy as 'fallback' treatment for UAE treatment failure or ineligibility; MRgFUS with myomectomy as 'fallback'; and myomectomy as the sole treatment. Cost-effectiveness was calculated in terms of US dollars per quality adjusted life year (QALY). A decision threshold of $50,000/QALY was used. In the model, women were assessed for eligibility for treatment, treated, and experienced adequate or inadequate symptom relief. Women were assumed to have additional treatment for inadequate symptom relief or recurrence. Event probabilities, costs, and quality of life measurements were taken from clinical and health economics literature, expert opinion, and an administrative claims database. Sensitivity analysis was conducted to evaluate uncertainty in the model parameters.

Results and Conclusions: In the base case analysis, the MRgFUS strategy was the least costly with average costs of $13025 and average QALYs of 5.00. The UAE strategy had average costs of $16777 and average QALYs of 5.00. For myomectomy, average costs were $13518 and average QALYs were 4.99. The optimal treatment strategy was sensitive to proportion of patients eligible for MRgFUS, probabilities of adequate symptom relief, costs of MRgFUS and myomectomy, and probabilities of recurrence for myomectomy and MRgFUS. Repeated simulations showed that the MRgFUS strategy was most likely to be found optimal. Changes in two or more of the sensitive parameters could increase or decrease the favorability of MRgFUS. Increasing the proportion of patients eligible for MRgFUS made the MRgFUS strategy more cost-effective. UAE was least likely to be cost-effective. MRgFUS can be a cost-effective option, and sensitive parameters should be further studied to improve the reliability of cost-effectiveness estimates.

Acknowledgements (Funding): Investigator time was funded by a research grant from Focus Ultrasound Foundation (Charlottesville, Virginia) (BB, JM, ES), and by NIH HD RC1063312 and R01060503 (ES &BB).

29-UF

Monday
15 October 2012

Topic: Uterine Fibroids
Presentation Type: Oral

A Multidisciplinary Approach to Uterine Leiomyomas: Rationale, Design, Early Results and Predictors of Undergoing Uterine-Preserving Treatment

Nelly Tan, Timothy McClure, Christopher Tarnay, David Lu, Michale Johnson, Steven Raman

University of California at Los Angeles, Los Angeles, California, United States

Background/Introduction: Fibroids are benign growth of the uterine smooth muscle. It occurs in 20 to 35% of all reproductive-age women; patients develop symptoms including pelvic pressure, menometrorrhagia, dysmenorrhea, urinary symptoms, and defecation problems. Treatment available include medical therapy, Magnetic Resonance guided Focused Ultrasound Surgery, uterine artery embolization, surgery (i.e. hysterectomy, myomectomy) and observation. Surgery can cause significant morbidity and is costly due to inpatient stay. Despite abundant literature supporting efficacy of non-surgical treatments, majority are treated surgically. We instituted a multi-disciplinary fibroid center in 2008 and we determined treatment outcomes for uterine leiomyoma after the implementation of a multidisciplinary fibroid center.

Methods: We performed a HIPAA-complaint, IRB-approved retrospective study of women consecutively evaluated at our multidisciplinary fibroid treatment center from July 2008 to August 2011. Pelvic MRI was obtained prior to a joint patient evaluation by our gynecology and radiology clinicians. After review of patients' history and physical and correlation with imaging findings, treatment options were offered to the patients and included conservative management (expectant management, medical therapy), uterine-preserving options (MRI-guided focused ultrasound ablation, uterine artery embolization, myomectomy, hysteroscopic resection) or hysterectomy. We performed simple linear logistic regression analysis to assess the effect of age, symptom (bleeding vs. bulk), presence of fibroid on MRI, size of fibroids, evaluation by radiology to predict whether a patient will undergo a uterine-preserving treatment or not. We performed a t-test for continuous variables and X2 test for categorical variables between the cohort that did and did not undergo a uterine-preserving treatment. Statistics were considered significant at $p = 0.05$.

Results and Conclusions: Of 446 phone inquiries, 213 (47.8%) women were evaluated in clinic and 205 satisfied inclusion criteria and comprised the study cohort. The mean age was 44.1 (SD 7.5). On MR Imaging, 193 (94.2%) had fibroids, 23 (11.2%) had non-fibroid conditions [21 (10.2%) had adenomyosis, 2 (1.0%) had ovarian endometrioma] and 15 (7.3%) had coexisting fibroid and non-fibroid conditions. Of 205 women, 112 (54.6%) had follow-up after the initial visit. Of these, 23 (20.5%) elected medical/expectant management and 88 (78.6%) patients underwent a total of 96 procedures. Thirty seven women (42.0%) underwent gynecological surgical resection and 51 (58.5%) underwent interventional radiology based treatment. Seventy seven (87.5%) had uterine-preserving treatment including laparoscopic myomectomy and 12 (10.7%) underwent hysterectomy. There was an association between women who presented with a history of non-conservative management of their fibroids and undergoing an interventional radiology based treatment (UAE, MRgFUS) over a gynecological procedure (7 vs. 0, $p=0.013$) as second line treatment. On simple linear logistic regression analysis, patients who were also evaluated by a radiologist had 6.0 increased odds of undergoing uterine preserving procedure compared to hysterectomy (95% CI 1.15-31.22).

A significant proportion of women with symptomatic fibroids presenting to our multidisciplinary clinic desired uterine-preserving treatment options; a multidisciplinary fibroid evaluation may facilitate the increased use of less invasive options over hysterectomy as primary therapy.

Acknowledgements (Funding): Focused Ultrasound Foundation Fellowship

30-UF

Monday
15 October 2012

Topic: Uterine Fibroids
Presentation Type: Oral

RELIEF - REgistry for Leiomyoma, International Efficacy of Focused Ultrasound

Jaron Rabinovici[1], Arik Hananel[2]

[1]Chaim Sheba Medical Center, Ramat Gan, Israel
[2]Focused Ultrasound Foundation, Charlottesville, Virginia, United States

Background/Introduction: During the last decade since the introduction of MR-guided Focused Ultrasound as a treatment for symptomatic uterine fibroids more than 8,000 treatments have been performed worldwide. Several small studies have indicated that Focused Ultrasound can provide women with symptomatic uterine fibroids with a non-invasive, efficacious and ambulatory treatment option that provides persistent relief of their symptoms.

However, as with many other new treatment paradigms, adoption by the clinical community and medical coverage, which are crucial for worldwide usage, have been limited. While demonstrating efficacy is the first required step for a new technology, the medical community, payers and other stakeholders are seeking high volume data demonstrating short and long-term safety, and clinical and cost effectiveness. The establishment of a worldwide registry might help achieve these goals and define the future role of Focused Ultrasound for the treatment of uterine fibroids.

Methods: A registry is a prospective, observational, exposure-registration follow-up study with the aim to determine the effectiveness of a treatment in clinical daily practice. Therefore, it offers the possibility of clinical data collection and comparison among a large number of patients with multiple confounding complications, wide age ranges, various socioeconomic and cultural backgrounds and differing healthcare situations.

Over the last year a unique collaboration between academia, a non-profit organization and industry was established for the creation of the RELIEF Registry. Partners include leading clinicians in the field of Focused Ultrasound for fibroids and the Focused Ultrasound Foundation with support from Philips and InSightec. RELIEF is designed to collect baseline and follow-up data (up to three years) on 1,000 patients from up to 20 sites worldwide, using Focused Ultrasound systems for symptomatic uterine fibroids. Data endpoints will include clinical symptoms, safety, patient satisfaction, and use of alternative treatments during the follow-up period. The registry will be led by a steering committee representing all involved parties.

Patients are expected to be recruited in 2013, and publications describing in detail the registry structure are planned for the near future.

Results and Conclusions: The RELIEF Registry can be a significant step in the quest of to define the role of Focused Ultrasound treatment for symptomatic uterine fibroids and to accelerate its worldwide adoption. It might serve also in the future as a template for the adoption of other Focused Ultrasound clinical applications.

Differences in Intratumoral Distribution of Doxorubicin Released From Temperature-Sensitive Liposomes During Hyperthermia, Ablation and Combined Treatment

Nicole Hijnen[1], Mariska de Smet[1], Edwin Heijman[2], Holger Gruell[2]

[1]Eindhoven University of Technology, Eindhoven, Netherlands
[2]Philips Research, Eindhoven, Netherlands

Background/Introduction: MR-HIFU treatment holds great promise as a non-invasive treatment option for malignant tumors. Optimization of heating protocols for ultrasound-mediated drug delivery using temperature-sensitive liposomes (TSLs)[1] can improve the treatment efficacy of the tumor as well as adjacent tissue. The latter is important for preventing reoccurrence. Not much is known on the influence of different heating protocols on the extravasation of TSLs and the distribution of the released drug in the tumor using MR-HIFU. Therefore different heating protocols were tested upon TSL injection (hyperthermia, ablation and their combination). We hypothesized that a combined treatment of hyperthermia-induced drug delivery followed by ablation might be the best approach. An MR contrast agent was incorporated in the TSLs to monitor the release in situ during the treatment.[2]

Methods: 111In labeled TSLs encapsulating doxorubicin (dox) and MR contrast agent (Gd-HPDO3A) were prepared and injected i.v. inrhabdomyosarcoma tumor bearing rats. Immediately after injection, MR-HIFU treatment was performed using a clinical 3T MR-HIFU with a dedicated small animal setup. Four groups were defined: control, hyperthermia alone [2x15min ~ 41°C], ablation alone [65°C], hyperthermia followed by ablation. R1 maps of the tumor were acquired pre injection and after every heating period. Animals were sacrificed at 90min post injection and further analyzed using SPECT/CT and histology.

Results and Conclusions: Local Gd-release was observed by an increase in R1 immediately after HIFU treatment, while no distinct effect was observed in the control group. Hyperthermia treatment resulted in a homogenous R1 change over the entire tumor, while after ablation treatment the enhancement was more limited to the tumor rim (Figure1). The R1 change coincided with the liposomal distribution pattern visible on SPECT and autoradiography. Fluorescence microscopy showed dox directly around the blood vessels in control tumors, while in the HIFU treated tumors the dox was spread over a larger area and also taken up by tumor cells further away from blood vessels (Figure2). Qualitative analysis showed that tumor uptake and subsequent delivery of dox was highest for the combined treatment (hyperthermia followed by ablation): combined > hyperthermia alone ≥ ablation alone >> control.

Figure 1. MR, SPECT/CT and autoradiography from excised tumor at t=90 min p.i. Red contour indicates tumor location. T=tumor, M=muscle.

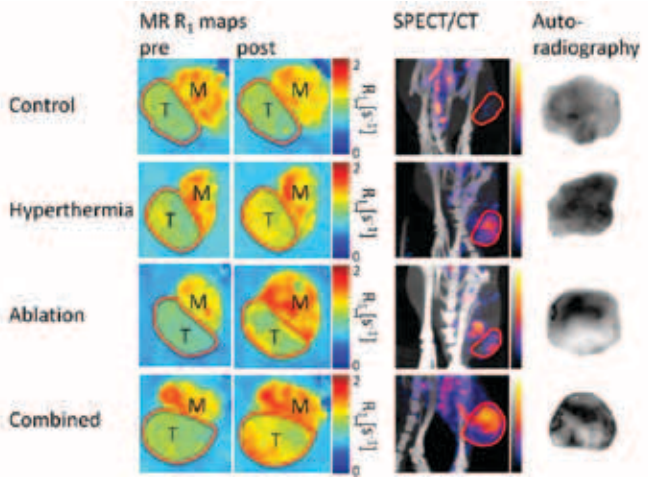

We conclude that HIFU treatment induced enhanced liposome accumulation and extravasation in the heated region and that deltaR1 is a good predictor of drug release from the liposomes. All heating strategies resulted in cellular uptake of dox, indicating that the drug became bioavailable and showed a deep penetration into the interstitial space upon heating with HIFU. As hypothesized, the combined treatment with hyperthermia and ablation gave the highest uptake together with a more homogenous intratumoral distribution. Since liposomes have a long circulation time and can benefit from the EPR effect the study will be repeated for 48 hours post injection.

Acknowledgements (Funding): This research was supported by the Center for Translational Molecular Medicine (VOLTA) and EU FP7 Sonodrugs (NMP-4-LA-2008-213706).

References:

1. Yatvin et al., *Science*. 1978 Dec 22;202(4374):1290-3.
2. de Smet et al., *J Control Release*. 2010 Apr 2;143(1):120-7.

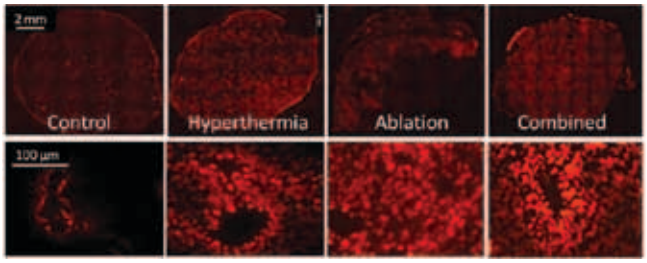

Figure 2. Fluorescence microscopy at t=90 min. p.i. from excised tumor. Lower row is a detail view of the upper row.

32-EA

Tuesday
16 October 2012

Topic: Emerging Applications
Presentation Type: Oral

Ultrasound-Triggered Release of Doxorubicin from Thermosensitive Liposomes Modified with Poly(N-Isopropylacrylamide-co-Propylacrylic Acid) Copolymers for Cancer Therapy

Tyrone Porter[1], Terene Ta[1], Eun-Joo Park[2], Nathan McDannold[2]

[1]Boston University, Boston, Massachusetts, United States
[2]Brigham and Women's Hospital/Harvard Medical School, Boston, Massachusetts, United States

Background/Introduction: Doxorubicin (DOX) is a chemotherapeutic agent that is widely used for cancer therapy. While potent against a variety of cancer types, the dose of DOX administered to patients is severely limited due to systemic toxicities, such as myelosuppression and cardiotoxicity. These toxic effects can be reduced significantly by packaging DOX within liposomes that are designed to accumulate within solid tumors after systemic administration. However, DOX must be released in a timely manner in order to be effective against the cancerous growth. To achieve this goal, we have developed a sterically-stable liposome surface-modified with a copolymer that is membrane-disruptive in mildly hyperthermic conditions. Furthermore, we employ MR-guided FUS (MRgFUS) to noninvasively heat solid tumors locally, thus triggering release of drugs encapsulated in the polymer-modified thermosensitive liposomes (pTSL) selectively within tumors. The combination of pTSL and MRgFUS can be used to improve the pharmacological profile of DOX, increasing its efficacy against localized malignancies while mitigating its systemic toxicities.

Methods: Copolymers composed of N-isopropylacrylamide and propylacrylic acid were synthesized via reverse addition-fragmentation chain transfer chemistry. The copolymers were terminated with a hydrophobic group, which was used to anchor the copolymer to the outer leaflet of the liposomal shell. Non-thermosensitive (NTSL), traditional thermosensitive (TSL), and pTSL were prepared via extrusion and remote loaded with DOX. For in vivo studies, rat mammary adenocarcinoma cells were injected subcutaneously in the hindlimb of Fischer rats. After IV injection of rhodamine-labeled liposomes, blood and tissue samples were collected at predetermined timepoints and assayed for fluorescence. For treatment studies, MRgFUS (f = 1.15 MHz) was used to heat solid tumors to a constant 43°C for 5 min after IV injection of free DOX or DOX-loaded liposomes. Rats from each treatment group were sacrificed immediately following FUS exposure and tumors were harvested and analyzed for DOX release. Additionally, the tumor volume in rats from each treatment group was measured over 14 days to evaluate tumor response to treatment.

Results and Conclusions: While the stability of pTSL was comparable to TSL in HEPES buffer and serum-containing media, pTSL had superior responsiveness to mild hyperthermia. The threshold temperature for 50% DOX release in HEPES buffer was 39oC for pTSL compared to 43oC for TSL. The lower threshold temperature resulted in a significant reduction in the thermal dose required for DOX release from pTSL compared to TSL. Both formulations had comparable biodistribution profiles in tumor-burdened rats, with the vast majority of liposomes being cleared through the liver and spleen and comparable percentage of injected liposomes accumulating in solid tumors (< 1%). pTSL released significantly more DOX than TSL in tumors heated via MRgFUS to 43oC, and this resulted in a stronger suppression of tumor growth over 14 days. Results show that pTSL are more responsiveness to mild hyperthermia than traditional TSL, releasing more entrapped drug at lower temperatures and thermal doses. Consequently, the combination of ultrasound-mediated heating and DOX-loaded pTSL was more effective than free drug and DOX-loaded TSL in the treatment of solid tumors.

Acknowledgements (Funding): This work was supported by the NIH (R25CA153955) and the Focused Ultrasound Foundation.

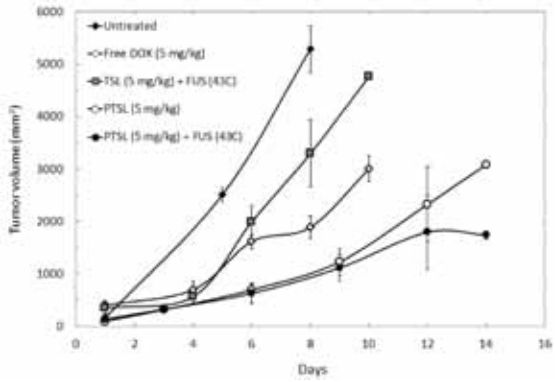

Efficacy of doxorubicin against tumor growth as a function of delivery approach. As shown, the combination of polymer-modified thermosenstive liposomes (pTSL) with ultrasound-mediated hyperthermia was most effective at arresting tumor growth.

33-EA

Tuesday
16 October 2012

Topic: Emerging Applications
Presentation Type: Oral

Mild Hyperthermia in Small Animals with A Sector-Vortex Phased-Array Transducer for Homogeneous Heating

Caitlin Burke[1], Ari Partanen[2], Matti Tillander[3], Marcelino Bernardo[4], Pavel Yarmolenko[4], Peter Choyke[4], James Mitchell[4], Bradford Wood[4], Matt Dreher[4]

[1]National Institutes of Health (NIH), Vienna, Virginia, United States
[2]Philips Healthcare, Bethesda, Maryland, United States
[3]Philips Healthcare, Vantaa, Finland
[4]National Institutes of Health, Bethesda, Maryland, United States

Background/Introduction: Mild hyperthermia (40-45°C) has shown great promise as an adjuvant cancer treatment due to its ability to improve effectiveness of radiotherapy and chemotherapy. Magnetic resonance guided high-intensity focused ultrasound (MR-HIFU) is a non-invasive image-guided method capable of accurate, precise and spatially localized, conformal delivery of mild hyperthermia. Clinical MR-HIFU systems are designed for human anatomy, which limits their use in a high throughput preclinical setting – a step necessary for rapid clinical translation. To address this challenge, a clinical software package was used to control heating with a pre-clinical sector-vortex transducer (similar shape to a clinical transducer but smaller heated region), on a scale suitable for rodent tumors. Performance of this system was evaluated in terms of accuracy and homogeneity of mild hyperthermia in vitro and in vivo.

Methods: The MR-HIFU system consisted of a 3MHz 8-channel sector-vortex phased-array transducer, 8-channel power generator, custom stage with integrated small animal MR coil (Philips Healthcare, Vantaa, Finland), and treatment planning/binary feedback temperature control software (Philips Healthcare, Vantaa, Finland). The transducer was driven in five unique operating modes (0-4), where the mode number indicates the number of times the element phases vary by 2π around the transducer circumference. Acoustic intensity distributions were simulated and verified using a needle hydrophone. Temperature maps orthogonal and parallel to HIFU beam axis were acquired on a 3T-MRI (Philips Healthcare, Best, Netherlands) using the proton resonance frequency shift method (dynamic=3s, voxel size=0.5x0.5x2mm). Sonications were performed in a tissue-mimicking phantom to characterize temperature accuracy and homogeneity. Sonication modes were evaluated in SCC subcutaneous tumors (~150-200mm3) on the hindlimb of mice for their ability to treat the entire tumor with mild hyperthermia (n=2).

Results and Conclusions: The acoustic field distribution became wider and yielded lower peak temperatures with increasing mode number, as determined by simulations and confirmed by hydrophone measurements. Hydrophone measurements yielded a single focal spot (>-3dB) with width of 0.5mm and length of 3.3mm (in beam axis direction) for Mode-0 (i.e. all elements in phase), and 8 separate foci in octagonal pattern for mode-4. In phantom, feedback-controlled sonications (target=40.5-41.0°C for 5min) produced mean temperatures that that were comparable across all modes (mean= 41.2±1.0°C, 41.2±0.9°C, 41.1±0.8°C, 40.8±0.6°C, and 40.8±0.5°C for modes 0, 1, 2, 3, and 4, respectively). Heating was more homogeneous for higher modes (T10-T90=2.54±0.04°C, 2.42±0.13°C, 2.05±0.08°C, 1.49±0.09°C, and 1.37±0.04°C, for modes 0, 1, 2, 3, and 4, respectively). Sonications in SCC subcutaneous tumors in mice resulted in a mean tumor temperature (average within the tumor) of 39.8±1.0°C, 40.0±0.8°C, and 40.1±0.8°C orthogonal to the HIFU beam axis, and 39.1±1.0°C, 39.3±0.7°C and 39.4±0.8°C parallel to the HIFU beam axis, for modes 0, 2, and 4, respectively. In vivo, temperature accuracy (average within 0.5±1.5°C of target temperature range) and homogeneity were not strongly dependent on mode (within the entire tumor, T10-T90 = 2.6±0.3°C, 2.1±0.4°C, and 2.2±0.3°C, for modes 0, 2, and 4, respectively).

A mild hyperthermia control algorithm was used within a clinical MR-HIFU control/treatment planning software suite to control a preclinical MR-HIFU system, demonstrating minimal temperature overshoot and accurate temperature maintenance. The sector-vortex phased-array system allows for homogeneous heating of the entire tumor in small animal models, potentially aiding clinical translation of MR-HIFU applications.

Acknowledgements (Funding): This work supported in part by the Intramural Research Program of the NIH. NIH & Philips have a Cooperative Research & Development Agreement & may share intellectual property.

34-EA

Tuesday
16 October 2012

Topic: Emerging Applications
Presentation Type: Oral

Enhanced MR-Guided HIFU Ablation of Rabbit VX2 Tumors In Vivo Using Phase-Shift Nanoemulsions

Jonathan Kopechek[1], Eun-Joo Park[2], Yong-Zhi Zhang[2], Nathan McDannold[2], Tyrone Porter[1]

[1]Boston University, Boston, Massachusetts, United States
[2]Brigham and Women's Hospital/Harvard Medical School, Boston, Massachusetts, United States

Background/Introduction: The clinical feasibility of MR-guided HIFU for ablation of solid tumors in deep-seated organs is limited by the high acoustic pressures and long treatment times needed (on the order of hours). It has been shown previously that microbubbles can accelerate HIFU-mediated heating, but microbubbles injected intravenously do not extravasate into tumors and thus have a limited effect on ablation of the extravascular space. In order to accelerate the rate of heating and enhance thermal ablation in tumors, we have developed a phase-shift nanoemulsion (PSNE) consisting of lipid-coated liquid perfluorocarbon droplets that are between 100 and 200 nm in diameter, in order to increase nanoparticle accumulation in tumors. Previous in vitro studies demonstrated that short, high-amplitude acoustic pulses can vaporize the liquid droplets into gas-containing microbubbles, which can locally accelerate heating through inertial cavitation. In this pre-clinical in vivo study, we examined the efficacy of vaporized PSNE on enhancing MR-guided HIFU-mediated heating and lesion formation in a rabbit VX2 tumor model.

Methods: All animal experiments were performed according to protocols approved by the Harvard Medical School Institutional Animal Care and Use Committee. Rabbit VX2 tumors were implanted into the thighs of 20 New Zealand White rabbits and experiments were performed two weeks later when the tumors were ~20 mm in length. PSNE (0.5 ml/kg) was injected through the ear vein for all experiments. The distribution of PSNE within the tumors was determined in an initial study by tagging the droplets with a gadolinium chelate. A custom-built 1.5 MHz MR-compatible HIFU transducer was used to sonicate targeted locations within the tumor. Each location was sonicated with a 100-cycle pulse for acoustic droplet vaporization (ADV), immediately followed with a 1 million-cycle HIFU pulse to drive cavitation, and the sequence was repeated for 30 seconds. A range of acoustic powers was tested. A portable ultrasound imaging system was used to capture PSNE vaporization and spatially map cavitation activity in the tumors. Changes in temperature were determined with MR thermometry measurements acquired before, during, and after sonication. Sonications and MR measurements were performed before and after injecting PSNE intravenously in order to evaluate the efficacy of PSNE on enhancing heating and lesion formation in the tumor.

Results and Conclusions: T1-weighted MR images of rabbit tumors before and after intravenous injection of gadolinium-tagged PSNE indicated accumulation of the nanoemulsion in the tumor interstitium (Figure 1). Acoustic vaporization of PSNE within rabbit tumor interstitium was observed for up to three hours after PSNE injection using B-mode images acquired from an ultrasound imaging array. Acoustic cavitation activity was detected in tumors only after vaporizing PSNE (Figure 2). MR temperature maps revealed that the thermal dose during sonication in rabbit tumors was significantly enhanced by vaporized PSNE, compared to controls without PSNE (Figure 3). These results suggest that PSNE could potentially improve the clinical feasibility of MRgHIFU by reducing the time and acoustic intensities needed to ablate solid tumors.

Acknowledgements (Funding): This work was supported by a grant from the National Institutes of Health (R21 EB009493).

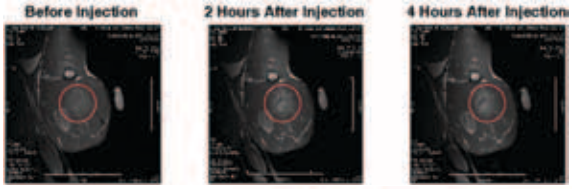

Figure 1. T1-weighted MR images indicating accumulation of gadolinium-tagged PSNE in rabbit tumors.

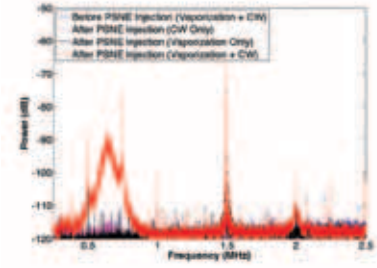

Figure 2. Power spectra from 650 kHz focused hydrophone, indicating cavitation activity in rabbit tumor only after vaporization of PSNE followed by continuous wave (CW) ultrasound.

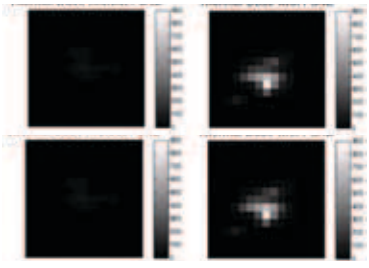

Figure 3. Thermal dose (in equivalent minutes) during sonication in rabbit tumors without (left) and with (right) PSNE.

35-EA

Tuesday
16 October 2012

Topic: Emerging Applications
Presentation Type: Oral

Pulsed Focused Ultrasound (pFUS) Induces Targeted Homing of Therapeutic Mesenchymal Stem Cells (MSC) to Kidneys During Acute Tubular Necrosis and Leads to Improved Renal Function

Scott Burks[1], Ali Ziadloo[1], Saejong Kim[1], Pamela Tebebi[1], Victor Frenkel[2], Joseph Frank[1]

[1]National Institutes of Health, Bethesda, Maryland, United States
[2]The Catholic University of America, Washington, D.C., United States

Background/Introduction: Stem cell therapies are promising, but targeted delivery to pathological loci following systemic infusion remains problematic. Circulating stem cells home by tethering to activated endothelium and actively transmigrating into the parenchyma in response to cytokine/chemokine gradients. Therapeutic stem cells can home to pathological loci during the acute inflammatory response, but fail to home after it has resolved. We have previously shown pFUS, likely through mechanotransduction, drives a transient local molecular biological response in healthy kidney tissue leading to enhanced homing permeability and retention (EHPR) of MSC to sonicated tissue. MSCs have demonstrated therapeutic benefit in models of acute tubular necrosis (ATN). We sought to examine if pFUS could further increase the number of MSC homing to diseased kidneys, during the acute inflammatory period or after its resolution, and whether increasing cell numbers at the pathological site has additional therapeutic benefit.

Methods: C3H mice were given a single injection of cis-platinum (15 mg/kg) to induce ATN. Kidneys were sonicated either unilaterally or bilaterally (1 MHz, 40 W, 5% duty cycle, 5 Hz repetition frequency) without microbubbles either 1 day or 4 days post-ATN. MSC were IV injected 2 hr after pFUS. At various times after treatment, mice were euthanized and tissues were harvested for physiological, histological, and molecular analyses.

Results and Conclusions: pFUS increases targeted homing of MSC to sonicated kidneys at both 1 or 4 days post-ATN. These represent time points where acute inflammation is ongoing and after its resolution. Mice were then treated with MSC alone or pFUS+MSC at 1 day post-ATN and assessed at day 5 post-ATN. pFUS+MSC-treated kidneys retained greater numbers of MSC compared to mice receiving MSC alone. Furthermore, targeting additional MSC with pFUS had greater protective effects than MSC alone. pFUS+MSC showed less pronounced disease histologically (necrosis and apoptosis) and pFUS+MSC mice had improved renal function, measured by blood urea nitrogen and serum creatinine, compared to mice that received MSC alone (Fig 1).

pFUS is a potentially powerful tool to noninvasively and nondestructively direct stem cell migration in vivo. pFUS drives a complex local biological response that can be capitalized for EHPR of therapeutic cells. pFUS provides spatiotemporal control over cell homing processes—it can increase the number of cells to a location and enables targeting of cells at late time points during disease when cells may no longer home by endogenous mechanisms. These results imply that increasing the number of cells homing to pathology can directly improve pathological outcomes and can greatly improve the efficiency and effectiveness of treatment strategies in cell therapy and regenerative medicine.

Acknowledgements (Funding): This research was supported by the Intramural Research Program at the National Institutes of Health Clinical Center and National Institute of Biomedical Imaging and Bioengineering.

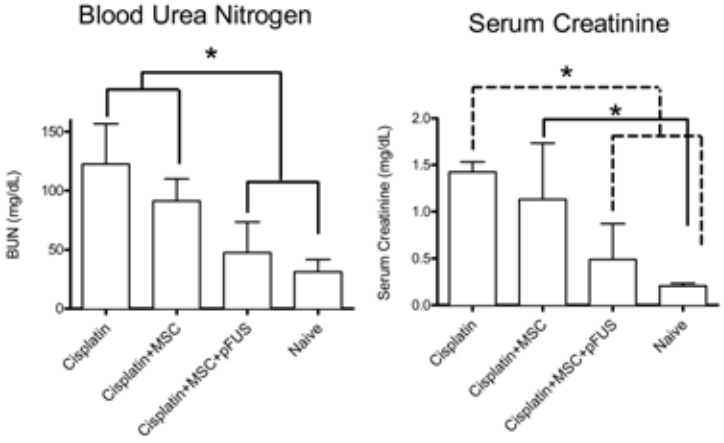

Figure 1. Renal function measured by blood urea nitrogen (BUN) and serum creatinine clearance. Mice were given cisplatinum on Day 0, followed by pFUS and/or MSC on Day 1. ATN was allowed to develop to Day 5 when mice were evaluated for renal function. Significant improvements in BUN clearance were noted when MSC were targeted using pFUS compared to mice that received MSC alone and statistical trends for improved creatinine clearance were also observed. Statistical significance ($p < 0.05$) is indicated by * and n=4-6 mice per group.

36-EA

Tuesday
16 October 2012

Topic: Emerging Applications
Presentation Type: Oral

Boiling Histotripsy: A Method of Tissue Emulsification using Millisecond-Long Pulses of High Intensity Focused Ultrasound

Lawrence Crum[1], Julianna Simon[1], Tatiana Khokhlova[1], Yak-Nam Wang[1], Joo-Ha Hwang[1], Vera Khokhlova[2], Michael Bailey[1]

[1]University of Washington, Seattle, Washington, United States
[2]Moscow State University, Moscow, Russian Federation

Background/Introduction: Background/Introduction: Most current clinical applications of high intensity focused ultrasound (HIFU) rely on heating and thermally injuring the targeted zone of diseased tissue. However, generating mechanical emulsification of tissue without or with some controlled degree of thermal coagulation can be beneficial for certain indications; for example, for treating cardiac arrhythmias and destroying tissue for conditions such as benign prostatic hyperplasia (BPH) and tumors of the liver, kidney, and prostate. In our previous work, a method termed boiling histotripsy was proposed to obtain mechanical emulsification of tissue non-invasively using millisecond bursts of ultrasound shock waves and repeated localized boiling [Canney et al., UMB 36(2), 2010; Khokhlova et al., JASA 130(5), 2011]. The clinical advantage of mechanical tissue ablation over traditional thermal ablation lies in the ability to create precise lesions with sharp boarders between treated and untreated tissues and with the ability to monitor the treatment with ultrasound imaging. There is also a possibility of maintaining the integrity of enzymes and proteins in tissue near the boundary of the lesion, which could potentially be used to enhance an immune response. In this work the results of feasibility studies to generate emulsified lesions under B-mode ultrasound guidance in various types of tissue ex vivo and in vivo are presented.

Methods: Boiling histotripsy lesions were created in ex vivo bovine heart and liver and in vivo in porcine liver and in subcutaneous tumors in mice (B16 melanoma). HIFU transducers operating at 2 MHz and 3.4 MHz were used in the exposures. The parameters of the pulsing protocols (65 – 100 MPa shock amplitudes, 1-500 ms pulse durations, and 0.01-0.1 duty factors) were varied depending on the extent of desired thermal effect. All exposures were monitored using B-mode ultrasound. Mechanical and thermal tissue damage in the lesions was evaluated histologically using conventional staining techniques (H&E and NADH-diaphorase). Thermal effects were quantified by measuring denaturation of salt soluble proteins in the treated area.

Results and Conclusions: The results of experiments performed in various ex vivo and in vivo tissues have confirmed the effectiveness of the boiling histotripsy method to mechanically ablate tissue. It was shown that the degree of the thermal effect can be controlled by varying the parameters of the pulsing scheme, while the size of a single lesion can be varied by the choice of HIFU frequency. In addition, it was shown that the treatment can be easily monitored in real-time using B-mode ultrasound imaging since millimeter-sized boiling bubbles are highly echogenic. The size and shape of emulsified lesions obtained in-vivo agreed well with those obtained in ex-vivo tissue samples using the same exposure parameters.

Acknowledgements (Funding): This work was supported by NIH EB007643 and 1K01EB015745 grants.

37-EA

Tuesday
16 October 2012

Topic: Emerging Applications
Presentation Type: Oral

Targeting Vascular Structures Noninvasively with Ultrasound Guidance

John Ballard[1], Andrew Casper[1], Dalong Liu[2], Islam Shehata[3], Alyona Haritonova[1], Emad Ebbini[1]

[1]University of Minnesota, Minneapolis, Minnesota, United States
[2]Seimens Medical, Issaquah, Washington, United States
[3]University of Minnesota, Cairo University, Minneapolis, Minnesota, United States

Background/Introduction: The feasibility of targeting atheromatous plaques noninvasively with ultrasound guided focused ultrasound surgery (USgFUS) by using an integrated dual-mode ultrasound array (DMUA) and diagnostic transducer is undertaken in this study to investigate a potential noninvasive treatment option for atherosclerosis.

Methods: A cohort of four familial hypercholesterolemic (FH) swine was enrolled due to their natural disposition to develop chronic atherosclerosis with similar pathogenesis to that of humans. During the intervention, the animal was placed under general anesthesia in a supine position. Diagnostic ultrasound and intravascular ultrasound (IVUS) with angiography guidance were used for characterization of an atheromatous plaque in the femoral artery of the animal. Upon verification of a plaque, the skin was cleaned and shaved before placement of a coupling bolus filled with degassed water. The integrated transducer assembly consisting of a 64-element fenestrated 3.5 MHz DMUA and linear array imaging probe inserted within the fenestration with a friction lock were mounted on a 3-axis positioning system. Imaging with both the DMUA and diagnostic probe were used for guidance of the femoral artery. Discrete and contiguous lesion formation was achieved with estimated focal intensities of 4000-5600 w/cm2 and 500-2000 msec duration were performed in multiple planes across the plaque. Imaging with both the DMUA and diagnostic transducer was interleaved with pulsed HIFU during therapy and stored for further analysis of the lesion formation. After the procedure, the animal was recovered and survived up to 7 days for histopathological analysis. Upon sacrifice, the femoral artery was pressure perfused and sections were fixed and stained with hematoxylin and eosin (H&E) to characterize HIFU-induced lesions.

Results and Conclusions: Localized thermal lesion formation indicative of discrete and contiguous thermal lesions for the given protocol respectively was histologically observed with the lesions containing necrotic cores and the periphery infiltrated by neutrophils. In addition, there were no apparent signs of perforation of the vessel or damage to the intima with all damage being confined to the plaque tissue. These results have shown the feasibility of targeting fine vascular structures such as atheromatous plaques for precise lesion formation with an integrated DMUA transducer. The ability of the treatment to affect the progression of atheromatous plaques is currently being investigated using a larger cohort of FH swine and longer follow up times.

Acknowledgements (Funding): This work is partially sponsored by a grant from International Cardio Corporation and NIH NIBIB (EB009750 & EB008191). The authors would also like to acknowledge American Preclinical Services, and Mitchell Troutman in particular for their help with the in vivo study.

38-BT

Tuesday
16 October 2012

Topic: Breast Tumors
Presentation Type: Oral

MRgFUS of Breast Cancer: Its Efficacy and Safety In the Clinical Studies

Hidemi Furusawa

Breastopia Namba Hospital, MIyazaki, Japan

Background/Introduction: Breast cancer is not the disease but just the living thing which someday will bring the real disease. The invasive breast cancer has already gone out from the breast to the systemic organs at the time of being diagnosed. Therefore the local treatment of breast cancer less contribute to the prognosis and the goal of it is to eradicate completely the cancer cells from the breast. This had been proven by some randomized clinical trials; mastectomy versus breast conserving therapy. On the other hand,MRI is the best modality in spatial resolution which can detect the ductal spread of the invasive breast cancer. Thermal ablation of breast cancer by HIFU under MRI guidance will be superior to US guidance. Two excision studies to investigate pathological efficacy and clinical safety of MRgFUS for breast cancer were conducted and their outcomes have been published. The excisionless study is on going.

Methods: To inspect clinical efficacy and safety of MRgFUS for breast cancer and to confirm iprovement in soft ware version-up. Non randomized studies. The main inclusion criteria: 1) well demarcated mass in contrast enhance MRI, 2) tumor size less than 15mm, 3) diagnosed by needle biopsy and confirmd receptor status. The main exclusion criteria: 1) pure type mucinous carcinoma, 2) tumor location which requires a high sonication angle. After diagnosis of no residual viable cancer, radiotherapy should be perfomed for the breast. The patients are followed by every three to six months contrast enhance MRI. The medical records and the documant files were looked back.

Results and Conclusions: Severe skin burn developed in one case of the excision study. The weighted elongated spot was developed to overcome the anterior vertical shift and to keep the skin away from burn. Seventy six patients were enrolled in the excisionless study and sixty three lesions were treated. The median age was 57 years old(29-79).The average tumor size was 11.0 mm(5-15). The median follow-up period was 53 months(2-84). Twenty seven cases have been followed for more than 60 months. There were no severe adverse events, no local recurrence and no distant recurremce cases. It is able to recognize efficacy in the excisionless clinical findings. The firmness is a physical characteristic of the treated region. It has last for several years. This finding faded away at the early time no radiation cases who were out of the study; commercial treatment. The most popular finding of mammoggrams is the oil cyst-like circumscribed mass with or without calcification. Only the distortion of the breast tissue is seen in a few cases. The ultrasonographical finding is the hypoechoic mass with heterogeneous internal echo and the posterior echo attenuation whch means the granuloma formation. Although the edema and /or inflammation is observed for several years in MRI, no enhanced mass is seen right after the initial treatment.

In conclusion, the cause of the anterior vertical shift are guessed the relation between the breast tissue interfaces on the pathway of ultrasound beams and the acoustic energy. The weighted elongate spot has been solving this issue. The efficacy of MRgFUS can be recognized physical and image findings. The ultrasonography may be not so useful as the follow-up image after treatment. The elastography will be useful to know the effectiveness. The mammographical findings suggest that the acoustic energy is too much to to treat the fat tissue rich breast. Radiotherapy likely to delay the wound healing. Although the number cases is still small and the follw-up priod is rather short, MRgfUS has the potential of replacing usual surgery. Strict case selection is essential.

39-BT

Tuesday
16 October 2012

Topic: Breast Tumors
Presentation Type: Oral

Clinical Study Design For the Evaluation of Volumetric MRI-Guided High-Intensity Focused Ultrasound of Breast Cancer Using A Dedicated MR-HIFU Breast System

Laura Merckel[1], Roel Deckers[1], Max Köhler[2], Willem Mali[1], Chrit Moonen[1], Lambertus Bartels[1], Maurice van den Bosch[1]

[1]University Medical Center Utrecht, Utrecht, Netherlands
[2]Philips Healthcare, Vantaa, Finland

Background/Introduction: A dedicated MR-HIFU breast system has been designed for MR-HIFU treatment of breast tumors. In this feasibility study, safety and treatment accuracy of MR-HIFU ablation in patients with breast cancer will be assessed using this dedicated system.

Methods: A total of 10 female patients with pathologically proven invasive breast cancer after large-core needle biopsy will be included for MR-HIFU treatment according to a treat-and-resect protocol. Prior to MR-HIFU ablation, all eligible patients will undergo dynamic contrast-enhanced T1-weighted imaging of the breast for planning purposes. MR-HIFU ablation is performed using a dedicated MR-HIFU breast system (Sonalleve Breast MR-HIFU, Philips Healthcare, Vantaa, Finland) in a standard 1.5 Tesla MRI scanner (Achieva, Philips Healthcare, Best, The Netherlands). The system consists of a water-filled table top with a breast cup in the center of the table (figure 1). Patients will be placed in prone position with the target breast in the water-filled breast cup, which is surrounded by eight separate 32-element focused ultrasound modules in a circle of 270 degrees (figure 2). Breast ablation will be performed using a volumetric ablation technique. During the sonications, fat-suppressed PRFS-based thermometry will be employed, which is complemented with a look-up-table-based mutibaseline approach to correct for temperature errors induced by respiration. The optimization and evaluation of the thermometry technique is reported in a separate abstract. Furthermore, dynamic T2 mapping will be performed to analyze whether this technique can further improve treatment safety by monitoring changes in temperature within the adipose breast tissue.

Results and Conclusions: At the moment of writing this abstract, our study protocol had recently been approved by the institutional review board of the University Medical Center Utrecht. The first endpoint of this study is treatment accuracy, which is defined as the agreement between ablated volumes and MR thermal dose predicted treatment volumes, and histopathology. This endpoint is achieved by partial tumor ablation. The residual non-ablated tissue can be used for appropriate tumor grading. The second endpoint of this study is safety, for which complications and adverse events during and after MR-HIFU treatment will be reported. In this treat-and-resect study, surgery will be performed between 48 hours and one week following MR-HIFU treatment. If indicated, patients will undergo a sentinel node procedure with peritumoral injection of a radioactive colloid just prior to surgery. Additional treatment and follow-up will be done according to standard clinical practice. The first patient inclusion is expected in August 2012. We expect to present the first results from treatment of patients with breast cancer using a novel and dedicated MR-HIFU breast system.

Acknowledgements (Funding): This research was supported by the Center for Translational Molecular Medicine (VOLTA).

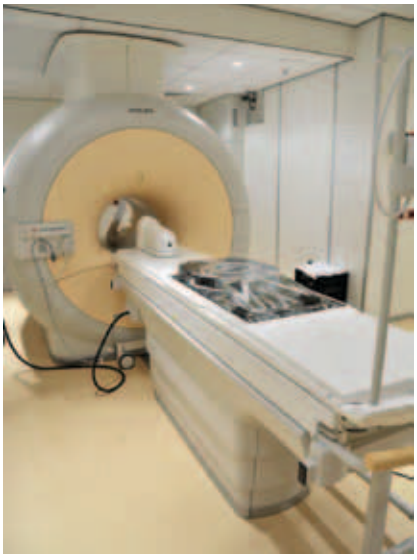

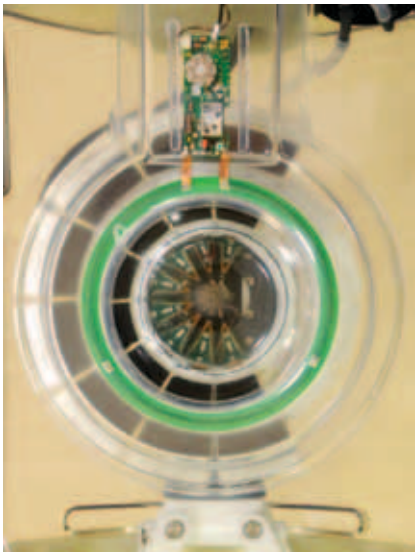

Left: The MR-HIFU breast platform consists of a water-filled table top which is integrated into a clinical 1.5 Tesla MRI scanner. During MR-HIFU treatment, the target breast will be positioned in the breast cup, which is positioned in the center of the table top.

Right: Eight separate focused ultrasound modules with 32 transducer elements each form a circular structure of 270 degrees surrounding the breast cup.

Ultrasound-Guided High-Intensity-Focused-Ultrasound (HIFU) Treatment of Breast Fibroadenoma

Roussanka Kovatcheva[1], Julian Stoinov[1], Jean Noël Guglielmina[2], Bernard Seror[2], Marc Abehsera[2]

[1]University Hospital of Endocrinology, Sofia, Bulgaria
[2]American Hospital of Paris, Neuilly Sur Seine, France

Background/Introduction: Breast fibroadenoma (FA) is the most common benign breast tumor in young women. It is a well-circumscribed lesion, easily distinguishable from normal breast tissue on ultrasound images. The diagnosis is based on the combination of clinical examination, imaging and non-surgical tissue biopsy. Surgical resection of the FA is achieved when the fibroadenoma is troublesome because of its size or location, or it is causing a major anxiety in the patient.

Ultrasound-guided High Intensity Focused Ultrasound (USg HIFU) is an alternative to the surgical treatment. HIFU penetrates through soft tissues and causes localized hyperthermia (around 80°C) responsible of irreversible cell damage, protein denaturation and coagulation necrosis, whereas overlying and surrounding tissues are spared. The objective of our study was to demonstrate the feasibility, safety and efficacy of USg HIFU in the treatment of the breast fibroadenoma.

Methods: To date, 23 patients at a mean age of 29 (16-52) have been treated. The HIFU treatment was performed with a focused piezoelectric transducer with 3 MHz resonant frequency. The ultrasound guidance was realized with an imaging transducer of 7.5 to 12 MHz frequency, integrated at the center of the treatment head, to allow perfect alignment between the imaging and the focal point.

The diagnosis of FA was confirmed with tissue biopsy and histology. Were excluded pregnant or lactating women, patients with microcalcifications at the mammogram, patients with history of breast cancer or with breast implant in the target breast. 16 patients presented one FA and 7 patients at least 2 FA. The lesions mean volume was 2.59 cm^3 (0,4 - 10,4 cm^3). The HIFU treatment was performed as an outpatient procedure using neurolept analgesia. All patients gave a written informed consent. The post treatment follow-up included physical examination at one week, ultrasound and Color Doppler examination every month (M) from M1 to M6, M9 and M12. Adverse events as edema, pain and skin damage were analyzed.

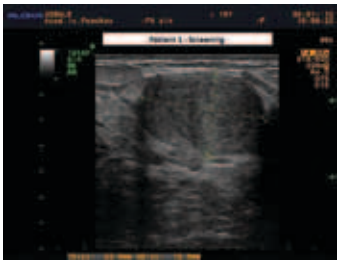

Figure 1. Patient 1: Ultrasonography performed 3 months post HIFU

Results and Conclusions: The average treatment time was around 1h23 (0h30-2h30). Volume reductions were on average 18.5% [1,5-44,4%] at M1 (n=15), 35% [6,4-62,7%] at M2 (n=13), 50.6% [28,8-77,4%] at M3 (n=10) (Figure 1, 2), 55.5% [40,8-64.6%] at M6 (n=4) and 68,5% (63,9-73%) at M12.

A patient who became pregnant one month after the HIFU treatment, showed a reduction of volume of 73% at M12 (Figure 3, 4) despite the total enlargement of the breast. Breastfeeding has been achieved without any complications. Three patients among 23 presented signs of skin irritation following the treatment that disappeared within 15 days. No other adverse events were observed.

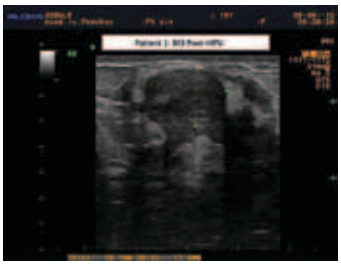

Figure 2. Screening ultrasonography of Patient 2. This patient has been treated by HIFU in May 2011

Conclusion: HIFU is a non-invasive and effective treatment method for breast FA, well tolerated by the patients. Preliminary results are encouraging and show that HIFU could be an alternative to surgery for benign breast tumors.

Acknowledgements (Funding): This study is funded by THERACLION France.

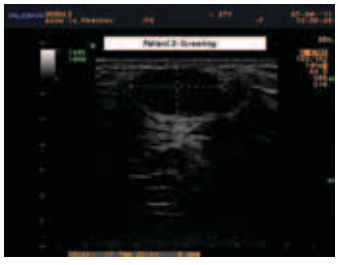

Figure 3. Patient 2: Ultrasonography performed 12 months post HIFU

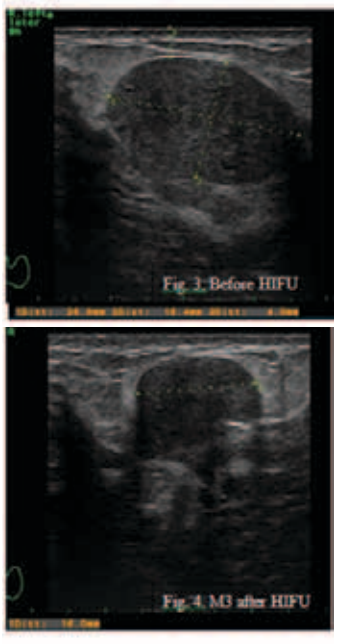

Figure 4. Screening ultrasonography of Patient 1. This patient has been treated by HIFU in March 2012

41-BT

Tuesday
16 October 2012

Topic: Breast Tumors
Presentation Type: Oral

In Vivo Evaluation of a Breast-Specific MRgFUS System in a Goat Udder Model

Allison Payne[1], Yi Wang[2], Henrik Odeen[2], Mahamadou Diakite[2], Leigh Neumayer[3], Nick Todd[2], Dennis Parker[2]

[1]Utah Center fo Advanced Imaging Research at University of Utah, Salt Lake City, Utah, United States
[2]University of Utah, Salt Lake City, Utah, United States
[3]Huntsman Cancer Institute, Salt Lake City, Utah, United States

Background/Introduction: Magnetic resonance-guided focused ultrasound (MRgFUS) has the potential to provide completely non-invasive treatments for women with breast cancer, adding to the treatment options available. In this work the efficacy of a breast-specific MRgFUS device[1,2] that has been developed by the University of Utah, Image Guided Therapy and Siemens is evaluated in an in vivo goat udder model. The volume of tissue ablated is assessed through the measurement of accumulated thermal dose and the non-enhancing tissue volume measured during delayed contrast enhanced MRI both immediately post-ablation and 14 days post ablation. Histological analysis was performed on a limited number of animals.

Methods: Eight female goats (22-52 kg) are currently enrolled or have completed the study. Six goats were actively nursing kids during the study. All experiments were conducted in a Siemens Trio 3T scanner. The pre-treatment protocol consisted of animal positioning, focal spot localization, and multi-contrast image acquisition (3-point Dixon, T2w TSE, T1w VIBE) for tissue type determination. Ablations were monitored using a real-time 3D segmented EPI MR temperature imaging sequence (TR/TE = 35/10 ms, FA = 15°, 2x2x2 mm, 4.9 s, FOV=256x190x28 mm, 752 Hz/pixel). A variable sized Z-pattern trajectory was used in all animals (1-2 planes with 10 mm spacing, 9-25 points/plane with 2 mm spacing, theat=45-60 s/point, Qacous=52-70W). Immediately post-treatment, delayed contrast-enhanced imaging was performed at several time points. The pre- and post-treatment imaging sequences were repeated approximately 14 days after MRgFUS treatment. One goat underwent a localized tissue-excision procedure 21 days after MRgFUS treatment. One goat was euthanized 21 days after the MRgFUS treatment for health reason unrelated to the study and the entire udder was removed for histological analysis.

Results and Conclusions: All animals tolerated the treatment very well, with the administration of minimal analgesics required. All goats were able to nurse their kids within 12 hours after HIFU ablation. To date, a mean volume of 1.93 cm^3 of tissue received a thermal dose of greater than 240 CEM43°C. Table 1 lists treatment results for each animal. The non-enhancing tissue volume was reduced by an average of 31% 14 days after the MRgFUS treatment. All ablated volumes appeared to have a hemorrhagic core immediately post-treatment. Animals with volumes ablated approximately 2 cm^3 or greater had significant edematous tissue present. This edematous tissue seems to correspond to a larger non-enhancing tissue volume when compared to the accumulated thermal dose volume (animals 4-6). Histological analysis shows features indicative of ischemic necrosis including vessel wall thickening, atrophic lobules and hyalinization of tissues.

The breast-specific MRgFUS system provides excellent SNR for accurate imaging during all aspects of the treatment. While there is some discrepancy between the thermal dose accumulated and non-enhancing regions in some animals, this system can ablate volume sizes appropriate for breast lesions with minimal near-field heating.

Goat No.	Total ablation time (min)	Max Temp Rise (°C)	Mean Temp Std (°C)	Max Temp Rise in near-field (°C)	Ablation Volume (cm^3)		
					> 240 CEM43°C	10 min. post-treatment	14 days post-treatment
1	1.35	26.7	0.25	3.1	0.42	0.23	n/a
2	14.5	33.0	0.66	4.2	1.23	1.1	0.9
3	12.0	39.9	0.90	4.4	1.17	0.95	0.24
4	24.5	39.5	0.44	2.1	1.93	4.42	4.31
5	24.0	43.1	0.28	3.4	3.21	6.12	**
6	15.0	39.1	0.62	4.9	3.60	2.88	**
7	**	**	**	**	**	**	**
8	**	**	**	**	**	**	**

Table 1. MRgFUS treatment results (**study still in progress). Near-field temperature measurements were obtained 2 cm proximal to the focal zone.

Acknowledgements (Funding): This work was funded by NIH grant R01 CA134599 and the Margolis Foundation.

References:

1. Payne, A. et al., *Med Phys*, 39, 1552, 2012.
2. Minalga, E. et al., *MRM*, 2012, in press.

42-BT

Tuesday
16 October 2012

Topic: Breast Tumors
Presentation Type: Oral

Optimizing MR Thermometry for Clinical Phase I Breast Tumor Ablation Study

Roel Deckers[1], Laura Merckel[1], Gerald Schubert[2], Maurice van den Bosch[1], Max Köhler[2], Lambertus Bartels[1]

[1]University Medical Center Utrecht, Utrecht, Netherlands
[2]Philips Healthcare, Vantaa, Finland

Background/Introduction: Several groups have shown that MR guided HIFU (MR-HIFU) holds promise for treating breast cancer[1,2]. To date, all patients have been treated in prone position on generic HIFU systems with the incident beam path directed towards the thoracic cage. This approach may result in significant heating and possible thermal damage of the tissues in the far field. Recently, a dedicated breast HIFU system was developed[3]. In this system an array of laterally sonicating transducer pads surrounds the free hanging breast thereby reducing the risk of excessive heating in the far field. At the time of writing of this abstract we have obtained IRB approval for performing a clinical phase I study in 10 patients to investigate safety and technical efficacy of this dedicated system. In preparation of the clinical study, we set out to optimize the PRFS-based thermometry sequence and the performance of the multi-baseline (MBL) algorithm for correcting respiration induced susceptibility artifacts in volunteers on this dedicated system[4].

Methods: All experiments were performed on a dedicated breast MR-HIFU system (Philips Sonalleve® Breast MR-HIFU, Philips Healthcare, Vantaa, Finland) integrated with a clinical 1.5-T MRI scanner (Achieva, Philips Healthcare, Best, The Netherlands). Volunteers (n = 10) were in the age of 25-60 years.

First, several prerequisites for the PRFS-based thermometry sequence were determined and fixed at the start of the optimization procedure, such as spatial resolution (1.67x1.67x5.0 mm3), number of slices (4), and the maximum acceptable dynamic scan time (3.5 s). Within these restrictions, the echo time (TE) and flip angle (FA) leading to the lowest temperature standard deviation were determined experimentally. Gradient Echo (GE) images with different TEs (10, 20, 30, 40, 50 ms) at and FAs (10, 20, 30, 40, 50°) were acquired during one breath hold (duration 15.6 s, 50 dynamics). The obtained temperature temporal standard deviation was calculated on a voxel-by-voxel basis.

T2* measurements were performed in glandular tissue using a multi-echo GE sequence (TR = 153 ms, 32 TEs, TE1/ΔTE = 1.23/2.0 ms, 1.6x1.6x5.0 mm3). T2*-values were determined by performing an exponential fit to the signal decay as function of increasing TE.

The best PRFS-based thermometry sequence found was then used for evaluating the performance of the MBL algorithm.

Results and Conclusions: Figure 1 shows a typical example of the temperature standard deviation as function of TE and FA. In all volunteers the optimal TE and FA were 30 ms and 20°, respectively. The experimentally found optimal TE corresponds closely with the T2* of the tissue which was found to be on average 33.3 ms for the glandular tissue in all volunteers. The experimentally found optimal FA corresponds to the Ernst angle (i.e. 19.9°) assuming a T1-value of 1266 ms[5]. Figure 2 shows temperature standard deviation maps during free breathing without (a) and with MBL correction (b). After MBL correction the temperature standard deviation is reduced to about 1.5° C.

Temperature standard deviation as function of echo time with a fixed FA of 30Â° (a) and as function of flip angle with a fixed TE of 30 ms (b).

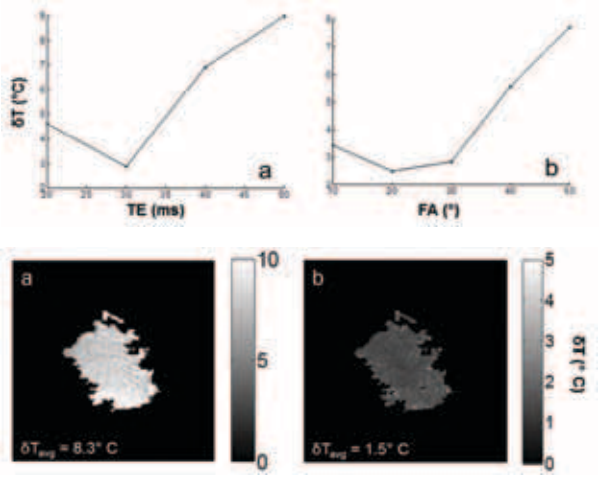

Temperature standard deviation maps during free breathing before (a) and after using the MBL (b) for correcting the respiration artifacts.

The optimization of the scan parameters as well as the use of the MBL algorithm was found to drastically improve the thermometry precision. The obtained optimal settings will be used for temperature monitoring during the upcoming phase I clinical trial for breast tumor ablation on this dedicated MR-HIFU system.

Acknowledgements (Funding): CTMM (VOLTA)

References

1. Huber, 2001, *Cancer Res.*
2. Gianfelice, 2003, *Radiol.*
3. Mougenot, 2011, *ISMRM*
4. Hey, 2009, *MRM*
5. Rakow-Penner, 2006, *JMRI*

43-BT

Tuesday
16 October 2012

Topic: Breast Tumors
Presentation Type: Oral

Internal Fiducial Tattoos Made with FUS for Surgical or Radiotherapy Image Guidance

Elizabeth Hipp[1], Xiaobing Fan[1], Ari Partanen[2], James Vosicky[1], Christopher Straus[1], Charles Pelizzari[1], Gregory Karczmar[1]

[1]University of Chicago, Chicago, Illinois, United States
[2]Philips Healthcare, Bethesda, Maryland, United States

Background/Introduction: Breast conservation is performed for cancer patients whenever possible. In order for this technique to be successful the lesion must be easily located for surgical removal and the subsequent post-resection tumor bed must be easily located for targeted radiotherapy. An internal fiducial tattoo mark, visible to the naked eye and conspicuous on imaging may be of interest. It is well known that FUS can induce visible lesions. This work investigates the use of FUS to create internal tattoo marks. Their visibility on MRI, CT and US are assessed.

Methods: New Zealand rabbits (n=6) were anesthetized, their hind limb placed in a degassed water bath. An integrated Philips MRgFUS platform was used for sonications and MR guidance. Images were acquired using a 3D T2W Turbo spin echo sequence (TR/TE =1000/130 ms, voxel size=1.2 mm). Dynamic temperature monitoring was performed using 2D fast field echo EPI (slice thickness 7 mm, in plane resolution 1.25 mm, temporal resolution 2.9 s). A sonication sequence consisting of a pulsed exposure followed by a volumetric ablation was performed. After sonication, rabbits were sacrificed and imaging was performed using clinical Philips CT and Siemens US. Surgical excision was performed and documented photographically. MRI and CT images were read by a radiologist who drew ROIs for statistical analysis and comparison. Comparing paired non-parametric groups was done with a Wilcoxon signed rank test.

Results and Conclusions: Of a total of 19 excised tattoos, approximately 79%, 63%, and 62% of them were visible on MRI, CT, and US, respectively. Using focused ultrasound, internal marks were created that could be detected on MRI, CT and with visual inspection at the time of surgical excision. MRI shows distinct and isolated tattoo marks generally presenting as a contiguous oval involving multiple muscle bundles, as previously reported. CT shows a radiolucent abnormal oval structure in the rabbit thigh muscles that is consistent with marks detected by MRI and found at excision. The average HU of the tattoos on CT is smaller than normal rabbit thigh muscle ($p<0.001$).

We have developed a method for marking in vivo muscle tissues. MRgFUS-generated tattoos are visible on MRI, CT and with visual excision. These marks or internal tattoos could guide surgical procedures. They may also provide fiducials for deformable registration CT. Further development is necessary to improve conspicuity for cone beam CT (which is sensitive to scatter and often masks low contrast objects) to assist in radiotherapy treatment planning. This preliminary preclinical study demonstrates that FUS may be useful for guiding surgical or radiotherapy procedures after continued development. Future work on marking other tissues – specifically those more closely modeling the fatty nature of the breast, is necessary.

Acknowledgements (Funding): The authors are grateful to the Focused Ultrasound Foundation, Philips Healthcare, and Elizabeth Lanzl for their support of this project.

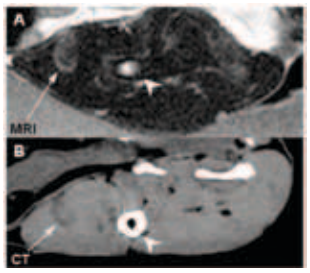

An example of a FUS tattoo shown on the MRI (A), and CT (B). The white chevron arrow marks the femur. The long arrow marks the tattoo. The displayed panel for each image is 11 cm Ã— 5 cm.

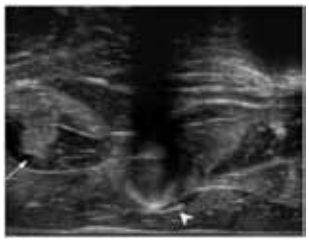

An example of the tattoo on ultrasound, with the wand below the image. The white chevron arrow marks the femur and the long arrow indicates the tattooed region of tissue. The displayed panel for this image is 5 cm Ã— 4 cm.

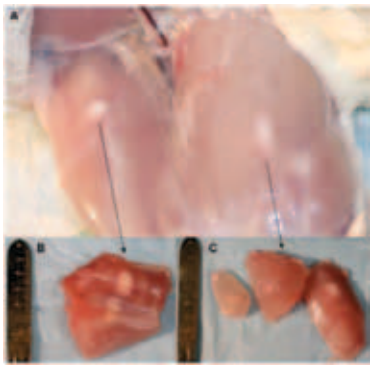

The tattoos in situ at excision (A), after cutting open split in half (B), and as three separate muscle bundles (C).

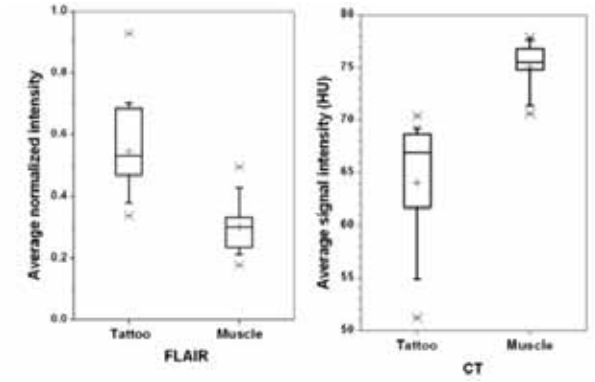

Box plots of the signal intensity (normalized to water) of the tattoos compared to the muscle as seen on FLAIR (left) MR images. Box plots of the signal intensity (HU) of the tattoos compared to the muscle as seen on the (right) CT images.

44-LD

Tuesday
16 October 2012

Topic: Prostate
Presentation Type:
Discussion

Near-Total Gland Ablation of Locally Confined Low and Intermediate Risk Prostate Cancer Using Magnetic Resonance Guided Focused Ultrasound Surgery (MRgFUS)

Abhijit Patil, Shrinivas Desai

Jaslok Hospital and Research Centre, Mumbai, India

Background/Introduction: In May, 2010, Jaslok Hospital and Research Centre, Mumbai, India has installed an ExAblate® Magnetic Resonance Guided Focused Ultrasound Surgery (MRgFUS) multi-application platform, (InSightec, Tirat Carmel, Israel), in the 1.5T GE (General Electric) MRI suite.

Locally confined prostate cancer is frequently an indolent disease which is currently being frequently over-treated by various radical treatment modalities involving a significant complication rate and long lasting morbidity. Due to the severity of therapeutic adverse events and morbidity from one hand and the frequent relatively low risk for disease progression, many patients are reluctant to undergo definitive treatments and instead they remain under active surveillance. However, active surveillance involves significant psychological and financial burden, as well as some risk for undetected cancer progression. Thus, focal or near-total gland ablation may offer to patients with low and intermediate risk prostate cancer a middle ground solution in which, the prostate tissue suspected to bear cancerous foci is ablated, while functional structures like rectum, urethral sphincters, bladder wall, and potentially the neurovascular bundles, are preserved.

To date, 5 near-total-gland-ablation-MRgFUS treatments were performed in our hospital for low and intermediate-low-risk prostate cancer patients, with proven locally-confined disease.

Methods: In the study were included patients aged 50 years or older with low-risk or intermediate- risk organ-confined prostate cancer, diagnosed by 12-core TRUS-guided endorectal biopsy; up to Gleason score of 7= 3+4 (Not 4+3 and no 5 scores); PSA <15 ng/dl and no contraindications to MRI; maximum prostate gland volume was not greater than 40cc. Patients should also be eligible for epidural or general anesthesia and willing and able to give consent and attend all study visits as defined in the protocol.

Results and Conclusions: By now we treated under this study protocol 5 patients with low and intermediate risk prostate cancer. All the patients were in the age group 50 to 85 yrs. All prostate volumes were less than 40cc and PSA LEVELS were between 5 to 15ng/ml before treatment. Cancerous foci were invisible on screening multifunctional MRI scans in all five patients. Neurovascular bundles were bilaterally preserved in the treatment of the two young patients, unilaterally preserved in treatment of one patient. These patients reported pre-treatment good erectile function.

In all the patients the suprapubic catheters were removed between 3 to 5 weeks. No incontinence was reported.

At 6 weeks follow-up, PSA levels dropped from baseline of 5 to 15ng/ml to 1to 3.8 ng/ml in all the 5 patients

Near-total gland ablation using Magnetic Resonance guided Focused Ultrasound seems like a potentially safe minimally invasive therapeutic alternative for young potent or elderly patients with low and intermediate risk prostate cancer, for whom surgery, cryoablation or radiotherapy might be aggressive and mutilating, however more data need to be obtained.

45-LD

Tuesday
16 October 2012

Topic: Prostate
Presentation Type: Discussion

Preliminary Clinical Experience of Treating Low-Risk Prostate Cancer with the Use of the ExAblate® Magnetic Resonance Guided Focused Ultrasound Surgery (MRgFUS)

Vladimir Turkevich, Sergey Kanaev, Aleksandr Nosov, Andrei Mishchenko, Maxim Molchanov, Sergei Rozengard

Petrov Research Institute of Oncology, Saint Petersburg, Russian Federation

Background/Introduction: In the ExAblate® system (InSightec, Haifa, Israel), focused ultrasound energy is transmitted from an endorectal transducer into the prostate. The rectal wall is protected from overheating by circulation of degassed cold water (14°C) circulated in a single use balloon enwrapping the endorectal transducer. In Petrov Research Institute of Oncology, (St. Petersburg, Russia), we were the first to use the ExAblate® system with a 1.5 T GE MRI, for treating patients with locally-confined low-risk prostate cancer. The current abstract presents preliminary results of the first eight that we patients treated with this device.

Methods: Patients with elevated PSA <10ng/ml; with previously confirmed or suspected prostate cancer where offered to participate in the study. Those who signed an informed consent were evaluated for their eligibility for the treatment. Evaluation included, MRI compliance, absence of previous or current rectal diseases, no previous therapies for prostate cancer, screening CT, multifunctional MRI, and mapping biopsies. Treatment was performed in the MRI suite, under epidural anesthesia with conscious sedation, and with continuous draining the urinary bladder by a Foley catheter. equipment. Patients were followed for 6 months and periodically evaluated for the occurrence and severity of adverse events; validated self-reported quality of life questionnaires were used to assess post-treatment quality of life, including, urinary symptoms, incontinence and sexual function. Preliminary efficacy was evaluated by repeated mapping biopsy at 6-month follow-up. In addition PSA levels were taken at baseline, and at 1, 3 and 6 months post-treatment.

Results and Conclusions: From Feb 2010 to Dec 2011, seven eligible patients underwent eight MRgFUS treatments. One patient underwent a second treatment due to a newly detected cancerous focus at 6-month follow-up mapping biopsy. More treatments are planned. Patients' mean age at treatment was 61.4 years (range, 49 to 71 years). All patients were stage 1C clinically. In Seven cases a single tumor focus was detected; one treatment was done for two biopsy proven tumor foci, both foci were separately targeted. Six patients were potent at before treatment, four of them returned to baseline sexual and erectile function within 3 months from treatment; for two of them, only one month follow-up is available by now, which is still too soon for post-treatment potency evaluation. According to these preliminary findings, ExAblate® has the potential of being a very attractive management option for patients with early low risk prostate cancer, encountering the dilemma of choosing between active surveillance and some definitive mutilating treatment. The ability to repeat the treatment without increased safety risk when a new cancerous focus is detected makes this treatment especially appealing in light of the current limitations to identify low grade, small, intracapsular cancer foci by imaging or biopsy.

46-LD

Tuesday
16 October 2012

Topic: Prostate
Presentation Type:
Discussion

MR-guided Focused Ultrasound Treatment in Patients with Organ-Confined Prostate Cancer: An Initial Experience

Young Taik Oh, Sung Joon Hong, Koon Ho Rha, Won Sik Ham, Mi-Suk Park, Kwang Hyun Kim, Dae Chul Chung

Yonsei University College of Medicine, Seoul, South Korea

Background/Introduction: Non-surgical treatment of prostate cancer is an emerging strategy in treatment of prostate cancer. The magnetic resonance (MR)-guided focused ultrasound (MRgFUS, ExAblate® 2100 System), integration of Therapeutic Focused Ultrasound with Magnetic Resonance Imaging, is a non-invasive thermal ablation device and can provide several advantages for the treatment of locally confined prostate cancer with MR thermometry, visualization of prostate tumor and monitoring the treatment to avoid/minimize damage to the neurovascular bundle. Therefore, MRgFUS has the potential of real-time personalized treatment modulation for achieving optimized treatment outcome. Here, we are presenting our initial experiences of MRgFUS for the treatment of organ-confined prostate cancer.

Methods: Among referred patients, 3 patients with prostate cancer were included in our initial screening process and finally 2 patients received the MRgFUS treatments. Prostate cancers were confirmed by transrectal ultrasound-guided biopsy. The suprapubic catheters (SPCs) were inserted into the bladder on both patients because urethra was included in ablation site. We evaluated the ablation volume and immediate clinical findings regarding first voiding time through urethra, indwelling time of SPCs, potency, any medical or surgical complications.

Results and Conclusions: The first patient showed 15 cc ablation volume and the first self-voiding occurred 8 days after procedure. He carried the SPC for 4 weeks. He showed same strength in potency. He complained discomfort around prostate but none of severe complications for 2month followed period. The second patient showed 17 cc ablation volume. The first self-voiding occurred 12 days after treatment and SPCs were removed at 15 days. Potency became weaken. He complained pain on buttock but none of severe complications for 19 days followed period. Although our experience was initial, MRgFUS treatment for prostate cancer seems to be safe and feasible treatment option for organ confined prostate cancer.

47-LD

Tuesday
16 October 2012

Topic: Prostate
Presentation Type:
Discussion

Feasibility Study to Evaluate the Safety and Preliminary Effectiveness of Focal MR-Guided Focused Ultrasound Surgery (MRgFUS) for Locally Confined Low-Risk Prostate Cancer: the First North American Experience

Sangeet Ghai, Uri Lindner, Masoom Haider, Walter Kucharczyk, Stuart McCluskey, Theodorus van der Kwast, John Trachtenberg

University Health Network, University of Toronto, Toronto, Canada

Background/Introduction: Prostate cancer (PCa) is one of the most frequently diagnosed cancers in the male population in the world. Men diagnosed with localized low risk prostate cancer and a significant life expectancy are usually offered the choice of two broad therapeutic options, either active treatment with surgery or irradiation with almost certain impairment in quality of life (i.e., sexual, genitourinary, or bowel dysfunction), or active surveillance (AS), with the low but real risk of disease progression and possibly death. Moreover, AS necessitates very long periods of careful clinical, biochemical, and histologic observation involving significant burden to the patient and health care systems, as well as long-term psychological pressure. The aim of focal treatment is to find in these men the best balance between oncologic control and maintenance of quality of life. Focal ablation of the index cancer, or the prostate section that harbors that cancer, could be very attractive for patients with low-risk cancers who are uncomfortable with the risks associated with active surveillance or the side effects of radical therapy.

Multi-parametric MRI (mp-MRI) imaging utilizing T2-weighted, diffusion weighted (DWI) and dynamic contrast enhanced MRI (DCE) represents the state of the art imaging technique for detection, localization, staging and also characterization of tumor aggressiveness of PCa. This advantage makes MRI the more suitable technique for targeting focal cancer lesions in the prostate. MRI can also identify nerve bundles and provide real-time MR thermometry, thereby allowing closed loop monitoring and controlling the treatment to ensure selective and adequate tumor ablation. Therefore, MR-guided focused ultrasound (MRgFUS) has the potential of focally treating prostate tumors (instead of the entire prostate), while reducing the risk of incontinence and impotence.

Purpose: To develope preliminary data to evaluate the safety and preliminary effectiveness of focal MRgFUS treatment of low risk prostate cancer.

Methods: A 51 year old patient with Gleason 6 (3+3) prostate cancer on previous biopsy was consented and enrolled in this IRB approved single-center, single-arm, prospective study. The patient was assessed for eligibility by mp-MRI, Transrectal extended mapping biopsy. No MRI target was identified on the mp-MRI, and a transrectal sixteen core mapping biopsy was performed as per protocol. This included 4 samples from peri-urethral locations (2 on each side), to map the medial extent of the tumor. Proximal end of each biopsy sample was inked. Biopsy results revealed Gleason 6 (3+3) cancer in right lateral and right medial samples at the level of the mid-gland, but not in the right peri-urethral samples. Since the tumor was not visible on T2w imaging, the treatment target volume included the two sectors from which the cores were positive. CT ruled out calcifications near the rectum, where the beam was supposed to pass. MRgFUS treatment was performed under general anesthesia one month after the biopsy as an outpatient procedure. A Foley's catheter was placed prior to treatment for continuous bladder drainage. Five macrosonications were required to treat the volume comprising the tumor. An additional regular sonication was used at the end to cover a marginal dose region at the lateral aspect of the region of treatment.

Results and Conclusions: The patient was in the magnet for a total time of 3.5 hours, of which the treatment time was approximately 70 minutes. The prescribed volume of treatment was 3.6cc (total prostate volume of 26cc). The immediate post-treatment non perfused volume (NPV) was 3.8cc. Foley's catheter was removed within 2 hours of the procedure and the patient was able to void spontaneously before discharge from the hospital 3 hours post treatment. There was no immediate complication following the procedure and the patient had no adverse symptoms at time of discharge. Also, there was no treatment related voiding or potency side effect at 1 week follow-up.

Efficacy will be assessed at 6 months post-treatment, using repeat extended transrectal mapping biopsy of the prostate and by periodic PSA. Post-therapy changes from baseline to 6 months in patient's status secondary to his prostate treatment and satisfaction from the

treatment will be assessed using the ICIQ-SF. SF-12, IPSS, and IIEF-15 questionnaires. We expect to treat 4 patients by the time of the Symposium in October.

Acknowledgements (Funding): The study has been sponsored by InSightec.

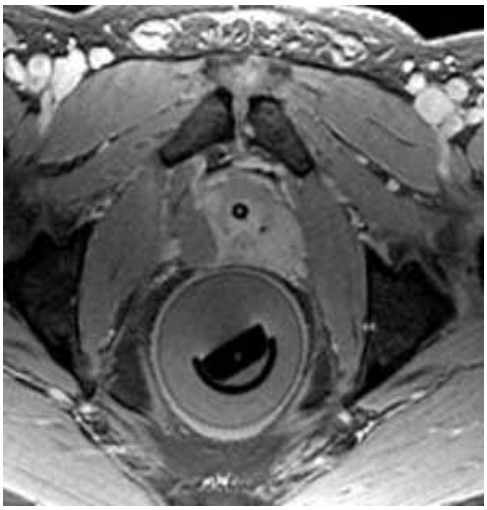

Gadolinum enhanced axial scan post ablation

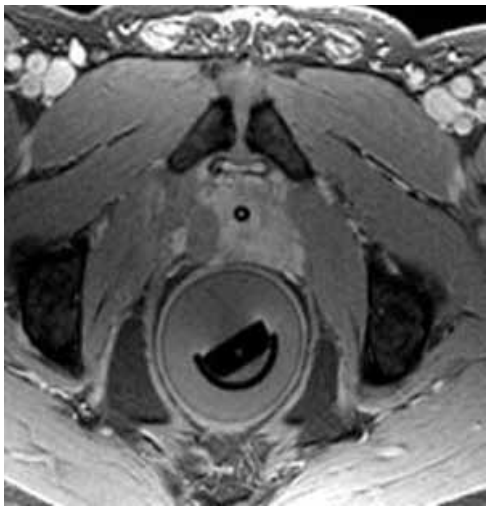

Gadolinum enhanced axial scan post ablation

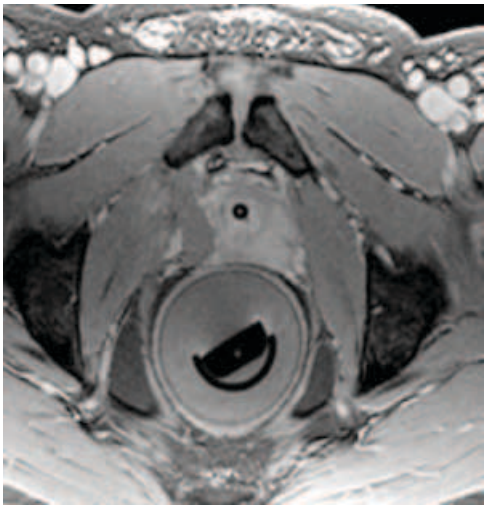

Gadolinum enhanced axial scan post ablation

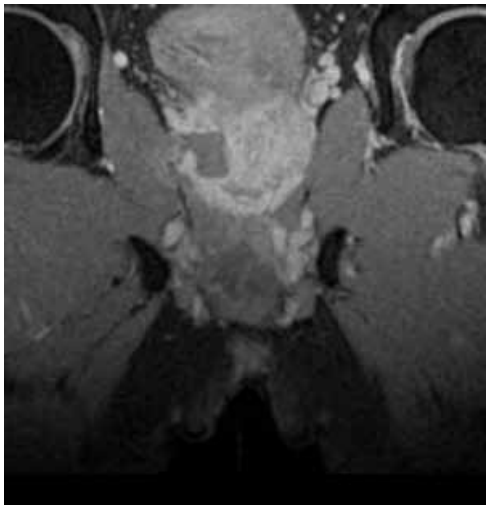

Gadolinum enhanced coronal scan post ablation

48-PR

Tuesday
16 October 2012

Topic: Prostate
Presentation Type: Oral

Evolution and Outcomes of 3 MHz High-Intensity Focused Ultrasound Therapy for Localized Prostate Cancer Over 15 Years

Christian Chaussy[1], Stefan Thüroff[2]

[1]University of Regensburg, Strasslach, Germany
[2]Klinikum Muenchen-Harlaching, Muenchen, Germany

Background/Introduction: High intensity focused ultrasound (HIFU) is an ablative therapy approach for localized prostate cancer (PCa), and over 30,000 procedures have been performed since its introduction 15 years ago.

Aim of the study is to describe the long-term cancer control and morbidity of HIFU with neoadjuvant transurethral resection of the prostate (TURP), the risk of metastatic induction with TURP, and the evolution of HIFU over time.

Methods: A database was searched for patients with primary localized PCa (T1-2, N0, M0, PSA < 50 ng/ml) with follow-up >1 year; those with previous long-term ADT, definitive PCa therapy, or any PSA-influencing therapy were excluded. All patients were treated with Ablatherm® HIFU devices; HIFU retreatment was offered to patients with biopsy-confirmed residual or recurrent PCa. Evaluation was performed in aggregate, and by stratification according to cohort group, risk group (D'Amico criteria), PSA nadir, and Gleason score. Phoenix definition was used for biochemical failure. Statistical analysis was performed using the Kaplan-Meier method, and univariate and multivariate analysis employing a Cox model.

Results and Conclusions: Of 704 study patients, 78.5% had intermediate- or high-risk disease. Mean (range) follow-up was 5.3 (2–14) years. HIFU retreatment rate was 22%. Cancer-specific survival was 99%, metastasis-free survival was 95%, and 10-year salvage treatment-free rates were 98% in low-risk, 72% in intermediate-risk, and 68% in high-risk patients. PSA nadir and Gleason score predicted biochemical failure.

Long-term follow-up with HIFU therapy found a high overall rate of cancer-specific survival and an exceptionally high rate of freedom from salvage therapy requirement in low-risk patients. Advances in technology and practice and the use of neoadjuvant TURP now allow the treatment of patients with any prostate size.

Acknowledgements (Funding): Funding by Lingen Foundation, Cologne, Germany

49-PR

Tuesday
16 October 2012

Topic: Prostate
Presentation Type: Oral

Medium Term Outcomes Following Primary Focal Therapy Using HIFU for Localised Prostate Cancer

Louise Dickinson[1], Hashim Ahmed[1], Neil McCartan[1], Alex Freeman[1], Alex Kirkham[1], Clare Allen[1], Richard Hindley[2], Mark Emberton[1]

[1]University College Hospital, London, United Kingdom
[2]Hampshire Hospitals NHS Foundation Trust, Basingstoke, United Kingdom

Background/Introduction: A limited number of prospective studies have evaluated the role of focal therapy for localised prostate cancer, demonstrating encouraging short-term cancer control with low rates of genito-urinary side-effects. We evaluated the medium term (>2 year) outcomes from trial patients followed-up within a prospective registry.

Methods: Of 118 men with localised prostate cancer (T1c-T3a, Gleason grade ≤4+3, PSA <20) treated (Sonablate® 500 HIFU) in 3 Phase I/II prospective ethics-committee approved trials (hemi, focal, or index lesion ablation), 88 have completed at least 24 months follow-up. Cancer control was assessed using histological outcomes (post-HIFU biopsies of treated or suspicious areas) and biochemical disease-free survival (BDFS) using Stuttgart (PSA nadir + 1.2ng/ml) and Phoenix (PSA nadir + 2ng/ml) criteria. Composite disease free status was defined as histological absence of disease, or BDFS in the absence of post-operative biopsies. Functional outcomes were assessed using validated patient questionnaires (IPSS, IIEF-15, UCLA EPIC-Urinary).

Results and Conclusions: Median follow-up was 32 months (range 24–69). Mean number of focal treatments was 1.2. There was one non-prostate cancer related death. Absence of any cancer was 72% (52/72), and absence of clinically significant cancer (≤3mm Gleason 3+3) was 86% (62/72) on post-operative biopsy. BDFS was 66% (57/87) and 82% (71/87) using Stuttgart and Phoenix criteria, respectively. Composite disease free status was 80% and 86%, using Stuttgart and Phoenix criteria, respectively. Four men (5%) required salvage radiotherapy or adjuvant hormones. Grade III rectal toxicity occurred in 1 man, with resolution on conservative management. Preservation of continence was 99% (86/87) pad-free, and 85% (56/66) leak-free pad-free. The rate of preserved erectile function was 89% (76/85), including 40% new PDE-5 inhibitor use (32/81).

Our results indicate that the short-term functional benefits of focal therapy seem to extend into medium term follow-up, alongside encouraging cancer control. Longer-term outcomes are still required.

Acknowledgements (Funding): These studies were supported by the National Cancer Research Network (UK), Medical Research Council (UK), Prostate Cancer Research Centre, Pelican Cancer Foundation, Prostate Action, and St Peters Trust.

50-PR

Tuesday
16 October 2012

Topic: Prostate
Presentation Type: Oral

Non-Invasive Treatment of Locally Non-Advanced Prostate Cancer: Phase I Study Using Magnetic Resonance Guided High Intensity Focused Ultrasound Technology and Excision Pathology for Efficacy Assessment

Alessandro Napoli, Michele Anzidei, Beatrice Cavallo Marincola, Fulvio Zaccagna, Gaia Cartocci, Fabrizio Boni, Carlo Catalano

University of Rome — Sapienza, Rome, Italy

Background/Introduction: The present choice of treatment for men with localized prostate cancer lies between active surveillance and radical therapy. Thus, the idea of treating only the cancer within the prostate and sparing the non-cancerous tissue in the prostate is quite appealing, yet very controversial. Furthermore, prostate cancer is dogmatically regarded as a heterogeneous and multifocal disease, and is therefore usually treated with a radical whole-gland approach. Radical prostatectomy is an effective therapy for patients with clinically localized prostate cancer. Despite improvements in surgical techniques, urinary incontinence and erectile dysfunction are not uncommon after radical prostatectomy. The International Task Force on Prostate Cancer and the Focal Lesion Paradigm, defined focal therapy for prostate cancer as a therapy that selectively ablates known disease while preserving existing functions, with the overall aim of minimizing lifetime morbidity without compromising life expectancy. Several techniques have been used in the focal treatment of prostate cancer—including microwave and radiofrequency ablation, cryotherapy, photodynamic therapy, and high-intensity focused ultrasound (HIFU) treatment. HIFU is, in several respects, ideally suited to the prostate. Thanks to the transrectal approach, there is little movement of the target because of respiration or reflection by overlying bone. A focal distance of 3 or 4 cm allows the generation of coagulative necrosis in treatment voxels less than 0.2 mL and allows a treatment volume that conforms to the shape of the prostate a degree of precision that may be beyond that of other techniques. Even so, complete ablation is likely to affect periprostatic tissues, including the neurovascular bundles containing the cavernosal nerves and the external urethral sphincter. Preservation of these structures and the patient's erectile and urinary function must be balanced against full treatment of the gland.

Purpose: To assess safety and initial effectiveness of non-invasive high intensity 3T MR guided focused Ultrasound (MRgFUS) treatment of localized prostate cancer in a phase I, treat and resection exploratory designed study.

Methods: 11 patients, scheduled to radical retropubic prostatectomy, with biopsy proven focal T2 prostate cancer, confirmed on a previous multiparametric MR exam including dynamic contrast enhanced (DCE) imaging (Gd-BOPTA, Bracco) with time to peak and mean transit time evaluation, underwent MRgFUS ablation (ExAblate®). Each subject was followed-up at 7 to 30 days after treatment with serum PSA levels prior to surgery. Pre- and post-ablative MR examinations were evaluated to analyze DCE differences.

Results and Conclusions: No significant complications were observed in all subjects during or immediately after the procedure. Tumor features on pre- and post-ablative MR examinations were found to differ on DCE imaging (increased time to peak, with corresponding decreased mean transit time after sonication). Post treatment PSA serum level decreased after initial increase. Procedure was validated by pathologist, that demonstrated extensive coagulative necrosis at the site of sonication surrounded by normal prostatic tissue with inflammatory changes. No residual viable tumor was observed within the treated area.

In conclusion, MRgFUS determines necrosis of prostate cancer that can be adequately evaluated by DCE, according to histopathology findings.

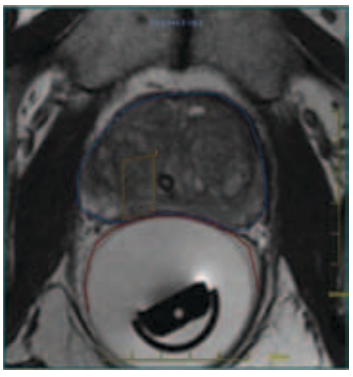

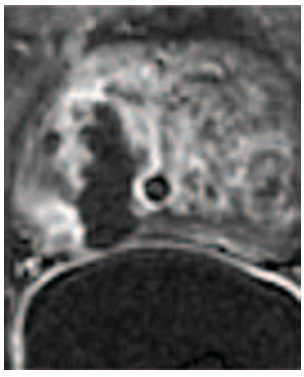

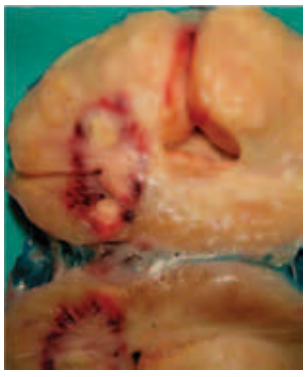

Left: Planning Stage

Center: ce-T1 fat sat axial image shows area on non-perfused volume consistent with coagulative necrosis in the region of treatment

Right: Radical prostatectomy was performed and the area of treatment is clearly visible at gross-pathology

51-PR

Tuesday
16 October 2012

Topic: Prostate
Presentation Type: Oral

Hemi Salvage HIFU in Patients with Radiorecurrent Prostate Cancer

Eduard Baco[1], Sebastian Crouzet[2], Erik Rud[3], Olivier Rouviere[2], Jean-Yves Chapelon[4], Viktor Berge[1], Albert Gelet[2]

[1]Oslo University Hospital, Oslo, Norway
[2]Hospices Civils de Lyon , Urology and Transplantation3, E. Herriot Hospital, Lyon, France
[3]Oslo University Hospital at Aker, Oslo, Norway
[4]Inserm LabTAU - U1032/Université de Lyon, Lyon, France

Background/Introduction: One third of patients treated with external beam radiation therapy (EBRT) for localized prostate cancer (PCa) experience local recurrence. Salvage treatment options include prostatectomy, cryoablation, and high intensity focused ultrasound (HIFU). Whole gland treatment in these patients offers acceptable cancer control, but carries a risk of severe urinary incontinence and reduction of QoL. In patients with unilateral local relapse, focal HIFU is feasible. The aim of this prospective study was to evaluate the effect of Hemi HIFU in patients with unilateral recurrence after EBRT.

Methods: Between 2009 and 2011 43 patients were prospectively included in 2 centers. Inclusion criteria were positive MRI and biopsy in one lobe diagnosing unilateral cancer after EBRT (41 pts) and after brachytherapy (2 pts). Median age was 69 years (51-78), pre HIFU PSA was 5.19ng/mL (3.47-6.91) and Gleason score was 7(≤7:28, ≥8:10, ND 7). Mean follow-up was 12 months. HIFU treatment was performed with Ablatherm®.

Results and Conclusions: The mean PSA nadir was 0.77 (0.51-1.04). Control biopsies (in 12 pts with rising PSA) were negative in 75% (n=9) and positive in 25% (n=3): in the treated lobe: 2, in the contralateral lobe: 1.

Disease progression ocurred in 10 pts (23%): local recurrence: 3 pts, metastasis: 4 pts and rising PSA without local recurence or proven metastasis in 3pts. Five patients received androgen deprivation and 1 redo-HIFU.

Severe incontinence occurred in 7% (n=3). The mean ICS score before/after treatment were score A: 0.51±0.27 / 2.30±0.59 and score B: 0.37±0.18 / 1.9±0,46. No significant change of EORTC-C 30 QoL and IPSS scores were observed: QLC30 35.07±8.57 VS 34.56±9.98; IPSS: 7.07±5.77 VS 8.84±5.72. The IIEF5 score decreased from 11.89±8.64 to 7.66±6.62.

In conclusion, hemi-salvage HIFU is efficient in patients with unilateral radio-recurrent PCa with a preserved QoL. It may offer comparable cancer control to whole gland treatment.

52-PR

Tuesday
16 October 2012

Topic: Prostate
Presentation Type: Oral

Clinical Evaluation of Transurethral MR-HIFU for the Treatment of Localized Prostate Cancer

Rajiv Chopra[1], Charles Mougenot[2], Elizabeth Ramsay[3], Mohamed Kazem[3], Linda Sugar[3], Masoom Haider[3], Laurence Klotz[3]

[1]UT Southwestern, Dallas, Texas, United States
[2]Philips Healthcare, Toronto, Canada
[3]Sunnybrook Health Sciences Centre, Toronto, Canada

Background/Introduction: Minimally-invasive image-guided treatments for localized prostate cancer offer the potential for targeted treatment of disease identified through imaging, and the sparing of surrounding sensitive structures. Magnetic resonance imaging is emerging as a powerful imaging technique for prostate tumor localization, while high-intensity ultrasound energy offers a means for targeted tissue destruction. Access to the prostate gland can be achieved through both transrectal and transurethral devices.

Transurethral ultrasound therapy offers some unique characteristics including the ability to deliver ultrasound directly to the prostate gland without passing through sensitive intervening tissues, the ability to deliver ultrasound continuously using a scanned device in order to achieve increased ablation rates, and the ability to deliver therapy from a simple disposable medical device. One of the perceived limitations of this approach is the challenge in treating out to the capsule of the prostate gland, a characteristic which is important in order for this to be used in the management of prostate cancer.

Methods: We have developed a system for transurethral ultrasound therapy at Sunnybrook Research Institute. The system is interfaced to a 3T MRI capable of providing up to ten planes of thermometry every few seconds. The temperature information is analyzed continuously during treatment and is used to adjust the output parameters of the transurethral device. This real-time temperature control is used to treat target volumes within the prostate gland.

Results and Conclusions: We are embarking on an NIH-sponsored clinical trial to evaluate the feasibility of treating target localized tumors in men diagnosed with prostate cancer. This presentation will describe the study objectives and design, as well as initial results obtained to date.

Acknowledgements (Funding): This study is supported by the NIH (5R21CA159550).

53-PR

Tuesday
16 October 2012

Topic: Prostate
Presentation Type: Oral

MR-Guided Closed-Loop Feedback Control of Transurethral Ultrasound Ablation For Treatment of Benign Prostatic Hyperplasia (BPH)

Punit Prakash[1], Andrew Holbrook[2], Vasant Salgaonkar[3], Peter Jones[3], Juan Plata[2], Serena Scott[3], Harcharan Gill[2], Donna Bouley[2], Kim Butts Pauly[2], Graham Sommer[2], Chris Diederich[3]

[1]Kansas State University, Manhattan, Kansas, United States
[2]Stanford University, Stanford, California, United States
[3]University of California at San Francisco, San Francicso, California, United States

Background/Introduction: A dual-sectored transurethral ultrasound device is under development for minimally-invasive MR-guided thermal therapy of BPH targets. Feedback control algorithms that modulate the power supplied to the ultrasound device may improve safety by restricting tissue temperatures to safe limits and terminating treatments once targets have been adequately heated. Real-time MR thermometry provides a means for assessing progress of the treatment and may enable automated control of procedures. The objective of this study was to design and evaluate in vivo a closed-loop feedback control algorithm to regulate maximal tissue temperatures and control the extent of therapeutic coverage to a defined outer boundary.

Methods: A catheter-based transurethral ultrasound applicator was designed, specific for MR-guided transurethral ablation of BPH targets in anterolateral regions of the prostate gland (Fig 1A and B). The applicator consists of independently powered, dual-sectored tubular ultrasound transducers (f ~7 MHz, 2 x 120° sectors, 3.5-4 mm OD, 10 mm L, Imax =7.5-14 acoustic W/cm2) enclosed in an expandable urethral cooling balloon (10 mm OD). A 3D acoustic-biothermal model implemented with the finite element method (FEM) was used to compute the energy deposition and transient temperature and thermal dose profiles during and after ablation. Independent proportional-integral controllers, with wind-up limits, were implemented to regulate peak temperatures (Tmax = 75 °C) in a 3 mm x 3 mm ROI positioned 5 mm from the balloon. Pilot-point point controllers for each active sector were implemented in 3 mm x 3 mm ROIs at the target boundary exceeded a specified threshold (Tmax = 50-56 °C). Prototype devices were fabricated and controllers implemented for integration into the 3T MRI environment and evaluated in tissue mimicking phantoms, ex vivo tissues, and 11 in vivo canine prostates. Imaging was performed with a custom endorectal coil and a 5" surface coil. An application specific interface was developed for fully integrated device localization, treatment planning, and multi-slice thermometry. A multi-slice GRE sequence (TE = 7.0 ms, TR = 95 ms, FOV = 15 cm × 15 cm, flip angle = 10°, BW = 10.4 kHz, and slice thickness = 5 mm) was used to prescribe three parallel axial thermometry slices for feedback control, an additional two coronal slices for monitoring temperature rise along the length of the prostate gland, and dual saturation bands to suppress incoming signal due to flow. Finally, a diffusion weighted sequence was implemented for acquiring ADC maps prior to, during or after ablation.

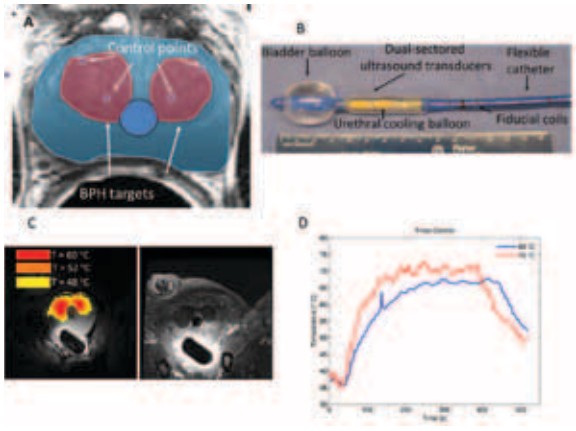

Figure 1. (A) Illustration of dual-sectored transurethral ultrasound targeting of anterior-lateral lobes of the prostate and ROIs for feedback control, (B) an MRI compatible dual-sectored transurethral ultrasound device, (C) temperature map from MR thermometry and contrast enhanced image after in vivo canine prostate ablation, and (D) illustration of maximum temperature regulation at T=70 Â°C and T= 65 Â°C during an in vivo canine prostate ablation.

Results and Conclusions: FEM simulations were used to determine controller gain parameters and temperature thresholds for determining treatment endpoint. For targets with a radial depth under 14 mm (t~5-6 mins), 55 °C is a suitable indicator of treatment endpoint, whereas for larger targets (r> 14 mm, t~7-12 mins), endpoint temperatures of 52-54 °C are suitable. In vivo experiments indicated the controller's ability to constrain tissue temperatures to within 2 °C of target temperatures in the range of 65-75 °C (Fig 1C and D). Simulations and in vivo experiments indicated that feedback control of maximum tissue temperature is not required for treating targets with radial depth < 14 mm. An integrated system for MR-guided, closed-loop feedback controlled transurethral ablation has been developed specific for treatment of BPH targets.

Acknowledgements (Funding): We acknowledge support through NIH grant R01CA111981.

54-PR

Tuesday
16 October 2012

Topic: Prostate
Presentation Type: Oral

Toward Real-Time Tissue Viability Mapping During MRgFUS in the Prostate

Juan Plata[1], Andrew Holbrook[1], Punit Prakash[2], Vasant Salgaonkar[3], Peter Jones[3], Harcharan Gill[1], Donna Bouley[1], Chris Diederich[3], Graham Sommer[1], Kim Butts Pauly[1]

[1]Stanford University, Stanford, California, United States
[2]Kansas State University, Manhattan, Kansas, United States
[3]University of California at San Francisco, San Francisco, California, United States

Background/Introduction: It has been described that the apparent diffusion coefficient (ADC) decreases by approximately 36% after a thermal ablation in the prostate. Interestingly, the decrease is the same if the ablation method was either high intensity ultrasound or cryoablation, even though the histology in these two cases is quite different. (J. Chen, MRM, 2008). Thus, the ADC may be a specific parameter indicating loss of tissue viability. The purpose of this work was to determine at what point during the treatment the ADC decreases and how it correlates with a thermal dose threshold of 240 min.

Methods: Three canine prostates were treated with high intensity ultrasound using multi-sectored transurethral applicators (3.5-4 acoustic Watts, 7MHz) under MR guidance in a 3T 750 MR scanner. During each treatment, ADC maps (b=1000 s/mm2, EPI, TE/TR=80ms/1250ms) and PRF temperature maps (GRE TE/TR=8ms/70ms) were acquired in an interleaved fashion. ADC and temperature values were recorded every 17 seconds. Peak temperature and ADC values were measured in each experiment. Using a linear regression on the first nine datapoints (before a thermal dose of 240 minutes was reached), a scaling factor for the ADC axis was determined so that temperature and ADC could be plotted on the same graph.

Results and Conclusions: Example images and region of interest measurements are shown in Figure 1. Initially, ADC increments track temperature increments. After a few minutes, the ADC increase stalls, even though the temperature is still increasing. This deviation occurs very close to a thermal dose of 240 minutes (dotted line in Figure 1). As the tissue returns to initial temperature, the ADC falls to a level substantially below the initial.

These results indicate that the correlation between ADC and temperature during treatment may be a sensitive marker for loss of tissue viability and that real-time maps indicating tissue viability may be possible.

Acknowledgements (Funding): We would like to acknowledge our grant support NIH R01 CA111981, NIH P01 CA159992, and an NSF Graduate Fellowship, as well as Wendy Baumgardner, Yamil Saenz, Anne Sawyer, and Kevin Epperson for their help with the in vivo experiments.

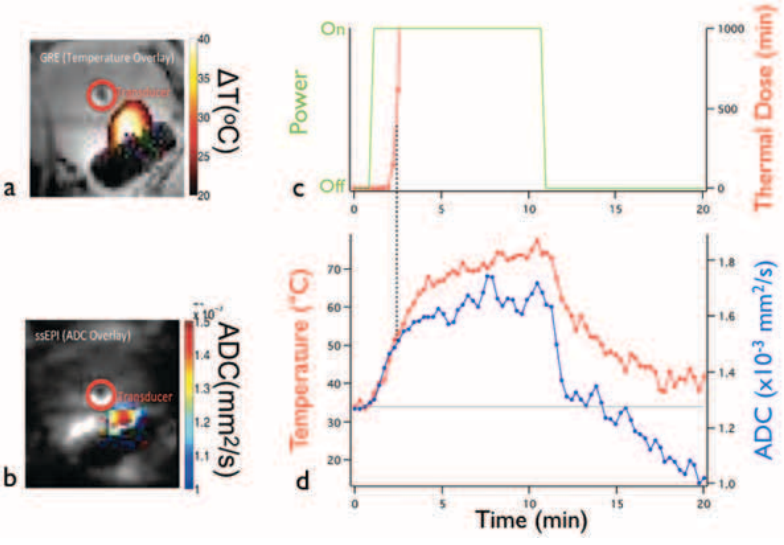

Figure 1
a) PRF temperature and b) ADC maps during high intensity ultrasound ablation of the prostate.
c,d) Measurements in an ROI indicate the ADC increase tracks the temperature increase until a thermal dose of about 240 minutes (dotted line), at which time the ADC curve begins to deviate from the temperature curve (arrow), eventually decreasing to a level substantially lower than the starting ADC.

55-PR

Tuesday
16 October 2012

Topic: Prostate
Presentation Type: Oral

MRI Guided Prostate Cancer Focal Ablation Using HIFU by Means of Image to Image Registration

Louise Dickinson[1], Yipeng Hu[2], Hashim Ahmed[1], Clare Allen[1], Alex Kirkham[1], Mark Emberton[1], Dean Barratt[2]

[1]University College Hospital, London, United Kingdom
[2]University College, London, United Kingdom

Background/Introduction: Multi-parametric (mp)MRI could be used to define the morphometry (location and limits) of a prostate tumour in order to allow greater precision in targeting focal therapies. This has hitherto not been possible so an anatomical zone has been declared the therapeutic target, with potentially large discrepancies between tumour and target volumes. We report on the use of tumour morphometry to inform the planning and conduct of therapy. The cases described are derived from a prospective Phase II multi-centre study of focal therapy using HIFU.

Methods: Non-rigid image registration software, developed in our institution, was used to transfer data on the location and limits of the index lesion as defined by mpMRI. Manual contouring of the prostate capsule and MR-visible lesion (histologically confirmed) was performed pre-operatively. A deformable patient-specific computer model capturing the location of the target lesion was registered to a 3D TRUS volume. Treatment volume could be added but not subtracted following registration, in order that cancer ablation was not compromised.

Results and Conclusions: MRI-TRUS registration was performed on 17 patients with MR visible lesions. The MRI-contoured lesion was visualised on the 3D TRUS images and compared with a prior manually-defined therapy plan. Two minor registration errors were attributed to temporary and correctable computer software issues. Time for registration took a mean 7 minutes (range 4 –16 minutes). Additional tissue was treated due to image-registration in 10/17 cases with a mean additional ablation time of 50 seconds (range 9 – 90 secs).

We have demonstrated that non-rigid MR-US registration is feasible, efficient and can locate lesions on ultrasound with potential for improved accuracy of focal treatments.

Acknowledgements (Funding): NIHR Biomedical Research Centre, The Prostate Cancer Charity, and US HIFU

56-BM

Wednesday
17 October 2012

Topic: Bone Metastasis
Presentation Type: Oral

Magnetic Resonance Guided Focused Ultrasound Surgery For Painful Bone Metastases Is A Safe and Effective Treatment In Patients For Whom Radiation Therapy Is Contraindicated: Results of a Multi-Center Phase III Trial

Mark Hurwitz[1], Dmitri Iozeffi[2], David Gianfelice[3], Abraham Kuten[4], Susan LeBlang[5], Junsung Choi[6], Pejman Ghanouni[7], Anne Roberts[8], Raphael Pfeffer[9], Sergey Kanaev[10]

[1]Dana Farber/Brigham Women's Hospital Cancer Center/ Harvard Medical School, Needham, Massachusetts, United States
[2]Rostov State Institute of Oncology, Rostov-On-Don, Russian Federation
[3]University Health Network Toronto, Toronto, Canada
[4]Rambam Medical Center, Haifa, Israel
[5]University Image Guided Therapy Center, Boca Raton, Florida, United States
[6]Moffitt Cancer Center, Tampa, Florida, United States
[7]Stanford University, Stanford, California, United States
[8]University of San Diego, La Jolla, California, United States
[9]Sheba Medical Center, Tel Hashomer, Israel
[10]Petrov Research Institute of Oncology, Saint Petersburg, Russian Federation

Background/Introduction: Osseous metastases are a daunting problem in oncology. Radiation therapy (RT) is the primary treatment for most patients with painful bone metastases however about one third do not get pain relief and others may have pain recurrence or not be candidates for RT. Magnetic resonance guided focused ultrasound surgery (MRgFUS) combines non-invasive focused ultrasound with MR guidance. Phase I-II studies demonstrated that MRgFUS resulted in high rates of pain relief with an excellent safety profile. A multi-center phase III trial, the first to assess a role for MRgFUS in oncology, was done to definitively assess efficacy of MRgFUS for treatment of painful bone metastases in patients for whom RT was not considered an appropriate option.

Methods: Patients with a painful bone metastasis amenable to MRgFUS treatment and NRS pain score ≥4 for whom RT was not considered appropriate (e.g. prior RT to painful site) were randomized 3:1 to MRgFUS or sham treatment. Study subjects were followed for 3 months. Sham subjects who were non-responders after 2 weeks were allowed to opt for cross-over MRgFUS treatment. Significant pain response was defined as decrease in worst pain NRS score ≥2 from baseline without increase in pain medication. Quality of life (QOL) measured by BPI-QoL, as well as safety were also evaluated.

Results and Conclusions: 134 subjects were included in an intent-to-treat analysis. Blinding of sham subjects was excellent. 94% of MRgFUS and 88% of sham subjects indicated belief they had received MRgFUS treatment. MRgFUS resulted in significant pain reduction. 67% (95%CI 57-76%) of 100 subjects in the MRgFUS arm had significant pain relief at 3 months compared to 21% of 34 sham subjects ($p<0.0001$) Median baseline and 3 month NRS scores in the MRgFUS and sham arms were 7.0 and 2.0 vs. 7.0 and 6.5 respectively. Clinically and statistically significant durable improvement in average BPI-QoL score: 2.4 at 3 months ($p<0.0001$), patient assessed well being, and function with MRgFUS but not sham treatment were noted. MRgFUS was well tolerated with transient treatment related pain the most commonly reported toxicity.

MRgFUS results in excellent rates of durable pain relief, improvement in QoL, and subject assessed well being and function for patients with metastatic bone pain who are not candidates for RT. Given these excellent results coupled with a favorable side effect profile, MRgFUS should be considered a primary choice for eligible patients when RT is contraindicated in treatment of painful bone metastases.

57-BM

Wednesday
17 October 2012

Topic: Bone Metastasis
Presentation Type: Oral

Clinical Results of Treatment Painful Bone Metastases with Magnetic Resonance Guided Focused Ultrasound.

Vladimir Turkevich, Sergey Kanaev, Valentina Savelyeva, Igor Dunaevsky, Andrei Mishchenko

Petrov Research Institute of Oncology, Saint Petersburg, Russian Federation

Background/Introduction: Magnetic Resonance guided Focused Ultrasound Surgery (MRgFUS) is an innovative technology combining non-invasive deposition of high intensity focused ultrasound energy into a specified target inside the body, with high resolution Magnetic Resonance Imaging (MRI) guidance and real-time thermal feedback. We present here results of a clinical trial conducted in our facility. The main objective of the trial was to evaluate safety and effectiveness of MRgFUS treatment of pain caused by bone metastases.

Methods: 31 patients with painful bone metastases were treated with the ExAblate® system (InSightec, Haifa, Israel) at Petrov Research Institute of Oncology, St. Petersburg, Russia. Immediately after procedure patients were examined for any adverse events and after a brief recovery discharged. Patients were followed up on 1 and 3 days, 1 and 2 weeks, 1, 2 and 3 months post treatment. During each visit, treatment safety was evaluated by recording and assessment of device or procedure related adverse events. Effectiveness of palliation was evaluated using the standard pain scale (0-no pain/10-worst pain imaginable) and by monitoring changes in the intake of pain-relieving medications. A reduction of 2 points or more on pain scale was considered a significant response to treatment. 17 patients were male and 14 female. Mean age was 55 years old (19-76). The primary cancers were: 19 breast, 4 stomach, 2 bronchus, 2 bladder, 4 other. Targeted lesions were 14 osteolytic, 8 osteoblastic and 9 mixed. 23 were pelvis metastases, 4 were located in the humerus bone and 4 were located in the ribs.

Results and Conclusions: No significant device or procedure related adverse events were recorded. 3 patients died during the follow-up period due to disease progression, thus 3 months follow-up data includes only results of 28 patients. All patients reported significant improvement in pain with no change in their medication intake. Mean worst pain score at baseline, 1 day, 3 days, 1 week, 2 weeks, 1, 2 and 3 months post-treatment was 6.9, 6.1, 5.1, 3.5, 2.6, 1.8, 1.2 and 0.9 respectively. MRgFUS can provide effective, safe and noninvasive palliative therapy for patients suffering from painful bone metastases. The ability to achieve rapid pain relief after only one treatment session, combined with the high safety profile of the procedure implies that MRgFUS has a significant potential for patients suffering from painful bone metastases.

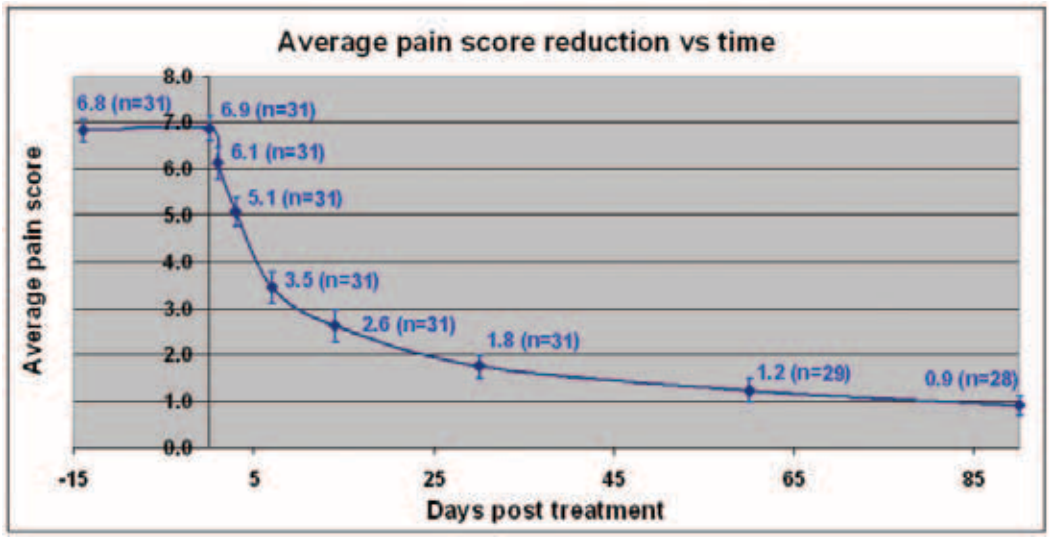

58-BM

Wednesday
17 October 2012

Topic: Bone Metastasis
Presentation Type: Oral

Primary Pain Palliation and Local Tumor Control in Bone Metastases Treated with Magnetic Resonance-guided Focused Ultrasound (MRgFUS)

Michele Anzidei, Alessandro Napoli, Beatrice Cavallo Marincola, Fulvio Zaccagna, Giulia Brachetti, Vincenzo Noce, Carlo Catalano

University of Rome — Sapienza, Rome, Italy

Background/Introduction: Bone is the most common organ for distant tumor metastases, especially in patients with cancers of the breast or prostate. Bone metastases can severely impair mobility and significantly contribute to a general decrease in quality of life. Current treatment strategies embrace analgesics, chemotherapy, hormonal therapy and bisphosphonates for systemic treatment, and radiation therapy, percutaneous ablation and surgical stabilization for local control.

At present external beam radiation therapy (EBRT) is the treatment of choice for clinically active bone metastases; however this has proven ineffective in 20-30% of cases and only temporarily effective in 27% of cases.

Initial studies have shown MRgFUS to be effective for pain control through thermal cell death and periosteal denervation induced by cortical heating relative to acoustic energy absorption; moreover there is evidence that a high intensity focused ultrasound beam can penetrate through the cortical bone to the medullary space producing thermal necrosis of cancer tissue. However, little is known about the potential effects of MRgFUS for primary pain palliation therapy in skeletal metastases.

Purpose: To evaluate the clinical performance of MRgFUS for the primary treatment of painful bone metastases and to assess its potential for local control of bone metastases.

Methods: This was a prospective, single arm research study with IRB approval. Eighteen consecutive patients (female: 8, male: 10; mean age: 62.7 ± 11.5 years) with painful bone metastases were enrolled. Patients were examined clinically for pain severity and pain interference according to Brief Pain Inventory-Quality of Life (BPI-QoL) criteria before and over the following 3 months after treatment. Computed Tomography (CT) and MR imaging were performed before and at 3 months after MRgFUS treatment. The non-perfused volume (NPV) was calculated in order to correlate the extension of the ablated pathological tissue in responder and non-responder patients.

Results: No treatment-related adverse events were recorded during the study. The evaluation of pain palliation revealed a statistically significant difference between baseline and follow-up values for pain severity and pain interference (p=0.001, both evaluations). In the evaluation of local tumor control, we observed increased bone density with restoration of cortical borders in 5/18 (27.7%) patients. According to MD Anderson (MDA) criteria, complete and partial response was obtained in 2/18 (11.1%) and 4/18 (22.2%) patients, respectively (Figure 1). NPV values ranged between 20 and 93%. Mean NPV values remained substantially stable after treatment (p=0.08). There was no difference in NPV values between responder and non-responder patients (46.7 ± 24.2% [25 – 90 %] vs. 45 ± 24.9% [20 – 93 %]; p=0.7).

Conclusion: MRgFUS can be safely and effectively used as the primary treatment for pain palliation in patients with bone metastases and has a potential role in local tumor control.

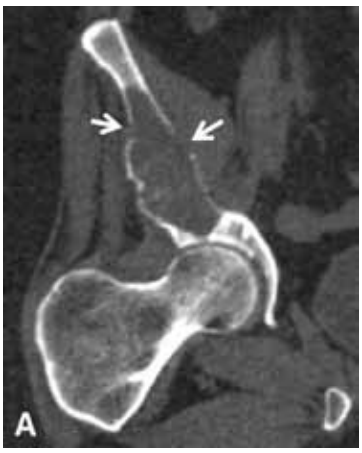

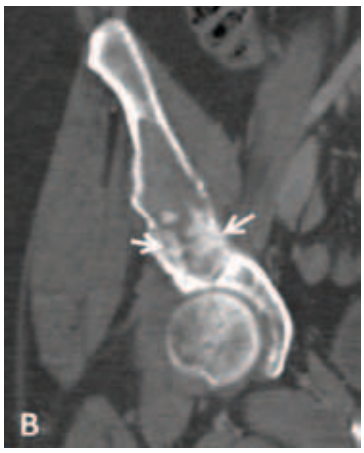

Figure 1a: Sixty-seven years old female with breast cancer. Pre-MRgFUS CT scan demonstrated the presence of a large osteolytic metastasis of the right iliac bone with cortical erosion (arrows).

Figure 1b: After 3 months from MRgFUS treatment CT scan revealed partial response of the lesion with evidence of de novo mineralization of the spongious bone (arrows) and partial restore of cortical borders.

59-BM

Wednesday
17 October 2012

Topic: Bone Metastasis
Presentation Type: Oral

A Comprehensive Quality Assurance Program for Bone Palliation Using MR Guided Focused Ultrasound: Fox Chase Experience

Lili Chen, Charlie Ma, Terry Richardson, Gary Freedman, Andre Konski, Joshua Meyer

Fox Chase Cancer Center, Philadelphia, United States

Background/Introduction: This work is aimed to develop a comprehensive quality assurance (QA) program to ensure the safety and efficacy of MR guided focused ultrasound (MRgFUS) treatment of bone metastases.

Methods: Seven patients with scapula (2), humeral head, sacrum, ilium, pubic ramus and acetabular bone metastases were treated using ExAblate® 2000 under MR guidance. In addition to the monthly and annual quality assurance (QA), pre-treatment machine calibration was performed before each treatment including the functionality of the treatment software, the mechanical motion control system and the patient safety devices. The effective ultrasound focal spot was verified with an acoustic phantom using MR thermometry. The patient was positioned on a gel pad. The interface between the treatment table, the gel pad and the patient was immersed in degassed water for acoustic coupling. Caution was taken to remove all gas bubbles between the interfaces. Treatment was performed under conscious sedation with an ACLS (Advanced Cardiovascular Life Support) certified registered nurse in the MRI room for the entire treatment procedure and working with the physician to provide an appropriate level of sedation. Continuous monitoring of vital signs (pulse, blood pressure, and oxygen saturation) was done with MRI compatible equipment plus a slave monitor in the control room.

Six to eighteen sonications were delivered for each patient treatment depending on the lesion size. Patients were treated with the following parameter: frequency 1 MHz, acoustic power 32 ± 4.0 to 96 ±11W and energy 628 ± 78 to 1859 ± 338J (20-30s sonication time). MR phase images were used to monitor the temperature changes in real-time. Based on the temperature feedback, the acoustic power was adjusted to reach designed temperatures (≥60 °C) for individual sonications (table 1). Pain was assessed using the visual analog scale (VAS).

Results and Conclusions: All seven patients tolerated the MRgFUS treatment well. No skin toxicity or other complications were observed. The VAS pain rating was significantly reduced over 7 patients from 8.0 ± 1.1 before treatment to 4.7 ± 3.0, 3.0 ± 1.5, 3.2 ± 2.8 and 3.4 ± 1.5 at one day, one month, two months and three months after treatment, respectively (figure 1). A comprehensive QA program has been developed for the MRgFUS system. Our data suggest that MRgFUS is a safe, effective and noninvasive treatment modality for palliation of bone metastases.

Acknowledgements (Funding): We would like to thank InSightec for their excellent technical support.

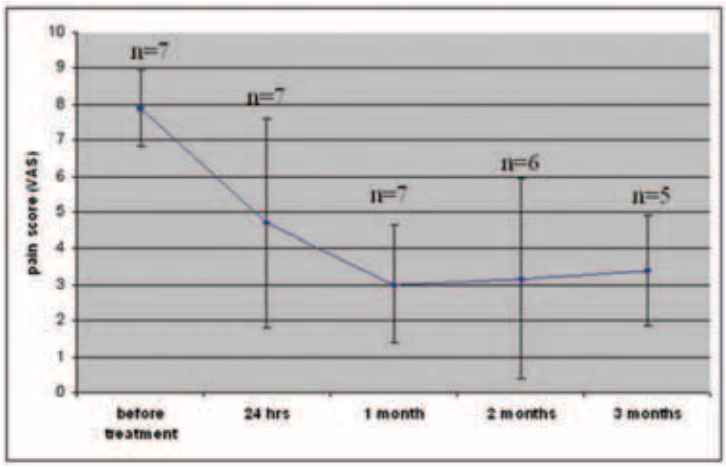

Figure 1. Pain scores after MRgFUS treatment. Two patients withdrew from the study one month and two months after treatment, respectively.

Pt #	Primary tumor	Treated site	Sonications	Acoustic power (w)	Energy (J)	Durations/ per sonication (s)	T (°C)
1	Breast	LT scapula	6	32 ± 4.0	628 ±78	20 ± 0	62±11
2	Prostate	RT rib/scapula	17	21 ± 4.0	628 ± 99	30 ± 0	66 ± 9
3	Breast	RT humeral head	9	42 ± 3.0	1005 ± 114	24 ± 3	77 ± 7
4	Breast	sacrum	18	79 ± 11.0	1607 ± 178	20 ± 0	69 ± 7
5	Colon	RT ilium	17	96 ± 11.0	1859 ± 338	20 ± 0	73 ± 11
6	Kidney	Pubic ramus	13	62 ± 15.0	1240 ± 293	20 ± 0	69 ± 12
7	breast	LT acetabular	12	78 ± 32.0	1605 ± 611	20 ± 0	65 ± 7

Table 1. Patient information and the FUS treatment parameters.

60-BM

Wednesday
17 October 2012

Topic: Bone Metastasis
Presentation Type: Oral

Volumetric MR-HIFU Ablation in a Patient with a Costal Metastasis and a Soft-Tissue Mass

Merel Huisman, Marco van Vulpen, Roel Deckers, Lambertus Bartels, Helena Verkooijen, Maurice van den Bosch

University Medical Center Utrecht, Utrecht, Netherlands

Background/Introduction: Magnetic Resonance-guided High Intensity Focused Ultrasound (MR-HIFU) has been proposed as a palliative treatment for painful bone metastases. Until recently, the ablation method consisted of point-by-point ablation. Volumetric ablation, as implemented on the Philips Sonalleve® MR-HIFU system, results in larger and more homogeneously ablated volumes than point-by-point ablation. In our institute, we recently started palliative treatment of painful bone metastases in patients who failed radiotherapy. In this case report we describe an exceptional patient who presented with a soft tissue mass.

Methods: An 86-year-old male with a history of a pulmonary sacromatoid carcinoma was referred to our center for palliative MR-HIFU treatment of a solitary, histology proven, inoperable painful costal metastasis, not responding to radiotherapy. Complaints were pain (VAS 4) as well as mass-related problems. Physical examination showed a non-painful, hard, infraclavicular mass and tenderness of the second rib (Figure1a). Contrast enhanced (CE)-MRI revealed a metastasis localized in the second right rib, extending to the third rib and pleura, with an enhancing, invasive, infraclavicular soft-tissue mass with a diameter of 6.0 x 5.8 cm (Figure 1b). A two-step approach was chosen to achieve both tumor debulking and pain palliation after informed consent was obtained. MR-HIFU ablations were performed with the Philips Sonalleve® system. First, under deep sedation with the patient in prone position, the infraclavicular mass was ablated in order to obtain local control. Under MR-guidance, 8 mm feedback cells (total volume of 11 ml) were placed in the center of the mass (Figure 2a) and alternatingly sonicated to avoid excessive skin heating. At a power of 100 W the temperature exceeded 70°C (Figure 2b). Directly after treatment a T1 CE-MRI with fat suppression showed a large non-perfused volume covering almost 75% of the tumor mass. Before the second treatment, 4 weeks later, the maximum point of pain was marked (Figure 3a) in order to obtain accurate focal ablation of the costal periosteum, presumably being the major source of pain. Under the same conditions as the first treatment, 4 mm treatment cells were placed adjacent to the cortex of the second rib. Heating to a temperature of 70°C was achieved at a power of 130 W (Figure 4).

Results and Conclusions: Three weeks after the first treatment, the mass was soft on palpation. CE-MRI exhibited a total lesion diameter of 5.6 x 4.3 cm with a large necrotic center (figure 3b). At the time of writing, the VAS score after the second treatment still had to be collected. No complications were seen and the overlying skin remained unaffected. Our experience shows that volumetric ablation with MR-HIFU is feasible in a complex bone metastasis with a large soft-tissue mass. Future application of volumetric MR-HIFU might include inoperable soft-tissue tumors. Currently, the procedure should be reserved for inoperable patients with persistent symptoms despite standard of care.

Figure 1a. 86-year-old male presenting with rib metastases and non-painful infraclavicular mass, hard on palpation. b. Transverse view of the right hemi thorax (CE-MRI T1 SPIR image) showing infraclavicular soft-tissue mass before treatment (arrow).

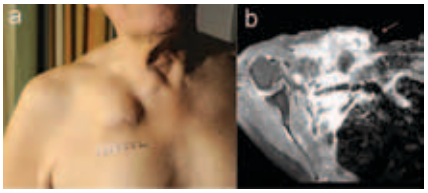

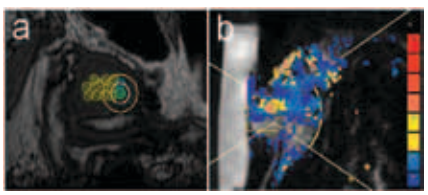

Figure 2. First treatment: soft-tissue ablation. a. 8-mm treatment cells placed in the center of the soft-tissue mass. b. Thermal mapping during sonicating: center of focus > 70°C (red).

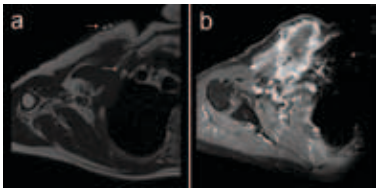

Figure 3. a. Transverse view of the right hemi thorax (T1 image) with markers at maximum point of pain (white arrow). Metastasis of second rib with soft-tissue components. Dashed arrow indicates targeted area for second treatment. b. CE-MRI T1 SPIR image 3 weeks post-treatment showing extensive central necrosis of soft-tissue mass (black arrow).

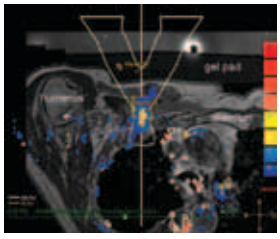

Figure 4. Transversal view of right hemi thorax with patient in prone position on a gel pad. Sonication of costal metastasis with temperature up to 70°C in the center of the focus.

61-BM

Wednesday
17 October 2012

Topic: Bone Metastasis
Presentation Type: Oral

Phase II Trial Design of MRI-Guided High Intensity Focused Ultrasound and Lyso-thermosensitive Liposomal Doxorubicin for Palliation of Painful Bone Metastases

Elizabeth Smith[1], Nicholas Borys[1], Sham Sokka[2]

[1]Celsion Corporation, Lawrenceville, New Jersey, United States
[2]Philips Healthcare, Andover, Massachusetts, United States

Background/Introduction: Prostate, lung and breast cancers are among the most common cancers in the US. Earlier diagnosis and improved care has led to an increased longevity among these patients as well as an increase in those living with secondary bone metastases. Bone metastasis occurs in about 70% of breast and prostate cancer patients. Pain is the principal and presenting symptom and the treatment goal is pain relief and normal activity restoration.

The standard of care for bone pain is external-beam radiation therapy (EBRT). EBRT suffers a 20-30% failure rate. About 27% of patients who receive initially successful EBRT will have pain recur within a few months. About 20-30% of patients with recurring pain will become ineligible for EBRT due to the dose load accumulation and to limitations in normal tissue tolerance. An additional draw back of EBRT is the repeated treatment regimen with 10 fractions over 2 weeks being typical in the US. An effective, single treatment option for bone pain would fill a serious growing medical need for oncology patients.

Lyso-thermosensitive liposomal doxorubicin (LTLD) [ThermoDox®] is a heat sensitive chemotherapeutic nanoparticle that is intravenously administered and systemically distributed. It is designed to release high concentrations of doxorubicin locally when temperatures >39.5 °C are applied to the desired region of treatment. Doxorubicin is known to be active against breast, prostate and lung cancers.

Magnetic resonance guided High Intensity Focused Ultrasound (MRgHIFU) [Sonalleve] uses real time MR imaging and thermography with focused ultrasound acoustic energy to non-invasively deliver desired levels of heat directly to a specified volume within the body without damaging intervening tissues. This MRgHIFU device has the unique ability to generate real-time temperature maps for feedback control of the treatment area as well as structures such as the skin or bowel.

We propose that a combination of LTLD and MRgHIFU will provide patients with painful boney metastasis benefits over either treatment alone, will greatly improve quality of life and will overcome the inherent short-comings of currently available pain-palliation therapies. A 52 patient, open-label, phase II trial designed to determine the safety and efficacy of combining LTLD and heat generated MRgHIFU for the palliation of painful bone metastases has been given clearance by USFDA. The study will have 2 arms. In one arm, the index lesion will have been previously treated with EBRT and yet remain painful. In the second arm the index lesion will be EBRT naive. Treatment will be identical for both arms.

All patients will receive a single LTLD infusion followed by an ablative heat treatment cycle which has been developed to enhance the combined benefits of LTLD and MRgHIFU heating. The heat radiating from the bone after ablative HIFU will lead to the regional release doxorubicin resulting in a large concentration gradient of doxorubicin causing cell death in the ablation zone and peri-ablation margin where there may be micrometastasis. The temperature gradient surrounding the ablation zone will facilitate additional LTLD uptake and release in the target area, especially in the periosteum and the vasculature supplying the tumor.

Methods: Phase II study objectives, design, enrollment criteria, and endpoints will be presented.

Results and Conclusions: None available at this time.

Acknowledgements (Funding): This work is jointly supported by Celsion Corporation (Lawrenceville, NJ) developer of ThermoDox® and Philips Healthcare (Andover, MA) developer of Sonalleve.

62-BM

Wednesday
17 October 2012

Topic: Bone Metastasis
Presentation Type: Oral

Effects of HIFU Ablation on Bone Metastases: From MRI, SPECT/CT and MicroCT Point of View

Sin Yuin Yeo[1], Aaldert Elevelt[2], Katia Donato[2], Bert van Rietbergen[1], Holger Gruell[2]

[1]Eindhoven University of Technology, Eindhoven, Netherlands
[2]Philips Research, Eindhoven, Netherlands

Background/Introduction: Bone metastases, which occur in 70% of advanced prostate cancer patients, are devastating diseases that cause cancer-induced bone pain and reduce patients' quality of life. In recent years, Magnetic Resonance guided High Intensity Focused Ultrasound (MR-HIFU) has been proposed as an alternative palliative treatment to radiation therapy. However, there are insufficient preclinical evidences to demonstrate the effects of MR-HIFU treatments on bone metastases. Therefore, we setup a preclinical bone metastases model with osteoblastic lesions and performed HIFU ablation to assess the effects of MR-HIFU. Imaging techniques, such as MRI, SPECT/CT and microCT, and behavior tests were used to assess the effects of HIFU treatment on bone and its' efficiency in alleviating pain.

Methods: Rat prostate cancer cells (MATLyLu) were injected in the femurs of 9 months old Copenhagen rats. Tumor growth and bone activity were monitored using MRI and SPECT/CT, respectively. The degree of pain was scored by monitoring limb usage after tumor inoculation. Two weeks post injection of tumor cells, HIFU ablation (55°C) was performed using a single point sonication cell behind the femur with a Philips Sonalleve 3T MR-HIFU system. Effects of ablation were evaluated 7 days post HIFU using MRI and SPECT/CT in combination with 99mTc-MDP. Post mortem, the tumor carrying and control limbs were excised and subjected to microCT analysis (30µm voxel size, 1024x1024 pixels, 360ms integration time). Changes in bone volume, density and trabecular structures were analyzed.

Results and Conclusions: Animal without HIFU treatment showed tumor outgrowth on 18 days after tumor inoculation (T2W), increased 99mTc-MDP uptake on SPECT/CT images due to increase bone activity and limping behavior due to pain. However, animal with HIFU ablation showed no tumor outgrowth, lower 99mTc-MDP uptake as compared to non treated group (Figure 1) and normal limb usage, suggesting tumor control effect of bone ablation. Post mortem microCT analyses demonstrated that femur without HIFU treatment showed an increase in bone volume, but have lower bone density, confirming formation of woven bone as a consequence of tumor cells injection (Figure 2). The microCT analysis of bone after HIFU treatment is ongoing. Histology will be performed to assess the cellular effects of HIFU ablation on bone.

Acknowledgements (Funding): This research was supported by the Center for Translational Molecular Medicine (HIFU-CHEM).

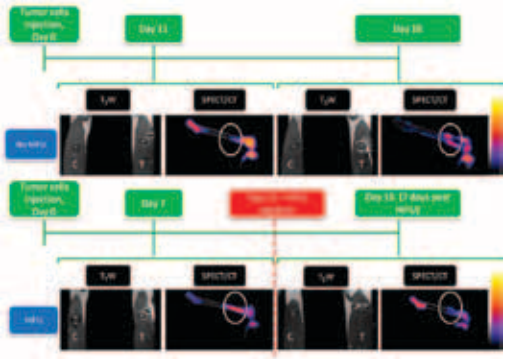

Effects of HIFU ablation on bone metastases. T2W = T2-weighted; white arrow = tumor outgrowth; white arrow head = edema; white circle= 99mTc-MDP uptake; T= Tumor carrying limb; C= Control limb.

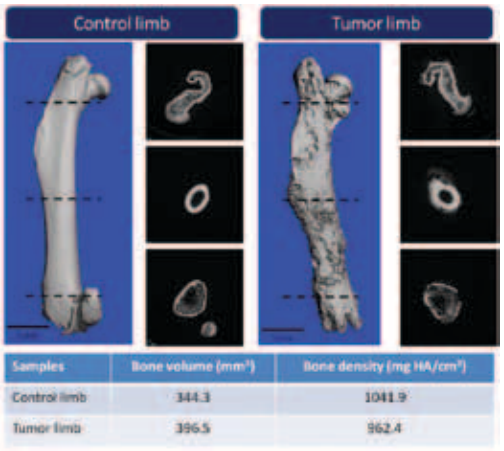

MicroCT images demonstrating increase bone volume on tumor limb (right) as compared to control limb (left).

63-BN

Wednesday
17 October 2012

Topic: Bone Non-Metastasis
Presentation Type: Oral

Osteoid Osteoma: Preliminary reSults of a Non-Invasive Treatment Using Magnetic Resonance Guided Focused Ultrasound

Beatrice Cavallo Marincola, Alessandro Napoli, Michele Anzidei, Fulvio Zaccagna, Luca Bertaccini, Carlo Catalano

University of Rome — Sapienza, Rome, Italy

Background/Introduction: Osteoid osteoma is a painful albeit benign bone lesion that usually affects younger subjects between 10 and 20 years. The most frequent symptom is localized bone pain that flares nocturnally; prompt relief is usually achieved with nonsteroidal anti-inflammatory drugs.

Once diagnosis has been established, conventional therapy options include surgery, pharmacological and/or percutaneous treatment. Since surgical resection can be challenging in many cases, minimally invasive therapies are increasingly the primary option at many centers. At present radiofrequency (RF) ablation, as opposed to excision with hollow needles and drills, cryotherapy and interstitial laser photocoagulation is the most popular of the various percutaneous techniques, with the percentage of patients reporting complete clinical success ranging between 85 and 98% at one year. Despite the high success rate of RF ablation, the only true non invasive treatment for tumor-related pain has, until recently, been pharmacological therapy. Due to the high acoustic energy absorption of cortical bone, Magnetic Resonance guided Focused Ultrasound technique (MRgFUS) may produce thermal damage to periosteal structures (including nerves, i.e. periosteal neurolysis) and can potentially penetrate into the medullary bone determining coagulative necrosis of sub-cortical lesions. The purpose of this study was to determine the feasibility and initial clinical efficacy of MR guided Focused Ultrasound (MRgFUS) for pain relieve in patients with osteoid osteoma.

Methods: This prospective, IRB approved study involved 7 consecutive patients (6 m; 1f; mean age, 21) with clinical and imaging diagnosis of Osteoid Osteoma; all patients underwent MRgFUS ablation after giving their informed consent. Lesions located in the vertebral body were excluded, while lesions in proximity to joints or neurovascular bundles were included. The number of sonications and the energy deposition used during the treatment were recorded. Treatment success was determined at clinical and imaging follow-up at 1, 3, and 6 months post-treatment. A visual Analog Pain Score (VAS) was used to assess changes in symptoms.

Results and Conclusions: Treatment was carried out using a variable number of sonications (mean 4±1.8) with a mean energy deposition of 866±211 J. There were no treatment- or anesthesia-related complications. A statistically significant (p=0.001) difference was noted between the overall pre- and post-treatment mean VAS scores (8.3±1.6 and 0.6±1.5, respectively). Six of the 7 treatments were conducted with complete clinical success (Figure 1). A single patient with intramedullary osteoid osteoma had pain recurrence after 2 weeks, requiring surgery. At imaging, edema and hyperemia associated with typical osteoid osteoma, gradually disappeared in all lesions.

In conclusion, treatment of osteoid osteoma using MR guided Focused Ultrasound can be performed safely with a high rate of success and without apparent treatment related morbidity.

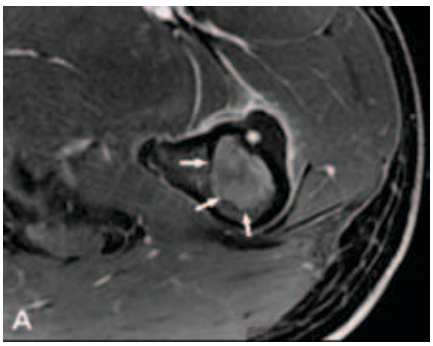

Figure1a: 21-year-old male with subperiosteal osteoid osteoma of the left femur. A) Axial GRE T1 weighted with gadolinium shows the presence of a highly perfused nidus (asterisk), a large periosteal reaction and enhancing area within the spongious bone due to the presence of hyperemia (arrows).

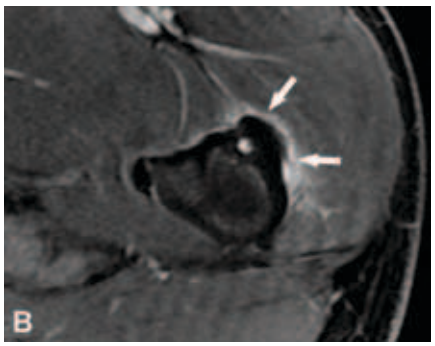

Figure1b: After MRgFUS treatment the enhancing nidus is still present; the ablation zone surrounding the periosteum is visible (arrows) while no enhancement of the medullary bone is seen. The patient referred complete symptoms relief with no more medication intake.

64-BN

Wednesday
17 October 2012

Topic: Bone Non-Metastasis
Presentation Type: Oral

Role of Magnetic Resonance Guided Focused Ultrasound Surgery (MRgFUS) in Treatment of Patients with Lumbar Facetal Arthropathy.

Abhijit Patil, Shrinivas Desai

Jaslok Hospital and Research Centre, Mumbai, India

Background/Introduction: We, at Jaslok Hospital and Research Centre, Mumbai, India have Installed Magnetic Resonance Guided Focused Ultrasound surgery (MRgFUS) at Jaslok Hospital and Research Centre, Mumbai, India in May 2010. We are doing treatments for Symptomatic Uterine Fibroids, Adenomyosis, Bone Metastasis and Prostate Cancer presently. In Future, we aim to do Brain and Breast surgeries with MR Guided Focused Ultrasound Unit.

Methods: MRgFUS unit consists of 1.5 Tesla GE HDXT MR Machine and InSightec ExAblate® 2100 Focused ultrasound system.

A group of 20 patients in age group 40 to 80 years were included in the study. 15 Male and 5 Female patients were included in the study complaining of low backache without radiculopathy. A diagnostic MRI Lumbar spine was done in all patients followed by CT scan. Following criteria were used for selection of patients.

1) Low backache without significant radiculopathy.

2) Degeneration of facets joints with presence of osteophytes, thickened capsular ligaments and ligamentum flavum.

All these patients were clinically evaluated by the neurologists to rule out radiculopathy. 10 of the Positive patients were taken up for diagnostic injection of facetal joints with a combination of steroid and local anesthetic medications (Inj. Kanacort (40 mg) and 0.5% Bupivacaine in 1:2 ratios). Pre treatment, post injection, post treatment (1, 3 and 6 months) NRS and Oswestry Disability Scores were plotted in all patients. The remaining 10 Patients underwent MRgFUS for their facet joints based on their MRI and CT Features only. Effectiveness of palliation was evaluated using the standard 11-points Numerical Rate Scale (NRS): 0-no pain, 10-worst pain imaginable and by monitoring changes in the intake of pain-relieving medications. Reduction of 2 points or more on pain scale was considered a significant response. Those who experienced significant reduction in NRS Scores after diagnostic injections were only taken for treatment with Magnetic Resonance Guided Focused Ultrasound Surgery (MRgFUS).

Results and Conclusions: All patients having Facetal arthropathy on MRI of Lumbar Spine showed significant improvement in NRS scores on Facetal injections of steroid and local anesthetic medications. These patients were taken for treatment with Magnetic Resonance Guided Focused Ultrasound Surgery (MRgFUS). Treatment was done under mild sedation. Total of six facets joints were targeted predominantly involving L3-L4, L4-L5 and L5-S1 intervertebral disc levels.3-4 sonications were given at each Facet Joint with maximum energy up to 700 Joules. Each Sonication lasted for about 14 to 18 seconds followed by cooling phase of 60-90 seconds. Approximately 20 to 25 sonications were given for each treatment and lasted for 1 to 2 hours. Immediate evaluation of the patients was carried out with post contrast MRI Study.

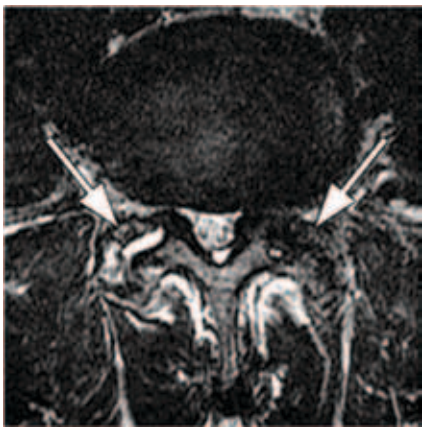

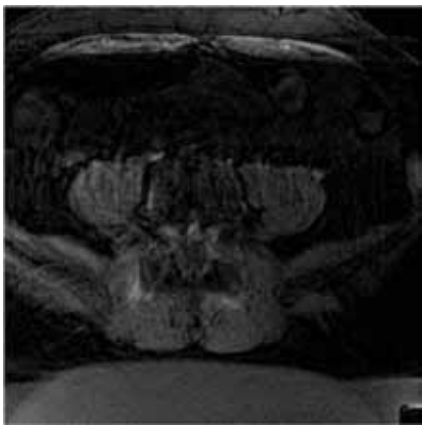

A follow up with NRS Scores and Oswestry Disability Scores were calculated after 1 week, 1 month, 3 and 6 months after treatment. There were approximately 65 -70% reductions in NRS and 60-65% reduction in Disability Scores respectively at 6 months follow-up.

There is significant improvement in pain scores on follow up in patients treated with Magnetic Resonance Guided Focused Ultrasound Surgery (MRgFUS). No adverse events were observed after the treatment. MRgFUS can be used as an effective non-invasive tool for treatment of Lumbar Facetal Arthropathy.

65-BN

Wednesday
17 October 2012

Topic: Bone Non-Metastasis
Presentation Type: Oral

Toward T1-Based Thermometry in Cortical Bone Using Ultrashort Echo-Time MRI

Wilson Miller

University of Virginia, Charlottesville, Virginia, United States

Background/Introduction: A major advantage of MR guidance for HIFU therapy is the ability to remotely monitor and quantify the induced temperature changes. For HIFU treatment of bone tumors, conventional MR thermometry can map the temperature rise in the soft tissue adjacent to the treated lesion, but cannot directly detect a temperature rise in solid tumor mass or bone itself. The purpose of the present work is to demonstrate that the local T1 increase due to focused thermal sonication can be combined with ultrashort echo-time (UTE) pulse sequence techniques to directly visualize HIFU-induced temperature rise in cortical bone.

Methods: Although MR has not traditionally been used to image the skeleton, due to the extremely short T2 relaxation time of cortical bone, UTE pulse sequence techniques can capture this short-lived signal and allow direct MR imaging of bone. We have implemented a custom 3D UTE pulse sequence on a 3T whole body MR scanner (Siemens Trio) to investigate applications of this technique. For the present demonstration, a section of beef long bone was imaged during focused ultrasound ablation using a table-top HIFU system (FUS Intruments). Ultrasound power was 25W and imaging voxel resolution was 0.8-1.0 mm isotropic for the images shown here.

Results and Conclusions: Figure 1 shows one slice of a 3D UTE image (TE=0.03 ms) together with an identical scan using an echo time typical of conventional fast gradient-echo MRI (TE=2.5 ms). The 0.8mm slice is oriented perpendicular to the bone segment, and shows a cross section through the middle of the bone. The bone marrow is intact and is visible in both images, whereas the surrounding cortical bone is visible only in the UTE image. The third image was obtained by subtracting the second image from the first, which suppresses signal from the water and fatty marrow and enhances visualization of the bone itself. Figure 2a shows UTE and conventional-TE images of a 1mm slice oriented parallel to the long bone segment. Bone signal intensity on the UTE image is similar to that of the surrounding water bath. Figure 2b shows UTE images of the same slice before and during FUS application. The focal spot is evident as a dark spot just inside the bone margin on the image acquired during sonication, similar to the signal loss on soft-tissue MR images due to the temperature rise during thermal ablation. In both cases, the signal decrease arises from the T1 increase with temperature.

This demonstration shows that it is possible to directly detect a thermal MR signature in bone using UTE pulse sequences. With further development it may be possible to perform quantitative thermometry in bone, similar to conventional T1-based thermometry in soft tissue, using such techniques. More generally, UTE pulse sequences may find other uses in MRgFUS such as in-situ bone density mapping for correcting beam aberrations.

Acknowledgements (Funding): Author supported in part by Siemens Medical Solutions.

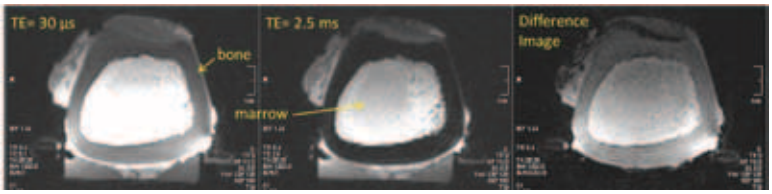

UTE image (left) and conventional-TE image (middle) showing cross section of long bone. MR signal from cortical bone is evident on the UTE image, and is enhanced in the difference image (right).

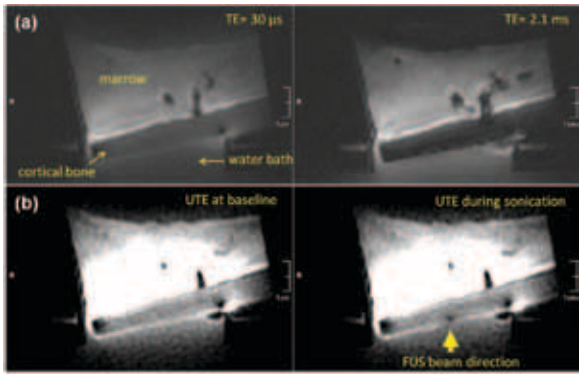

(a) UTE image (left) and conventional-TE image (right) showing longitudinal section of long bone. (b) UTE images before (left) and during (right) ablative sonication. The location of the focal spot within the bone is evident on the sonication image.

66-FD

Wednesday
17 October 2012

Topic: Foundation
Presentation Type: Oral

The Journal of Therapeutic Ultrasound

Arik Hananel[1], Robert Muratore[2]

[1]Focused Ultrasound Foundation, Charlottesville, Virginia, United States
[2]Quantum Now LLC, Huntington, New York, United States

Background/Introduction: Publications in therapeutic ultrasound have been growing for the past four decades. In order to serve this growing demand, the Journal of Therapeutic Ultrasound (JTU) has been launched. JTU is an online, open access journal designed to accelerate the adoption of focused ultrasound.

The journal website (JTUltrasound.com) is currently accepting manuscripts of research articles, case reports, reviews, meeting reports, and study protocols. Appropriate topics include translational and clinical research in all areas of therapeutic ultrasound, including stimulation, inhibition, destruction, or modification of tissue function or structure via focused ultrasound.

As an online journal, color images and supplemental materials such as audio and video files are readily accepted and publication rapidly follows review. As an open access journal, authors retain full rights to their papers through the Creative Commons license, and papers will be freely available and thus easily accessible to developing countries and the popular press.

JTU serves as the official journal of the Focused Ultrasound Foundation and the International Society for Therapeutic Ultrasound. Our distinguished editorial board of twenty-six members represents ten countries. Author fees are waived through 2014.

Acknowledgments: Support is provided by the Focused Ultrasound Foundation.

67-FD

Wednesday
17 October 2012

Topic: Foundation
Presentation Type: Oral

Bio Mechanisim

Jessica Foley[1], Jean-François Aubry[2], Arik Hananel[1]

[1]Focused Ultrasound Foundation, Charlottesville, Virginia, United States
[2]University of Virginia, Charlottesville, Virginia, United States

Background/Introduction: Focused ultrasound is a medical technology platform that can produce a variety of biological effects in tissue that enable its many potential clinical indications. With an emphasis on the clinical applications of focused ultrasound currently under investigation and those planned for the near future, this talk will provide an overview of focused ultrasound-induced bioeffects and their underlying thermal and mechanical mechanisms. It is these bioeffects that are the foundation for new focused ultrasound therapies with the potential to provide alternative or complementary treatments to improve the quality of life for millions worldwide.

68-LV

Wednesday
17 October 2012

Topic: Liver
Presentation Type: Oral

HIFU Ablation for Hepatocellular Carcinoma: Updated Clinical Applications

Feng Wu

Institute of Ultrasonic Engineering in Medicine and Clinical Centre for Tumour Therapy, Chongqing, China

Background/Introduction: Noninvasive, image-guided thermal ablation with extracorporeal high-intensity focused ultrasound (HIFU) has received increasing interest in the past decade for the treatment of patients with hepatocellular carcinoma (HCC). The purpose of this presentation is to introduce our clinical trials and the recent development of using ultrasound-guided HIFU device for the treatment of HCC patients.

Methods: Clinical trials using HIFU ablation started in 1998, and an extracorporeal ultrasound-guided HIFU system (Model-JC, Haifu Tech Co., Ltd, Chongqing, China) was employed for the treatment of early- and advanced-stage HCC patients at Chongqing, China. Since then, the same device has been introduced into the Europe and Asia, and HIFU clinical trials have been performed for treating hepatic cancers in the UK, Italy, Japan and Hong Kong.

Results and Conclusions: The histological trials showed that HIFU can precisely cause coagulation necrosis in targeted HCC lesions. Small tumor blood vessels were completely destroyed. Follow-up imaging including contrast-enhanced MRI and CT revealed a positive therapeutic response and an absence of viable tumor cells in the treated-tumor. HIFU combined with TACE demonstrated better survival benefit in HIFU plus TACE than ones in TACE alone in patients with advanced-stage HCC. Better survival data have been achieved in patients with unresectable HCC. In addition, HIFU can successfully treat HCC lesions in difficult locations, which are close to the diaphragm, big hepatic blood vessels, heart, gallbladder and bowel.

HIFU ablation is a safe, effective, and feasible for the treatment of hepatocellular carcinoma. It will provide a noninvasive therapy for HCC patients.

69-LV

Wednesday
17 October 2012

Topic: Liver
Presentation Type: Oral

Magnetic Resonance guided Focused Ultrasound (MRgFUS) Treatment of Primary Pancreatic and Hepatic Cancer: Preliminary Experience in Tumor Control

Michele Anzidei, Alessandro Napoli, Beatrice Cavallo Marincola, Fabrizio Boni, Luca Bertaccini, Vincenzo Noce, Carlo Catalano

University of Rome — Sapienza, Rome, Italy

Background/Introduction: Hepatocellular carcinoma (HCC) and pancreatic cancer probably represent two of the most challenging abdominal tumors from a therapeutic point of view, mostly due to the peculiar anatomy of the involved organs, to their vascular relationship and to the very poor response to conventional chemotherapy. At present, while percutaneous ablation techniques and transarterial embolization are feasible therapeutic alternatives in HCC in selected cases-, surgery represents the only available approach to treat patients with pancreatic cancers and percutaneous treatment is reserved only for palliative scopes. Small animal models have established that high-intensity focused ultrasound can ablate areas of normal liver and pancreas, also determining the energy thresholds for tissue destruction at these sites. Moreover, both hepatic and pancreatic lesions have been successfully treated with focused ultrasound under conventional echographic guidance. This therapeutic system has the advantage of being a non-invasive ablative technique and also the possibility to be repeated if necessary with very limited possible complications. As compared to this latter approach, MR guided focused ultrasound ablation (MRgFUS) introduces the advantage of real time monitoring of treatment effects, allowing a more precise ablation of the lesion and a more accurate in-treatment patient management. This technique has been widely used for the ablation of uterine fibroids, bone metastases and breast cancer, while its application to the treatment of HCC and pancreatic cancer remains still in its preliminary phases.

The purpose of this study was to evaluate the feasibility of MRgFUS ablation in selected pancreatic and hepatic primary tumors.

Methods: After giving their informed consent 3 patients with histologically proven unresectable pancreatic adenocarcinoma and 1 patient with unresectable right lobe HCC (3 males, 1 female; age range 58-72) underwent MRgFUS treatment on a dedicated 3T unit featuring the ExAblate® 2100 system (InSightec). The system is composed by a 200-element transducer located within the MR table. The MR guidance allows a detailed depiction and visualization of the lesion; moreover, the use of the proton resonance frequency (PRF) shift method allow a real time monitoring of the temperature inside the target lesion and the adjacent anatomical structures, in order to ensure adequate tissue ablation and safe ablation margins. The treatment was performed in general anesthesia with breath control. After the procedure, gadolinium-enhanced gradient echo T1-weighted sequences were performed in order to evaluate the ablated area and the absence of possible local complications. Clinical and imaging follow-up was performed with both MR and CT at 3 and 6 months after treatment respectively for the patient with HCC and those with pancreatic cancer.

Results and Conclusions: Treatment was successfully performed in all patients without any adverse events during or after the procedure. MR images acquired immediately after treatment demonstrated necrosis of ablated area within the lesion in all cases; in particular the HCC was completely non-enhancing. At short term clinical follow-up, all the patients with pancreatic cancer referred reduction of pain symptoms due to infiltration of the celiac plexus. However follow-up imaging demonstrated recurrence of pathologic tissue within the ablated area, even if there was no local progression of the disease. Two patients with pancreatic cancer underwent radiotherapy after treatment, while the remaining one underwent another MRgFUS ablation.

In conclusion, our preliminary clinical experience suggests that MRgFUS is a feasible and repeatable ablative technique in patients with unresectable and device-accessible hepatic and pancreatic lesions.

70-LV

Wednesday
17 October 2012

Topic: Liver
Presentation Type: Oral

MR-Guided Focused Ultrasound Induced Hyperthermia For Enhancing Drug Delivery in a Pancreatic Cancer Mouse Model

Navid Farr[1], Nicole Hijnen[2], Esther Kneepkens[2], Yak-Nam Wang[1], Samantha D'Andrea[1], Donghoon Lee[1], Holger Gruell[3], Joo-Ha Hwang[1]

[1]University of Washington, Seattle, Washington, United States
[2]Eindhoven University of Technology, Eindhoven, Netherlands
[3]Philips Research, Eindhoven, Netherlands

Background/Introduction: Pancreatic cancer has one of the lowest survival rates because current therapies are ineffective. Dense stromal tissue and poor vascular perfusion, limits drug penetration and uptake into the tumor tissue. Growing evidence indicates that hyperthermia in combination with temperature sensitive liposomal (TSL) drug delivery can lead to increased organ perfusion and drug extravasation resulting in high local drug concentration. Enhanced drug delivery may be achieved using Magnetic Resonance-guided High Intensity Focused Ultrasound (MR-HIFU) in conjunction with a heat triggered drug delivery system. MR-guided heating methods enable accurate and precise spatial and temporal control of heating.

Methods: Three different mouse models of pancreatic tumors were used for these studies: a transgenic mouse model (KPC) that spontaneously develops pancreatic ductal adenocarcinoma, an orthotopic model, and a heterotopic subcutaneous model. A dedicated small animal setup integrated into a 4-channel MR receiver coil (Philips Healthcare) was used as add-on to a 3T clinical MR-HIFU system (Sonalleve®, Philips Healthcare). Mice were treated by targeting sonications (1.2 MHz frequency, 7W acoustic power) in 5-10 minute increments with a total time of 30 minutes after injection of TSLs co-encapsulating doxorubicin and the MRI contrast agent. Temperature changes during sonications were monitored by a gradient echo based echo planar imaging (EPI) sequence with EPI factor 7, TR/TE: 62/20 ms, flip angle 20 degree, dynamic scan time 3.9s, and voxel size RL0.8mmFH0.9mm. After each treatment fraction, drug release from the TSL was probed by the acquisition of maps of the tumor and bladder longitudinal relaxation rate (R1). A small gel phantom was placed beside the mouse to monitor the magnetic drift for temperature correction. Mice were sacrificed immediately after treatment and tumor tissue was collected. All samples were evaluated for drug concentration.

Results and Conclusions: Hyperthermia therapy in mouse pancreatic cancer tumor models was successful using a clinically available MR-HIFU system. Preliminary fluorescence evaluation of the samples revealed increased focal nuclear uptake of doxorubicin in tumors treated with MR-HIFU hyperthermia with systemically administered doxorubicin loaded TSLs.

Acknowledgements (Funding): This project is supported by funding from the Focused Ultrasound Foundation and Philips Healthcare.

71-LV

Wednesday
17 October 2012

Topic: Liver
Presentation Type: Oral

Clinical Evaluation of a Toroidal High Intensity Focused Ultrasound Transducer Used Intra-Operatively for the Treatment of Liver Metastases

David Melodelima[1], Jeremy Vincenot[2], Yao Chen[3], Aurelien Dupre[3], Jean-Yves Chapelon[4], Michel Rivoire[3]

[1]National Institute of Health and Medical Research - INSERM, Lyon Cedex 03, France
[2]INSERM, Lyon, France
[3]Centre Leon Berard, Lyon, France
[4]Inserm, U1032, LabTau/Université de Lyon, Lyon, France

Background/Introduction: In this study an ultrasound device that uses a toroidal HIFU transducer guided by ultrasound imaging was evaluated clinically for the treatment of colorectal liver metastases during an open procedure. Our long-term objective is to associate HIFU with hepatic resection. Here we report the first clinical results obtained on six patients with liver metastases and scheduled for elective surgical resection of their tumors. The principal objective was to validate the effectiveness, tolerance and safety of the HIFU parameters defined during preclinical studies. In addition, the response to HIFU was assessed using the ultrasound imaging probe integrated in the HIFU device and compared directly with histological analysis.

Methods: It was planned to include 6 patients in this Phase I trial. A 85% ablation rate success was required to continue the study (Phase II). Secondary endpoint was preciseness of ultrasound imaging to visualize HIFU ablations. The transducer has a toroidal shape 70 mm in diameter and is divided into 8 radial ultrasound emitters of 4.16 cm2 each. The radius of curvature is 70 mm to enable treatment of the deepest regions of the liver and each of the 8 emitters is divided into 32 individual transducers operating at 3 MHz. A 7.5 MHz ultrasound imaging probe was placed in the centre of the device to guide the treatment. The imaging plane was aligned with the HIFU focal zone. Two single thermal ablations were created in each patient after laparotomy and just before the planned liver resection.

Results and Conclusions: Twelve HIFU lesions were performed. All were visible on ultrasound images. Consistent with our previous experience, the demarcation between ablated and non-ablated tissue was apparent in ultrasound images as a hypoechoic boundary and a large central hyperechoic zone. The dimensions measured on ultrasound imaging were correlated (r=0.92) with dimensions measured during histological analysis. The average coagulated volume obtained from a 40 s total exposure in the liver was 5.6 ± 2.6 cm3 (1.9 – 11.4) with an average diameter of 21.6 ± 4.5 mm (12.0 – 28.0) and an average depth of 28.4 ± 6.3 mm (20.0 – 43.0). The patients have tolerated the treatment well. There was no hemodynamics and respiratory changes. No HIFU-related complications occurred during surgery and 30 days postoperatively. The ultrasound imaging probe integrated in the HIFU device enabled exploration of 88% of the liver.

This HIFU treatment using a toroidal transducer is feasible, safe and well tolerated. The HIFU approach presented in this study is characterized by the brevity of the treatment (40 seconds for one single ablation of 5-6 cm3). This device is capable of achieving selective ablation of predefined liver regions. Ultrasound imaging evidence of complete ablation of the target region can be taken to infer histological success.

Acknowledgements (Funding): This work was supported by funding from the Canceropole Lyon Auvergne Rhone Alpes (PDC 2006.4.8)

72-LV

Wednesday
17 October 2012

Topic: Liver
Presentation Type: Oral

FUSIMO - A European Project on Patient-Specific Modeling and Simulation of FUS in Moving Organs

Stefan Braunewell[1], Jenny Dankelman[2], Thomas Langø[3], Jürgen Jenne[4], Michael Müller[5], Yoav Levy[6], Mario Bezzi[7], Christine Tanner[8], Calin Tiu[9], Daniel Outmazguine[10], Matthias Günther[1], Andreas Melzer[11], Tobias Preusser[1]

[1]Fraunhofer MEVIS, Bremen, Germany
[2]Delft University of Technology, Delft, Netherlands
[3]SINTEF, Trondheim, Norway
[4]mediri GmbH, Heidelberg, Germany
[5]IBSMM Engineering spol. s r.o., Brno, Czech Republic
[6]InSightec Ltd., Tirat Carmel, Israel
[7]Universita Degli Studi Di Roma La Sapienza, Rome, Italy
[8]ETH Zürich, Zürich, Switzerland
[9]MEDIS Foundation, Campina, Romania
[10]GE Healthcare, Tirat Carmel, Israel
[11]University of Dundee, Dundee, United Kingdom

Background/Introduction: Focused Ultrasound (FUS) application to moving organs is still a great challenge due to several complexities. Processes affecting the outcome of FUS therapy range from the movement of the target, the physiology of the organs down to the energy disposition in the tissue and the heat transfer within the body. To empower the physician to perform safe, effective and efficient ablation of tumours in moving organs requires software support. In the 4.74 million € EU project FUSIMO (2011-2013), a patient specific model of the relevant processes involved in MR-guided FUS therapy is developed to simulate the outcome of the therapy. In this talk, an overview of the FUSIMO project will be given.

Methods: The software assistance developed within FUSIMO comprises a set of models for the respective physical and biophysical processes during FUS; an abdominal organ model simulates the patient specific motion and the influence on ultrasound application. This model will include geometric structures of organs, muscles and bones relevant for the target region. A patient specific target organ/tumour model captures the physiology and the tissue's reaction to the therapy. Finally a tissue model simulates the energy distribution, tissue heating and cooling. All model components are individualized to the patient under treatment by relevant parameters, which are extracted from imaging (MR and/or US). All components are integrated into a clinically applicable software system. This system as well as the model components will be validated in both phantom ex vivo and soft embalmed human cadavers.

Results and Conclusions: The FUSIMO software demonstrator will incorporate multi-level models for FUS application in moving organs. It shall support the physician in assessing the feasibility of the intervention, predicting and optimizing the outcome, detecting potential risks and avoiding them, as well as monitoring the progress and tracking deviations from the planned procedure. Having an integrated and validated system will facilitate the application of MR-guided FUS on moving abdominal organs such as the liver or kidney.

Acknowledgements (Funding): The research leading to these results has received funding from the European Union's Seventh Framework Programme (FP7/2007-2013) under grant agreement n° 270186.

73-LV

Wednesday
17 October 2012

Topic: Liver
Presentation Type: Oral

Ultrasound Thermography In Vivo: Tissue Property Measurements Using Subtherapeutic High Intensity Focused Ultrasound

Alyona Haritonova[1], Dalong Liu[2], Andrew Casper[1], John Ballard[1], Jeunghwan Choi[1], John Bischof[1], Emad Ebbini[1]

[1]University of Minnesota , Minneapolis, Minnesota, United States
[2]Seimens Medical, Issaquah, Washington, United States

Background/Introduction: We have recently demonstrated the first in vivo real-time ultrasound thermography (UST) system based on our speckle tracking approach to imaging temperature change. The sensitivity of the approach to small changes in temperature (~1oC) has been demonstrated in the presence of tissue motions and deformations due to breathing and blood vessel pulsation. Furthermore, the temperature fields can be updated at relatively high frame rates (80 - 150 fps) with high spatial resolution (~0.3 mm). The high spatial and temporal resolution of UST, together with the heat localization ability of subtherapeutic HIFU, make it possible to measure local tissue properties like absorption, diffusivity, and stiffness. In order to validate these measurements, however, we have designed an approach to register real-time UST with histology samples obtained after localized lesion formation experiments in a small-animal model.

Methods: HIFU lesion formation was performed with a 3.5MHz fenestrated dual mode ultrasound array (DMUA), where the central opening accommodates a SonixRP imaging probe (Ultrasonix, Canada). The Copenhagen rat received HIFU treatment in both hind limbs, with two lesions formed per therapeutic plane (avg. intensity ~4300 W/cm2). High frame rf data was collected before, during and after lesion formation procedure. The rat was sacrificed 4hrs post therapy; at which point a solution of nitro blue tetrazolium was perfused through the animal. The tissue was then fixed in a 10% formalin bath and submitted for histological processing. Formalin-fixed hind limbs were scanned with a 9.4T MRI and US to obtain 3D structural volumes. In addition, an ultrasound 3D volume was acquired at the time of therapy. Coherent point drift (CPD) registration algorithm [Myronenko, 2010] was performed on the 3D US, MRI and gross tissue volumes.

Results and Conclusions: The results from the CPD registration algorithm are presented in Figure 1, where a cross-section through a therapeutic plane is captured with gross photography (A), an in vivo ultrasound (B), and 9.4T MRI (C). Two lesions formed in the therapeutic plane are outlined by the white rectangles, with the Figure 1D depicting a histological equivalent of the lesion on the right. The CPD registration method relies on utilization of 3D volumes obtained in vivo and post fixation to overlay multimodality volumes. The subtheraputic thermography data is presented in Figure 2, where 2D temperature evolution is outlined in the beginning (Frame A), middle (Frame B) and the end (Frame C) of the heating cycle. Ability to correlate gross tissue photographs and histological cross-sections with the thermography maps allows for localized tissue property measurement at the lesion location and direct comparison with histological evaluation.

Acknowledgements (Funding): We would like to thank UMn Center for Magnetic Resonance Research for their assistance with the MRI scan. This work is supported by "Ultrasound Thermography and Thermometry In Vivo" - Samsung funded project # 00025422.

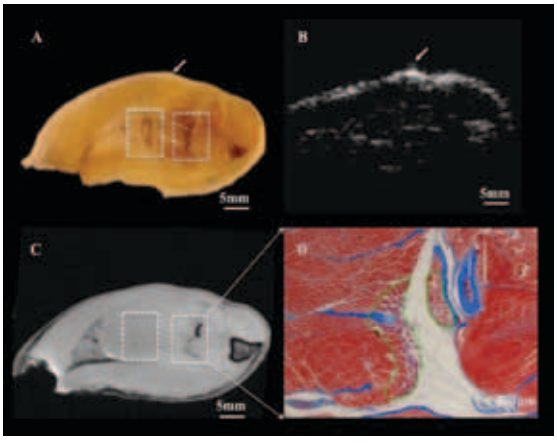

Figure 1. Gross cross-section of the therapeutic plane (A) co-registered with the in vivo ultrasound (B) and 9.4 MRI (C). The arrows highlight the presence of edema on gross and ultrasound images and white rectangles outline two lesions formed during therapy; (D) depicts the histological equivalent of the lesion on the right stained with the Masson's trichrome.

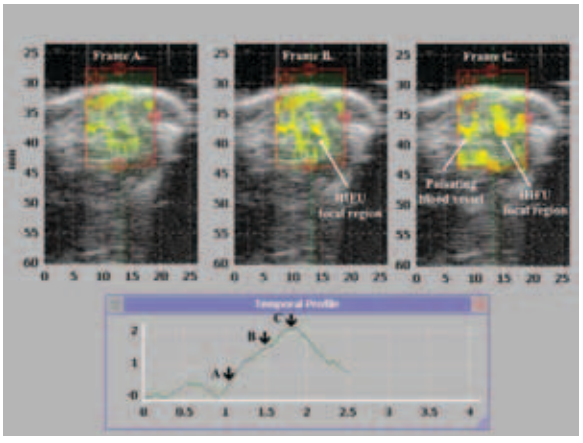

Figure 2. Temperature evolution during a subtherapeutic HIFU shot delivery in a Copenhagen rat. Frame A, B and C represents different time points at the time of HIFU heating.

74-LV

Wednesday
17 October 2012

Topic: Liver
Presentation Type: Oral

In-Vivo Evaluation of Acoustic Intensity Based Element Selection for Optimal Intercostal Firing

Martijn de Greef[1], Matti Tillander[2], Julius Koskela[2], Joost Wijlemans[1], Mika Ylihautala[2], Lambertus Bartels[1], Chrit Moonen[1], Mario Ries[1]

[1]University Medical Center Utrecht, Utrecht, Netherlands
[2]Philips Healthcare, Vantaa, Finland

Background/Introduction: One of the challenges of HIFU-therapy of hepatic lesions is sonication across the thoracic wall. To avoid tissue damage in the vicinity of the ribs two basic approaches have been suggested, both selectively de-activate individual transducer elements: Marquet et al.[1] used echo-graphic data from the transducer elements to identify and deactivate obstructed channels. However, currently most clinical HIFU-systems are not equipped with echo-graphic capabilities. Quesson et al.[2] proposed MRI based deactivation, based on a projection of the ribs onto the transducer. Here, we present a de-activation algorithm based on rapid acoustic simulations of the beam propagation in a two-layer model. The proposed approach is validated in both ex-vivo and in-vivo experiments.

Methods: Element switch-off was studied in-vivo in a porcine animal model. The animal was positioned prone, feet-first on a clinical MR-HIFU system (Sonalleve V2, Philips Healthcare, Vantaa, Finland). General anesthesia and mechanical ventilation were applied and all sonications were performed in breath-hold. After T2-weighted anatomical TSE imaging (voxel size: 1.5x1.5x1.5mm3), an ablation volume was placed such that the beam cone overlapped with the right lower part of the thoracic cage. At mid-rib position, the ribs within the beam cone were delineated to define a surface on which the acoustic intensity was evaluated per element. Based on an intensity threshold, with an attempt to limit the rib temperature increase to 10°C, according Tillander et al.[3], transducer elements were selectively disabled. The resulting temperature evolution was compared with experiments using the full transducer aperture and equal power levels. Rib heating was measured with both PRF MR-thermometry and two thermocouples, one placed in front of the ribs, one in an adjacent area. Post-intervention, detailed acoustic simulations using a stochastic acoustic ray-tracer (Mougenot et al.[4]) were performed to study rib exposure in detail.

Results and Conclusions: The results show that element switch-off based on acoustic intensity calculations is an effective strategy to limit undesired heating in the thoracic wall. The main disadvantage of the approach is the requirement to obtain and to segment high-resolution MRI of the thoracic anatomy during therapy. On the other hand, the method takes both refractive and diffractive effects into account and allows to investigate the spatial distribution of the acoustic energy exposure for each transducer element individually. Furthermore, the method is compatible with other imaging modalities such as CT and can thus also be used in therapeutic pre-planning to predict the required aperture reduction, essential for the evaluation of the anticipated treatment duration and overall feasibility.

Acknowledgements (Funding): This research was supported by the Dutch Center for Translational Molecular Medicine (CTMM, project VOLTA).

References:

1. F. Marquet F, et al. *Phys Med Biol.* 2011 Nov 21;56(22):7061-80.
2. B. Quesson, et al. *Med Phys.* 2010 Jun; 37(6):2533-40.
3. M. Tillander, et al. *Proc. of the 12th Int. Symposium on Therapeutic Ultrasound* 2012, A-239.
4. C. Mougenot, et al. *Med Phys.* 2012 Apr;39(4):1936-45.

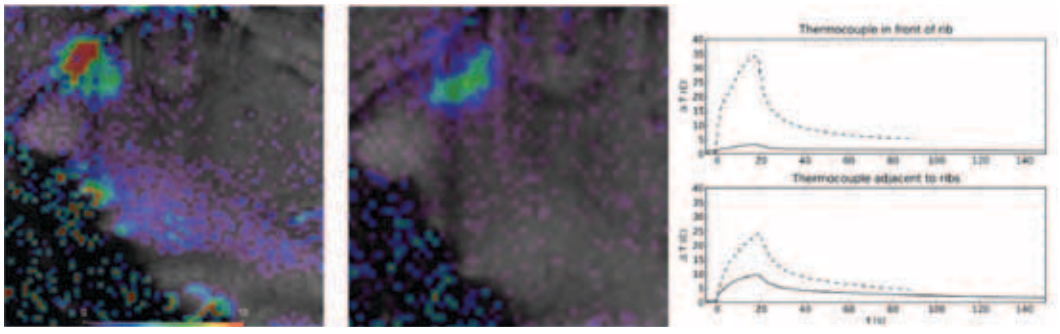

Coronal PRFS MR Thermometry slice during sonication without rib protection (left), with rib protection (center) and temperature rise as measured with thermocouples (right). Dashed lines correspond to the sonication without rib protection, solid lines to sonication with rib protection.

75-LV

Wednesday
17 October 2012

Topic: Liver
Presentation Type: Oral

T2-Based MR thermometry in Adipose Tissue Layers for HIFU Near-Field Monitoring

Paul Baron[1], Mario Ries[1], Martijn de Greef[1], Roel Deckers[1], Max Köhler[2], Jukka Tanttu[2], Lambertus Bartels[1]

[1]University Medical Center Utrecht, Utrecht, Netherlands
[2]Philips Healthcare, Vantaa, Finland

Background/Introduction: High intensity focused ultrasound (HIFU) treatment of uterine fibroids and of lesions in liver and breast is complicated by the risk of undesired near field heating, which potentially leads to cutaneous/subcutaneous tissue damage. In particular adipose tissue layers are at risk due to the high ultrasound absorption, lower specific heat capacity, and lower heat conductivity compared to those in aqueous tissues. Since the commonly used PRFS-based MR-Thermometry method is unsuitable for measurements in these areas, we evaluated dynamic T2 mapping for monitoring the temperature decrease in adipose tissue during the cool down period of the treatment cycle. The feasibility of this approach was investigated for liver HIFU ablation in an in vivo porcine model

Methods: *Ex vivo calibration:* For calibration of the apparent T2 temperature dependence, a subcutaneous adipose tissue sample was obtained directly postmortem and kept above room temperature. A temperature stabilized MRI-compatible closed-circuit water bath was employed to vary the temperature of the sample in four steps from 24 to 45°C and subsequently back to 24°C. A fiber optic probe was used to determine when the temperature had been stable for 15 minutes. Subsequently, at each temperature step a dual echo turbo spin echo sequence (TE= 38 and 180ms, TR=376ms, TSE factor=40, Voxel size =1.75x1.75x5mm3, 3 s/scan, SPIR water suppression) was used for T2 quantification using the calibration data.

In vivo experiment: The liver of one pig was sonicated in prone position using a clinical MR-HIFU system (Sonalleve, Philips Healthcare, Vantaa, Finland) integrated into a 1.5-Tesla MR scanner (Achieva, Philips Healthcare, Best, The Netherlands). A volumetric sonication cell of 8-mm diameter was placed 1.5cm deep in the liver, and sonicated with an acoustic power of 300W for 20s in order to achieve a lethal thermal dose. Dynamic T2 mapping was used for temperature monitoring in the subcutaneous adipose tissue layer of ≈5mm thickness using the same pulse sequence as for the calibration experiment. The cooling time constant was estimated by fitting the mean temperature of the beam path intersection with the image slice with a mono-exponential decay function. The thermometric precision per voxel was obtained as the temperature change temporal standard deviation calculated from 5 dynamic scans acquired prior to sonication.

Results and Conclusions: *Ex vivo calibration:* The T2 temperature dependence was found to be linear with a coefficient of 5.3 ms/°C (fig 1a). The T2 temperature dependence was found to be completely reversible during heating and cooling of the sample (figure 1a).

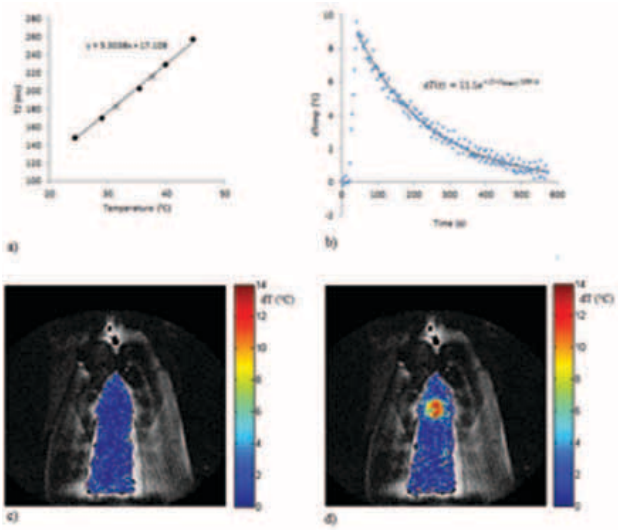

Figure 1. a) T2-temperature dependence during heating (dots) and cooling (crosses). Note the absence of any hysteresis in the evaluated temperature range. b) Temperature change in the near-field during sonication. c) Temperature change map before sonication and d) at peak temperature.

In vivo experiment: In the porcine adipose tissue T2 based temperature changes were observed (figure 1c and d). A cooling time constant of 3min and 20s was found for this sonication (figure 1b). The thermometric precision in the near field was 1.1°C (range 0.2-3.8°C).

The reversibility and linearity of the T2-temperature dependence of adipose tissue allowed to continuously monitor the temperature in the subcutaneous tissue layers during cool-down. The temperature change and precision showed heterogeneities, likely reflecting the varying water/fat fractions in a voxel. The cooling time can be expected to be geometry and subject specific, and underlines the need for individual observation of the cool down process to avoid cumulative heating of subcutaneous tissue. Future studies need to explore the inter-individual variation of the T2-temperature dependence and confirm this dependency at other field strengths.

Acknowledgements (Funding): This research was supported by the Center for Translational Molecular Medicine (VOLTA WP1).

76-LV

Wednesday
17 October 2012

Topic: Liver
Presentation Type: Oral

Intrapleural Fluid Injection for MR-HIFU Ablation in the Subdiaphragmatic Liver

Joost Wijlemans[1], Maurice van den Bosch[1], Martijn de Greef[1], Gerald Schubert[2], Lambertus Bartels[1], Mika Ylihautala[2], Chrit Moonen[1], Mario Ries[1]

[1]University Medical Center Utrecht, Utrecht, Netherlands
[2]Philips Healthcare, Vantaa, Finland

Background/Introduction: One of the challenges for the clinical implementation of MR-HIFU for liver tumor ablation, is that the lung overlaps the cranial part of the liver in the costophrenic angle. The resulting air-tissue interface creates a barrier for the propagation of the ultrasonic waves. As a consequence, ablation of tumors in the cranial part of the liver is challenging, since a major part of the beam cone is obstructed. In this study we present a technique of intrapleural fluid injection (i.e. to fill the costophrenic angle with fluid) for the creation of an acoustic window during hepatic HIFU ablation. We demonstrate the feasibility of this technique in vivo during HIFU ablation of the subdiaphragmatic part of a porcine liver.

Methods: After induction of general anesthesia on an adult swine (80kg), ultrasound imaging was used to locate the costophrenic angle of the right pleural cavity and an 18 Gauge intravenous infusion catheter was inserted into the intrapleural space under ultrasound guidance. Degassed normal saline (0.9% NaCl) was injected into the intrapleural space until the costophrenic angle was filled, which was confirmed by repeated T2-weighted MRI. Cardiac frequency, blood pressure and oxygen saturation were monitored during intrapleural fluid injection. Subsequently, the pig was positioned in right decubitus position on a clinical 1.5T MR-HIFU system (Sonalleve, Philips Healthcare, Finland). One 4mm volumetric ablation cell (400W, 20s) was placed cranially in the right liver lobe, so that 80% of the ultrasonic beam cone intersected with the newly created acoustic window. The sonication was conducted during breath hold and under MR-guidance using PRFS-thermometry. No measures were taken to prevent rib heating during sonication. After the experiment the animal was sacrificed and the parietal and visceral pleura, the diaphragm and the liver were inspected for procedure-related damage

Results and Conclusions: The ultrasound-guided intrapleural injection of 200ml of saline solution was sufficient to fill the right costophrenic angle and to displace the right lung 1.5cm cranially. Cardiac frequency and blood pressure remained stable during and after the procedure; oxygen saturation remained 100%. The HIFU sonication resulted in a peak temperature of 56.3 °C in the designated ablation area as presented in Figure 1. Significant heating was observed in the vicinity of the ribs in the beam path due to the obstruction of ~40% of the beam cone. This is also a likely explanation of the low target temperature despite the 400W sonication power. The post-mortem examination evidenced no thermal damage to lung, pleura or diaphragm, except a small needle puncture on the visceral pleural of the right lower lung lobe. In conclusion, intrapleural fluid injection can be used to create an acoustic window for MR-HIFU ablation of the subdiaphragmatic liver segments. This technique may enable MR-HIFU ablation of cranially located liver tumors in clinical practice.

Acknowledgements (Funding): This study was performed within the framework of CTMM, the Center for Translational Molecular Medicine, project VOLTA (grant 05T-201). We are grateful to Young-sun Kim for his advice on injection techniques.

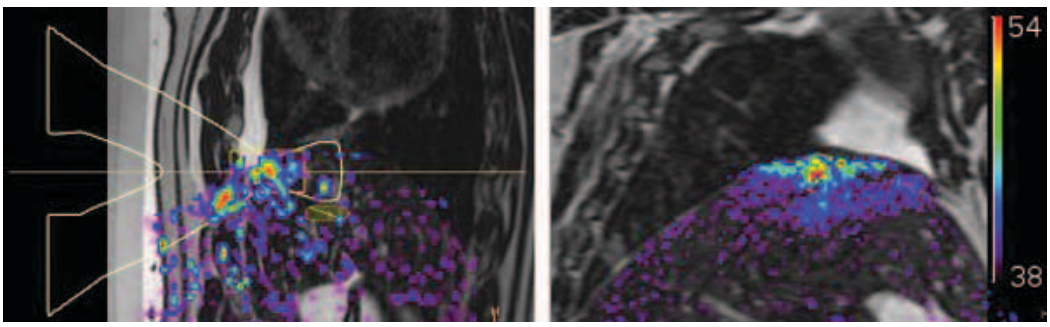

Figure 1. Overlay of MR-thermometry at peak temperature over the T2-weighted anatomical images in sagital (left) and coronal (right) view. The normal saline injection displaced the lung cranially and allowed the sonication of a liver area located only 1 cm below the diaphragm.

77-LV

Wednesday
17 October 2012

Topic: Liver
Presentation Type: Oral

Suitability of a Tumour-Mimicking Material for the Evaluation of High Intensity Focused Ultrasound Ablation Under Magnetic Resonance Guidance

Samuel Pichardo[1], Jon Kivinen[2], Laura Curiel[1], David Melodelima[3]

[1]Thunder Bay Regional Research Institute, Thunder Bay, Canada
[2]Lakehead University, Thunder Bay, Canada
[3]National Institute of Health and Medical Research - INSERM, Lyon Cedex 03, France

Background/Introduction: In the present study we propose the use of an agarose-based tumour-mimic for MR targeting and thermometry maps during HIFU exposures. In the search and validation of new clinical applications for HIFU, animal models play an important role. Models similar to the anatomy and physiology of humans have been used. For the treatment of hepatic tumours with HIFU, pigs are a common model, but results to develop human hepatocarcinomas in this model are still inconclusive. As a result, hepatic applications for HIFU are usually studied in a combination of models using VX2 tumours in rabbits to validate the therapy response and HIFU lesions performed on healthy pigs to validate the size of coagulation and the safety of the device. However, these models do not provide a complete tool to ensure that the targeting and complete treatment of the intended area is achieved. And since achieving controlled margins is important to ensure that the treatment is complete, an alternative model for studying the accuracy of HIFU and other thermal treatments has to be explored.

Methods: MRI experiments were conducted using a 3T MR scanner (Achieva®, Philips). HIFU exposures were conducted using an MRgHIFU clinical system (Sonalleve®, Philips). The tumour-mimic was prepared with a mix of 3% agarose, 3% cellulose, 7% glycerol, 0.05% methylene blue and sterile water. Thermal conductivity, thermal diffusivity and volumetric heat capacity of the tumour-mimic were obtained using a thermal constants analyzer. Relaxation times T1 and T2 were obtained on the 3T MR scanner and a 500 MHz NMR. The acoustic absorption of the tumour-mimic was calculated by comparing MR thermal maps and simulations of the rise of temperature using the heat transfer equation. MRgHIFU validation under ex vivo conditions was performed with 25 liver samples with an embedded 1.5 cc tumour-mimic. In vivo validation was done using Six New Zealand 3 kg rabbits with 1 cc of tumour-mimic injected in the left and right thighs.

Results and Conclusions: The relaxation times at 3T were 1679±15 ms for T1 and 41±1ms for T2. The mimic was clearly visible on T1-weighted images showing an average mimic-muscle CNR of 34.8±4.7 for ex vivo samples and mimic-muscle CNR of 31.8±5.6 for in vivo samples. On T2-weighted images the contrast was lower with an average mimic-muscle CNR of 4.6±3.6 for ex vivo samples and mimic-muscle CNR of 5.3±3.7. MR thermometry maps were performed during HIFU. Absorption of the tumour-mimic was found to be 63% of attenuation losses. The average temperature when the sonication was done at the tumour-mimic was 67.6±8.0°C in vitro and 67.6±5.0°C ex vivo. The average temperature for sonications at tissues was 68.4±8.7°C ex vivo (liver) and 66.0±2.6 C in vivo (muscle), with no significant difference between tissue and tumour-mimic ($p>0.05$). The tumour-mimic behaviour when using MR-guided HIFU was similar to tissues, showing that this mimic can be used as an alternative to tumour models for validating MR-guided HIFU devices targeting.

Acknowledgements (Funding): This work was partly supported by funding provided by the Natural Sciences and Engineering Research Council of Canada.

(See figures, next page)

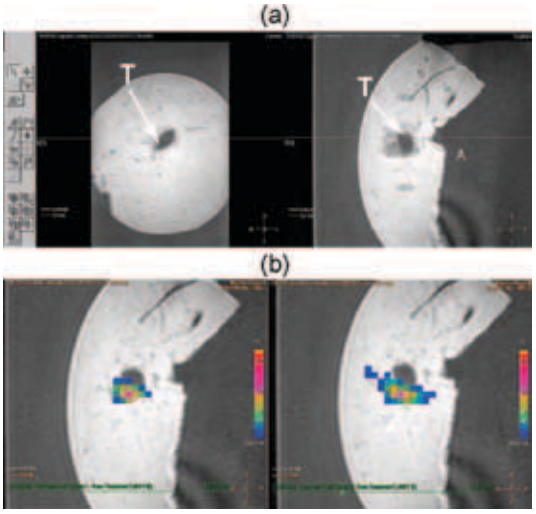

Heating using the Sonalleve system on ex vivo samples: a) screen used for targeting the tumour-mimic with the planned lesions appearing in light grey and b) thermometry map at the point of maximum temperature rise during two neighbouring exposures. The tumour-mimic is shown by the arrow marked T.

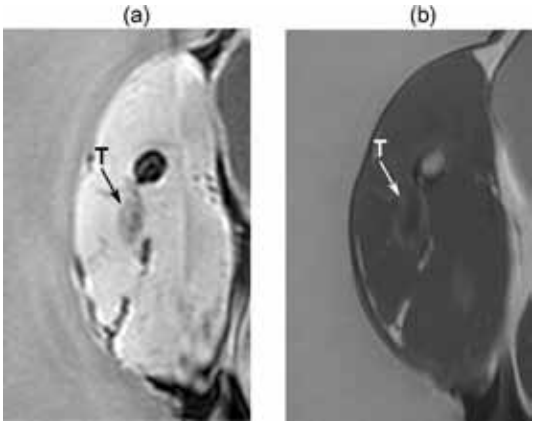

MR images of the tumour-mimic injected into a rabbit thigh: a) T1-weighted gradient echo (TE/TR=3.5/7ms, FOV=150x150x100mm, 2.5 mmslice thickness, 140x135 acquisition matrix, 320x320 reconstruction matrix, flip angle 10 degrees, ETL=45, 4 NEX) and b) T2-weighted turbo spin echo (TE/TR=36/2500 ms, FOV=200x200x39mm, 4 mm slice thickness, 348x400 acquisition matrix, 448x448 reconstruction matrix, flip angle 90 degrees, ETL=15, 2 NEX). The tumour-mimic is shown by the arrow marked T

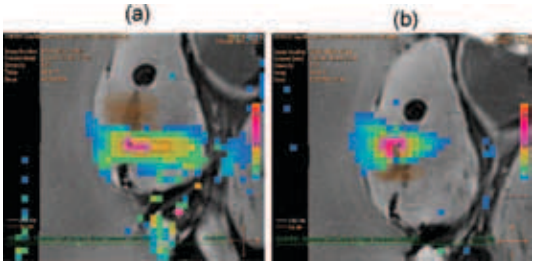

MR thermometry obtained during a sonication in vivo for two different cases: a) with the heating following the expected beam shape and b) one of the cases where irregular heating was observed at the tumour-mimic

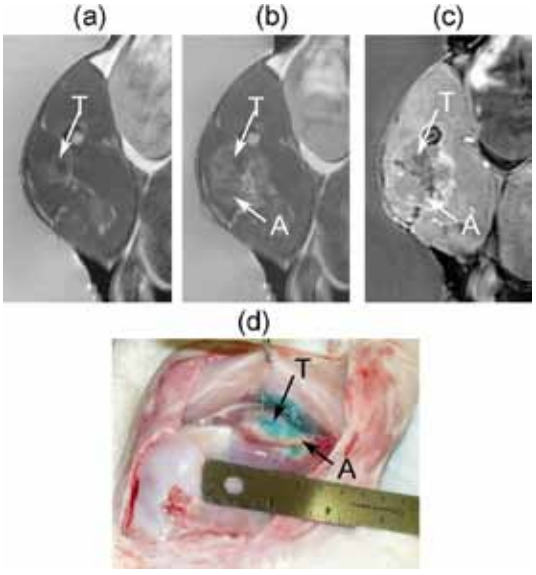

Images of the tumour-mimic in vivo: a) T2-weighted spin echo after ablation; c) contrast-enhanced T1-weighted after ablation; and d) the correspondent picture of the tissue obtained after euthanasia. The tumour-mimic is shown by the arrow marked T and the ablation by the arrow marked A.

78-LV

Wednesday
17 October 2012

Topic: Liver
Presentation Type: Oral

MR-HIFU Drug Paintbrush: Large Volume, Conformal Mild Hyperthermia with MR-HIFU Used To Trigger and Monitor Release From Image-Able, Temperature-Sensitive Liposomes

Pavel Yarmolenko[1], Elma Carvajal Gallardo[2], Ari Partanen[3], Ashish Ranjan[4], David Woods[4], Ayele Negussie[4], Caitlin Burke[5], Lambertus Bartels[6], Mark Dewhirst[7], Bradford Wood[5], Matt Dreher[1]

[1]National Institutes of Health, Bethesda, Maryland, United States
[2]Image Sciences Institute, University Medical Center Utrecht, Utrecht, Netherlands
[3]Philips Healthcare, Bethesda, Maryland, United States
[4]Center for Interventional Oncology, Radiology & Imaging Sciences, Clinical Center, National Institutes of Health, Bethesda, Maryland, United States
[5]National Institutes of Health, Vienna, Virginia, United States
[6]University Medical Center (UMC) Utrecht, Utrecht, Netherlands
[7]Duke University, Department of Radiation Oncology - Durham, Durham, North Carolina, United States

Background/Introduction: Chemotherapy of solid tumors may be improved by spatio-temporal control of drug delivery, a concept known as drug dose painting, where a desired concentration of drug may be deposited in a specific region, often with image guidance. Dose painting may be achieved with a combination of image-able low temperature-sensitive liposomes (iLTSL) and local mild hyperthermia (HT) using magnetic resonance guided high-intensity focused ultrasound (MR-HIFU). Clinical translation of this drug-device combination largely depends on development of algorithms that enable conformal heating of large volumes in a variety of shapes. Objectives of this study were to: 1) develop a mild hyperthermia (~41°C) algorithm for MR-HIFU to conformally heat large volumes (>2cc) of tissue, 2) characterize the algorithm's performance in vitro and in vivo, and 3) examine its utility in drug dose painting with iLTSL.

Methods: A large volume, conformal HT algorithm was implemented on a clinical MR-HIFU platform (Sonalleve, Philips Medical Systems, Vantaa, Finland), combining electronic and mechanical HIFU steering. The ability of the system to deliver HT was evaluated in terms of temperature accuracy and stability, as well as spatial accuracy (spatial offset = average distance to target from all heated voxels [>40°C]), in a phantom and in vivo (Vx2 tumor and thigh muscle in a rabbit). iLTSL release was triggered with MR-HIFU mild hyperthermia and monitored in real time (through changes in tissue T1) simultaneously with MR thermometry, using the variable flip angle approach.

Results and Conclusions: In phantom, the system quickly heated the intended region to the 41°C target (heat-up <5.5min for target cross-sectional area, perpendicular to beam path <8.8cm2). Mean temperature was stably maintained (±1°C) for the prescribed duration (10min). Cross-sectional area of the heated volume tightly conformed to the prescribed area (spatial offset=0.04±0.51mm). Performance was similar in vivo (heat-up<2.2min for target cross-sectional area <2.9cm2), albeit with slightly more temporal variation in mean temperature (±1.6°C) and slightly lower spatial accuracy (spatial offset=1.0±2.2mm). After injection of iLTSL and a 10min baseline observation, subsequent HT for 25min (area=3.3cm2) resulted in contrast agent concentration of 0.43±0.07mM in heated tumor, compared to 0.20±0.04mM in adjacent unheated muscle. No noticeable real-time changes in T1 were detected following iLTSL administration before heating in the above experiment, likely due to a relatively low sensitivity of the variable flip angle sequence to T1 changes. However, when iLTSL was injected during stably-maintained HT, it reduced T1 below a pre-hyperthermia baseline, suggesting that T1 decrease due to contrast agent release from iLTSL is relatively large compared to the well-documented (and observed) increase in T1 due to heating. Stable pre-hyperthermia baseline, undetectable T1 changes due to iLTSL without heating, and stable tissue T1 during maintenance of HT before iLTSL injection can be used to mathematically solve for changes in T1 that occur mostly due to hyperthermia-triggered iLTSL content release.

Large volume conformal hyperthermia with a clinical MR-HIFU platform enabled HT of variable shapes and sizes that are typical of lesions encountered in clinical oncology. Orchestration and real-time quantification of iLTSL content release with MR-HIFU could be used in conjunction with the large volume mild hyperthermia algorithm to enable drug dose

painting in large target lesions of variable shape. This drug-device combination is a novel tool not currently available in clinical oncology.

Acknowledgements (Funding): This work was supported through the Huygens Scholarship Program in the Netherlands, the NIH Intramural Research Program at the Center for Interventional Oncology and a CRADA with Philips Healthcare. The authors would like to thank Dr. Chrit Moonen's laboratory in Utrecht, the Netherlands for the RealTI toolkit that was instrumental to the implementation of the large volume HT algorithm. Part of this work was recently presented at ISTU 2012 in Heidelberg, Germany.

79-LV

Wednesday
17 October 2012

Topic: Liver
Presentation Type: Oral

Targeted Drug Delivery By Focused Ultrasound Mediated Hyperthermia Combined with Temperature Sensitive Liposomes

Astrid Gasselhuber[1], Matt Dreher[2], Ari Partanen[3], Pavel Yarmolenko[2], Bradford Wood[2], Dieter Haemmerich[1]

[1]Medical University of South Carolina, Charleston, South Carolina, United States
[2]National Institutes of Health, Bethesda, Maryland, United States
[3]Philips Healthcare, Bethesda, Maryland, United States

Background/Introduction: Temperature sensitive liposomes (TSL) are drug carriers that release content (usually chemotherapy agent) above a threshold temperature, typically ~40 ºC. In combination with localized hyperthermia facilitated by high-intensity focused ultrasound (HIFU), targeted drug delivery for cancer treatment applications can be achieved. A variety of physiological, biological, biophysical, TSL, and drug parameters affect hyperthermia-mediated drug delivery from TSL. Computer simulations provide a means to efficiently examine effects of these parameters. Among other benefits offered by computer simulations, they can suggest optimal delivery strategies by enabling detailed examination of heating algorithms (e.g. varying temperature and time), varying tumor transport parameters (e.g. vessel permeability, perfusion), and modifying TSL properties (e.g. release rate). Here, we present a mathematical model that combines a heat-transfer model with a drug delivery model to simulate both HIFU-induced tissue heating and hyperthermia-mediated drug delivery from TSL-encapsulated doxorubicin. We use this model to examine a different heating regimen, and present results of an in-vivo study for comparison.

Methods: HIFU heating in tissue was simulated using a heat-transfer model based on the bioheat equation, including heat-induced cessation of perfusion. A spatio-temporal multi-compartment pharmacokinetic model simulated intravascular release of doxorubicin from TSL, its transport into interstitium, and cell uptake. Two heating schedules were simulated, each lasting 30 min: (1) hyperthermia at 43 ºC (HT) and (2) hyperthermia followed by a high-temperature (50 ºC for 20 s) pulse (HT+). As preliminary model validation, in vivo studies were performed in thigh muscle of a New Zealand White rabbit, where local hyperthermia with a clinical magnetic resonance-guided HIFU system was applied following TSL administration.

Results and Conclusions: HT produced a defined region of high doxorubicin concentration (cellular concentration ~15-23 μg/g) in the target region. Cellular drug uptake was directly related to HT duration, with increasing doxorubicin uptake up to ~2 h. HT+ enhanced drug delivery by ~40% compared to HT alone. Temperature difference between model and experiment within the hyperthermia zone was on average 0.54 ºC. Doxorubicin concentration profile agreed qualitatively with in vivo fluorescence profile. Computational models can predict temperature and delivered drug from combination of HIFU with TSL. Drug delivery using TSL may be enhanced by prolonged hyperthermia up to 2 h or by local cessation of vascular perfusion with a high-temperature pulse following hyperthermia.

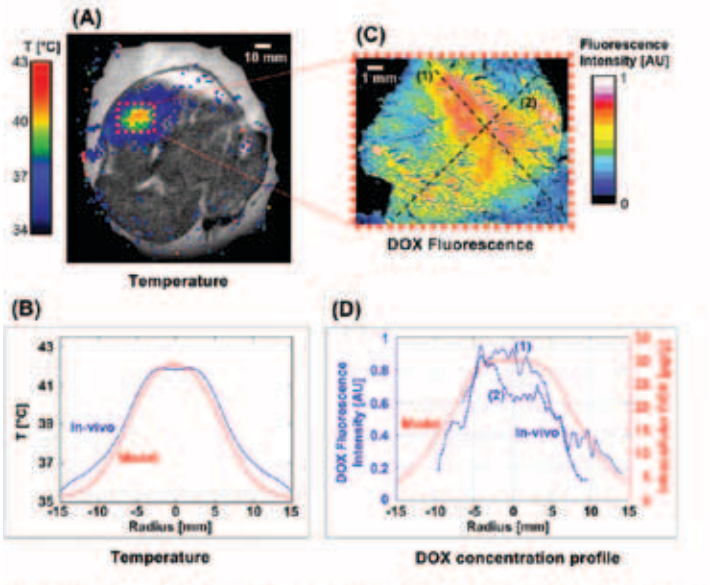

Figure 1. (A) Temperature map during *HT* measured via MR Thermometry, overlaid on pre-procedural proton density-weighted coronal image of rabbit thigh muscle. (B) Radial temperature profile (time-averaged over *HT* duration) from *in vivo* study (blue), compared to model (red). Profile location in model was chosen such that it traversed maximum temperature point (see Figure 2A, white dashed line). Temperature deviation between simulation and *in vivo* study was 0.54 °C (mean over 15mm radius). (C) DOX distribution measured via fluorescence microscopy in extracted tissue sample. (D) DOX fluorescence profile (blue) in two orthogonal directions (dashed lines marked (1) and (2) in (C), compared to DOX concentration profile from computer model (red).]

Acknowledgements (Funding): This work was supported by NIH grants R01CA118990, R21CA135519 to DH, by the NIH Center for Interventional Oncology and NIH Intramural Research Program, and by a cooperative research agreement between NIH and Philips. NIH and Celsion Corp. have a Cooperative Research and Development Agreement. Part of the work was conducted in a facility constructed with support from the National Institutes of Health, Grant Number C06 RR018823 from the Extramural Research Facilities Program of the National Center for Research Resources.

P-80-BO

Tuesday
16 October 2012

Topic: Bone
Presentation Type: Poster

MR-Guided Focused Ultrasound Improves Pain but Not Opioid Requirement

Joshua Meyer, Charlie Ma, Gary Freedman, Andre Konski, Terry Richardson, Lili Chen

Fox Chase Cancer Center, Philadelphia, Pennsylvania, United States

Background/Introduction: Palliative radiation therapy is a standard treatment for metastatic disease to the bone. However, for patients who do not benefit from or are not candidates for radiation, there is no standard palliative therapy. MR guided focused ultrasound (MRgFUS) is a treatment technique that can be employed to heat periosteal nerves to ablative temperatures, with the goal of decreasing pain. We evaluated the effect of this treatment on opioid analgesic requirement.

Methods: All patients had metastatic disease to the bone and were treated with MRgFUS using the Exablate 2000 system. Primary tumor histologies included: breast, prostate, colon and renal cell carcinomas. Metastatic sites included: scapula (2), humeral head, sacrum, ilium, pubic ramus, and acetabulum. Appropriate anesthesia was achieved utilizing conscious sedation, and frequently a periosteal injection of local anesthetic prior to treatment. Six to eighteen sonications were delivered in order to adequately treat each lesion. Pain was scored using the visual analog scale (VAS), and all analgesic medication were recorded. All opioids were converted into morphine equivalents; each patient's pre-treatment opioid requirement was normalized to 1 for the sake of comparison. All data were collected prior to treatment and at 1 week, 1 month, 2 months and 3 months post treatment.

Results and Conclusions: Seven patients were treated with MRgFUS. All treatments were completed without complication. The VAS improved over time, with the following scores: 8.0 +/- 1.1, 4.7 +/- 3.0, 3.0 +/- 1.5, 3.2 +/- 2.8, and 3.4 +/- 1.5 at pre-treatment and one week, one month, 2 months and 3 months post treatment, respectively. However, the number of normalized morphine equivalents did not differ significantly over time. The values at the same visits were: 1 +/- 0, 0.78 +/- 0.39, 1.38 +/- 1.43, 1.34 +/- 1.45, and 1.56 +/- 1.43 (Figure 1). No significant relationship could be drawn between energy, acoustic power, or temperature and treatment effect. However, it was noted that the largest percent decrease in opioid requirement was in the two patients with the lowest starting doses. The patient with the best response also achieved the highest mean energy.

In conclusion, in this small series of patients, MRgFUS was more effective at decreasing VAS score than opioid requirement. It is possible that a more profound improvement may be exhibited in patients with lower opioid requirements prior to treatment.

Acknowledgements (Funding): We would like to thank InSightec for their technical support and expertise.

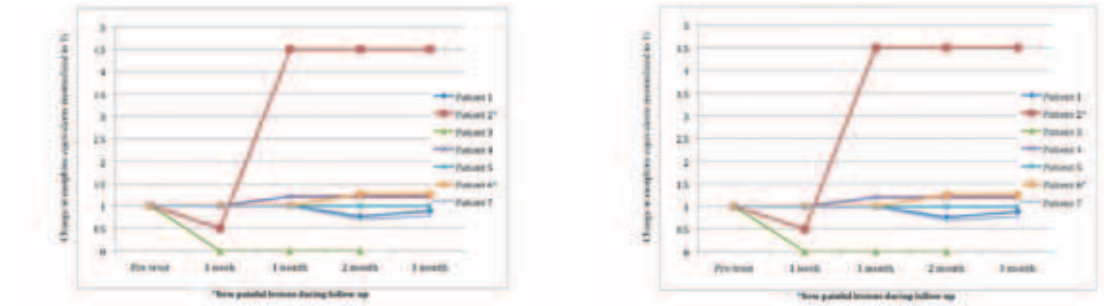

P-81-BO

Tuesday
16 October 2012

Topic: Bone
Presentation Type: Poster

MR-Guided FUS for the Noninvasive Treatment of Pain of Osteoarthritic Knees

Masashi Izumi, Motohiro Kawasaki, Takahiro Ushida, Masahiko Ikeuchi, Hirofumi Namba, Tomonari Kato, Toshikazu Tani

Kochi Medical School, Nankoku, Japan

Background/Introduction: Knee Osteoarthritis (OA) ranks among the most common disabling conditions in the elderly. A major symptom of knee OA is chronic knee pain which has a significant effect on patients' quality of life. Although total knee arthroplasty is the validated and reliable treatment for alleviating refractory knee pain, there are some patients who are at high risk during surgery and other patients who are not willing to undergo surgery. On the other hand, we have already reported the pain relieving effect of MR-guided FUS (MRgFUS) treatment in bone metastasis and lumbar facet joint OA. Here, we have created a novel, noninvasive treatment for relieving pain of knee OA using MRgFUS.

Methods: The study protocol was approved by the institutional review board of Kochi Medical School. Eight patients (2 males and 6 females with a mean age of 78 years) who had medial knee pain and tenderness were included. All patients had Kellgren-Lawrence grade-4 varus OA, and preoperative 100-mm pain visual analog scale (VAS) during walking was 75 ± 11 mm (mean ± SD). Prior to MRgFUS, patient underwent local anesthesia with 0.75% ropivacaine to the treated sites. A strappable transducer of ExAblate 2100 system (InSightec Ltd.) was fixed to the medial side of the knee. Sonications were applied to just below the rim osteophyte of medial tibia plateau, the insertion site of deep medial collateral ligament. The primary outcome measure was VAS pain score. Using a hand-held pressure algometer, pressure pain threshold (PPT) at the treated sites was also evaluated at one month after treatment.

Results and Conclusions: Fugure 1 shows VAS pain score at each follow-up time point. Although there were two non-responders, the other 6 cases showed good pain relief at the final follow-up. In particular, Case 1 and Case 4 had long-lasting pain alleviation. Case 2 and Case 3 underwent total knee arthroplasty one month after MRgFUS. In responders, PPTs (N) of medial tibia plateau were significantly increased after treatment (38.2 [27.4-51.9] vs 59.8 [49.0-62.7] (pre- vs post-, median [range]) in anterior, 34.3 [27.4-41.2] vs 53.9 [44.1-53.9] in middle, 28.4 [26.5-37.2] vs 48.0 [40.2-49.0] in posterior part, $p<0.05$), which suggested denervation of nociceptive nerve terminals. There were no obvious complications associated with the treatment. In conclusion, MRgFUS is a promising option for the noninvasive pain management of osteoarthritic knees.

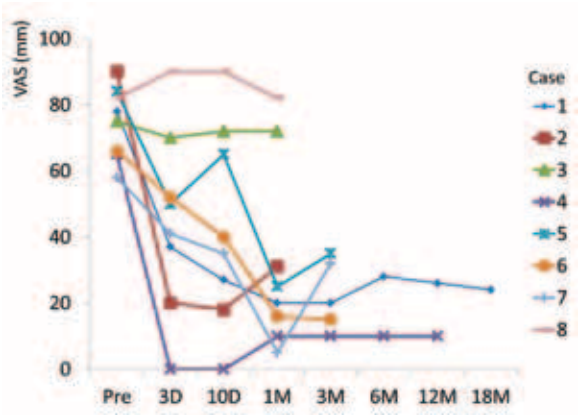

Figure1. VAS pain score at each follow-up time point

P-82-BO

Tuesday
16 October 2012

Topic: Bone
Presentation Type: Poster

Pain Palliation in Patients with Bone Metastases Using MR-guided Focused Ultrasound with Conformal Bone System: A Preliminary Report

Mi-Suk Park[1], Soohyeon Lee[2], Hye Jin Choi[1], Itay Rachmilevitch[3], Ori Atar[4], Young Taik Oh[1]

[1]Yonsei University, Severance Hospital, Seoul, South Korea
[2]Severance Hospital, Seoul, South Korea
[3]InSightec, Israel, Israel
[4]InSightec, Tokyo, Japan

Background/Introduction: Noninvasive thermal ablation using magnetic resonance (MR)-guided focused ultrasound (MRgFUS) of body system (Exablate 2000 system) has been reported to be clinically effective for palliation of pain caused by bone metastasis. Here, we are presenting the feasibility, safety, and effectiveness of MRgFUS with conformal bone system for pain palliation in patients with bone metastases.

Methods: Fifteen patients with painful bone metastasis were referred for the MRgFUS procedure with conformal bone system. Treatment safety was evaluated by assessing the device related complications. Effectiveness of pain palliation was evaluated using the visual analog pain score (VAS), and measurable changes in the intake of opioid analgesics.

Results and Conclusions: Five procedure in four patients were performed. Mean follow-up time was 43 days. 80% of the patients reported significant pain improvement from 3 days after treatment. Average VAS score was reduced form 6.4 prior to treatment to 4.4 at 3 days, 3.2 at 7 days, and 1.8 at 1 month post treatment. Second degree skin burn on the opposite site of the transducer was seen in one patient. No device-related severe adverse event were recorded.

The results suggest that MRgFUS with conformal bone system has the ability to provide an accurate, effective, and safe noninvasive palliative treatment for patients with bone metastasis.

Acknowledgements (Funding): This study is supported by a grant of InSightec (BM012) and a research fund of Korea Research Foundation (2012).

P-83-BO

Tuesday
16 October 2012

Topic: Bone
Presentation Type: Poster

Pain Palliation in Patients with Bone Metastasis. Randomized Trial Comparing MRgFUS and EBRT: Analysis of Treatment Response by Using Functional Diffusion Maps

Daniel De Oliveira, Giulia Brachetti, Vincenzo Noce, Beatrice Cavallo Marincola, Alessandro Napoli, Carlo Catalano

University of Rome — Sapienza, Rome, Italy

Background/Introduction: Bone is the most common organ for distant tumor metastases, especially in patients with cancers of the breast or prostate. Bone metastases can severely impair mobility and significantly contribute to a general decrease in quality of life. Owing to progressively improved treatments for primary tumors, the incidence of distant metastases has increased and long-term management of clinical effects has become determinant. Current treatment strategies embrace analgesics, chemotherapy, hormonal therapy and bisphosphonates for systemic treatment, and radiation therapy, percutaneous ablation and surgical stabilization for local control.

At present external beam radiation therapy (EBRT) is the treatment of choice for clinically active bone metastases. Magnetic Resonance (MR) guided Focused Ultrasound (MRgFUS) is a non-invasive treatment modality that combines the ablative properties of high-intensity focused ultrasound with MR imaging for target definition and real time guidance and monitoring.

Monitoring changes during therapy with multifunctional imaging can provide invaluable information on the in vivo mechanisms of action of therapeutics and of likely patient outcomes. A number of studies have reported on the multiparametric approach for monitoring the effects of conventional therapies. Diffusion-weighted MRI (DWI) allows the detection of a variety of malignancies. Lesion detection and characterization using DWI largely depends on the increased cellularity of solid or cystic lesions compared with the surrounding tissue. This increased cellularity leads results in restricted diffusion as indicated by reduction in the apparent diffusion coefficient (ADC). Low pretreatment ADC values of several malignancies have been shown to be predictive of better outcome. DWI can assess response to systemic or regional treatment of cancer at a cellular level and will therefore detect successful treatment earlier than anatomical measures.

For both ERBT and MRgFUS, little is known about the treatment response in bone metastases using DWI to determine variations at cellular level that might predict clinical outcome.

The purpose of our study was to investigate and compare the response to MRgFUS and EBRT treatments of painful bone metastases by using diffusion-weighted magnetic resonance imaging with apparent diffusion coefficient.

Methods: This prospective, double arm, randomized study with EBRT serving as control arm, received IRB approval. 36 consecutive patients (female:15 male:21 mean age:60.3) with painful bone metastases were enrolled. 18 patients underwent MRgFUS treatment, using ExAblate 2100 system (InSightec), and 18 patients underwent EBRT. Pain palliation was evaluated by visual analog scale (VAS), pain questionnaires and changes in the patients' medication.

All patients underwent ce-MRI (3T Discovery, GE; gd-BOPTA, Bracco) before treatment and at 1, 2, and 3 months afterward. MRI protocol included DWI sequences with five b factors (0–800 sec/mm2) and ADC maps were obtained. The average ADC values for each lesion were analyzed in comparison between pre- and post-treatment.

Results and Conclusions: No treatment-related adverse events were recorded for both arms. Statistically significant difference between baseline and follow-up VAS values and medication intake for both MRgFUS and EBRT patients ($p<0.05$) was noted. DWI showed substantial increase in mean ADC values after treatment for both MRgFUS (pre:1080,6±269 mm^2/sec; post: 1577,5±311,6) and EBRT (pre:1313,3±424,3 mm^2/sec; post:1777,9±386,3); there were no significant statistical differences in ADC shift following between MRgFUS and ERBT ($p>0.5$). Progressive decrease in VAS values positively correlated to an increase in mean ADC values ($p>0.01$) for both treatment modalities.

In conclusion, MRgFUS is a promising noninvasive treatment modality for successful

palliation of bone metastasis and has potential for tumor control as compared to ERBT. MRgFUS treatment determines bone metastasis cell damage similarly to ERBT as demonstrated by linear ADC modification.

P-84-BO

Tuesday
16 October 2012

Topic: Bone
Presentation Type: Poster

Pain Palliation of Bone Metastases: Steps Towards a Pre-Clinical Protocol

Aaldert Elevelt[1], Sin Yuin Yeo[2], Katia Donato[1], Huub ten Eikelder[2], Alon Rozen[2], Yvonka van Wijk[2], Dragan Bosnacki[2], Holger Gruell[1]

[1]Philips Research, Eindhoven, Netherlands
[2]Eindhoven University of Technology, Eindhoven, Netherlands

Background/Introduction: Advanced prostate cancer often metastasizes to bone and leads to cancer-induced bone pain. Treatments for these patients are mostly palliative and the state of the art treatment used for these patients is external beam radiation therapy, which results in pain reduction in 70-80% of the patients. In recent years, Magnetic Resonance guided High Intensity Focused Ultrasound (MR-HIFU) has been proposed as an alternative treatment. Preliminary clinical studies have shown that patients subjected to MR-HIFU treatments reported pain relief. However, there is insufficient preclinical evidence to demonstrate the safety and effects of MR-HIFU treatments. Therefore, we developed a preclinical model developing osteoblastic bone lesions and subjected it to MR-HIFU treatments. Here, we will present the first results with respect to the MRI an SPECT based characterization.

Methods: Tumor growth was monitored on a 3T Achieva MR system using T2- weighted-TSE at 7, 14 and 21 days after tumor injection. At 21 days, tumor vascularization was investigated using T1-weighted-DCE-MRI. SPECT/CT was used in combination with 99mTc-MDP on the same days as the MRI to follow osteoblastic activity. After positioning the animal in the MR-HIFU setup, (fig 2) HIFU treatment was performed using a single 2 mm cell with the focus point just behind the bone. The temperature in the focus point was increased up to 55°C. Temperature FEM simulation models are being setup to translate the soft tissue temperature into that of bone.

Results and Conclusions: T2-weighted MRI showed tumor growth over time (fig 1B). SPECT/CT images showed an increase in 99mTc-MDP uptake, indicating an increase in bone activity (figure 1A). T1-weighted DCE-MRI acquired 21 days after tumor injection showed high vascularization at tumor rim and necrotic core due to rapid tumor growth (figure 1C).

MR-HIFU animal setup allowed treatment of bone, without harming critical structures such as bladder and spine (figure 2). The temperature map shows an area of high temperature around the bone, which correlates with the edema seen in the post-ablation T2-weighted scan. The temperature map suggests that the shape of the temperature profile is influenced by the presence of bone. Temperature FEM simulation models to determine the temperature of bone cortex is ongoing work of which results will be shared at the FUSF meeting.

Acknowledgements (Funding): This research was supported by the Center for Translational Molecular Medicine (HIFU-CHEM).

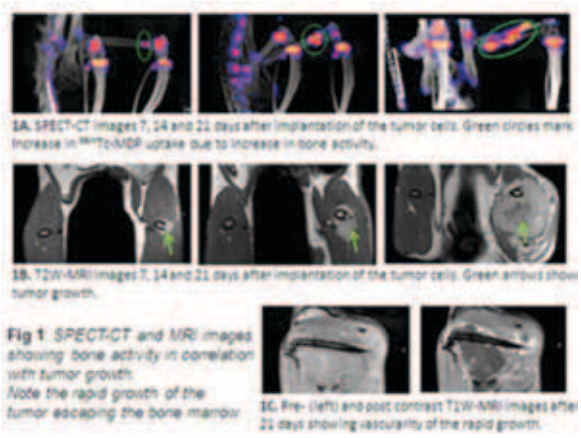

Fig 1 *SPECT-CT and MRI images showing bone activity in correlation with tumor growth. Note the rapid growth of the tumor escaping the bone marrow.*

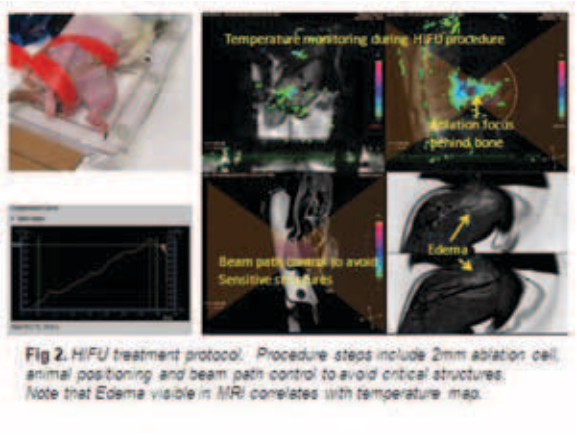

Fig 2. *HIFU treatment protocol. Procedure steps include 2mm ablation cell, animal positioning and beam path control to avoid critical structures. Note that Edema visible in MRI correlates with temperature map.*

P-85-BO

Tuesday
16 October 2012

Topic: Bone
Presentation Type: Poster

Use of MRgFUS in the Management of Surgically Untreatable Bone Lesions

Armando Conchiglia, Lorenzo Maria Gregori, Francesco Arrigoni, Luigi Zugaro, Antonio Barile, Carlo Masciocchi

University of L'Aquila, L'Aquila, Italy

Background/Introduction: MRgFUS was used on bone lesions in which surgery would be too demolitive.

The lesions included in this study are all primary tumors.

Methods: From November 2011, we used MRgFUS (ExAblate InSightech, Haifa, Israel) on nine surgically untreatable bone lesions, including four osteoid osteomas located in the femoral epiphysis (n.1), in the tibial diaphysis (n. 2), in the talus (n. 1); two chondroblastomas of the knee tibial plateau (n. 2) with an average diameter of 30 mm; two fibroangiomas of the humeral head (n. 1) and foot (n. 1); one periosteal chondroma of the femoral neck (n.1).

Eight patients received epidural anesthesia. General anesthesia was administered in one case to obtain more cooperation by the patient given the young age (12 year old).

Results and Conclusions: All patients were assessed by CT and c.e. MRI before and after treatment. After treatment with MRgFUS, all but one patients showed regression in painful symptomatology with a mean VAS decreasing from 7.9 to 2.3. In the patient with periosteal chondroma of the femoral neck no improvement in symptomatology was observed.

MRI with gadolinium performed after the procedure showed a reduced enhancement in seven patients. In two cases (periosteal chondroma and fibroangioma of the foot), no differences with the pre-procedural imaging were appreciated.

In the first case, the presence of calcifications did not allow a satisfactory ablation of the lesion. In the second case, the verification phase did not produce a perfect matching.

In no case did we find major complications.

In conclusion, though the need of further and larger studies, in our experience the use of MRgFUS in case of surgically untreatable lesions has proved to be a safe and effective treatment.

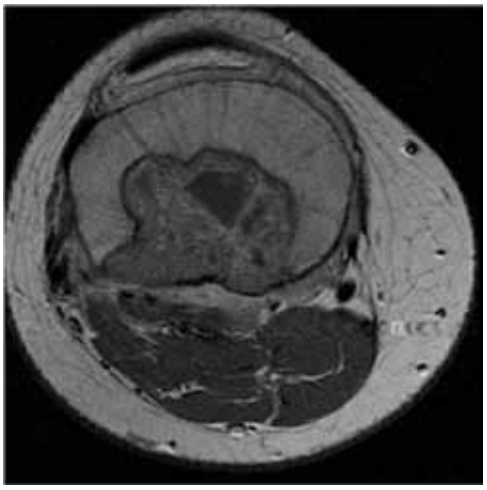

Chondroblastoma of proximal tibial epiphysis. Axial c.e.T1 weight image shows enhancement of the lesion before treatment

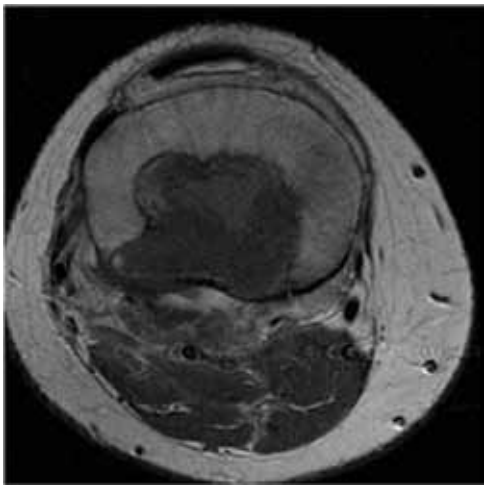

Chondroblastoma of proximal tibial epiphysis. Axial c.e.T1 weight image shows marked reduction of the enhancement after treatment

P-86-BR

Tuesday
16 October 2012

Topic: Brain
Presentation Type: Poster

A Magnetic Resonance Imaging and Histological Comparison of Focused Ultrasound, Radiofrequency, and Gamma Knife Radiosurgery Lesions in Swine Thalamus

Mohamad Khaled[1], Justin Hilliard[2], Robert Frysinger[1], Jason Sheehan[1], Max Wintermark[1], Maria-Beatriz Lopes[1], Jeff Elias[1]

[1]University of Virginia, Charlottesville, Virginia, United States
[2]University of Florida, Gainesville, Florida, United States

Background/Introduction: Stereotactic radiofrequency (RF)lesioning and gamma knife radiosurgery (RS) have been utilized for decades to perform lesioning of deep subcortical nuclei. The exact nature of MRI and histological maturation of the lesion remains incompletely understood. Recently MR-guided focused ultrasound (FUS) has been used to produce precisely defined lesions in deep brain structures.

The aim of this study is to directly compare radiographic evolution and histopathologic characteristics of lesions produced by each of Radiofrequency, GammaKnife and Focused Ultrasound in an swine model.

Methods: Piglets (Sus scrofa domesticus) weighing between 13 and 20 kilograms were divided into three lesioning cohorts. Each animal was treated with a unilateral stereotactic thalamotomy based on standard clinical practice, utilizing one of three lesioning modalities: focused ultrasound (FUS), radiofrequency (RF), or gamma knife radiosurgery (RS).

FUS and RF cohorts were assessed with MR imaging and histology at acute (<72 hours), subacute (1 week), and chronic / late 1-3 month) time points. The RS cohort was assessed at subacute and chronic.

Results and Conclusions:

MRI: FUS and RF lesions evolve similarly by MR imaging. By 48 hours, three concentric zones appear on T2 weighted sequences representing necrosis (inner zones 1 and 2) and perilesional, vasogenic (outer zone 3) edema. This perilesional edema subsides by 10 days, and the lesion size diminishes over 3 months. There were no blood products demonstrated on gradient echo (GRE) imaging throughout the study.

Gamma knife radiosurgery is associated with a much different evolution of imaging findings with less distinct lesions by 3 months.

Histology: The histological appearance of the thalamus was similar for FUS and RF throughout the evolution to a mature lesion. In the acute period for both, the lesions appeared consistent with an acute infarction with axonal swelling and the infiltration by macrophages. At one week, a circumscribed lesion is present with dense macrophage infiltration and early neovascularization. Finally at 3 months, the mature lesions are more circumscribed with dense fibrillary gliosis. The gamma knife radiosurgical lesions presented a much different histology with poorly circumscribed lesions at 3 months and edema and macrophage infiltration extending well beyond the lesion in into the overlying white matter.

FUS produces well defined lesions that are comparable to RF ablation in the brain both on MRI and histologically with a similar evolution through time. RS produced lesions that are less well defined at 3 months and are associated with white matter injury outside of the lesion.

Acknowledgements (Funding): Focused Ultrasound Foundation provided the funding for this study.

P-87-BR

Tuesday
16 October 2012

Topic: Brain
Presentation Type: Poster

A Model for Predicting Temperature Change in Brains From CT Data and Sonication Settings

Alisha Geldert, Richard Booth, Arik Hananel, John Snell, Matthew Eames

[1]Focused Ultrasound Foundation, Charlottesville, Virginia, United States

Background/Introduction: The temperature elevation at the focal point of a FUS brain system is difficult to predict. The skull reflects and attenuates acoustic energy depending on its shape and material properties. In response to local heating during and between sonications, edematous changes occur, and heat dissipates at a variable rate. In the UVA ET study, surgeons produced precise high temperatures by sonicating repeatedly, slowly increasing power and holding time constant, producing incremental increases in temperature until a lesion was produced. This method is slow.

Methods: A model to predict peak temperature elevation from sonication intensity (watts) and duration (seconds) was developed. On its own, the model predicts temperature with R2 = 0.67. Then, using regression analysis, we found a linear combination of focused ultrasound device data (InSightec ExAblate 4000, Tirat Hakarmel, Israel) that predicts the residual error in our model for peak temperature elevation. The combination of these two methods predicts temperature with R2 > 0.8.

We also developed a method for using actual heating data from low-energy spot localization sonications to further improve this prediction.

Results and Conclusions: Using CT summary data alone, it is possible to predict temperature rise in a patient with a standard deviation of 2 degrees celsius – smaller at low temperatures. With low-energy heating data, the standard deviation can be further decreased. As more data become available, both the CT-alone and CT-plus-heating methods can be further improved.

Acknowledgements (Funding): FUS Foundation

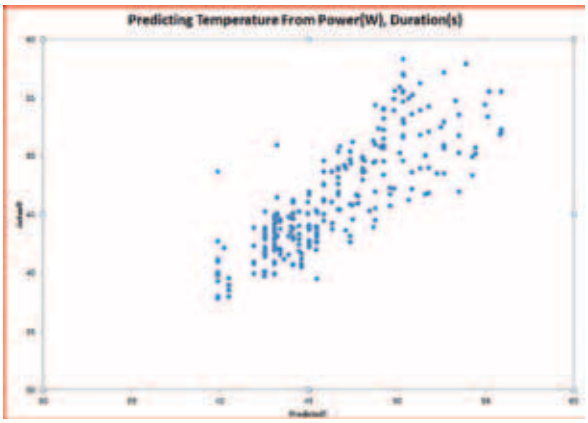

Graph showing prediction of temperature from Power and Duration of sonication

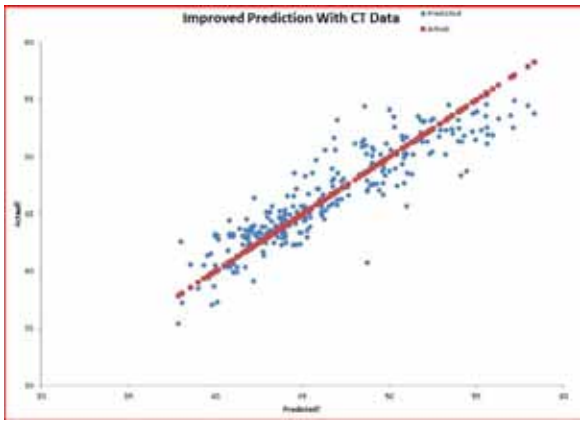

Graph showing prediction of temperature from Power, Duration, and FUS device data

P-88-BR

Tuesday
16 October 2012

Topic: Brain
Presentation Type: Poster

An Implantable Ultrasound Device for Repeated Opening of the Blood-Brain Barrier: A Preclinical Toxicological Study on Primates

Catherine Horodyckid[1], Michael Canney[2], Alejandra Uzcategui Pedroza[3], Alexandre Vignot[4], Pascal Merlet[5], Cyril Lafon[6], Jean-Yves Chapelon[6], Alexandre Carpentier[1]

[1]CarThera/Pitie-Salpetriere Hospital, Assistance Publique - Hôpitaux de Paris, Paris, France
[2]CarThera, Lyon, France
[3]Inserm, U1032, LabTau, Lyon, France
[4]CarThera, Paris, France
[5]CEA, IR4M, SHFJ, Orsay, France
[6]Inserm LabTau - U1032/Université de Lyon, Lyon, France

Background/Introduction: Brain tumor prognosis is presently poor due to the low response of patients to chemotherapy treatments after surgery. The main limitation to the efficacy of chemotherapy in the brain is the blood-brain barrier (BBB). It has been shown that delivery of pulsed ultrasound in combination with echogenic microbubbles can temporarily disrupt the BBB to deliver drugs that normally can not reach interstitial brain tissue. Since primary brain tumors are a diffuse whole brain pathology, we have developed a device for a large and temporary BBB opening by using an unfocused ultrasound device that can be easily used in routine outpatient clinical practice during repeated chemotherapy sessions. The device is implanted in a skull burr hole in order to circumvent absorption and aberration of ultrasound by the skull and induces minimal artifacts on magnetic resonance imaging (MRI). Our previous studies in dogs and rabbits have shown that the BBB can be opened over a broad region within the brain and allow for uptake of chemotherapy agents with no acute or sub-acute effects for acoustic pressures of less than 0.8 MPa using a 1 MHz transducer. The purpose of this study was to determine if BBB opening can be reproduced in an animal model with a cerebral volume closer to the size of humans. In addition, toxicity of repeated BBB opening by unfocused ultrasound was analysed on magnetic resonance imaging and behaviour scales.

Methods: Three primates were included in the study. A 12-mm diameter craniotomy was performed after which a 10-mm diameter, unfocused, 1 MHz ultrasound transducer was placed on the dura-matter, fixed to the skull, and left implanted for 3 months. BBB opening was performed every 15 days by connecting the transducer to an external generator using a transdermal needle connection. The transducer was operated in pulse mode with a burst length of 25 ms and a pulse repetition frequency of 1 Hz for 120 seconds. Peak acoustic pressure levels from 0.6 MPa to 0.8 MPa were used and a microbubble contrast agent (Sonovue, Bracco Imaging, France) was intravenously injected (0.1cc/kg) during sonications. MRI imaging was performed after sonications to observe BBB opening using T1-gadolinium contrast images. The behavior of each primate was analyzed using a neurological behaviour animal scale.

Results and Conclusions: MRI images acquired after sonication showed a T1-contrast enhancement area underneath the transducer that corresponded well with the acoustic field of the transducer and did not show hemorrhagic or ischemic processes. Pre-treatment MRI signals were used as control data. The T1-contrast enhancement area indicated a 4.5 cm depth and 0.9 cm diameter region of BBB opening. An oedematous zone, without mass effect, was observed on FLAIR images, and resolved by day 2. At day 15, MRI control showed strictly normal brain in all primates, with a totally closed BBB. The behavior of all of the primates appeared to be normal. We confirmed that unfocused ultrasound can temporarily open the BBB at an acoustic pressure of 0.8 MPa (1 MHz) without any induced hemorrhagic effect.

Acknowledgements (Funding): Work supported by CarThéra SAS

P-89-BR

Tuesday
16 October 2012

Topic: Brain
Presentation Type: Poster

Behavioral and Motor Control Studies of Repeated FUS Induced BBB Openings in Mice

Oluyemi Olumolade, Shutao Wang, Gesthimani Samiotaki, Elisa Konofagou

Columbia University, New York, New York, United States

Background/Introduction: Focused Ultrasound (FUS) in combination with microbubble ultrasound contrast agent has been demonstrated to non-invasively disrupt and open the blood brain barrier (BBB) while causing no gross structural damage to cerebral tissue or vasculature. However, little focus has been shed on the ability of FUS to consistently and reversibly open the BBB at repeated, serial applications. Further, the assessment of behavior after BBB opening has also not yet been established. The main goal of this study was to examine any behavioral changes that could be attributed to multiple BBB openings in mice.

Methods: A total of 55 C57BL/6 mice were divided into 11 groups (n=5) and were studied for varying periods, up to 3 months. Mice received either monthly or biweekly FUS treatments. Parameters for FUS sonication are as follows: The transducer frequency was set to 1.5 MHz, peak rarefractional pressure in situ was 0.45 MPa for 60 seconds, burst rate was 10 Hz and 500 cycles. FDA approved microbubbles (Definity™) were intravenously injected prior to sonication. The brain region targeted was the Caudate Putamen, an essential brain region for motor control. In order to best assess potential deficits, mice received repetitive (either monthly or biweekly) unilateral treatment to the left caudate putamen. Upon completion of sonications, mice underwent MRI to confirm and assess volume of the BBB opening. One day following FUS procedure, behavioral testing was conducted. The mice were placed in a custom made open field test chamber located in a soundproof, isolated room and free to explore the field. Visual tracking software (Noldus) was used to record distance traveled, as well as turn angle. Upon completion of the open field test, the animals were allowed to rest before being placed on the accelerating rotating rod (rotarod), where they were required to maintain balance and motor coordination for a fixed period (180 seconds).

Results and Conclusions: In the open field test, two indicative factors of potential brain damage were the total distance traveled and the rotation direction. There was no difference in terms of increased or decreased distance traveled between the BBB-opened and control groups in both the biweekly and monthly treated mice. Similarly, there was no affinity for a particular turn angle in the sonicated compared to the control animals. In the rotarod test, overall, animals were able to complete the test successfully. The behavioral assessment of the mice using open field and rotarod suggests that repeated opening of the BBB in the caudate putament using FUS paired with microbubbles over several months under the parameters used do not cause motor impairment and behavioral changes. This indicates the potential safety of repeated or long-term drug delivery using the FUS methodology.

Acknowledgements (Funding): The study was supported by the Kinetics Foundation.

P-90-BR

Tuesday
16 October 2012

Topic: Brain
Presentation Type: Poster

Computational Multi-Scale Modeling of Blood-Brain Barrier Disruption with Focused Ultrasound

Wolfgang Wiedemair[1], Adamos Kyriakou[2], Esra Neufeld[2], Dimos Poulikakos[1], Niels Kuster[2], Vartan Kurtcuoglu[1]

[1]ETH Zurich, Zurich, Switzerland
[2]IT'IS Foundation/BIWI/ETHZ, Zurich, Switzerland

Background/Introduction: It has been shown reproducibly that the sonication of intravascular ultrasound contrast agents (UCA) with focused ultrasound (FUS) can result in local, reversible blood-brain barrier disruption (BBBD) without the production of lesions or apparent neurological damage. However, because of the complexity of the mechanical, physiological and thermal interactions between the ultrasonic waves, the UCA microbubbles (MBs), blood and tissue, the exact mechanism of BBBD remains largely unknown. We aim to investigate the physical conditions inside the tissue during BBBD, specifically addressing the impact of individual parameters such as the frequency, intensity and duration of the ultrasound (US) waves, the type and concentration of the UCA as well as the characteristics of the transducer.

Methods: We are developing a computational multi-scale model capable of capturing the microscopic, mesoscopic and macroscopic physics of BBBD. On the microscopic level, the modeling focuses on the interaction of individual MBs with the incident pressure field, the resulting cavitation and the thereby created microcirculation in the vessel. A lumped parameter model (LPM) for the mechanical stresses generated at the endothelial interface as a function of UCA properties and US pressure characteristics will be derived. The impact of blood perfusion and pressure distribution on the local bubble concentration will be considered on the mesoscopic level using a porous medium model coupled to a three-dimensional flow network representation of major blood vessels. At the macroscopic level, the pressure field distribution is calculated based on detailed anatomical models that take into account variation of skull thickness, tissue parameters and local UCA concentration. Linking of the scales allows the LPM to obtain intravascular pressure and shear stress levels based on the macroscopic pressure field and the local bubble concentration derived from the mesoscopic level.

Results and Conclusions: In order to calculate the macroscopic pressure distribution, full-wave, non-linear 3D ultrasound solvers optimized for propagation in anatomical models at high resolutions have been implemented. In addition, flow and thermal solvers were developed, which can be coupled with the acoustic solvers in order to simulate acoustic streaming and FUS induced temperature increase. The microscale interaction between sonicated MBs and the enclosing microvessel is captured by a multiphysics framework based on a modified Rayleigh-Plesset equation accounting for bubble shell characteristics and explicitly incorporates mobile, deformable red blood cells and a compliant vessel structure. It predicts microflow characteristics and the mechanical conditions at the endothelium. These results could constitute valuable input for an advanced model of BBBD and drug crossing.

The implementation of the macroscopic and microscopic models has been completed. The next step will be the extraction of an LPM and the coupling of the two scales. The modeling environment will provide valuable insight into physical processes involved in FUS induced BBBD and might one day be used to optimize treatments in a patient-specific manner.

Acknowledgements (Funding): This study was supported by the Swiss National Science Foundation through NCCR Co-Me.

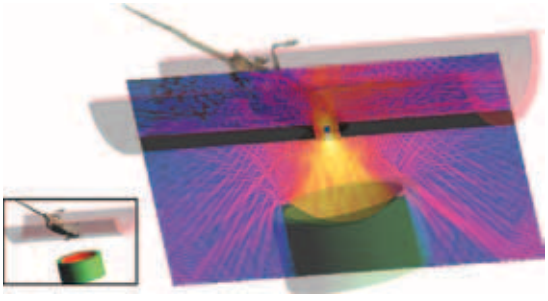

Figure 1. 3D model replicating an experimental setup of Blood-Brain Barrier disruption in live mice through the combined use of UCA microbubbles and FUS produced by a single element transducer (left) and the resulting pressure distribution in a plane through the acoustic focus (right).

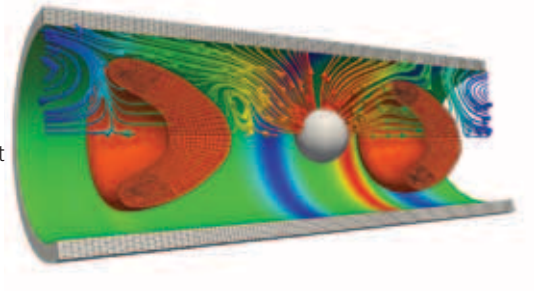

Figure 2. Microscopic flow conditions created by a single insonated microbubble during expansion inside a compliant capillary vessel with explicit incorporation of red blood cells. The streamlines represent the current flow field and are colored according to local pressure while the colors at the vessel interface indicate wall shear stress levels.

P-91-BR

Tuesday
16 October 2012

Topic: Brain
Presentation Type: Poster

Correcting Phase Aberrations at Multiple Treatment Sites in Transcranial Brain HIFU

Scott Almquist, Nick Todd, Dennis Parker, Douglas Christensen

University of Utah, Salt Lake City, Utah, United States

Background/Introduction: In transcranial focused ultrasound treatments, differences in acoustic properties between the skull and surrounding tissue can cause significant beam phase aberrations, resulting in defocusing and imprecise localization of the beam. We present a method for rapidly correcting phase aberrations at multiple arbitrary treatment points, and demonstrate its usefulness with experimental results.

Methods: Aberrations caused by varying tissue geometries in the beam path can largely be corrected by introducing compensating phase offsets to each element of a phased-array transducer. We calculate these offsets utilizing the Hybrid Angular Spectrum (HAS) beam simulation method.[1] The HAS technique quickly and accurately calculates the pressure pattern throughout the entire insonated 3D volume using standard acoustic values for each tissue type. We calculate the pressure pattern attributed to each individual element of the phased array throughout the entire volume that encompasses all possible focal sites. Therefore, choosing additional sites does not require any additional pattern calculations. The ensemble of these pressure patterns is computed in parallel on an Nvidia Tesla GPU within 34 seconds for our transducer. Phase offsets are then determined such that constructive interference can be created at any chosen treatment site. Experimental verification was carried out using a 1-MHz, 256-element phased-array transducer propagating a beam through an anatomically realistic plastic skull embedded in agar targeting a pork sample inside the skull. The model was placed inside a Siemens 3T MRI and temperature measurements were obtained using a 3D segmented EPI gradient echo sequence while heating for 30 seconds at 40 acoustic watts. We compared the beam's strength and position within the focal region using our phase correction method to that obtained with no applied correction for three separate treatment sites: at the geometric focus and steered 5 mm away from the geometric focus in two transverse directions.

Results and Conclusions: The result for the treatment site steered laterally 5 mm from the geometric focus in the coronal plane is given in Figure 1. This figure shows the maximum temperature observed during the scans both for the case when a) no phase correction is applied to the elements, and b) phase correction is employed. In all cases observed for all treatment sites, phase correction resulted in an increase in maximum temperature achieved. Additionally, with phase correction the maximum temperature was always observed at the correct axial voxel location, whereas without phase correction the maximum temperature was as much as 5 mm away from the intended treatment location. Thus phase aberration correction provides for more efficient treatment and more accurate beam positioning.

Reference:

1. U. Vyas and D. Christensen, *IEEE Proc.* UFFC 59(6), June 2012.

Acknowledgements (Funding): The authors gratefully acknowledge support from Siemens Healthcare AG, the FUS Foundation, the Ben and Iris Margolis Foundation, and NIH grants R01 CA87785 and R01 CA134599.

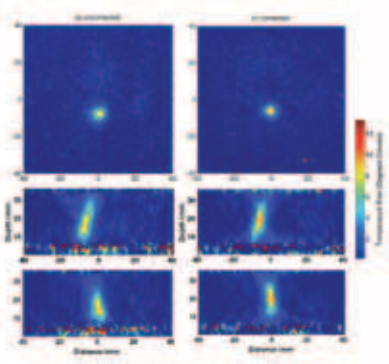

Figure 1. Maximum temperature achieved within the focal region for an ultrasound exposure through the skull model when steered 5 mm away from the geometric focus in the coronal plane using a) no phase correction, and b) phase correction. Coronal (top), sagittal (middle) and transverse (bottom) slices are shown. Voxel size is 1 mm isotropic.

P-92-BR

Tuesday
16 October 2012

Topic: Brain
Presentation Type: Poster

Delivery of Biodegradable PEGylated PLGA Nanoparticles Across the Blood-Brain Barrier with MR-Guided Focused Ultrasound

Kelsie Timbie[1], Grady Miller[1], Elizabeth Nance[2], Ji Song[1], Alexander Klibanov[1], Justin Hanes[2], Richard Price[1]

[1]University of Virginia, Charlottesville, Virginia, United States
[2]Johns Hopkins University, Baltimore, Maryland, United States

Background/Introduction: Drug delivery across the blood-brain barrier (BBB) has proven difficult and limits treatment options for most central nervous system diseases, including glioblastoma, Parkinson's and Alzheimer's. Focused ultrasound (FUS) in conjunction with microbubbles (MBs) enables non-invasive, localized disruption of the BBB. We have previously demonstrated the delivery of fluorescent polystyrene tracer nanoparticles (NPs) across the BBB. Here, we tested whether long-circulating biodegradable PEGylated PLGA NPs , capable of controlled drug release, could be delivered across the BBB using FUS and MBs. Specifically, we examined the distribution pattern of PEGylated PLGA NPs after FUS/MB mediated delivery at 0.6 MPa and 0.4 MPa in the rat brain.

Methods: Poly(lactic-glycolic acid) (PLGA) NPs covered with a dense polyethylene glycol (PEG) coating and tagged with AlexaFlour 555 or AlexaFlour 647 were fabricated. The NPs were 94 nm in diameter, with a surface charge of -3.2 mV. Rats were anesthetized, and 10 ug/g body weight NPs were intravenously coinjected with 3.5E4/g body weight polydisperse albumin MBs. Ultrasound sonication was initiated immediately following NP/MB injection using a focused 1 MHz transducer with 3 coordinate motor control (FUS Instruments). Using 3T MR guidance, four locations were sonicated in each rat, two at 0.6 MPa and two at 0.4 MPa. Locations were chosen to minimize structural variation within the brain. Sonication continued for 2 minutes at a 0.05% duty cycle. Following sonication, rats were intravenously injected with 0.3 uL/g body weight gadolinium and MR imaged to verify BBB opening. Rats were euthanized one hour post sonication to maximize uptake of NPs. Rat brains were perfused with heparinized saline, desiccated in a concentrated sugar solution overnight, and frozen in OCT at -80°C. Brains were cryosectioned and stained with an endothelial label (BS-I lectin 480) before being imaged with a confocal microscope. NP coverage was calculated as number of red pixels over total number of pixels. Fraction of NPs not in endothelial cells (ECs) was determined by subtracting the lectin image from the NP image and dividing by total number of red pixels. Fraction of EC area containing NPs was calculated by multiplying the lectin image by the NP image and dividing by the total number of green pixels. All values were compared to a contralateral "no-ultrasound" control region.

Results and Conclusions: NP coverage showed an ultrasound pressure dependent trend, while relative NP distribution and EC area containing NPs did not. Notably, over 70% of NPs were found outside of the endothelium at both 0.4 and 0.6 Mpa, on average. Figure 1 depicts NP coverage, EC area containing NPs and the fraction of NPs lying outside of endothelial cells normalized to a "no-ultrasound" control. NP coverage was 19.5±8.3 fold higher than control at 0.6 MPa, and 4.7±0.9 fold higher at 0.4 MPa (significant). EC area containing NPs was similar at 0.6 MP and 0.4 MPa but still several-fold higher than control, at 7.0±5.2 and 2.6±1.7, respectively. The fraction of NPs not in ECs was fairly constant across all groups, with both 0.6 MPa and 0.4 MPa showing only a 2 fold increase over control, on average. Analysis of the confocal images indicated that treatment with ultrasound and MBs greatly increased NP delivery across the blood-brain barrier in a pressure dependant manner. While NP delivery across the BBB using FUS has been previously demonstrated, this technique has not been applied to long-circulating biodegradable particles, which are appealing for controlled-release applications. The fairly high percentage of ECs receiving NPs in conjuction with the large percentage of NPs that penetrated beyond the endothelium are promising indicators of a NP distribution pattern that would effectively deliver drug throughout the targeted region.

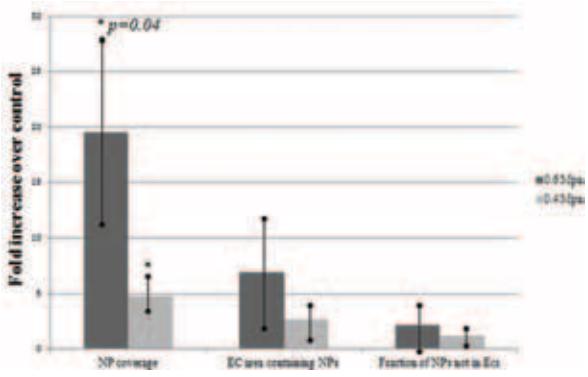

Figure 1. Fold increase over "no-ultrasound" control regions in nanoparticle coverage, endothelial cell area containing nanoparticles, and fraction of nanoparticles not in endothelial cells at 0.6 MPa and 0.4 MPa. Error bars are standard deviation, n=3.

Acknowledgements (Funding): This project is supported by the Focused Ultrasound Foundation and NIH R01 CA164789.

P-93-BR

Tuesday
16 October 2012

Topic: Brain
Presentation Type: Poster

Detection and Characterization of Intracranial Cavitation Activity

Arne Voie, Thilo Hoelscher

University of California at San Diego, San Diego, California, United States

Background/Introduction: This presentation will describe a year-long Foundation-funded project to study cavitation using a 220 kHz transcranial FUS system. We sought to characterize cavitation and determine the effects of different skull anatomy on both cavitation activity and the ability to detect it.

Methods: The PCD capability of the ExAblate 4000 was compared to an external broadband PCD system, using brain-mimicking material (BMM) in both calvaria and full skulls. The FUS PCD system analyzes a pass band between 75 kHz and 150 kHz, and we examined whether this somewhat limited range was sufficient to differentiate between stable and inertial cavitation compared to the broadband PCD system. We used both continuous wave (CW) and pulsed wave (PW) ultrasound transmission in the course of this project. We sought to determine whether PCD signals obtained using PW contained any information that might be used to locate the source of the cavitation. We also positioned the FUS PCD elements in various locations on the interior surface of the transducer to determine whether one orientation was optimal. We evaluated three positions: on the transducer rim oriented toward the lateral sides of the skull; on the transducer rim oriented toward the front and back of the skull; deeper in the transducer, oriented up toward the parietal bones.

Results and Conclusions: Cavitation Sensitivity: The FUS PCD was found to be more sensitive than the broadband system to detection of both stable and inertial cavitation. Cavitation Characterization: Stable cavitation was indicated by the presence of the ½ f0 subharmonic and inertial cavitation by a marked increase in spectral energy in the pass band accompanied by the emergence of the 1/3 f0 and 2/3 f0 subharmonics in the spectral plots. In general cavitation thresholds were lower when CW was used. Cavitation Localization: The highly reverberative environment of the hemispherical transducer makes true cavitation localization very challenging, however we found that cavitation may be localized to a coarse extent, such as differentiating between a skull source or brain source, or being closer to one PCD element than another. These findings may lay the groundwork for more precise localization in some future effort. We found the parietal bone orientation to produce the best results in terms of cavitation thresholds and also localization information.

Acknowledgements (Funding): Supported by a grant from the Focused Ultrasound Foundation

P-94-BR

Tuesday
16 October 2012

Topic: Brain
Presentation Type: Poster

Ex-vivo Feasibility Studies of Brain Sonication Under MR-Guidance

Alexander Volovick[1], Timur Saliev[2], Sam Eljamel[2], Roos Eisma[2], Andreas Melzer[2]

[1]InSightec, Tirat Carmel, Israel
[2]University of Dundee, Dundee, United Kingdom

Background/Introduction: MR-guided high focused ultrasound (MRgHIFU) offers a new approach for treatment of neurological disorders in non-invasive manner. To the present, some clinical experience of using MRgHIFU has been already gained, which includes tumour ablation, management of neuropathic pain and essential tremor (Hynynen, UMB. 1998; Martin, et. al. Ann Neurol. 2009; McDannold, et.al. Neurosurgery. 2010). Apart of direct eradication of malignant cells, the targeted delivery of anti-cancer drugs across the blood-brain barrier by ultrasound assistance has been suggested. (Deng, Ther Deliv. 2010). The application of MRI for ultrasound treatment significantly increased the efficacy of brain therapy. First of all, it allows a precise localization of treated area by using different MR sequences. Secondly, MRI provides a real-time temperature mapping, which is based on Proton Resonance Frequency (PRF) shift of hydrogen protons.

Despite of recent progress in MRgHIFU neurological applications, some questions remain unsolved, including optimization of ultrasound protocol, methods of beam focusing and safe sonication of targets at different depths and localization inside the brain tissue. As a model for research to resolve these issues, the use of Thiel embalmed cadavers has been proposed. This embalming technique relies on a water-based mixture of glycol, salt compounds and very low amounts of volatile formaldehyde to effect tissue fixation (Thiel, Ann Anat. 1992). The method benefits from a lifelike flexibility of body, excellent color preservation (muscle, viscera and vasculature), undetectable odor and relative long-time conservation. Besides, the Thiel embalmed cadavers are both MR and Ultrasound compatible/safe. Those factors make the Thiel embalmed cadaver a perfect model for testing medical technologies for non-invasive therapy.

Methods: The cadaver (#837) used for experiments was female, age at death 84. Prior to craniotomy, the MR-scanning was conducted on MRI machine (Signa HDxt 1.5 Tesla, GE Healthcare, USA). The cadaver head was inserted into 8-channel Brain coil. T2 weighted imaging was performed with echo time of 85 msec and a very large repetition time to allow the imaging in a single acquisition. In addition, a modified Fiesta scan (TE/TR=4.2/8.1, BW=62.5 kHz) was done as to localize the possible artefacts produced by cadaveric gases in the brain. After scanning, the craniotomy was performed, which included the incision of the scalp (forming a skin flap), drilling multiple holes and removal of bone cap. The dura were not damaged. In order to achieve an optimal interface, an ultrasonic gel was used to fill the gap between the transducer and the dura. After defining the target area, 14 sonications were carried out by using different sonication parameters (apertures, locations and acoustic power). Sonication was performed by MR-compatible HIFU machine (CBS ExAblate 2100 system) with portable transducer. The ultrasound frequency was 0.5 MHz.

2 different MR coils were exploited for brain treatment (1-5 with head coil and the rest with 8 channels body coil). The thermal feedback for was provided by MRI machine (PRF-thermometry) for monitoring of the heat in focal point. Beside of this, MR-Acoustic Radiation Force Imaging (MR-ARFI) was conducted in order to evaluate mechanical properties of treated brain tissue.

In order to validate of MRgHIFU efficacy the MRgHIFU the same acoustic protocol was tested on ultrasound gel phantom (MR-safe).

Results and Conclusions: Imaging: High quality of brain MR-imaging was established with good preservation of white-grey matter differentiation (Fig.1).

Craniotomy: The wide craniotomy allowed a proper focussing of ultrasound beam indicating a strong correlation between size of the aperture and HIFU efficacy.

Heating effect: The detected increase of temperature at the focal point was linear to the level of acoustic energy. This linearity is very promising and might have clinical relevance.

Elastography: The acquired results of MR-ARFI measurements demonstrated that the brain tissue of Thiel embalmed cadaver is more elastic comparing to the normal one. It could be

related to the effect of Thiel embalming solution on bio-mechanical properties of the tissues (Fessel et al., Ann Anat. 2011).

Conclusion: The experiments demonstrated that Thiel embalmed cadaver is convenient model for experimentation and validation of MRgHIFU, particularly for optimization of treatment protocol.

Acknowledgements (Funding): 1) Project FUSIMO ("Patient specific modelling and simulation of focused ultrasound in moving organs") funded under the EU's Seventh Framework Programme for Research and Technological Development. 2) Fellowship from Focused Ultrasound Surgery Foundation. 3) NANOPORATION project funded from the European Community's Seventh Framework Programme.

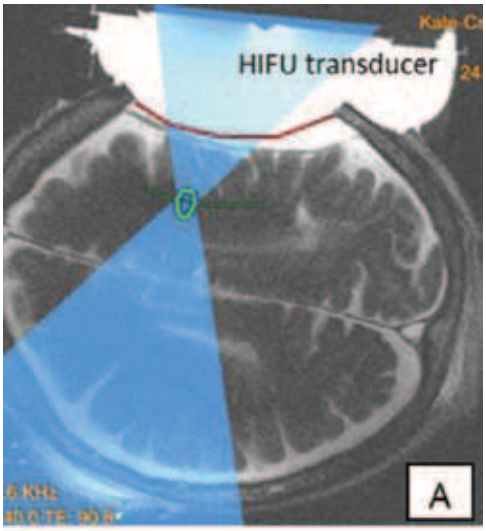

Figure1. A) MR-image: HIFU transducer (beam path) and brain

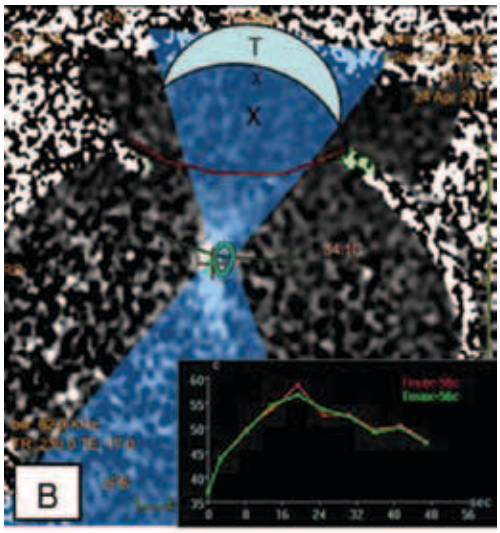

Figure1. B) PRF thermal map with temperature graph

P-95-BR

Tuesday
16 October 2012

Topic: Brain
Presentation Type: Poster

Improved Temperature Accuracy in Transcranial MRgFUS with Hybrid Thermometry

Viola Rieke[1], Ron Instrella[2], Jarrett Rosenberg[2], Kim Butts Pauly[2]

[1]University of California, San Francisco, San Francisco, California, United States
[2]Stanford University, San Francisco, California, United States

Background/Introduction: Clinical applications for MR-guided focused ultrasound in the brain have included tumor ablation and neuropathic pain management, and may potentially include the treatment of Parkinson's disease, tremor, and epilepsy. During the FUS ablation accurate temperature measurements are necessary to insure patient safety. Temperature reconstruction is currently performed using single baseline subtraction, which cannot account for motion-induced errors. Previously, we have investigated a hybrid thermometry approach that combines the advantages of multi-baseline and referenceless temperature reconstruction (Hybrid MB/R). Here, we present an analysis of the improvements in temperature accuracy using the Hybrid MB/R thermometry method in volunteers and patients undergoing transcranial MRgFUS.

Methods: Consecutive sagittal brain images were acquired over four minutes from three normal volunteers without heating (GRE, TE/TR = 11.7/23.9 ms, BW = 12.2 kHz). Thirty images were available as a baseline library and 50 images were used for analysis. We compared single baseline, multi-baseline with 30 library images, hybrid with a single library image (Hybrid SB/R), and Hybrid MB/R with 30 library images. In datasets from patients undergoing transcranial MRgFUS, we reconstructed a total of 40 sonications (5 sagittal and 3 coronal datasets in each patient, imaging parameter: GRE, TE/TR = 18.6/37.6 ms, BW = 7.36 kHz). Since only a single image was acquired before ablation in these datasets, only single baseline subtraction and Hybrid SB/R were compared. To determine the accuracy of the hybrid method compared to the other methods, nonparametric tolerance intervals (99% coverage with 99% confidence) were calculated in three ROIs selected in the brain outside the heating area. In addition, the percentage of ROI pixels with a temperature error exceeding +/- 1ºC was calculated.

Figure 1. Distribution of temperature errors of the different methods for a single ROI in all volunteer datasets.

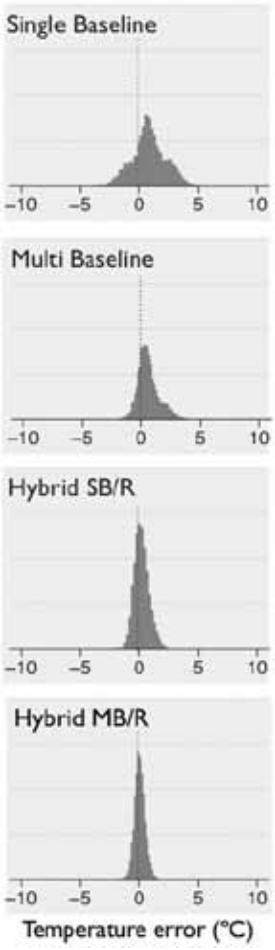

Results and Conclusions: Figure 1 shows the distribution of temperature errors of a single ROI for all volunteers. Table 1 summarizes the results of the statistical analysis of a single ROI for volunteers and patients (sagittal datasets). The results show that Hybrid MB/R and SB/R thermometry achieves substantially lower errors than single and multi-baseline subtraction. The volunteer data also shows that Hybrid MB/R and SB/R perform better than multi-baseline, which is not able to correct errors from non-repetitive motion. The graphs and table illustrate that Hybrid MB/R and SB/R thermometry has less bias towards positive errors compared to the baseline subtraction methods. These bias errors are typical for susceptibility induced background phase changes that are automatically corrected by the referenceless component in the hybrid method.

	Method	99% Tolerance Interval	pixels with error > 1ºC
Volunteers	Single baseline	-2.6ºC to 4.3ºC	52%
	Multi-baseline	-1.6ºC to 2.8ºC	27%
	Hybrid SB/R	-1.3ºC to 1.7ºC	11%
	Hybrid MB/R	-1.0ºC to 1.1ºC	2%
Patients	Single baseline	-3.1ºC to 2.2ºC	37%
	Hybrid SB/R	-1.2ºC to 1.3ºC	5%

Table1. Results of a single ROI of all volunteer datasets and all sagittal patient datasets. The 99% tolerance interval indicates the limits within which 99% of future observations with each method should fall with 99% confidence. Differences between hybrid and non-hybrid number of pixels exceeding a 1ºC temperature error are significant at $p < 0.0001$ by McNemar test.

In summary, the analysis of our data shows that hybrid multi-baseline and referenceless thermometry achieves significantly higher temperature accuracy than baseline subtraction methods in both volunteer and patient images.

Acknowledgements (Funding): This research is supported by NIH R00HL097030, P01 CA159992 and R21EB011559.

P-96-BR

Tuesday
16 October 2012

Topic: Brain
Presentation Type: Poster

Improving MR Image Quality for FUS Treatments: Initial Results From an Ultrasound-Compatible RF Coil

Mike Jones[1], J Rock Hadley[2], Emilee Minalga[2], John Snell[3], Arik Hananel[3], Matthew Eames[3]

[1]High Field LLC, Saint Paul, Minnesota, United States
[2]Utah Center for Advanced Imaging Research, Salt Lake City, Utah, United States
[3]Focused Ultrasound Foundation, Charlottesville, Virginia, United States

Background/Introduction: Focused ultrasound has been explored for more than 50 years as a non-invasive thermal lesioning tool for neurosurgery. A new approach using MRI for guidance and thermometry, and focusing algorithm for delivery of acoustic energy through the skull has the potential of finally gaining clinical acceptance. However trans-cranial MR guided Focused Ultrasound, (tcMRgFUS), still have technical limitations.

Placement of clinical MRI coils in or around the therapeutic transducer provides challenges both due to the transducers mechanical design, and the nature of the procedural environment requiring the coil to be submerged in cooled degassed water bath, (acoustic medium), and exposed to the high level of acoustic transmission, (could cause adverse effects on patient safety). Here we'll present an initial evaluation of a "shoot through" MR coil for tcMRgFUS therapy.

Methods: The setup used a cadaver skull filled with a tissue mimicking material to simulate a patient head. The head mockup was placed inside an upright tilted 220 kHz transducer of an ExAblate Neuro system integrated to a GE Discovery MR750 3T MRI. A "shoot through coil", designed for a minimal obstruction of acoustic energy, and consisting of two water resistant, single channel loops was placed 2 cm away from sides of the cadaver skull, (Figure 1).

T2-weighted, T1-weighted spin echo, and FSPGER thermal sequences were acquired in the sagittal and coronal planes, (orthogonal and parallel to the coils), in a dry and wet setup, using the "shoot through" coil and body coil (Body coil is one currently used for tcMRgFUS therapy). Each of the resulting 12 body-coil prototype-coil image pairs were evaluated in terms of signal-to-noise improvement.

Results and Conclusions: Initial results show an average SNR improvement of 215% and 470% in the middle of the brain for T2w and the T1w in water filled and dry setup respectively. The thermal imaging show a 450% improvement in the thermal standard deviation in water filled setup.

Our next step is evaluating the interaction between coil and acoustic transmission.

In conclusion, initial results show enhancement of imaging quality in this simulated clinical setup. Enhancing MRI image quality during tcMRgFUS will improve its safety and efficacy profile as well as advance its acceptance.

Acknowledgements (Funding): Focused Ultrasound Foundation

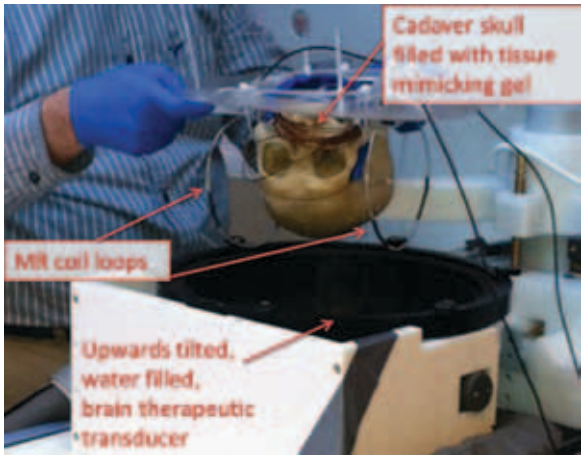

Figure 1. Ex vivo coil imaging setup

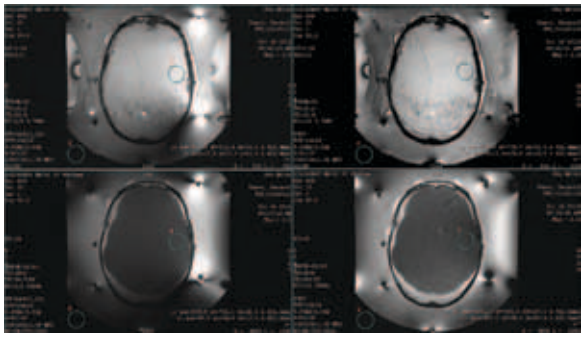

Figure 2. T2-weighted and TMAP MR images acquired with the body coil and prototype coil.

P-97-BR

Tuesday
16 October 2012

Topic: Brain
Presentation Type: Poster

Transcranial MRg-FUS Treatment Envelope

Matthew Eames, Arik Hananel, John Snell

Focused Ultrasound Foundation, Charlottesville, Virginia, United States

Background/Introduction: MR-guided focused ultrasound has been used in recent years to successfully treat neurosurgical targets in the thalamus as a part of small clinical trials in North America and Europe. These anatomical targets are positioned near the geometric center of the skull convexity, which reduces the challenges of transcranial refocusing to those associated with bone thickness, while also avoiding a concern regarding the ultrasound incident angle at the skull surface and unintentional heating of bone near the focus. However, other neurosurgical targets – including the cingulate gyrus for the treatment of OCD, the hippocampus for the treatment of epilepsy, and many locations for the treatment of brain tumors – present significant challenges.

In order to assess and improve device performance in the context of these clinical indications, it is necessary to understand where in the intracranial volume therapeutic levels of FUS can be delivered in a safe and targeted manner.

We present an initial thermal mapping study of two ex-vivo human skulls with both a 220kHz and 710kHz MR-guided focused ultrasound system.

Methods: A custom-molded thermal phantom was used to fill the skull cavity with a brain-mimicking material that would heat in response to focal ultrasound energy and provide signal change in associated MR thermometry. CT-based skull refocusing was performed through the ExAblate Neuro, planning workstation, (InSightec LTD, Haifa, Israel). Through a combination of mechanical transducer positioning and electronic steering, 220kHz sonications spaced at 1cm intervals in the axial imaging plane were performed at 200W acoustic power for 15 seconds. This was repeated in axial planes spaced 1cm apart in order to cover a full hemisphere of the skull. The same procedure was repeated at 710kHz for the same skull, and both transducers were used to sonicate a second ex-vivo skull specimen in the same manner.

Results and Conclusions: Initial results indicate more efficient delivery of FUS energy to the center-of-mass of the skull cavity, with some preferential heating lateral of center, medially above the orbits, and when very close to bone. Both treatment envelope datasets are overlaid on MR images of the corresponding cadaveric brain anatomy.

In conclusion, this efficiency-mapping study will provide the basis of a study into methods for improving efficiency of delivery of FUS energy to identified minimum-efficiency areas. Such a study would involve adjusting the acoustic aperture, apodization, and simulation studies to improve efficiency in these areas.

Acknowledgements (Funding): FUSF internal

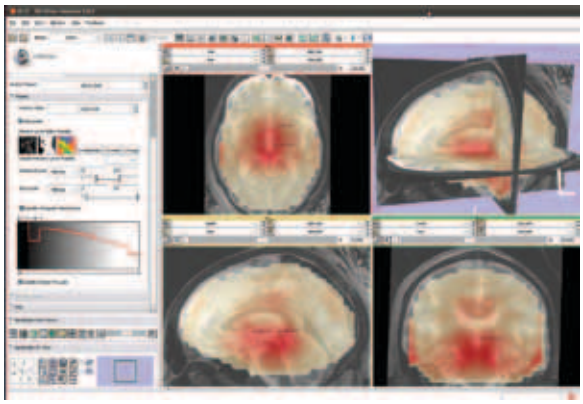

Treatment Envelope at 220kHz

P-98-BR

Tuesday
16 October 2012

Topic: Brain
Presentation Type: Poster

Increased Blood-Tumor Barrier Permeability and Enhanced Doxorubicin Delivery Into Rat Glioma by MRI Guided Focused Ultrasound and Microbubbles

Juyoung Park, Muna Aryal, Yong-Zhi Zhang, Natalia Vykhodtseva, Ferenc Jolesz, Nathan McDannold

Brigham and Women's Hospital / Harvard Medical School, Boston, Massachusetts, United States

Background/Introduction: Although the blood vessels in many brain tumors are permeable, this permeability is heterogeneous. This heterogeneity, along with other factors such as increased interstitial pressures and efflux pumps hinders the effective delivery of chemotherapy and other anti-cancer drugs. This study used MRI methods to characterize the permeability changes of the "blood-tumor barrier" (BTB) induced by focused ultrasound (FUS) bursts and IV injected microbubbles in 9L glioma-bearing rats and the resulting payload of a chemotherapy agent, doxorubicin (DOX).

Methods: Male Spraque Dawley rats (n=25) were implanted with 9L glioma cells in both hemispheres of the brain. At 10-12 days after the implantation, one of the resulting brain tumors was sonicated transcranially. The tumor and a narrow surrounding rim was covered by five sonications using a 690 kHz FUS transducer; the non-sonicated tumor in the other hemisphere served as a control. For BTB permeabilization, 10 ms bursts at 0.8 MPa were applied at 1 Hz for 60s. Each sonication was combined with IV injection of a microbubble ultrasound contrast agent (Definity; 10 μl/kg). MRI contrast agent (Magnevist) and DOX were injected immediately after the last sonication. The BTB permeability was assessed by calculating of the transfer coefficient (Ktrans) for the Magnevist using dynamic contrast enhanced (DCE)-MRI before and 30 min after sonication. The rats were sacrificed at 1 hr after the last sonication, at which time the DOX concentration in both tumors were measured by fluorometric analysis.

Results and Conclusions: The mean Ktrans in the tumor was 0.0163±0.0069 min-1 before sonication and 0.0316±0.0085 min-1 30 min after sonication. DOX concentrations in the sonicated tumor area were 2.5-fold higher than in the non-sonicated tumor area. Also, a linear correlation was found between the DOX concentration and the Ktrans measured 30 min after sonication (R: 0.78). These data suggest that FUS-induced BTB disruption can substantially increase BTB permeability and augment DOX delivery in this brain tumor model. In addition, an MRI contrast agent may be use as a surrogate tracer to estimate drug delivery to the brain tumor after FUS-induced BTB disruption.

Acknowledgements (Funding): This work was supported by National Institutes of Health (P41 RR019703, P41EB015898 and RC2NS069413) as well as a gift from Betty Brudnick.

P-99-BR

Tuesday
16 October 2012

Topic: Brain
Presentation Type: Poster

Safety Evaluation for Temporary Disruption of Blood-Retinal Barrier Using MR-Guided Focused Ultrasound and Microbubbles

Juyoung Park[1], James Akula[2], Costas Arvanitis[1], Yong-Zhi Zhang[1], Natalia Vykhodtseva[1], Nathan McDannold[1]

[1]Brigham and Women's Hospital/Harvard Medical School, Boston, Massachusetts, United States
[2]Children's Hospital Boston and Harvard Medical School, Boston, Massachusetts, United States

Background/Introduction: The blood-retinal barrier (BRB) prevents most systemically-administered drugs from reaching the retina and is a major obstacle to the use of drugs for treatment of retinal disease. This study evaluated whether burst ultrasound applied with a circulating microbubble agent can safely disrupt the BRB.

Methods: Five overlapping targets on the retina were sonicated in rats and rabbits through the cornea and lens using a 690 kHz focused transducer. For BRB disruption, 10 ms bursts was applied at 1Hz for 60 s with peak rarefactional pressure (PRP) amplitudes of 0.40-0.67 MPa in rats, and 0.8 MPa in rabbits; each sonication was combined with an IV injection of a microbubble ultrasound contrast agent (Definity; 20 μl/kg). During some of the sonications, acoustic emissions from the microbubbles were recorded in order to characterize the microbubble dynamics. An MRI contrast agent (Magnevist) was intravenously injected immediately after the last sonication, and serial T1-weighted MR images were acquired every 5 min for 25 min to confirm the BRB disruption. Electroretinograms (ERG) were performed after the sonications to evaluate retinal function.

Results and Conclusions: In rats (n=25), we observed BRB disruption as extravasation of a systemically injected MRI contrast in the targeted retinal area, which then leaked into the vitreous. BRB disruption was observed at pressure amplitudes as low as 0.48 MPa; it was always observed at 0.6 MPa and above. At 0.6 MPa, the BRB disruption was not detected after an additional MRI contrast injection 3.5 hrs following the sonication. Histology findings at 24 hrs indicated that most of the sonicated regions appeared unaffected. Only one sonication target in the retina showed clusters of extravasated erythrocytes (petechaie) in the nuclear layer. Sonication at 0.6 MPa produced no evident changes in the ERG. When acoustic emissions were recorded, only strong harmonics were observed; no ultra-harmonic or no broadband signals were evident. In rabbit experiments (n=2), we also observed BRB disruption at 0.8 MPa. These results demonstrate that temporary BRB disruption can be produced without retinal functional changes using FUS combined with circulating microbubbles for the targeted ocular drug delivery. Also, we found that BRB disruption can be achieved in a larger eye.

Acknowledgements (Funding): This work was supported by National Institutes of Health (P41 RR019703, P41EB015898 and RC2 NS069413) as well as a gift from Betty Brudnick.

P-100-BR

Tuesday
16 October 2012

Topic: Brain
Presentation Type: Poster

Microbubble-Type Dependence of Focused Ultrasound Induced Blood Brain Barrier Opening

Shutao Wang, Gesthimani Samiotaki, Jameel Feshitan, Oluyemi Olumolade, Elisa Konofagou

Columbia University, New York, New York, United States

Background/Introduction: Focused Ultrasound (FUS) in combination with ultrasound contrast agents (UCA) has been used to non-invasively induce reversible blood brain barrier (BBB) opening in both rodents and non-human primates. The goal of this study was to investigate the effects of clinically approved UCA (DefinityTM) and custom-made polydispersed microbubbles on the BBB opening in mice.

Methods: The custom-made polydispersed microbubbles, which primarily composed of phosphocholine lipid and perfluorobutane gas, were formed through mechanical activation (ViamixTM). The concentration and volume distribution of both the custom-made microbubbles and activated DefinityTM (lipid-shelled, gas content: octofluoropropane) were measured by a multisizer, and were diluted to 6×108 #/ml prior to injection. A total of 18 black wild-type mice (3 per group) were used in this study, and each mouse received either DefinityTM or custom-made microbubbles (1 ml/g body weight) via tail vein injection. Although both types of microbubbles were polydispersed, the volume distribution of DefinityTM peaked around the diameter of 3 mm (0.67%), while the volume percentage of custom-made microbubbles stabilized around 0.5% for diameters of 4.5 mm and above. Immediately after the microbubble administration, FUS sonications were given with the following parameters: frequency of 1.525 MHz, pulse length of 10 ms, pulse repetition frequency of 10 Hz, peak rarefactional acoustic pressures of 0.3, 0.45 MPa, and 0.6 MPa, and a sonication duration of 60 s. The BBB opening was confirmed after treatment through T1-weighted MRI with intraperitoneal injection of gadodiamide (300 ml). The permeability of the sonicated regions was imaged using a previously reported model-based approach and dynamic contrast enhanced (DCE) MRI. The volume of BBB opening using 3D MRI was quantified for the different pressures with both types of microbubbles. In addition, the closing timeline was established for each animal and histology was performed to evaluate the safety of the treatments one week after treatment.

Results and Conclusions: The permeability of the treated region using the two types of microbubbles did not show significant difference ($P > 0.05$) for FUS pressure levels of 0.45 MPa and 0.6 MPa, while custom-made microbubbles showed significantly high permeability ($P < 0.01$) at the lower pressure of 0.3 MPa. The volumes of BBB opening showed similar trends at all pressure levels across the two types of microbubbles. Furthermore, mice treated with custom-made microbubbles exhibited longer BBB closing timelines compared to those treated with DefinityTM. The results from this study indicate that the gas and shell material of microbubbles may have significant effects on FUS induced BBB opening at low pressure levels, possibly due to higher levels of stable cavitation of custom-made microbubbles. Nonetheless, this difference becomes less significant for high FUS pressure levels where inertial cavitation typically occurs.

Acknowledgements (Funding): This study was supported in part by NIH R01EB009041, NIH R01AG038961, NIH MH059244, and the Kinetics Foundation.

P-101-BR

Tuesday
16 October 2012

Topic: Brain
Presentation Type: Poster

MR Compatible Positioning Device for Guiding a Focused Ultrasound System for the Treatment of Brain Diseases

Nicos Mylonas[1], Christakis Damianou[2]

[1]Frederick Institute of Technology, Limassol, Cyprus
[2]MEDSONIC, LTD, Limassol, Cyprus

Background/Introduction: A prototype magnetic resonance imaging (MRI)-compatible positioning device that navigates a focused ultrasound (FUS) transducer is presented. The positioning device has 3 user-controlled degrees of freedom that allow access to brain targets using a lateral coupling approach. The positioning device can be used for the treatment of brain cancer (thermal mode ultrasound) or ischemic stroke (mechanical mode ultrasound).

Methods: The positioning device incorporates only MRI compatible materials such as piezoelectric motors, ABS plastic, brass screws, and brass rack and pinion.

Results and Conclusions: The robot has the ability to accurately move the transducer thus creating discrete and overlapping lesions in rabbit brain in vivo.

A simple, cost effective, portable positioning device has been developed which can be used in virtually any clinical MRI scanner since it can be placed on the table of the MRI scanner. This system can be used to treat in the future patients with brain cancer and ischemic stroke.

P-102-BR

Tuesday
16 October 2012

Topic: Brain
Presentation Type: Poster

MR Guided Focused Ultrasound Surgery for Trigeminal Neuralgia: A Cadaveric and Laboratory Feasibility Study

Stephen Monteith[1], Jason Sheehan[1], Neal Kassell[1], Max Wintermark[1], Ricky Medel[1], Matthew Eames[2], John Snell[2], Eyal Zadicario[3], Javier Grinfeld[3], Jeff Elias[1]

[1]University of Virginia, Charlottesville, Virginia, United States
[2]Focused Ultrasound Foundation, Charlottesville, Virginia, United States
[3]InSightec, Tirat Carmel, Israel

Background/Introduction: Microvascular decompression, stereotactic radiosurgery, and percutaneous techniques are effective treatments for trigeminal neuralgia , but each procedure is associated with operative morbidity and a failure rate. Transcranial MR guided Focused Ultrasound Surgery (MRgFUS) is evolving as a treatment modality in neurosurgery. Until now, the trigeminal nerve (TN) was felt to be beyond the treatment envelope of existing high frequency MRgFUS systems. In this study, we explore the feasibility of targeting the TN in a cadaveric model. Assessment of temperature changes in anatomical structures of interest such as the internal acoustic canal (IAC) were performed using computer simulations and in an in vitro skull phantom model fitted with thermocouples.

Methods: Six trigeminal nerves from four cadavers were targeted. High resolution 3D volumetric sequences were performed on a 3T MRI to clearly delineate the TN. The cadaver was positioned into a focused ultrasound transducer (ExAblate Neuro, 650Khz system – InSightec, Israel) and the MRI system using a stereotactic frame. The focus of the transducer was centered at the trigeminal root entry zone (REZ), allowing targeting at the REZ and the cisternal segment. Real-time two dimensional thermometry was performed during sonications. Post-hoc MR thermometry was performed on a computer workstation at the conclusion of the procedure to analyze temperature effects at neuro-anatomical areas of interest. Using a cadaveric skull and gel phantom, the region of the TN was targeted and temperature changes in regions of interest in the skull base were measured using thermocouples.

Results and Conclusions: Using the MRgFUS system, a focal thermal rise of minimal temperature was performed in the pons to confirm accurate targeting using real time MR thermometry. Sequential sonications of 25-1500W for 10-30 seconds were successfully performed along the length of the TN starting at the REZ. Real time MRI thermometry confirmed the temperature rise as a narrow focus of heating by a mean of 10 degrees Celsius. Post-procedural thermometry calculations and thermocouple experiments in a phantom skull demonstrated minimal heating of critical surrounding structures including the skull base, cranial nerves, and cerebral vessels. For a REZ target, inclusion of 'no pass regions' through the petrous bone decreased collateral heating in the IAC from 16.7 without blocking to 5.7 degrees with blocking. Similarly, for a mid cisternal target, collateral heating at the IAC was improved from a 16.3 degree rise to 4.9 degrees.

In conclusion, this study demonstrates focal heating of up to 18 degrees Celsius in a cadaveric TN at the REZ and along the cisternal segment with transcranial MR Guided focused ultrasound. Significant heating of the skull base and surrounding neural structures did not occur with implementation of no pass regions. However, in vivo studies are necessary to confirm the safety and efficacy of this potentially new, noninvasive treatment.

Acknowledgements (Funding): Focused Ultrasound Foundation

P-103-BR

Tuesday
16 October 2012

Topic: Brain
Presentation Type: Poster

MR Sub-Sampling Strategies for Transcranial MRgFUS Applications

Henrik Odeen, Nick Todd, Mahamadou Diakite, Allison Payne, Dennis Parker

University of Utah, Salt Lake City, Utah, United States

Background/Introduction: Transcranial MRgFUS requires accurate temperature measurements with high spatio-temporal resolution over the fully insonified 3D field of view (FoV) to assess treatment and monitor heating in both near-field tissue-bone interfaces and the treatment site. To achieve high spatio-temporal resolution over the large FoV many researchers utilize sub-sampling of k-space in conjunction with e.g. parallel imaging, constrained reconstruction or model based reconstruction algorithms. Here we present a comparison between two sub-sampling schemes, which are reconstructed with a constrained reconstruction method as well as a model predictive approach.

Methods: Subsampling schemes Two different subsampling schemes were implemented in a 3D Segmented EPI sequence on a Siemens 3T MRI scanner (Tim Trio, Siemens Healthcare AG, Erlangen, Germany). The even sub-sampling (ESS) scheme fully sampled the read out (kx) and slice (kz) directions, and evenly sub-sampled the phase encode direction (ky). The second scheme, taking advantage of the fact that most of the energy of k-space is located in the center, applied a variable density subsampling (VDSS) pattern in the ky-kz plane (kx was fully sampled). The ky-kz plane was divided into regions, where the central region was fully sampled every time, and the outer regions were sampled with increasing reduction factors (R), see figure 1.

Temporally Constrained Reconstruction (TCR) In the previously described TCR algorithm[1,2] the sequence of temperature images is obtained by iteratively minimizing a cost function consisting of a constraint term and a data fidelity term using a gradient descent method.

Model Predictive Filtering (MPF) In the previously described MPF approach[3] a forward prediction of the Pennes bioheat equation (PBE) is used in conjunction with the sub-sampled data to predict the temperature. An initial low-power heating was performed to determine the parameters for the PBE.[3,5]

Experiment HIFU heating was performed on ex vivo chicken tissue. The PBE calibration heating and the experiment heatings were performed with 15/30 W for 29.6/48.1 s, respectively. Imaging parameters included voxel size=1x1x3 mm3, TR = 33 ms, TE = 12 (for fully sampled "truth" and ESS) and 20 (for VDSS) ms, EPI factor=7, bandwidth=752 Hz/pixel, tacq=3.7 s. For the calibration run and fully sampled "truth" the imaging matrix was 128x77x10. To achieve the same reduction factor (R=7) for ESS and VDSS the ESS matrix was 128x98x54, and the VDSS matrix was 128x126x44.

Results and Conclusions: Figure 2 shows 3 orthogonal views of the HIFU focal spot for a fully sampled "truth" heating, and for the VDSS and ESS schemes, both reconstructed with MPF and TCR. Figure 3 shows temperatures as a function of time.

Data acquired with the VDSS underestimates the maximum temperatures both with TCR and MPF reconstructions, while data acquired with the ESS scheme performs well with both reconstruction algorithms. In general the MPF algorithm provides a more accurate fit to the temperature measurements than the TCR algorithm. The cause of this systematic offset for the VDSS scheme is still under investigation.

Acknowledgements (Funding): This work was supported by Siemens Healthcare, The Focused Ultrasound Foundation, The Ben B. and Iris M. Margolis Foundation, and NIH grants R01s CA87785, EB013433, and CA134599.

References:

1. Adluru et al. *MRM* 57:1027:1036 (2007).
2. Todd et al. *MRM* 62:406-19 (2009).
3. Todd et al. *MRM* 63:1269-79 (2010).
4. Cheng and Plewes *JMRI* 16:598:609 (2002).
5. Roemer et al. *Int. J. Radiat. Oncol. Biol. Phys* 11:1539:1550 (1985)

(See figures, next page.)

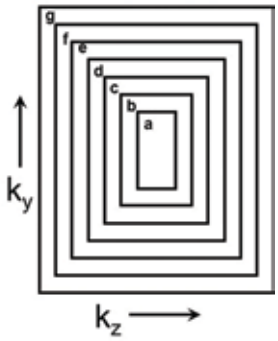

Figure-1 Variable sampling density in ky-kz. The center region (a) is fully sampled every time point, and regions (b) through (g) are sampled with increasing R ranging from 3 (b) to 13 (g).

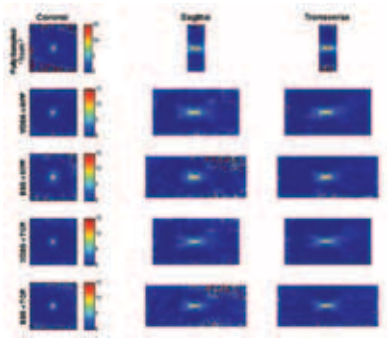

Figure-2 Columns show coronal, sagittal, and transverse views of the HIFU hotspot, respectively. Rows show data for; fully sampled "truth", VDSS + MPF, ESS + MPF, VDSS + TCR, and ESS + TCR, respectively.

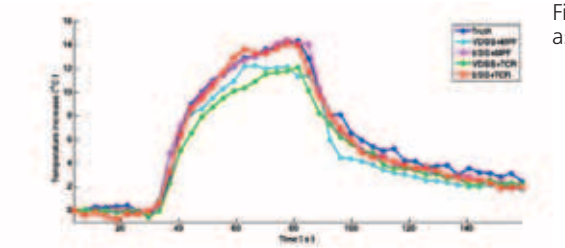

Figure-3 Temperature increase as a function of time.

P-104-BR

Tuesday
16 October 2012

Topic: Brain
Presentation Type: Poster

MRgFUS for Glioma Patients: Case Report

Daniel Coluccia[1], Javier Fandino[2], Beat Werner[1], Ronald Bauer[3], Jenny Kienzler[2], Bettina Gers[3], Ernst Martin[1]

[1]Zurich, Switzerland
[2]Aarau, Switzerland
[3]St. Gallen, Switzerland

Background/Introduction: Precision and sparing of normal tissue together with non-invasiveness make high focused ultrasound a potentially ideal method for brain interventions. While high focused ultrasound is increasingly applied for tumor ablation in uterine, liver and prostate tumors in preclinical and clinical settings, the use in brain tumors is less examined. We present the first results of our feasibility and safety study of noninvasive, MR guided high focused ultrasound surgery (MRgFUS) in a glioma patient.

Methods: A 32 year old patient with a histologically confirmed glioblastoma with a cystic mass in the region of the left thalamus was included in our study. Due to the location within eloquent brain tissue, surgical removal was not considered and the patient was treated with chemo- and radiotherapy. As the cystic portion of the tumor did cause symptomatic mass effect, an omaya reservoir with a catheter into the cyst was placed in order to allow repeated aspiration. Two months after the initial diagnosis the patient was included for a MRgFUS procedure (ExAblate4000®, 650kHz). Interpretation of the data was supported by additional phantom studies.

Results and Conclusions: A total of 8 sonication sessions were performed each with 10-15 seconds duration. Energy range was 500-6750J, while the power range was 50-450W. Thermometry data did not show adequate heating in the target volume (Tmax = 40°C, dT = 3°C) and the procedure was stopped in order to avoid any risk. No harmful effect could be registered and the patient showed an overall good tolerance to the intervention. According to our analysis including also phantom studies, the catheter material in the close vicinity to the target volume (about 15mm) was likely to impede appropriate focussing, while catheter material outside the skull did not show interference.

In conclusion, sonication with an energy range up to 6750J could safely be performed in the partially cystic glioma tumor, while an ablative effect was absent presumably because of an impediment of a high temperature spot due the catheter material. Further investigation are needed to evaluate the feasibility of noninvasive brain tumor ablation and the influence of foreign material in the brain on the sonication effect.

P-105-BR

Tuesday
16 October 2012

Topic: Brain
Presentation Type: Poster

Permeability and Reversibility Timeline Study of the Focused-Ultrasound Induced Blood-Brain Barrier Opening at Distinct Pressures and Pulse Lengths In Vivo

Gesthimani Samiotaki, Oluyemi Olumolade, Elisa Konofagou

Columbia University, New York, New York, United States

Background/Introduction: Impermeability of Blood-Brain Barrier (BBB) remains the biggest challenge in the brain drug delivery. Focused Ultrasound (FUS) in conjunction with microbubbles has been shown to open the BBB locally, non-invasively and reversibly. In this study the FUS pulse length (PL) and peak-negative pressure (PNP) are studied as two major parameters in predicting and controlling the BBB opening permeability and its recovery timeline using MRI.

Methods: The FUS (1.5 MHz) was used together with Definity® microbubbles (IV 1 µl/g, 1:20 diluted in PBS) and its PL ranged from 67 µs to 6.7 ms while the PNP varied between 0.30 MPa and 0.60 MPa, with a PRF of 10 Hz. T1-weighted and Dynamic Contrast Enhanced (DCE) MRI using gadodiamide (IP 300 µl/ 25 g) was used to quantify the volume of opening and the transfer rate from blood to the brain (Ktrans). The reversibility timeline was also measured, and safety was assessed using H&E staining 7 days later.

Results and Conclusions: The permeability and volume of opening were both found to increase with the PNP and PL, but saturated at high PNPs or PLs. At the lowest (67 µs) PL, the opening PNP threshold was higher, the average Ktrans was equal to 0.010 ± 0.002 min-1, the opening volume was 5.38 ± 5.34 mm3, and closing occurred within 4 h from opening. At 0.67- and 6.7- ms PLs, the Ktrans reached the same plateau of 0.025 min-1 at both 0.45 MPa and 0.60 MPa, with opening volumes of 13.39 ± 5.94 mm3 and 18.56 ± 11.12 mm3, and 16.10 ± 5.98 mm3 and 22.16 ± 5.38 mm3, respectively. At 0.30 MPa, only the longest (0.67 ms and 6.7 ms) PLs were found capable of inducing BBB opening, while closing occurred within 24 – 48 h. Correlation between the time required for closing and the Ktrans on the day of opening was shown to follow a logarithmic relationship, while the opening duration increased with the opening volume. In all the cases studied, no histological damage was detected, indicating the safety of the methodology with the parameters used.

In this longitudinal study, the dependence of the BBB opening permeability, volume and duration on the PL and PNP was established. At the lowest PNP (0.30 MPa), a longer PL is required to induce BBB opening, indicating that the FUS needs to be applied over a minimum period of time to induce BBB opening. Above the 0.67ms PL threshold, there is no significant difference in opening among different PNPs, indicating that the most significant interaction of the FUS with the microbubbles occurs in the first few FUS cycles. Longer PLs and higher pressures within the ranges studied have an effect on the BBB opening volume and duration, but not on the safety of the methodology within the pressure range studied.

Acknowledgements (Funding): This study was supported in part by NIH R01 EB9041.

(See figures, next page.)

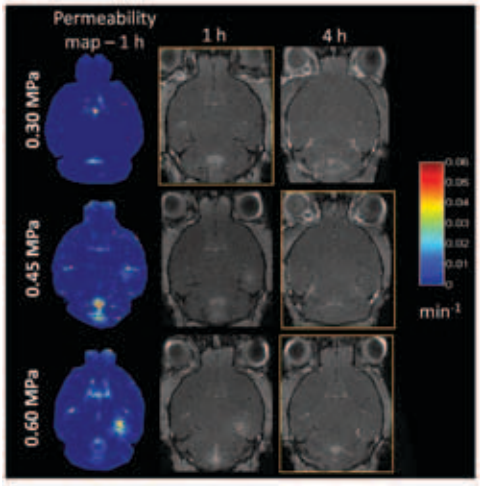

Horizontal permeability maps after FUS, followed by T1-weighted images of the reversibility timeline for all PRPs with a PL of 67 ?s. Yellow frames denote BBB closing. Images following the detected closing, confirm that BBB remained closed.

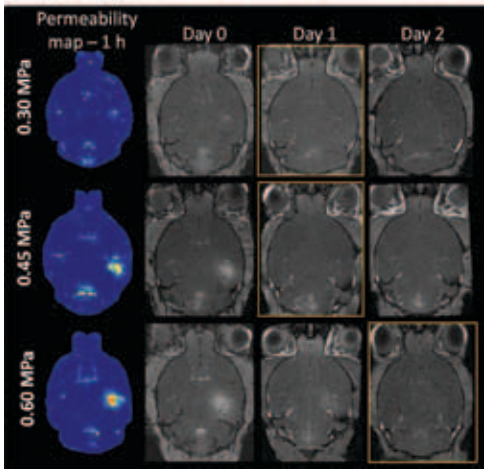

Horizontal permeability maps after FUS, followed by T1-weighted images of the reversibility timeline for all PRPs with a PL of 0.67 ms. Yellow frames denote BBB closing. Images following the detected closing, confirm that BBB remained closed.

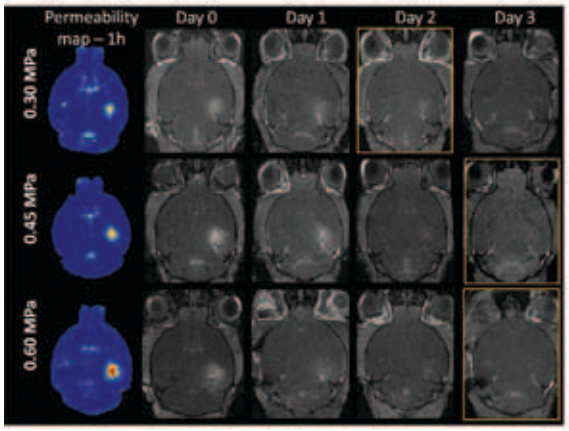

Horizontal permeability maps after FUS, followed by T1-weighted images of the reversibility timeline for all PRPs with a PL of 6.7 ms. Yellow frames denote BBB closing. Images following the detected closing, confirm that BBB remained closed.

P-106-BR

Tuesday
16 October 2012

Topic: Brain
Presentation Type: Poster

Phase Aberration Correction Using Simulation and MR-ARFI for Transcranial MR-Guided Focused Ultrasound Surgery

Urvi Vyas, Elena Kaye, Kim Butts Pauly

Stanford University, San Francisco, California, United States

Background/Introduction: Spatial inhomogeneities in the cranium cause aberrations in the location and shape of the beam's focus in transcranial MR-guided focused ultrasound surgery. CT-based correction techniques approximate acoustic parameters from Hounsfield units and require co-registration between the CT and MR images. Current implementations of MR-ARFI based corrections require many ultrasound sonications (4 x the number of elements).1 In this paper, we propose a hybrid technique that uses a simulation to find the phase aberrations that are consistent with an experimentally measured MR-ARFI displacement image of the focal spot.

Methods: The hybrid simulation/MR-ARFI technique iteratively modifies the simulation aberrations to minimize the difference between simulated and experimental radiation force patterns. The experimental radiation force pattern is derived from an MR-ARFI displacement image while the simulation radiation force pattern uses the fast Hybrid Angular Spectrum2 beam simulation technique that simulates the effect of attenuation, reflection and refraction of the ultrasound beam in heterogeneous media. Experiments were conducted by applying random numerical phase aberrations to a planar 1024-element 550 kHz phased-array transducer (InSightec). Random aberrations (1024, one for each element) were applied to the transducer during transmission and the experimentally acquired MR-ARFI displacement image in a gel phantom was used as an input to the optimization routine.

Results and Conclusions: After the optimization, the corrected aberrations were applied to the transducer and the resulting MR-ARFI image was compared to the aberrated and the unaberrated images. The results are shown in Figure 1. A single loop of the hybrid simulation/MR-ARFI technique results in a 10% increase of the focal displacement compared to the aberrated case.

Conclusion: Using one MR-ARFI image and no a priori information about the applied phase aberrations, the hybrid simulation MR-ARFI technique improves the quality of the beam's focus. The effect of additional MR-ARFI images (<5) to the technique will be investigated in future work.

Acknowledgements (Funding): Grant Support: P01 CA 159992, R21 EB011559

References:

1. E. Herbert IEEE TUFFC 56(11), 2388-2399
2. U. Vyas IEEE TUFFC 59(6), 1093-1100

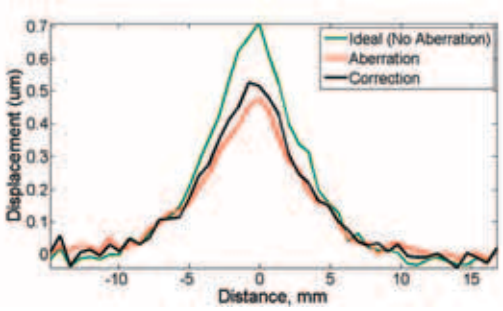

Figure 1. Profiles through the MR-ARFI displacements at the focal spot are shown for the three cases indicated. The estimated aberrations were obtained using only one MR-ARF image. The initial phase aberration estimate for the hybrid technique was not based on any a priori information.

P-107-BR

Tuesday
16 October 2012

Topic: Brain
Presentation Type: Poster

Thermal Ablation in Normal Canine Brain Using a Multi-Element Interstitial Ultrasound Device

Michael Canney[1], Kevin Beccaria[2], Catherine Horodyckid[3], Cyril Lafon[4], Jean-Yves Chapelon[4], Alexandre Carpentier[2]

[1]CarThera, Lyon, France
[2]Pitie-Salpetriere Hospital, Assistance Publique - Hôpitaux de Paris, Paris, France
[3]CarThera / Pitie-Salpetriere Hospital, Assistance Publique - Hôpitaux de Paris, Paris, France
[4]Inserm, U1032, LabTau / Université de Lyon, Lyon, France

Background/Introduction: Thermal ablation of brain tumors is a promising treatment modality that can be used as an alternative or adjuvant therapy to conventional treatments involving surgical resection, radiotherapy, and chemotherapy. Recent clinical studies using laser heating applicators have demonstrated that interstitial thermal ablation is well tolerated by patients and can be used for the management of both primary and metastatic brain tumors. The principal limitation of existing devices is the lack of control over the geometry of the heated volume. In this work, a multi-element interstitial ultrasound device was developed that allows for greater control over the geometry of the heated region. The device was tested in vivo in healthy canine brain to examine the feasibility of using such a device for thermal ablation of brain tumors.

Methods: A multi-element interstitial device was developed that operated at output surface intensities of up to 30 W/cm2 at a frequency of 6 MHz. The device consisted of 56 elements, each 1 mm2, oriented on 7 faces of a 3.2-mm diameter support and was enclosed by a cooling envelope. Heating was monitored during experiments in five healthy beagle canines using a 1.5T magnetic resonance imaging (MRI) system to obtain 3D real-time temperature maps using the proton resonance frequency shift with a thermal sensitive echoplanar sequence. The ultrasound applicator was inserted in the brain after a 1.5 cm diameter craniotomy and multiple heating experiments were performed in each canine. After treatment, contrast-enhanced T1-weighted gadolinium images were obtained and compared with predicted regions of thermal necrosis from thermal dose calculations. Long-term followup was performed in 2 dogs at up to 21 days after ablation to examine inflammation and long-term characteristics of lesions.

Results and Conclusions: Temperatures of greater than 60°C were induced in vivo during heating and regions of ablation of up to 5 cm3 were visible on post-treatment MR images. Regions of thermal ablation were visible on T1-gadolinium contrast enhanced images and compared well with predicted regions of thermal necrosis using calculations of thermal dose. Thermally ablated regions in the brain resulted in regions of liquefactive necrosis that showed gadolinium enhancement throughout the treated region with a sharp demarcation (<0.5 mm) between liquefied and healthy tissue. Interstitial thermal ablation using multi-element ultrasound applicators is a promising treatment modality for brain tumors.

Acknowledgements (Funding): Work supported by CarThera SAS.

P-108-BT

Tuesday
16 October 2012

Topic: Breast Tumors
Presentation Type: Poster

3-D Graphical Modeling for FUS Device Design

Robb Merrill[1], Allison Payne[2], J Hadley[1], Emilee Minalga[1], Dennis Parker[2]

[1]Utah Center for Advanced Imaging Research, Salt Lake City, Utah, United States
[2]University of Utah, Salt Lake City, Utah, United States

Background/Introduction: Medical equipment laboratories are relying more and more on the computer-aided design and simulation of their prototype devices in an effort to reduce hardware development costs and manage the increased complexity of modern imaging technology. MRI scanners support an ever-increasing number of advanced functions, i.e., a greater number of coil receive channels and the integration of interventional hardware. Realistic computer modeling has greatly facilitated the task of optimizing device functionality on such an ever-increasing scale of complexity.

A significant limitation to the design of complex MRI coils and integrated interventional devices has been the absence of adequate digital models of the human anatomy and scanner hardware. Mathematical programming suites such as Matlab have successfully simulated the electromagnetic, thermal, and acoustic physics of magnetic resonance guided focused ultrasound (MRgFUS) treatments and systems with relatively simple geometries. However, the mechanical layout of hardware devices relative to the human subject is very cumbersome to analyze and predict in non-graphical software packages. Modeling the organic nature of human anatomy has presented a considerable challenge to geometric design in programs with rigidly mathematical user interfaces.

Advanced 3-D design software has been used to design and construct a dedicated MRI guided breast FUS device as well as the RF coil arrays for a transcranial MRgFUS device. Because FUS treatment during scan time requires accurate temperature monitoring, the implementation of a dedicated MRI coil was of chief concern during the design process of each device to obtain maximum coil SNR and temperature accuracy. After placing a human model 'patient' inside an accurate scanner model, device hardware can be designed around the patient within the scanner bore to achieve maximum patient comfort and treatment region access.

Methods: Human models were created in SolidWorks 3-D modeling software for FUS brain and breast treatment. Clinical MRI scans were consulted for approximate feature location. Brain and breast treatment hardware devices were rotated through their maximum ranges of adjustability to detect mechanical interference with the patient table and scanner. "Treatable Volume" regions were obtained by sweeping the ultrasound focal region through the full range of mechanical and electronic transducer steering.

Figure 1. Breast FUS (X-section)

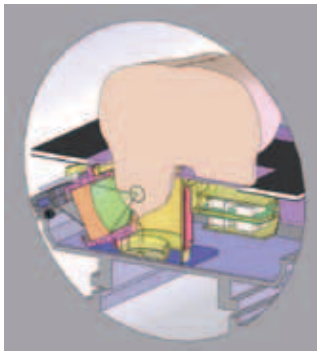

Figure 2. Human Model

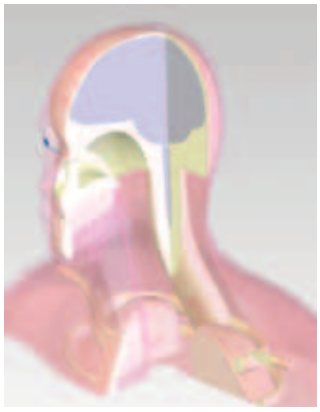

Results and Conclusions: Inexpensive 3-D human models were developed using SolidWorks CAD software that provided sufficient anatomical detail for relevant body parts. Hardware and coils of various sizes and configurations can be easily applied and precisely arranged relative to the models.

Discussion: Body parts of approximate location and shape were deemed sufficient for coil simulation due to variability of human anatomy. Additional time can be invested to produce finer and more accurate detail of organs, or to adjust the location and size of individual organs (e.g. depth and diameter of carotid arteries) to model treatment of non-average patients.

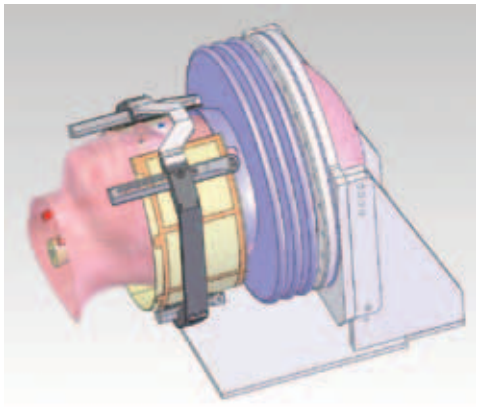

Figure 3. Brain FUS

Acknowledgements (Funding): This work is supported by NIH grants R01 CA134599 and R01 EB013433 and the Ben B. and Iris M. Margolis Foundation.

P-109-BT

Tuesday
16 October 2012

Topic: Breast Tumors
Presentation Type: Poster

Estimation and Correction of Phase Aberrations for a Lateral MRgFUS Breast System

Alexis Farrer, Scott Almquist, Yi Wang, Allison Payne, Dennis Parker, Douglas Christensen

University of Utah, Salt Lake City, Utah, United States

Background/Introduction: MR-guided focused ultrasound surgery (MRgFUS) has potential use as a non-invasive breast cancer therapy. Our group has designed and built a custom system in which the phased-array transducer is located laterally to the breast being treated.[1] It has been shown for another breast system using laterally positioned wide-view transducers that phase distortion, caused by varying tissue acoustic properties, can lead to significant broadening of the pressure pattern at the focus.[2] We used simulations to assess whether such focusing distortion in a typical breast would be present for our system, which uses a transducer with a smaller numerical aperture. We also applied a phase correction technique to the transducer elements to observe potential improvement in the focusing strength and accuracy.

Methods: Our breast system allows considerable flexibility in the mechanical and electronic positioning of the ultrasound beam in the breast.[1] It employs a 256-element, 1.0-MHz phased array with a 10-cm focal length and 14 x 10-cm outer dimensions. To simulate the effects of varying breast tissue properties on the focus, we segmented a 3D breast image volume (121 x 75 x 93.5 mm^3) from a volunteer (0.5 x 1.0 x 0.5 mm resolution) into five tissue types: skin, breast fat, fibroglandular, fibroadenoma, and water. Using the Hybrid Angular Spectrum (HAS) method[3] implemented in MATLAB, we calculated the pressure pattern throughout the breast for a focal location that was electronically steered 5.0 mm away from the geometric focus, as shown in Figure-1. Literature values[4] were used for the speed of sound, density and attenuation of each tissue type. We next calculated the phase values for each transducer element that would correct for the aberrations in this model using the following procedure: We propagated a wave from each individual element throughout the 3D model (employing parallel computation on a GPU) and stored each complex array. At an arbitrary voxel chosen for the focus, we found the phase associated with each element's pressure pattern and used the conjugate of that value to adjust the driving excitation to the elements.

Results and Conclusions: As seen in the close-up view in Figure-2a, the pressure pattern at the focus for the inhomogeneous breast model is relatively displaced and spread out compared to that calculated in a water-only homogeneous medium for the same exposure conditions (Figure-2c). Such distortion could potentially compromise the accuracy and efficiency of MRgFUS treatments. When the phase aberration correction procedure is applied, the beam's focus is sharpened (Figure-2b), approaching the pattern found in a water-only homogeneous medium (Figure-2c). Although the expected breast phase aberration for the moderately sized transducer used in our system is less severe than that expected with wider view transducers, it is likely to present enough of a detriment to treatment accuracy to require a phase aberration correction technique, especially for more heterogeneous breasts. Further work will allow for analysis of phase aberrations and phase correction in phantoms and ex vivo tissues.

Figure 1. Segmented breast model, with the focused beam propagating horizontally. The phased-array transducer is positioned on the left (not shown).

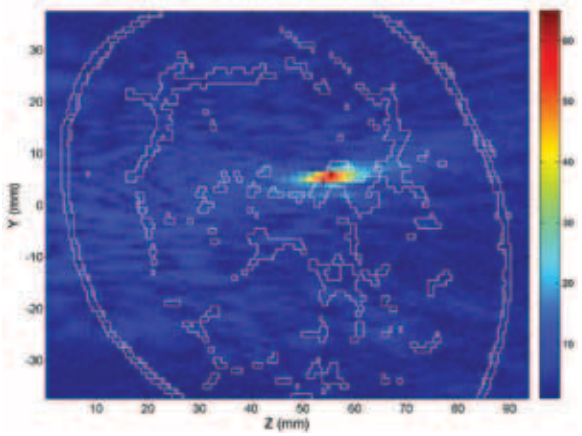

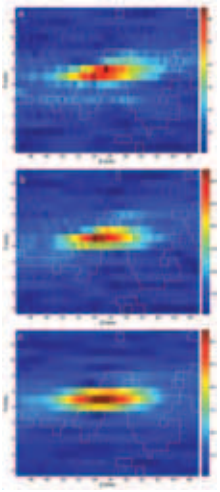

References:
1. A. Payne et al., *Med. Phys.* (39)1552, 2012.
2. C. Mougenot et al., *Med. Phys.* 39(4), April 2012.
3. U. Vyas and D. Christensen, *IEEE Proc.* UFFC 59(6), June 2012.
4. F. Duck, *Physical Properties of Tissue* (Academic, New York), 1990.

Acknowledgements (Funding): The authors gratefully acknowledge support from Siemens Healthcare AG, the FUS Foundation, the Ben and Iris Margolis Foundation, and NIH grants R01 CA87785 and R01 CA134599.

Figure 2. Close-up pressure patterns at the focus for a) inhomogeneous breast model; b) inhomogeneous breast model using phase-corrected excitation; and c) water-only homogenous model. Each voxel is 0.5 x 1.0 mm.

P-110-BT

Tuesday
16 October 2012

Topic: Breast Tumors
Presentation Type: Poster

High-Frequency Ultrasound Mapping of Tumor Vascular Hypoxia As a Targeting Modality for Focused Ultrasound Ablation to Complement Ionizing Radiotherapy

Nathan Koonce[1], Xin Chen[2], David Lee[3], James Raleigh[4], Robert Griffin[1]

[1]University of Arkansas for Medical Sciences, Little Rock, Arkansas, United States
[2]Stanford School of Medicine, Palo Alto, California, United States
[3]Harvard Medical School, Belmont, Massachusetts, United States
[4]UNC School of Medicine, Chapel Hill, North Carolina, United States

Background/Introduction: The emergence of stereotactic radiotherapy (SRT) has led to studies investigating the impact of stromal sensitivity on therapeutic outcome in solid tumors. While there have been conflicting reports, blood vessel response to SRT appears to play a significant role in local tumor control. Hypoxia is a well-studied physiological barrier to radiation and chemotherapy and we hypothesize that vascular hypoxia attenuates SRT response and may play a crucial role in revascularization of recurrent tumors. A method to identify and destroy regions of vascular hypoxia in solid tumors with HIFU could reduce treatment times and greatly improve overall tumor control. Based on the idea that nitroimidazole, markers for hypoxia, produce detectable cell surface antigens on radiobiological hypoxic cells we report here our initial investigation of targeted microbubbles for detecting endothelial/blood adjacent cell hypoxia. From our results, we surmise that antibody-targeted high-frequency ultrasound mapping of endothelial/blood adjacent-hypoxia may be an improved approach for focused ultrasound ablation of these areas to complement radiation or chemotherapy. Our prior work on PET/MRI-guided focused ultrasound (PET/MRgFUS) with 18F- misonidazole for detection of regional tumor hypoxia and selective ablation of these areas proved that a rationale for combined HIFU and radiotherapy exists. However, this approach is inefficient in spatial resolution of tumor hypoxia and cumbersome for clinical translation.

Methods: Balb/c mice bearing 4T1 murine breast carcinoma tumors were subjected to 18MHz high-frequency ultrasound imaging of streptavidin target-ready microbubbles conjugated to biotinylated anti-pimonidazole antibody, MBpimonidazole, 2-3 hours following intraperitoneal injection of 75 mg/kg pimonidazole or saline for in vivo detection of binding specificity. In vivo targeted contrast agent was quantitatively correlated with pimonidazole antigen presence using Vevo CQ software.

Results and Conclusions: Perfused endothelial or other cells in contact with the circulation at levels of radiobiological hypoxia were detected with MBpimonidazole and the contrast mean power was found to be 17-fold higher than in negative control tumors (animals not injected with pimonidazole), mean±SEM (110.8±23.64 vs. 6.25±2.842, $p=0.0118$). Ongoing efforts are toward 3D contrast-enhanced ultrasound mapping of the MBpimonidazole binding pattern as a template for treatment planning with HIFU to destroy these areas. This study captures the first appraisal of non-invasive detection of tumor vascular hypoxia using targeted microbubbles and ultrasound contrast imaging providing an attractive treatment planning tool for focused ultrasound ablation as an adjuvant to chemo/radiotherapy.

Acknowledgements (Funding): Work supported by NCI/NIH CA44114 and FUSF

P-111-BT

Tuesday
16 October 2012

Topic: Breast Tumors
Presentation Type: Poster

MRI Based Heterogeneity Correction for Large Aperture HIFU Transducers

Mario Ries[1], Max Köhler[2], Julius Koskela[2], Matti Tillander[2], Chrit Moonen[1]

[1]University Medical Center Utrecht, Netherlands
[2]Philips Healthcare, Vantaa, Finland

Background/Introduction: The risk of undesired tissue damage to thoracic cage, heart and lung during MR guided HIFU ablations of breast tumors can be greatly reduced if a phased array transducer design with a lateral beam direction is used in combination with a large aperture.[1,2] However, such designs are intrinsically more susceptible to focus aberrations due to heterogeneous tissue within the beam path.

Recently, a compensation for these focus aberrations by combining high resolution MRI measurements of the tissue distribution with acoustic simulations of the propagation path has been suggested.[3] The result is a phase correction for each individual transducer element, allowing to reestablish the original form of the focal point.

The work presented here validates this compensation strategy with both acoustic simulations and pressure measurements on human breast-tissue samples.

Methods: A human breast tissue sample was placed asymmetrically in a Philips Sonalleve® breast HIFU-ablation system (Philips, Vantaa, Finnland), which is integrated in a clinical 1.5T Philips Achieva MRI (Philips, Best, The Netherlands). In order to evaluate the maximum dephasing of the transducer elements due to different propagation paths to the ablation area, a lateral water filled recess was created using a mylar film separation, as shown in figure a). High-resolution MRI images (3D T2-weighted gradient recalled fast field echo with a resolution of 0.8×0.8×0.9mm) were used to create a 3D description of the adipose tissue compartments within the HIFU beam path. Combined with celerity measurements similar to,[3] this allows to perform a simulation of the acoustic propagation of the waves from each individual transducer element and to estimate the resulting phase differences in the targeted focal spot. These are applied as corrections on the HIFU system during the actual ablation process. The results have been validated by direct acoustic measurements.

Results and Conclusions: Figure b) shows the pressure distribution of the focal point area in coronal direction if no aperture corrections are applied. Compared to an unobstructed sonication, the peak beam intensity is reduced by 50%. Although a simple two-fold power compensation can reestablish the original peak pressure intensity, the focal point area (FWHM) increases from initially 0.5x0.5mm2 to 1.2x3.1mm2 as shown in c). In comparison, a matching phase and amplitude correction based on acoustic simulations leads to the same peak pressure intensity, while maintaining the original focal point shape as shown in figure d).

Although the effectiveness of the proposed correction method is in practice limited by the spatial resolution of the MR images and the accuracy of the tissue celerity quantification, the presented first experiments under realistic conditions showed very encouraging results: An optimal focal point shape allows to increase ablation efficiency and thus to reduce the risk of undesired tissue damage in adipose tissue layers in the near-field. The proposed method is non-invasive and compatible with a standard interventional pre-planning and thus a step towards optimal treatment efficiency of MR-guided HIFU ablations in heterogeneous tissues such as the human breast. Future work includes an analysis of the required MR-resolution and accuracy of the tissue celerity on biological tissue samples.

Acknowledgements (Funding): The authors like to acknowledge the FUS Foundation for financial support.

References:

1. Moonen CTW et al. Berlin: Springer; 2006. p. 183-2000.
2. C. Mougenot et al., Large Aperture Transducer Designed for MR-HIFU Treatment of Breast Tumors. ISTU 2011
3. Mougenot C, et al. *Med Phys.* 2012 Apr;39(4):1936-45.

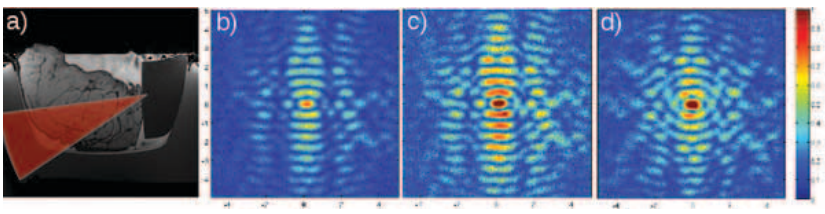

The MR-image (a) indicates the acoustic propagation path through the breast sample. (b) to (c) show the corresponding pressure map in the focal point area without correction (b), with a global amplitude correction (c) and with a matched phase and amplitude correction (d).

P-112-BT

Tuesday
16 October 2012

Topic: Breast Tumors
Presentation Type: Poster

New Nanodroplet Formulation Offers Enhanced HIFU Tissue Ablation Compared to Microbubbles

Linsey Phillips, Connor Puett, Paul Sheeran, Paul Dayton

[1]University of North Carolina, Chapel Hill, North Carolina, United States

Background/Introduction: We have developed a new low-boiling point perfluorocarbon emulsion composed of decafluorobutane (b.p.=2°C) and dodecafluoropentane (b.p.= 30°C) for enhanced thermal delivery during high intensity focused ultrasound (HIFU) ablation. Microbubbles are known to enhance thermal delivery, however they can shield energy deposition to deeper tissues, and are too large to extravasate. Our new nanodroplets are 240 +/- 65 nm in diameter, small enough to extravasate into tumor tissue, and are inherently more sensitive to ultrasound due to their low boiling point. We hypothesized that these nanodroplets would increase HIFU ablation lesions in tissue-mimicking phantoms compared to microbubbles or agent-free controls.

Methods: A 1:1 ratio nanoemulsion of decafluorobutane and dodecafluoropentane with phospholipid shells was generated by condensation. Mean nanodroplet size was 240 +/- 65 nm. Mean microbubble size was 2.1+/- 0.5 µm microbubbles or nanodroplets were added to individual albumin-acrylamide tissue-mimicking phantoms. Final concentration per phantom ranged from 2.5 x 104 to 2.5 x 107 per ml. Continuous wave HIFU was applied to phantoms by a focused 1 MHz array (TIPs, Philips). Phantoms were maintained at 37°C and sonicated at 4 MPa for 20 seconds. Acoustic pressure was varied from 2-4 MPa containing nanodroplets or microbubbles. Ellipsoid lesion volumes were calculated from lateral and axial dimensions measured by calipers. One-way ANOVA analysis was applied to compare lesion volumes over the range of droplet concentrations. T2-weighted magnetic resonance (MR) imaging was performed on phantoms pre and post ablation.

Results and Conclusions: HIFU lesion formation was visible by T2-weighted MR imaging (Figure-3) and ultrasound imaging (Figure-1). The addition of nanodroplets or microbubbles significantly increased the size of lesions in the phantoms in response to HIFU. Lesion size was highly dose dependent. Microbubbles, resulted in the formation of lesions at the surface of the phantoms away from the target site. Especially in high concentrations, microbubbles shielded deep lesion formation (Figure-1). Lesions in nanodroplet phantoms formed around the acoustic focus (Figure-2). Non-targeted lesion formation was not observed in the agent-free mold around the nanodroplet phantom indicating the absence of non-targeted heating. All other acoustic parameters being constant, equally sized lesions formed in nanodroplet phantoms (1e5 NDs per ml) at half the pressure (2MPa) compared to agent free phantoms (4MPa). This study demonstrates that our new nanodroplets containing a low boiling point PFC enhance HIFU ablation in a tissue mimicking phantom. Importantly, these agents induce targeted lesion formation at the site of interest while avoiding non-targeted heating.

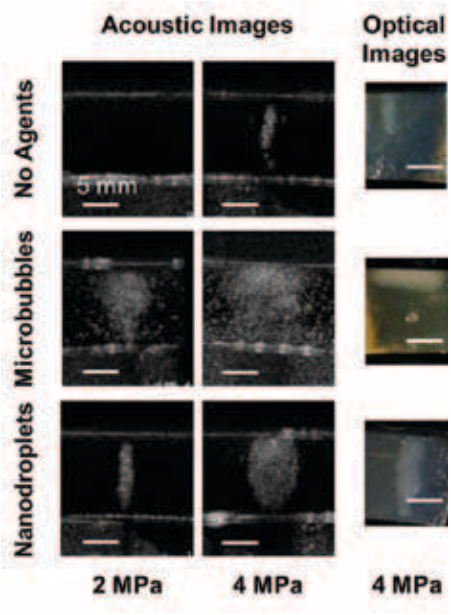

Figure 1. Acoustic and optical images of tissue mimicking phantoms containing no agents (control), microbubbles, or nanodroplets. Lesions formed in response to continuous wave HIFU for 20s at 1MHz using a peak negative pressure of 2 or 4 MPa (white scale bar = 5 mm).

Acknowledgements (Funding): Funding for this project is supported by an NIBIB grant # 1R21EB011704-01 to PAD, and an NIH postdoctoral fellowship to LCP.

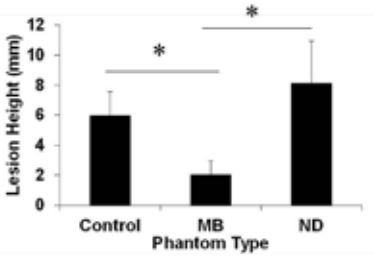

Figure 2. HIFU induced lesion volumes (mean Â± S.D., n ? 7) in albumin-acrylamide phantoms containing 2.5 to 10 Âµl of microbubbles (MB) or nanodroplets (ND).

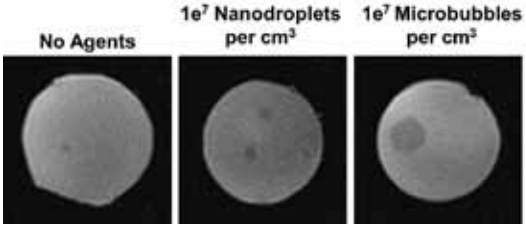

Figure 3. T2 weighted MR images of phantoms post HIFU (4MPa continuous 1MHz ultrasound for 20 seconds) ablation. One lesion was created in the agent-free and microbubble phantoms, while two are visible in the nanodroplet phantom.

P-113-BT

Tuesday
16 October 2012

Topic: Breast Tumors
Presentation Type: Poster

Partico-Kinetics and Drug Release Analysis of Nanoparticles for Image Guided FUS

Elena Rosca[1], Michael Wright[1], Andrew Miller[1], Wladislaw Gedroyc[2], Maya Thanou[1]

[1]King's College London, London, United Kingdom
[2]Imperial College London, London, United Kingdom

Background/Introduction: High Intensity Focused Ultrasound with Magnetic Resonance Guidance (MRgFUS) is a clinically used technique which has emerged recently as a treatment approach for several diseases. Due to its capability for precisely localized drug delivery (focal drug delivery) there has been a lot of interest in using FUS for targeted drug delivery. The success of this approach is highly dependent on the time when the temperature triggered activation is initiated and thus kinetic studies of the nanoparticles are absolutely essential. The success of this approach is highly dependent on the time when the temperature triggered activation is initiated and thus kinetic studies of the nanoparticles are absolutely essential. However, such investigations are not feasible with MRI due to its low sensitivity, thus we propose the use of optical imaging to determine the optimal time for the initiation of the focused ultrasound activation of drug release.

Methods: Temperature sensitive liposomes containing a unique Near Infrared (NIR) and DOTA (either with Gd3+ or with Eu3+) lipids are formed using the standard method of lipid film hydration followed by sonication and extrusion to create particles with diameters of130 nm. The liposomes were loaded with Topotecan via a pH gradient. The kinetic profile of the nanoparticles delivered via tail vein injections in SHO (SCID hairless outbred) mice was monitored using an in vivo imaging system (Maestro). Time course curves of the tumour accumulation were created from the quantification of unmixed images (images from which the background was subtracted). The drug release was studied by application of an external heat source and quantified by the fluorescence signal of the drug.

Results and Conclusions: The particles demonstrated very good short term stability at 37°C in high serum concentration (<10% release in 80% serum after 1 hour incubation) and relatively good long term stability (<45% release in 20% serum after 24 hours). Due to the strong NIR fluorescence profile in association with the multispectral analysis of the images it is possible to follow the particle kinetics immediately after intravenous administration and up to 28 hours post injection. Peak tumour accumulation of the particles was observed to occur between 5 to 10 hours post injection in IGROV?1 subcutaneous tumours. Ex-vivo biodistribution can also be quantified using the NIR signal and corroborated by time resolved fluorescence of Eu3+. Heating the tumour to 45°C using an external heat source (analogous to FUS-induced hyperthermia) for 5 min led to an increase in fluorescence intensity of the Topotecan 2 to 3 times over the signal of the unheated tumour. The significantly increased fluorescent signal indicates the rapid release of the drug at increased Temperatures.

In conclusion, most studies investigate tumour accumulation at 24 hours post injection which is not optimal. Our results show that nanoparticles accumulate in tumour to provide the maximum signal significantly earlier. Knowing these parameters will help designing the therapeutic MRgFUS scheme. Using fluorescent imaging tools we can study the effect of different parameters such as nanoparticle size, PEGylation, targeting moieties and tumour types on the kinetic profiles of particles to maintain focal drug delivery upon activation by FUS.

Acknowledgements (Funding): We thank the EPSRC for their support of this research.

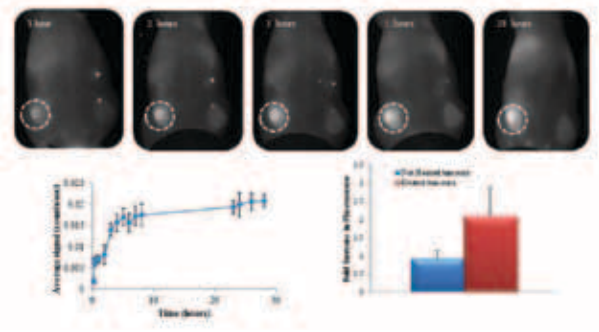

Time course of Nanoparticle accumulation in tumour along with quantification of accumulation and drug release upon heating

P-114-BT

Tuesday
16 October 2012

Topic: Breast Tumors
Presentation Type: Poster

Simultaneous Temperature Mapping in Fat and Aqueous Tissue Using 3D Hybrid PRF-T1 Technique During MRgHIFU

Mahamadou Diakite, Henrik Odeen, Nick Todd, Allison Payne, Dennis Parker

University of Utah, Salt Lake City, United States

Background/Introduction: Accurate temperature mapping in tumor and surrounding tissue throughout a thermal therapy procedure is essential to ensure the safety and efficacy of the treatment. MRI temperature imaging based on the water proton resonance frequency (PRF) work well in aqueous tissues. Unfortunately, the PRF shift with temperature does not apply to lipid protons, since there is no hydrogen bonding among the methylene protons that supply the bulk of the fat signal. However, the spin-lattice relaxation time, T1, has been found to obey a linear relationship with the temperature in a number of fatty tissues.[1] Here we present a sequence implementation for simultaneous 3D fat and water temperature imaging based on a Two Point Dixon (2PD) fat and water separation and the Variable Flip Angle (VFA) T1 mapping technique.[2]

Theory: A new 2PD hybrid PRF-T1 sequence was implemented from a 3D segmented Flyback EPI sequence. The sequence was implemented by alternating two flip angles (FAs) and two echo times (TE, TE+Δ) between measurements and every other two measurements respectively. TE and (TE+Δ) are the echo times when water and fat are in phase and out of phase, respectively. The two FAs were computed to minimize T1 variance as described previously.[3] The temperature maps are acquired in four measurements (Fig 1). The Water and Fat images were separated using the extended 2PD method[4-7] for both flip angles. The T1 map was computed using the fat only images at both FAs.

Methods: All MR imaging was performed using in-house built 4-channel RF receive surface coils on the Siemens TIM Trio 3T MRI scanner (Siemens Healthcare, Erlangen, Germany). Multiple HIFU heating experiments were performed on human breast fat embedded in ex vivo pork samples (Fig 2.a). The mixture of these tissues was used as a substitute for the human breast. Images were acquired with the 2PD hybrid PRF-T1 sequence throughout the heating and cooling of the sample. Acquisition parameters were: TR/TE/TE+Δ=40/14/15.1ms, 1.6X1.6X3.0 mm resolution, 8 slices, 128X64 image matrix, echo train = 9, FAs= 10?/49?, and scan time = 4.3 sec/measurement. To determine the correlation of T1 with temperature, a fiberoptic temperature probe (OpSens, Inc, Quebec, Canada) was positioned near the focal zone.

Figure 1. Schematic diagram of the simultaneous fat and water temperature imaging using the Two Point Dixon Hybrid PRF-T1.

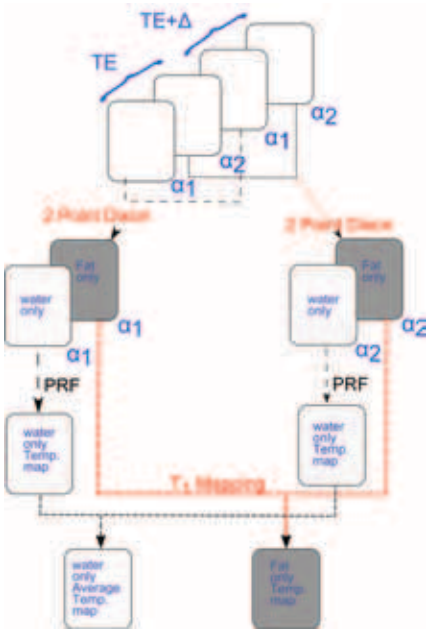

Results and Conclusions: Although not currently practical for clinical applications due to the long acquisition time (16 sec for one complete fat/water temperature map), the proposed technique shows the capability of determining temperature in mixed tissue (fat+water) over a 3D volume. To reduce the acquisition time, a parallel imaging method (GRAPPA) is being implemented on the 2PD hybrid PRF-T1 sequence. With an appropriate multi-element RF coil, GRAPPA can reduce the acquisition time by 4 or more without sacrificing accuracy of the temperature maps. Results from GRAPPA+2PD hybrid PRF-T1 will be presented in future work.

Acknowledgements (Funding): This work was supported by the Ben B. and Iris M. Margolis Foundation, Siemens Medical Solutions, and NIH grants R01CA134599 and R01EB013433.

References:

1. Hynynen et al. *MRM* 43(6):901-4 (2000).
2. Deoni et al. *MRM* 49:515-526 (2003).
3. Diakite et al. Poster 1768, *ISMRM*, Montreal, Canada.
4. Coombs et al. *MRM* 38(6):884-9 (1997).
5. Skinner et al. *MRM* 37(4):628-30 (1997).
6. Xiang et al. *MRM* 56(3):572-84 (2006).
7. Schmidt et al. *JMRI* 27(5):1122-9 (2008).

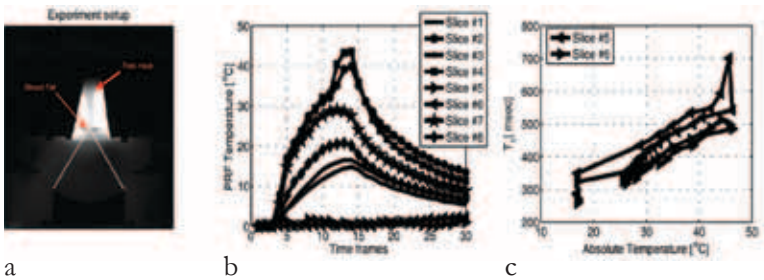

a b c

Figure 2. a. Experimental setup. b. PRF temperature profile of the water based tissue (pork) over a 2x2 ROI chosen in all slices at the center of the focal zone. c. Absolute T1 as a function of absolute temperature over a 2x2 ROI chosen in Fat near the tip of the temperature probe. During the heating T1 increased linearly with temperature (dT1/dT= 8.7ms/?C).

P-115-EA

Tuesday
16 October 2012

Topic: Emerging Applications
Presentation Type: Poster

Displacement Sensitivity Analysis Of Shear Wave Propagation Introduced By A Transient High Intensity Focused Ultrasound Using A Gradient Echo Sequence

Jiming Zhang[1], Pei-Herng Hor[1], Raja Muthupillai[2]

[1]University of Houston, Houston, United States
[2]St. Luke's Episcopal Hospital, Houston, United States

Background/Introduction: MR elastography is based on the excitation of a mechanical motion and the subsequent measurement of the shear waves velocity in biological tissue (1). By applying a displacement-encoding gradient (DEG), the local displacement of the tissues was recorded as the accumulated phase in the complex MR signal. In order to accurately estimate the shear wave velocity, displacement map at different phase shifts between the DEG and the excited mechanic motion needs to be acquired so as to track the shear wave propagation. In the case of shear wave excited by a transient high intensity focused ultrasound (t-HIFU) the displacement sensitivity (Accumulated phase divided by instantaneous displacement) will change at different phase shift. However the displacement sensitivity was normally assumed to be constant. This work will demonstrate the reconstruction of the displacement wave propagation by applying a dynamic displacement sensitivity function.

Methods: All experiments were performed on a 1.5T MR scanner equipped with a 256 channel spherical shell HIFU transducer (Sonalleve, Philips).

MRI Data acquisition: A phase contrast based gradient-echo pulse sequence was modified to include motion-sensitizing gradients between the RF excitation pulse and the spatial encoding gradients. MR acquisition parameters were: voxel size: 2.0 x 2.5 x 7 mm3; FOV: 180 x 180 mm2; TR/TE/flip angle = 29 ms/18 ms/12°; bandwidth: 110 Hz/pixel; scan time: 4.4 s. The duration and gradient strength of the symmetric bipolar motion encoding gradient (MEG) was 8 ms and 28.6mT/m. A coronal slice bisecting the plane of the HIFU focus was imaged, and the displacement encoding direction was set perpendicular to the slice-select direction.

HIFU- MRI scanner Interface: The scanner triggers the HIFU device to emit a 4 ms, 250W burst of ultrasound (1.2 MHz) focusing at 6.7 cm within a gel phantom. A phase shift (t) at 0.4 ms intervals between the application of HIFU and motion encoding gradient captured wave propagation. (Figure 1)

Data Analysis: 1) Construct a phase difference image from the two sets of raw data (acquired with opposing polarities of displacement encoding gradient) after correcting for the background phase; 2) Calculate the displacement sensitivity at different phase shift based on the given displacement encoding gradient and the t-HIFU excitation; 3) Reconstruct the displacement map at different phase shift by applying dynamic displacement sensitivity.

Results and Conclusions: The acquired phase maps at phase shift of 0.1 ms (Left) and 1.3 ms (right) were shown in Figure 3. The displacement sensitivity function of phase shift was shown in Figure 2. By using different displacement sensitivity at different phase shift, the reconstructed displacement maps were shown in Figure 4. The displacement map at low displacement sensitivity was very noise and was not reliable.

The results from this preliminary study demonstrate that the displacement sensitivity needs to be dynamically considered in tracking the displacement wave at different phase shift. This method provides a foundation for optimizing the MR motiong encoding gradient at different phase shift for transient MR elastography.

Acknowledgements (Funding): This study was partly funded by Ronald MacDonald fund at St. Luke's Episcopal Hospital and Texas Center for Superconductor at University of Houston, and research support from Philips.

(See figures, next page.)

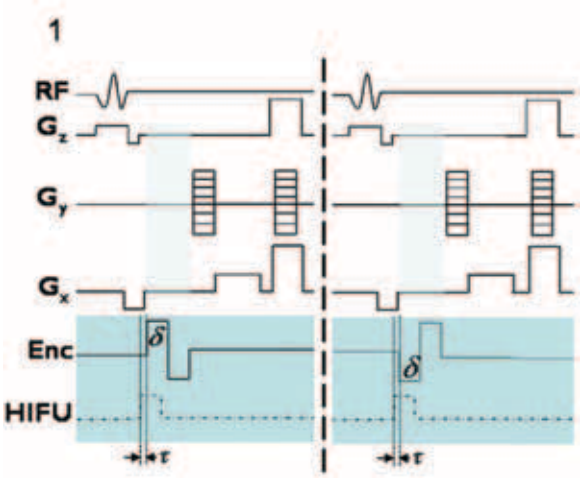

Figure 1. The MRI pulse sequence with displacement encoding gradients

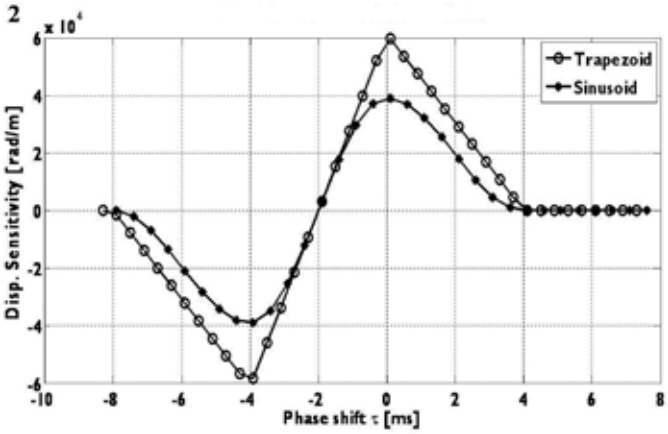

Figure 2. Displacement sensitivity of different phase shift using bipolar trapezoid and sinusoid displacement encoding gradients

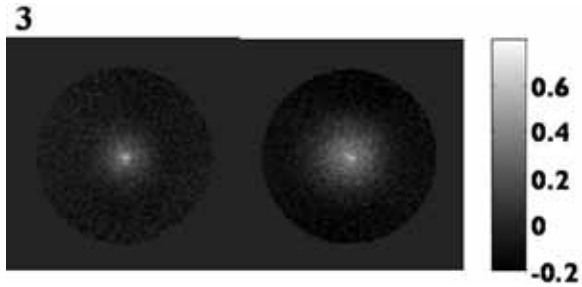

Figure 3. Accumulated phase [rad] at two different phase shift 0.1 ms (Left) and 1.3 ms (right) between the t-HIFU excitation and bipolar DEG

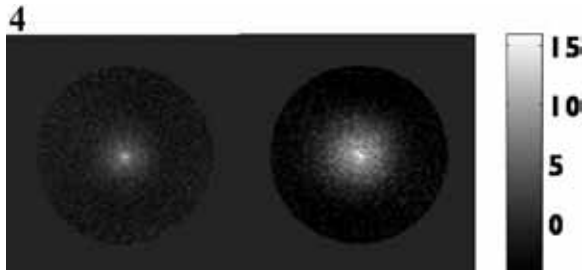

Figure 4. Reconstructed displacement map at two different phase shift of 0.1 ms (Left) and 1.3 ms (right) by applying the corresponding sensitivity function

P-116-EA

Tuesday
16 October 2012

Topic: Emerging Applications
Presentation Type: Poster

Effects of MRI Contrast Agents During HIFU Ablation Therapy

Nicole Hijnen[1], Aaldert Elevelt[2], Holger Gruell[2]

[1]Eindhoven University of Technology, Eindhoven, Netherlands
[2]Philips Research, Eindhoven, Netherlands

Background/Introduction: MR contrast agents, such as Gd-DTPA, are used to improve tumor delineation for diagnosis and treatment optimization. The use of a Gd-contrast agent in combination with HIFU ablation was avoided due to safety concerns. Therefore we investigated the use of Gd-DTPA shortly prior MR-HIFU thermal ablation therapy with respect to transmetallation, trapping and long term deposition of gadolinium (Gd) in the body. As an addition we investigated the effect of a Gd-DTPA on the accuracy of temperature mapping sequences.

Methods: The stability of Gd-DTPA at temperatures (T = 37°C, 65°C, 80°C) relevant for HIFU ablation therapy was investigated in vitro using a transmetallation assay. Potential trapping, dechellation, and long term retention of Gd was investigated in vivo by conducting MR-HIFU ablation treatment on both rat muscle and subcutaneous tumor (9L glioma) using a clinical 3T MR-HIFU system. A human equivalent dose of Gd-DTPA (0.6 mmol/kg bw) was injected via a tail vein catheter just prior ablation (≤ 5 minutes). Before and after therapy, R1-maps of the target location were acquired. Animals were sacrificed 2 hours or 14 days post injection (n = 4 per group, 40 animals total) and Gd-content in the tissue and carcass was determined using Inductively Coupled Plasma techniques (ICP).

The effect of Gd on the accuracy of temperature mapping was assessed by monitoring the temperature measurement error in correlation with the change in contrast agent concentration.

Results and Conclusions: In vitro, the amount of dechelated Gd3+ was dependent on the temperature. Temporal trapping of Gd-DTPA in the coagulated tissue was observed on R1 maps acquired within two hours after ablation, an effect confirmed by ICP analysis (3 times more Gd3+ was found in the treated muscle volume than in control muscle tissue). Two weeks after therapy, the absolute amount of Gd3+ present in the coagulated tissue was low. There was no significant increase in Gd-content in the principal target organs for translocated Gd3+ions (liver, spleen and bone) between the HIFU and sham treated animals and an in vivo relaxivity of 4.6 mmol-1s-1 was found in the HIFU ablated volume. Both results indicate intact Gd-DTPA.

A linear relation between the variation in contrast agent concentration and temperature measurement error was observed, ranging from 0-5°C when using human equivalent doses.

In conclusion, MR-HIFU treatment does not increase the transchellation of Gd-DTPA. In small tissue volumes, no significant effect on the long-term in vivo Gd retention was found. However, care must be taken with the use of PRFS based MR thermometry for HIFU guidance in combination with Gd3+, as the susceptibility artifact induced by Gd3+ can severely influence treatment outcome.

Acknowledgements (Funding): This research was supported by the Center for Translational Molecular Medicine (Volta)

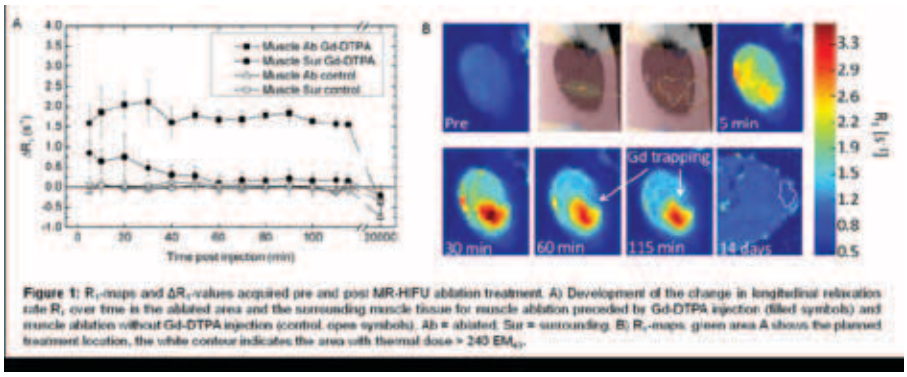

Figure 1: R_1-maps and ΔR_1-values acquired pre and post MR-HIFU ablation treatment. A) Development of the change in longitudinal relaxation rate R_1 over time in the ablated area and the surrounding muscle tissue for muscle ablation preceded by Gd-DTPA injection (filled symbols) and muscle ablation without Gd-DTPA injection (control, open symbols). Ab = ablated, Sur = surrounding. B) R_1-maps, green area A shows the planned treatment location, the white contour indicates the area with thermal dose > 240 EM_{43}.

P-117-EA

Tuesday
16 October 2012

Topic: Emerging Applications
Presentation Type: Poster

Effects of Using MR Thermometry for Estimation of HIFU SAR, Beam FWHM, and Tissue Thermal Diffusivity

Christopher Dillon, Nick Todd, Joshua de Bever, Allison Payne, Dennis Parker, Douglas Christensen, Robert Roemer

University of Utah, Salt Lake City, Utah, United States

Background/Introduction: Recent work has shown that a new analytical method for obtaining HIFU SAR patterns from experimental temperature data is significantly more accurate than the traditional linear method and promises to be a valuable tool in improving SAR predictive software.[1] This method estimates the maximum focal SAR, the lateral full width at half maximum (FWHM) of the HIFU beam, and the thermal diffusivity (K) of the tissue, important parameters for planning and control of thermal therapies. Although magnetic-resonance temperature imaging (MRTI) during therapies is extremely valuable, random and systematic errors in MRTI temperature measurements may propagate into temperature-based estimations of tissue properties and treatment parameters. This study presents simulation and experimental results assessing the effects of MRTI noise, temporal averaging, and spatial averaging on HIFU temperature measurements and SAR, FWHM, and K estimates.

Methods:

Simulations: SAR was simulated using the Hybrid Angular Spectrum technique[2] for several focal zone sizes. High resolution temperatures were then calculated with a finite difference solver and used as input for MRTI simulation code that included various levels of zero-mean noise (STDV=0 to 2 deg C), temporal averaging (tacq=1 to 8 s), and spatial averaging (Res=0.5 to 2.0 mm isotropic).[3] For each set of MR parameters, SAR, FWHM, and K were estimated from a fit to the simulated temperature versus time curves in a 3x3 or 7x7 voxel region centered on the beam axis.

Experiments: HIFU heating experiments were performed in ex vivo pork loin. Temperatures were acquired using MRTI with varying degrees of noise, temporal averaging, and spatial averaging. SAR, FWHM, and K were estimated in each case using temperature data from a 7x7 voxel region centered on the beam axis.

Results and Conclusions: The simulation study showed that under noisy conditions, the interquartile range of maximum SAR, FWHM, and K estimates was reduced by up to 50%, 85%, and 80%, respectively, by fitting a 7x7 voxel region when compared to fitting a 3x3 voxel region. Simulated temporal averaging caused small changes in temperature values (<2% change) and estimates of SAR (<5% change), FWHM (<1% change), and K (<5% change). Simulation results also demonstrated that a spatial resolution with voxel size of 1x1x3 mm3 or smaller (1x1x1 mm3 for isotropic voxels (see figure)) is required to keep errors in temperature and all estimations less than 10%. Preliminary experimental results verify the conclusions of the simulation study, namely that fitting to a larger voxel region mitigates noise effects, temporal averaging effects are relatively small, and spatial resolution plays a major role in the accuracy of MR temperatures and estimates of SAR, FWHM, and thermal diffusivity.

Acknowledgements (Funding): The authors gratefully acknowledge support from Siemens Healthcare AG, the FUS Foundation, the Ben and Iris Margolis Foundation, and NIH grants R01 CA87785, R01 EB013433, and R01 CA134599.

Spatial averaging effects on simulated (a) MR temperatures and (b) maximum SAR, (c) FWHM, and (d) K estimates for isotropic voxel dimensions and several beam sizes.

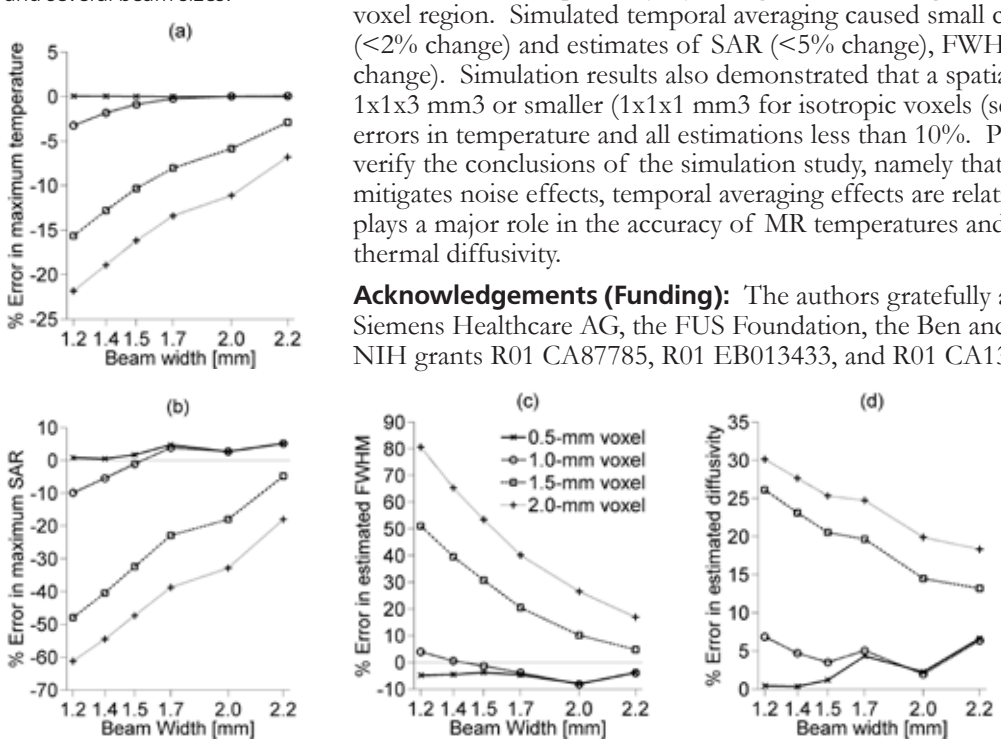

References:

1. Dillon et al 2012 *Phys Med Biol* 57 4527-44
2. Vyas and Christensen 2012 *IEEE Trans Ultrason Ferroelectr Freq Control* 59 1093-100
3. Todd et al 2011 *Magn Reson Med* 65 515-21

P-118-EA

Tuesday
16 October 2012

Topic: Emerging Applications
Presentation Type: Poster

Enhanced Delivery With MRI-Guided Pulsed Focused Ultrasound: Lessons in Translation From a Rabbit Model

Brian O'Neill[1], Howard Vo[1], Christof Karmonik[1], King Li[2]

[1]The Methodist Hospital Research Institute, Houston, Texas, United States
[2]Wake Forest School of Medicine, Winston-Salem, North Carolina, United States

Background/Introduction: Pulsed focused ultrasound treatment has been successfully applied as a means of enhancing targeted drug delivery in murine tumor models. There are challenges, however, with interpreting those results due to the dominant role played by the boundary conditions in the acoustical, thermal, and mechanical physics of such a small tissue volume. In this study, translational research using MR thermometry-guided focused ultrasound for targeted drug delivery in rabbit muscle was performed to develop a new understanding of the mechanism behind this effect and to find a practical approach for clinical translation.

Methods: Thigh and calf muscles of female New Zealand White rabbits weighing 3 to 4 kg were treated as a model of bulk tissue. Drug uptake was modeled by uptake of Gd-based MR contrast agent following treatment. FUS power, duty cycle and treatment duration were varied to generate different levels of thermal and mechanical energy deposition, with peak power varying from 10-277W, duty cycle from 0.7-100 % at a repetition rate of 1 Hz, and treatment length from 20-600s per sonication. Temperature was monitored during treatment using MR thermometry, and thermal dose calculated from treatment temperature profiles. Changes in T2-weighted and contrast-enhanced (CE) MR signal were assessed immediately following treatment and again at later times between 12 and 48 hrs. Over 200 sonications were performed in 25 animals. To avoid any possibility of lingering effects, each leg was treated once. Following euthanasia, legs were collected for histology. Evan's Blue dye injection prior to euthanasia assisted in marking treatment locations.

Results and Conclusions: Contrary to earlier conclusions from mouse studies, the only achievable effect in bulk tissue with these parameters was thermal in nature. For sonications lasting 1-2 minutes, peak temperatures of 49.4-52.5 ºC gave the greatest probability of an enhanced delivery effect without significant thermal necrosis. A positive result was visible as edema on T2-weighted MR images immediately after treatment. However, the peak of MR contrast uptake appears between 12 and 36 hrs, and was driven largely by an acute inflammatory response. These results suggest improved local contact between drug and cells is achieved in terms of both temporal and spatial distribution. Although the details may vary, we believe this general approach will work consistently for a variety of tissues, and may therefore be used to improve drug delivery to solid tumors in humans.

Acknowledgements (Funding): This work was funded by NIBIB grant R01 EB009009.

P-119-EA

Tuesday
16 October 2012

Topic: Emerging Applications
Presentation Type: Poster

Feasibility Studies of Organ Ablation by MR-Guided Focused Ultrasound on Ex-Vivo Kidney Model

Timur Saliev, Ioannis Karakitsios, Sarfraz Ahmad, Helen McLeod, Stewart Fleming, Andreas Melzer

University of Dundee, Dundee, United Kingdom

Background/Introduction: The data of UK statistics demonstrate that 19 new kidney cancer cases have been registered for every 100,000 males and more than 11 for every 100,000 females (crude incidence rate) (Office for National Statistics on request, UK. October 2011). MRI-guided ultrasound therapy has been considered as an alternative to classic methods of cancer treatment, particularly for tumours of a kidney. It provides an opportunity of ablation of malignant tissues in non-invasive and highly controllable manner. Despite those obvious advantages, this method requires an optimization as to become a standard modality for cancer treatment in hospitals. The purpose of this work was to examine the response of kidney tissue on applied high acoustic energies under MR-guidance. The kidney organ model was represented by explanted Thiel-embalmed kidney from human cadaver and non-embalmed animal kidney (porcine). The Thiel embalming is a novel method for post-mortem preservation of body's life-like properties (Thiel, W. Ann Anat 174(3): 185-195, 1992). It makes a cadaver an excellent model for medical training purposes, particularly for minimally invasive interventions. It has been hypothesized that Thiel embalming process results in changing chemical / physical properties of the tissue. Those changes might effect on tissue response to ultrasound propagation and finally on heating effect. To scrutinize this assumption, the sonicated tissues were subjected to histological analysis. Besides of Thiel-embalmed kidney, the porcine explanted kidney was exploited for validation of the response of intact tissue on high intensity ultrasound.

Methods: The explanted kidney has been placed in the sonication chamber. The size of the chamber: 20 x 20 cm and depth 6 cm. It has aperture on the bottom (11.4 x 10.4 cm) covered by polyethylene film (thickness 60 microns). As to provide a proper interface between organ and ultrasound transducer the solid Gel Pad has been placed on the bottom of the chamber (Gel Pad UF 25 mm, ASM000352, Insightec Ltd). The kidney has been fixed to the Gel Pad by wooden sticks for stabilization. Then the chamber has been filled with degassed water and covered by acoustic absorber as to avoid the formation of standing waves and backscattering of the ultrasound beam. The kidney was scanned on MR machine (Signa HDx 1.5 Tesla, GE Healthcare) by using the following parameters: TE 80.9, TR 2300, Bandwidth 31.3 KHz. The sonication was performed by MR-guided High Focused Ultrasound machine (ExAblate 2000 UF system, InSightec, Israel). After planning MR-scanning and defining regions of the treatment, the tissue was ablated by ultrasound at high acoustic powers. The 2 sonication areas were chosen in renal medulla region (on MR coronal images). The scheme of sonication set-up is given in Figure 1.

After MR-guided sonication, the explanted kidney (both: from human cadaver and porcine one) was subjected to biopsy for further histological analysis.

Results and Conclusions: First sonication spot was treated with acoustic energy 1064 Joules and total sonication time was 120 sec. The ultrasound frequency was the same for all treatments as 1.15 MHz. In the first focal point the temperature rise was observed at the focal point with maximal peak at 640 C (SD±1). The second sonication was performed on another region with the same acoustic energy 1064 Joules, but the treatment time was doubled (240 sec). In this spot the highest temperature was detected as 65.40 C (SD±1). Despite of continuous sonication of the same area the maximal temperature did not exceed 65.40 C, which might be associated with high level of detected cavitation events. It has been thought that the inertial cavitation leads to formation gaseous micro-bubbles, which are responsible for deflection and attenuation of ultrasound signal (Nyborg 2006; Ashokkumar, Lee et al. 2010; Stride and Coussios 2010).

The sonication of Thiel embalmed explanted kidney by HIFU did not result in ablation of the tissue. This might indicate that Thiel solution changed the morphology and structure of the tissue and made it irresponsive to applied acoustic energy. These results do agree with data of histological analysis of sonicated Thiel-embalmed kidney tissue, where signs of the ablation were not detected. The basic concept of HIFU ablation is an induction of severe

intracellular and extracellular protein denaturation and loss of molecular structure. But the process of embalming tissue in Thiel solution may lead to irreversible morphological changes in the cells, which make impossible to elicit protein denaturation by applied high acoustic energy.

In opposite to the results from Thiel embalmed kidney, the samples from ablated porcine kidney demonstrated evident signs of tissue disruption triggered by ultrasound (Fig.2 A, B).

The results suggest that the level of tissue ablation directly correlates with the time of treatment, where elongated sonication would be more effective for therapy.

The histological data from explanted animal kidney model clearly indicate the feasibility of ablation of the kidney tissue by high focussed ultrasound. These findings demonstrate the potential of MR-guided ultrasound surgery as a modality for non-invasive cancer treatment of abdominal organs.

Acknowledgements (Funding): 1) Project FUSIMO ("Patient specific modelling and simulation of focused ultrasound in moving organs"), funded under the EU's Seventh Framework Programme for Research and Technological Development.

2) Fellowship from Focused Ultrasound Surgery Foundation.

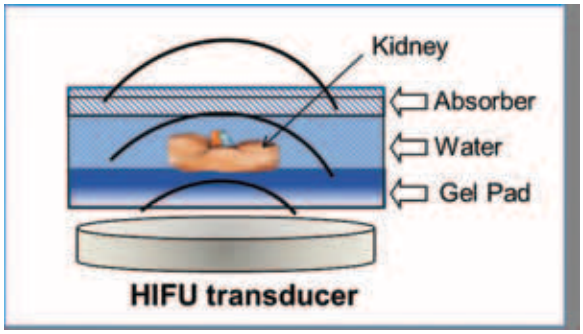

Figure 1. Schematic draw of sonication set-up

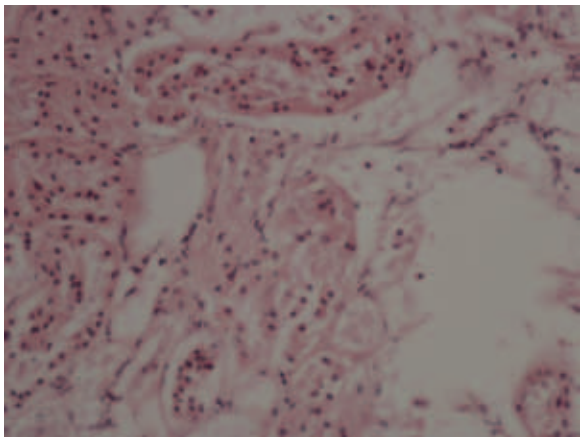

Figure 2. Disruption of kidney tissue caused by high focused ultrasound. A) Sonication time 120 sec

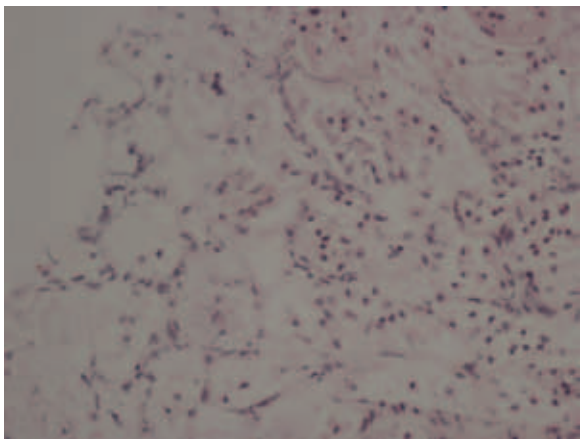

Figure 2. Disruption of kidney tissue caused by high focused ultrasound. B) Sonication time 240 sec

P-120-EA

Tuesday
16 October 2012

Topic: Emerging Applications
Presentation Type: Poster

HIFU-Induced Localized Hyperthermia Further Enhances Anticancer Efficacy of Systemic Doxorubicin Than Conventional Hyperthermia: Experimental Study Using SCC-7 Xenograft Model in Mice

Sun Young Chae[1], Young-sun Kim[2], Min Jung Park[2], Hyunchul Rhim[2], Jung Hee Lee[2], Hyo Keun Lim[2]

[1]SAIHST, Sungkyunkwan University, Seoul, South Korea
[2]Samsung Medical Center, Seoul, South Korea

Background/Introduction: Hyperthermia is known to enhance chemotherapeutic efficacy by raising tissue temperature to 42~43 degree C. However, existing conventional hyperthermia using nonspecific external heat source is not clinically useful due to excessive body temperature elevation. Therefore, the need for hyperthermia localized to cancer has arisen, which could be realized by HIFU (high-intensity focused ultrasound). The purposes of this experimental study were to assess technical feasibility of HIFU-induced localized hyperthermia and to evaluate enhancement of anticancer efficacy of systemic doxorubicin(DOX) by HIFU-induced localized hyperthermia(HH) as compared to that by conventional hyperthermia(CH).

Methods: For in-vitro test, DOX(4microgram/ml) uptakes into SCC-7(mouse squamous cell carcinoma) cells were qualitatively compared between 37 degree C and 42 degree C by measuring fluorescence using a confocal microscopy. SCC-7 cells were subcutaneously injected into the thigh area of Balb/c-nude mice to form 7-8mm tumors. For in-vivo test, the mice were randomly classified into one of control (n=8), CH(n=6), HH(n=6), DOX-alone(n=8), CH+DOX(n=5), or HH+DOX(n=7) group. CH and HH was induced by merging the tumor into warmed water(42 degree C, for 5min prewarming+10min hyperthermia) and the preclinical animal HIFU system (for 10min/spot, 4 spots; TIPS, Philips Healthcare), respectively. HIFU parameters were optimized in an iterative manner and temperature changes in the tumor were verified with direct measurements using a thermocouple. DOX(1mg/kg, IV) was administrated before each treatment. Tumor growth curve of each group was compared. Coagulation necrosis in the tumor was assessed with TTC stain.

In vitro test, confocal microscopic fluoroscence intensity by intranuclear uptake of DOX was more prominent at 42 degree C than 37 degree C in a time-dependent manner.

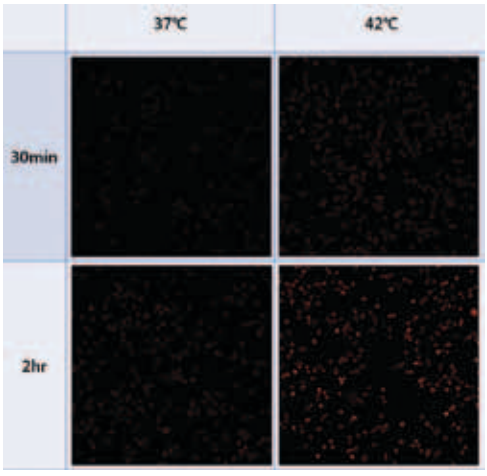

Results and Conclusions: In in-vitro test, the intensity of fluorescence by intranuclear uptake of DOX was more prominent at 42 degree C than 37 degree C in a time-dependent manner. The optimal parameters of HIFU sonications were found to be frequency=1MHz, PRF=5Hz, power=12W, duty cycle=50%, and spacing=3mm that reached the equilibrium (42-43 degree C) at 60sec. In in-vivo test, HH+DOX group (relative volume: 5.95±1.0) showed the most prominent tumor growth suppression as compared to all the other groups (control, 17.6±2.1; CH, 16.4±1.5; HH, 17.8±2.6; DOX-alone, 14.3±0.9; CH+DOX, 13.3±1.5) ($p<0.05$). There was no intra-tumoral coagulation necrosis or procedure-related complication.

In conclusion, HIFU was able to safely induce hyperthermia localized to the tumor, which enhanced anti-cancer efficacy of systemic doxorubicin further than conventional hyperthermia did.

Acknowledgements (Funding): This study was supported by the Basic Science Research Program through the National Research Foundation of Korea (NRF) funded by the Ministry of Education, Science and Technology (#2011-0006504)

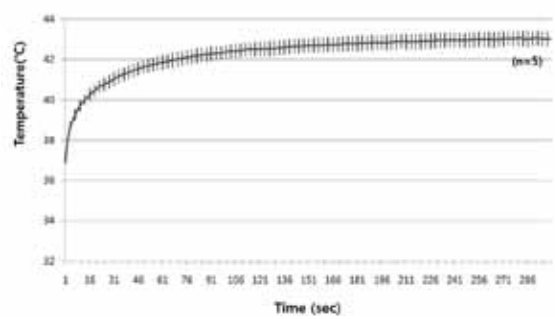

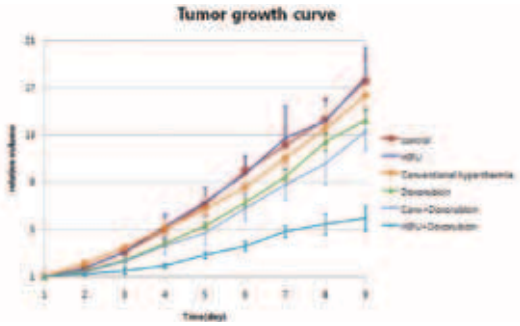

Left: In vivto test, Intratumoral temperature changes using optimized HIFU parameter which was directly measured by a thermocouple.

Right: In vivo test, tumor growth curves after systemic doxorubicin therapy with or without conventional or HIFU-induced hyperthermia

P-121-EA

Tuesday
16 October 2012

Topic: Emerging Applications
Presentation Type: Poster

Imageable Nanoparticles for Magnetic Resonance Guided Focused Ultrasound Targeted Drug Delivery in Tumours.

Roman Gonitel[1], Michael Wright[2], Karen Shaw[2], Gavin Kenny[2], Elena Rosca[2], Maya Thanou[2], Wladislaw Gedroyc[1]

[1]Imperial College London, London, United Kingdom
[2]King's College London, London, United Kingdom

Background/Introduction: Failure to successfully treat a range of cancers stems from a direct relationship between the effective dose to eliminate cancer cells and the unspecific action of the anticancer agents that compromises the organism. A solution would be to deliver the anticancer agents locally to the tumour cells while limiting their bioavailability at any other sites in the body. To this purpose, the field of non-invasive Magnetic Resonance-Guided Focused Ultrasound (MRgFUS) has emerged which aims to combine inducible release drug carriers and FUS protocols which allow concentration of the therapeutic agents in the vicinity of the tumour.

Liposomal nanoparticles have been designed to date, which combine their thermosensitive properties and high intensity focused ultrasound (HIFU) to enable local drug delivery. An incorporated contrast agent would facilitate the visualisation of nanoparticles in vivo and application of the releasing HIFU "trigger" at the optimal time to make the drug maximally available to the cancerous cells and minimally available elsewhere. Further, due to the accumulation of the nanoparticles in the tumours, the contrast agent would allow detection and delimitation of the tumour size allowing a finer targeting of drug release. Here we report the design and development of such nanoparticle using Gd3+-labeled lipid for MRgFUS drug delivery.

Methods: Liposomes were prepared with commercially available phospho- and lyso-lipids having Gd-DOTA-DSA (1,4,7,10-tetraazacyclododecane-1,4,7,10-tetraaceticacid-N,N-Distearylamidomethylamine and DSPE-PEG (1,2-distearoyl-sn-glycero-3-phosphoethanolamine-N-[amino(polyethylene glycol)-2000, loaded with or without Gadovist®(Bayer). Nanoparticle relaxivity and release behaviours were described using a 9.4T MR system (Bruker), and an ICP/MS technique, using Elan ICP/MS system (Perkin Elmer).

Results and Conclusions: Designed formulation showed to be thermosensitive at 42oC while having robust stability at lower temperatures in different environments, including high serum concentrations. Gd3+-labeled lipid nanoparticle and liposomes encapsulating Gadovist® showed equivalent levels of R1 relaxivity to liposomes encapsulated Gadovist® (R1=0.3) and T1 shortening (both at ~1.85s for 1mg/ml lipid concentration) at 37oC. We further present data on the optimisation and the effect of targeted HIFU thermosensitive nanoparticle application in cancer. In conclusion we have designed a novel nanoparticle that is tractable by non-invasive methods and is capable of delivering drugs . This nanoscale liposomal technology will prove useful for a variety of applications of both medical and research purposes.

Acknowledgements (Funding): The work was funded by EPSRC.

P-122-EA

Tuesday
16 October 2012

Topic: Emerging Applications
Presentation Type: Poster

In Situ Produced Microbubbles via a Microfluidic Device for Enhanced Drug Delivery

Adam Dixon, Ali Dhanaliwala, Johnny Chen, Alexander Klibanov, Brian Wamhoff, John Hossack

University of Virginia, Charlottesville, Virginia, United States

Background/Introduction: The application of intravascular ultrasound (IVUS) to circulating microbubbles (MBs) in vivo enhances drug delivery to the vessel wall. In this framework, drug-loaded MBs are administered intravenously and subjected to an enhanced level of ultrasound via an IVUS catheter to achieve focal delivery. Unfortunately, MBs administered via systemic injection undergo rapid clearance from the blood stream, which limits drug concentration at the location of interest. To address this limitation, we propose the production of MBs directly within the vasculature by developing microfluidic devices that fit within the tip of a catheter and can produce MBs in real-time. By placing the catheter at the location of interest, MBs and drug are more likely to reach their intended target, thereby reducing the amount of drug that must be administered to a patient to achieve an effective dose. Here we demonstrate enhanced drug delivery to cells in vitro under flow by applying ultrasound to MBs produced in real-time by a microfluidic device.

Methods: Cell culture: Rat aortic smooth muscle cells (SMCs) were plated on coverslips and allowed to reach confluency for all in vitro experiments. Microfluidic device: Microfluidic devices were fabricated using poly-dimethyl-siloxane (PDMS) cast from a custom photoresist (SU-8) mold. The liquid phase, consisting of PEG40-stearate, glycerol, and propylene glycol dissolved in phosphate buffered saline (PBS), focuses a gas stream of nitrogen within the microfluidic device to continuously produce MBs (Fig 1b). Drug delivery: SMCs and the microfluidic device were placed in a parallel plate flow system to mimic arterial flow (Fig 1a). Calcein, a model drug that only enters permeabilized cells, was co-injected while MBs were produced. 1 MHz ultrasound was applied by a single-element transducer at peak negative pressures between 10 and 200 kPa.

Results and Conclusions: The microfluidic device produced 18 μm diameter MBs at a production rate of 330,000 MB/s. This production rate is several orders of magnitude larger than has been previously achieved with microfluidic devices and is sufficient to provide acoustic contrast immediately without additional concentration. Consistent calcein delivery was achieved when ultrasound was applied at peak acoustic pressures between 20 and 200 kPa (Figure-1c). Less calcein was delivered under flow conditions, suggesting that MB throughput, drug concentration, and ultrasound parameters must be optimized to enhance delivery. We demonstrate delivery of a model drug to SMCs using MBs produced by a microfluidic device in situ. By fabricating MBs at the catheter tip, we are able to achieve highly localized drug delivery to SMCs without the loss of drug associated with systemic injection. Future studies will replace calcein with drugs in order to observe a therapeutic effect following drug delivery.

Acknowledgements (Funding): This work was supported by National Institutes of Health NHLBI RO1HL90700.

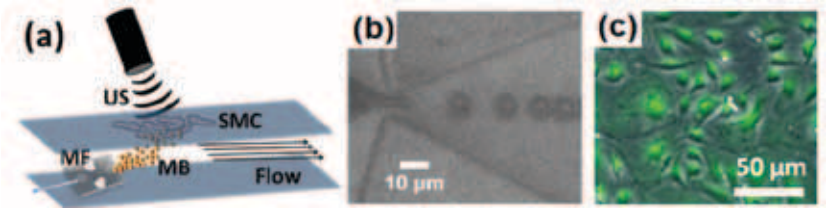

Figure 1. a) Schematic of the microfluidic device (MF) dispensing MBs and calcein within the parallel plate flow system. MBs are insonated near the SMC surface via a single element transducer (US) to enhance calcein delivery. b) High-magnification image of a microfluidic device producing MBs. c) Calcein delivery (green fluorescence) to SMCs within the parallel plate flow system.

P-123-EA

Tuesday
16 October 2012

Topic: Emerging Applications
Presentation Type: Poster

Intravascular Microbubble-Based Drug Delivery With Ultrasound

Joseph Kilroy, Alexander Klibanov, Brian Wamhoff, John Hossack

University of Virginia, Charlottesville, Virginia, United States

Background/Introduction: Lipid-shelled microbubbles (MBs) have demonstrated potential as drug delivery vehicles. Despite this potential, the application of MBs is constrained by anatomic barriers to ultrasound propagation (e.g. lung and bone). We propose combining intravascular ultrasound (IVUS) and MBs to achieve localized image-guided therapy in regions of the body otherwise inaccessible to ultrasound. A compact low frequency, high power, multifunction IVUS transducer capable of MB displacement, destruction / delivery, and imaging has been designed to provide localized MB therapeutics within the body. Our long-term goal is to provide localized delivery of antiproliferative agents following percutaneous transluminal angioplasty to prevent vessel restenosis and thereby overcome some of the limitations of drug eluting stents (drug fixed during initial design, fixed dosage, incomplete vessel wall coverage, etc.)

Methods: Finite element analysis was performed to optimize the dimensions of a high power piezoceramic transducer. Following IVUS characterization, drug delivery capabilities were tested by delivering calcein, a membrane impermeable fluorophore, to rat aortic smooth muscle cells (SMCs) cultured in Opticells. After co-injecting MBs (15x106/mL) and calcein (40 μg/ml), SMCs were treated with IVUS (center frequency (fc) = 5 MHz, Peak Negative Pressure (PNP) = 1.3 MPa, pulse repetition frequency (PRF) = 1-10 kHz). An acoustic radiation force (ARF) pulse (fc = 5 MHz, 40 cycle length, PNP = 600 kPa, PRF = 5 kHz, 1 min treatment) was applied to MBs flowing through a vessel phantom (diameter = 4.5 mm) at 100 mm/s - comparable to coronary flow - to evaluated ultrasound displacement of MBs. MBs carrying DiI, a lipid fluorescent dye, were drawn through an excised porcine artery at a rate of 95 ml/min. MBs were displaced (fc = 5 MHz, 40 cycle sine, PNP = 150 kPa, PRF = 4 kHz, 90 s treatment) then destroyed (fc = 5 MHz, 5 cycle sine, PNP = 1 MPa, PRF = 10 kHz, 90 s treatment) using IVUS. Following treatment, arteries were imaged en face to localize DiI delivery.

Results and Conclusions: A subdiced, 220 μm thick piezoceramic device with an fc = 6.9 MHz, a -6 dB fractional bandwidth = 60%, and an outer diameter of 1 mm was fabricated. The device successfully imaged a wire target. Fluorescence microscopy images indicated localized calcein delivery to SMCs only in ultrasound exposed regions (Fig 1A, green fluorescence). Ultrasound image intensity following microbubble infusion and ARF indicated localized microbubble accumulation in the flow phantom due to the IVUS (Fig 1B-C). Microscopy videos collected during IVUS insonation verified microbubble destruction at PNPs as low as 600 kPa. Finally, fluorescence microscopy images indicated localized DiI delivery only in ultrasound exposed regions of ex-vivo arteries treated with ultrasound and microbubbles under physiological flow conditions (Figure 2).

Acknowledgements (Funding): University of Virginia Biotechnology Grant T32 GM08715, US National Institute of Health NHLBI R01 HL90700

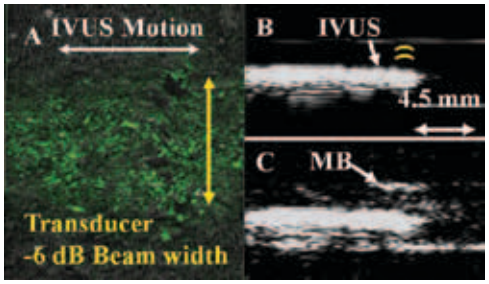

Figure1. A) Microscope image of in-vitro calcein delivery to rat SMCs in an Opticell using an IVUS transducer. B) Transcutaneous image of an IVUS transducer in a wall less flow phantom before microbubble infusion. C) Transcuatenous image of IVUS transducer in a wall less flow phantom channel following microbubble infusion and IVUS transmission.

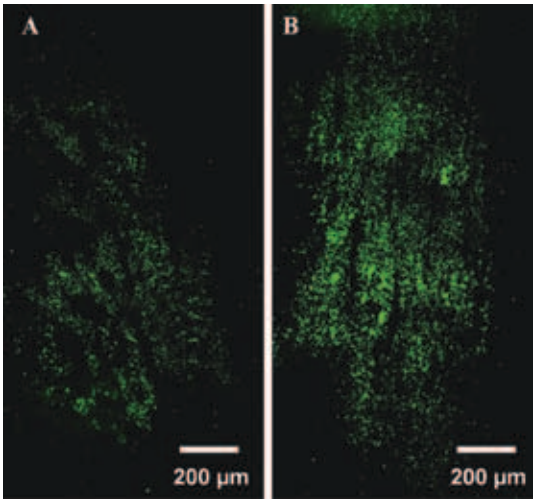

Figure 2. Microscope images collected following IVUS delivery of DiI microbubbles to an ex-vivo porcine artery. A) Top of artery following DiI delivery. B) Bottom of artery following DiI delivery.

P-124-EA

Tuesday
16 October 2012

Topic: Emerging Applications
Presentation Type: Poster

MatMRI+MatHIFU: Toolboxes for Real-Time Monitoring and Control of MR-HIFU

Samuel Pichardo[1], Tony Sinclair[1], Benajmin Zaporzan[1], Charles Mougenot[2], Ari Partanen[3]

[1]Thunder Bay Regional Research Institute, Thunder Bay, Canada
[2]Philips Healthcare, Toronto, Canada
[3]Philips Healthcare, Bethesda, Maryland, United States

Background/Introduction: Availability of open tools is a key feature to facilitate the development of pre-clinical research of Magnetic Resonance-guided High Intensity Focused Ultrasound (MR-HIFU). Development of pre-clinical set-ups for MRI and MR-HIFU research require often custom modifications that may not be compatible with clinic installations. Because the complexity of installations and limited access to technical support, acquisition of real-time data is not always ensured when new imaging techniques are being tested.

MatMRI is a toolbox that allows direct communication with a Philips MRI scanner in a Matlab environment, which is well-known in many laboratories. MatMRI performs real-time acquisition of magnitude and phase images that can be processed to estimate changes of temperature. Available functionality of MatMRI includes acquisition of individual slices and volumetric data. Analogously to MatMRI, MatHIFU is a toolbox for the control of the Philips Sonalleve MR-HIFU system. MatHIFU allows the execution of user-defined treatment protocols intended for applications such as thermal ablation or drug delivery.

Methods: MatMRI was based on the official tool for MRI data-dumping made by Philips Healthcare. Multi-threading capabilities were added to maximize real-time processing performance. Basic use of MatMRI involves four basic steps: initiate communication, subscribe to MRI data, query for new images and unsubscribe. If required, MatMRI can also pause/resume the MRI scanner and update on real-time the location and orientation of the images. MatHIFU performs the execution of protocols and allows real-time monitoring. Basic use of MatHIFU requires also four steps: preparation of protocol, initiate communication, execute protocol and monitor the state of execution

Results and Conclusions: MatMRI was integrated into existing software used to control a table designed for animal experimentation (FUS Instruments, Canada). The integration in the existing software was seamless and delivered real-time estimation of changes of temperature in a mouse model. Using MatHIFU and MatMRI, a complete new interface to control the Sonalleve system was developed to perform in vivo experiments allowing adapted conditions for the experimental model. Dynamic control of the HIFU system was added as functionality allowing the test of new control algorithms intended for hyperthermia applications.

MatMRI and MatHIFU leverage considerably the existing multi-million dollar investments by research centres and hospitals done in MRI and MR-HIFU infrastructure. These tools reduce the complexity required to conduct pre-clinical research and does not require any non-standard modification to the MRI and MR-HIFU installations, which simplifies the use of these tools in installations running a clinic operation. MatMRI simplifies considerably the efforts required to perform real-time measurements of MR data and its possibilities are beyond thermal applications including opportunities for motion tracking or MR-based elastography. MatHIFU facilitates the exploration of new therapeutic applications using the Philips MR-HIFU Sonalleve system by allowing execution of user-defined protocols and dynamic control of the HIFU hardware. Both matMRI and matHIFU are aimed to be freely available to other research groups under coordination of Philips Healthcare.

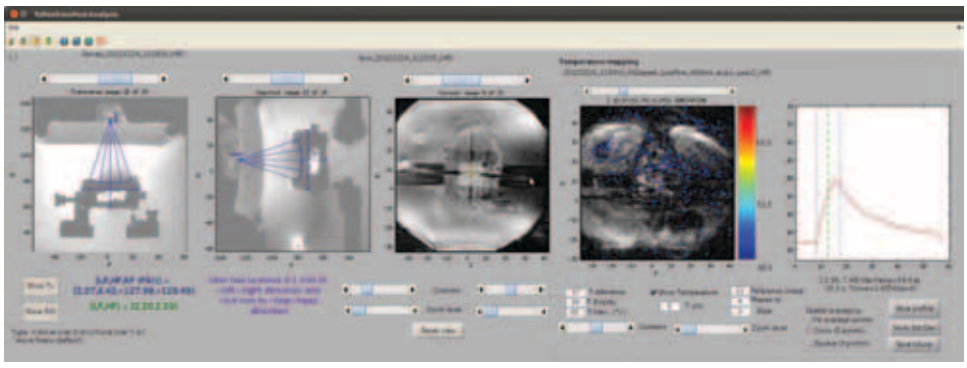

Example of use of MatMRI for the control of HIFU delivery. A graphic user interface was built to collect M2D sequences intended for positioning of a therapy transducer related to a target in a mouse flank. Once correct positioning is ensured, dynamic sequences are collected to reconstruct thermometry maps while HIFU is being delivered.

P-125-EA

Tuesday
16 October 2012

Topic: Emerging Applications
Presentation Type: Poster

MRI Compatible versus Safe HITU Transducers

Kyle Morrison[1], George Keilman[1], Ian Rivens[2], John Civale[2], Victoria Bull[2], Gail ter Haar[2]

[1]Sonic Concepts, Inc., Bothell, Washington, United States
[2]Institute of Cancer Research : Royal Marsden NHS Foundation Trust, London, United Kingdom

Background/Introduction: Magnetic resonance imaging (MRI) has become a predominant imaging modality in managing thermal effects introduced by high intensity therapeutic ultrasound (HITU). Obvious measures must be considered in eliminating ferrous materials into the magnetic field when developing any MRI Safe HITU transducer. In addition to being safe, an MRI Compatible HITU transducer must avoid signal loss and image distortion around the transducer placed within a magnetic resonance field. Susceptibility artifacts enhance image cloudiness around the transducers radiating surface and can compromise evaluating thermal effects.

Methods: Both gradient echo localizer and basic spin echo MR sequences have been performed on various mechanical structures to observe how a material's composition and shape can distort images in either case. Results indicate that a material's composition and shape present artifacts independent from one another; therefore both variables were treated separately in optimizing a susceptibility artifact-free transducer.

Results and Conclusions: The presented MRI Compatible transducer design and fabrication maintains 75% electrical to acoustic conversion efficiency, normally handling up to 150 Watts Continuous (CW) Power Acoustic Output at its fundamental resonance. The MRI Compatible transducer performs electrically different than an MRI Safe transducer and both configurations should be carefully considered for each specific study. Both MRI transducer designs are used in single element and array configurations up to 1024 elements ranging between 500 kHz and 5 MHz. MRI compatible temperature monitoring, water cooling and matching network components are integrated into all MR Compatible and Safe configurations while offering operation at each transducer's 3rd harmonic resonance.

Various materials susceptibility findings have provided useful results in optimizing passive cavitation detector, pulse-echo transducer and hydrophone designs for use in a magnetic resonance field.

Future work leads us to improving electrical shielding and electrical operating band uniformity of the MR Compatible HITU transducer without introducing susceptibility artifacts.

P-126-EA

Tuesday
16 October 2012

Topic: Emerging Applications
Presentation Type: Poster

Mri-Compatible Sectored Cylindrical Array for Spatially-Controlled Intracavitary Ultrasound Hyperthermia of Recurrent Rectal Cancer

Robert Staruch[1], Rajiv Chopra[2], Kullervo Hynynen[1]

[1]Sunnybrook Research Institute, Toronto, Canada
[2]UT Southwestern, Dallas, Texas, United States

Background/Introduction: Management of advanced rectal cancers includes radiation and chemotherapy prior to surgical tumor excision. Often there is recurrent disease in the rectal wall or in the pelvic floor after primary treatment. There is clinical evidence that hyperthermia combined with radiation could improve outcomes for patients with recurrent rectal cancers.

Previous studies have shown that intracavitary ultrasound heating applicators can be used to create a conformal region of mild heating in the prostate, through the use of multi-element heating applicators with independent power and frequency control.[1] With MRI-compatible devices, real-time MR thermometry can be used to monitor and control ultrasound output such that a desired region of heating is achieved and no thermal damage to surrounding organs is experienced.[2] Here we present an MRI-compatible transrectal ultrasound transducer consisting of a 12 element sectored cylindrical array capable of achieving spatially controlled heating of the rectal wall and surrounding tissue.

Methods: The array is based on the intracavitary ultrasonic applicators developed by Diederich[1] and Smith[2] for prostate hyperthermia. It was constructed using outwards-emitting half-cylindrical sections of PZT-4 material (15 mm OD, 15 mm length). Each section was sectored into three channels by scoring the inner electrode using a diamond wire saw. Four sections were arranged end-on-end and glued together using silicone to produce a 12-channel array that was then glued into an Ultem chassis. The 12 elements were individually powered and matched at 1.615 MHz. Acoustic coupling was achieved by circulating degassed water through a latex sheath sealed to the device.

MR compatibility and the ability to achieve spatially controlled heating in an ex vivo bovine tissue sample were assessed in a clinical 3T imager. Device localization was achieved using T2-weighted fast spin echo images, and tissue heating was monitored by PRF shift MR thermometry using a fast SPGR sequence.

Results and Conclusions: Figure 1 depicts a longitudinal T1-weighted image of the device positioned for sonication in an ex vivo tissue sample, demonstrating its MR compatibility. Figure 2 depicts temperature maps demonstrating spatially controlled temperature elevations of 5 to 8 degrees C. Figures 2 and 3 demonstrate the longitudinal and axial heating pattern of a single element driven at 4W of electrical power. The axial image in Figure 4 demonstrates the ability to modulate the spatial heating pattern around the device, by driving two of three elements in one half-cylindrical section at 5.5W, while the third element was driven at 0W.

We are developing an MRI-compatible intracavitary hyperthermia device for the treatment of recurrent rectal cancer. Here we have demonstrated its MR compatibility and ability to modulate spatial heating patterns in tissue.

References:

1. Diederich and Hynynen. *Med Phys* 1990.
2. Smith et al. *Int J Rad Oncol Biol Phys* 1998.

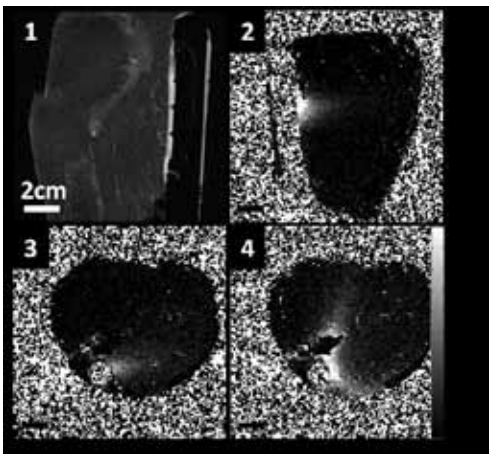

MR images of MRI-compatible transrectal ultrasound array. 1: T1-weighted FSE image, 2-4: temperature maps calculated from FSPGR images during ex vivo ultrasound heating. Scale bar, 2 cm.

P-127-EA

Tuesday
16 October 2012

Topic: Emerging Applications
Presentation Type: Poster

Multiple-Focus Strategy for Volume Ablation Using Dual Mode Ultrasound Array (DMUA) Systems: Uniform Tissue Ablation in a Fraction of the Time

Islam Shehata, John Ballard, Andrew Casper, Erik Cressman, Emad Ebbini

University of Minnesota, Cairo University, Minneapolis, Minnesota, United States

Background/Introduction: One of the key advantages of HIFU is the ability to create small, precise and trackless lesions noninvasively. However, to create larger volumes such as those required to ablate body tumors, stacking of single lesions is necessary to create uniform volume ablation. Unfortunately, such a procedure is a lengthy one and is a main limitation towards the wide clinical acceptance of HIFU in fibroid and oncological applications. We investigate the feasibility of using a double focus strategy to construct volume ablation in-vitro and report how adoption of this strategy can reduce the total ablation time when compared to conventional single focus strategy.

Methods: Fresh bovine heart tissue blocks were degassed and held in degassed water (23 °C) opposite a 3.5 MHz, 64-element fenestrated DMUA (Imasonic, France) with a diagnostic imaging probe confocally aligned in the central coaxial fenestration. Two strategies for volume ablation at a depth of about 12 mm were used and compared. For the single focus strategy, a grid of 4 X 8 points was targeted using raster scan of single focus patterns (1.25 sec, ~ 5600 W/cm2). As an example of multiple focus strategy, the single focus pattern was replaced by a double focus pattern, ± 2 mm laterally from the geometric focus. The 4 X 8 grid was targeted using 16 double foci shots (2.75sec, ~ 2400 W/cm2). Inter-lesion spacing and waiting time between shots was fixed for both strategies at 1 mm and 1 min. Tissue samples were cut immediately after each experiment; photographs of grossly ablated tissue were taken and compared.

Results and Conclusions: Localized volumetric lesions without significant cavitation were formed by both strategies. The extent of the thermal damage along the elevation and lateral axes was found to by about 4.5 x 8 mm and 4.5 x 9 mm for the single and double focus strategies, respectively. Furthermore, the total ablation time (exposure + waiting) was 31 min and 40 sec for the single focus whereas it was reduced to 15 min and 44 sec for the double focus strategy. No gaps were seen throughout the volume produced with the double focus strategy but small gaps were observed in the single focus case. During therapy with either technique, no significant echogenic changes were detected by conventional B-mode imaging.

Results clearly demonstrate the feasibility of using a double focus strategy for uniform volume ablation. Using the double focus strategy allowed for a significant (~ 50%) reduction in total ablation time when judged against the single focus strategy for comparable size ablated volume. As such, the double focus strategy, and a multiple focus strategy in general, can be valuable to reduce the time required for HIFU therap.

Acknowledgements (Funding): Grant from the Institute for Engineering in Medicine (IEM) at the University of Minnesota. The authors would like to acknowledge Dalong Liu for his efforts.

P-128-EA

Tuesday
16 October 2012

Topic: Emerging Applications
Presentation Type: Poster

Numerical and Experimental Evaluation of a Novel Ultrasonic Transducer for Superficial Tumor Ablation

Adamos Kyriakou[1], Esra Neufeld[1], Duo Chen[2], Eduardo Moros[2], Niels Kuster[1], Gal Shafirstein[3]

[1]IT'IS Foundation/BIWI/ETHZ, Zurich, Switzerland
[2]University of Arkansas for Medical Sciences, Little Rock, Arkansas, United States
[3]Roswell Park Cancer Institute, Buffalo, New York, United States

Background/Introduction: Thermal ablation of solid malignancies is being performed with energy sources such as microwaves and laser. All these modalities, however, are invasive, as they require percutaneous access to the tumor. Focused Ultrasound (FUS) is an alternative method in which the ultrasonic beams propagate through tissues and create a sharply defined focus in the tumor causing coagulation necrosis without harming the overlying or surrounding tissues.

Numerous parameters, such as bone structures, air cavities, transducer positioning and the focus steering pattern, can affect ultrasonic ablation and determine the success of the therapy. A software tool that simulates the propagation of ultrasonic waves in complex scenarios is needed to understand and optimize treatment. A novel numerical framework was developed to analyze a prototype of a novel, line-focused, ultrasonic transducer (SonoKnife) for the ablation of superficial tumors.

Methods: The software framework includes explicit linear and nonlinear acoustic solvers (parallelized for CPU and GPU systems). Thermal solvers for modeling ultrasound induced temperature increase and lesion formation were also developed and can be coupled with the acoustic solvers. Numerical studies on the interactions between ultrasonic waves and biological tissues can be performed with this framework by running 3D simulations of full wave propagation in inhomogeneous anatomical models.

Numerical simulations of the SonoKnife in homogeneous and inhomogeneous (layered) tissue setups were performed with FOCUS and the new framework for a wide range of frequencies. Hydrophone measurements of the US field were conducted inside a water-tank. Additionally, 3D acoustic and thermal simulations of a detailed anatomical model with an inserted tumor in the vicinity of the neck were performed (not feasible with FOCUS).

Results and Conclusions: The pressure fields from the FOCUS simulations and the hydrophone measurements were compared with the full wave simulations using the Gamma dose distribution comparison method and by comparing the acoustic focus characteristics. Good agreement of the focus size and shape as a function of frequency was obtained. The Gamma method revealed differences in the sub-maxima of the pressure field predictions of the two numerical approaches. Further measurements are required to elucidate these differences.

A novel software platform for effectively simulating full wave propagation in complex anatomical models with a resolution better than 0.1mm was developed, integrated in a flexible framework and validated. SonoKnife, a novel transducer used for superficial tumor ablation was evaluated with the software tool in realistic setups. Powerful simulation tools will help to optimize therapy outcomes and understand the importance of the various parameters in relevant clinical scenarios.

Acknowledgements (Funding): This study was supported by the Swiss National Center of Competence in Research (NCCR), NCI RC1 CA147697, NSF (EPS-0918970) and ASTA (G1-35321).

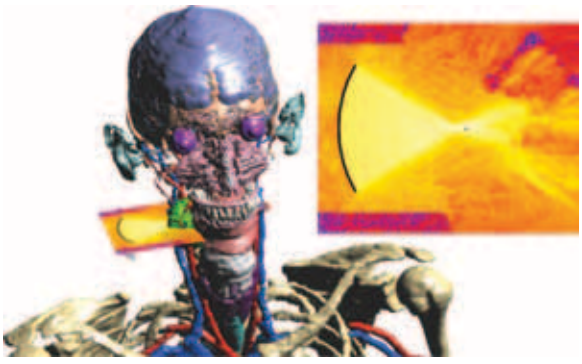

Simulated 3D model of a patient with a squamous cell carcinoma (bright green object) in the neck area ablated with the SonoKnife (a novel HIFU transducer for superficial tumor ablation). The full model and the resulting pressure distribution are shown on the left. The pressure distribution on a plane through the center (marked with a point in the distribution) of the tumor is displayed on the right to show the impact of bone structures (e.g. vertebrae) and air-filled cavities (e.g. internal air in the trachea and esophagus).

P-129-EA

Tuesday
16 October 2012

Topic: Emerging Applications
Presentation Type: Poster

Physical Properties of an Egg White-Based Blood Mimicking Fluid

Yunbo Liu, Subha Maruvada, Keith Wear, Bruce Herman, Gerald Harris

Food and Drug Administration/CDRH/OSEL/DSFM, Silver Spring, Maryland, United States

Background/Introduction: An egg white-based blood mimicking fluid (BMF) was developed and characterized as a blood coagulation surrogate for the acoustical and thermal evaluation of therapeutic ultrasound, especially high intensity focused ultrasound (HIFU) devices.

Methods: Physical properties, including coagulation temperature, frequency-dependent attenuation, sound speed, thermal conductivity and thermal diffusivity, were measured as a function of temperature (20 - 95°C). The fluid viscosity was quantified at room and body temperature. With the addition of Nylon particles in the solution, the backscattering coefficient of the BMF was measured and compared before and after a complete thermal coagulation.

Results and Conclusions: For a 30s thermal exposure, the egg white-based BMF (3 mm thickness) started to denature at 65°C and coagulate into an elastic gel at 85°C. The coagulation temperature can be lowered by adding a small amount of acid solution to the BMF. The temperature-dependent ultrasound attenuation and other physical parameters were found to be similar to the reported values of blood. These properties make this egg white-based blood mimicking fluid a useful tool for pre-clinical bench testing of therapeutic ultrasound devices.

P-130-EA

Tuesday
16 October 2012

Topic: Emerging Applications
Presentation Type: Poster

Pulsed Focused Ultrasound (pFUS) Is a Nondestructive Modality That Provides "Tunable" Control Over Targeted Homing of Mesenchymal Stem Cells (MSC) and Endothelial Precursor Cells (EPC)

Scott Burks, Ali Ziadloo, Saejong Kim, Joseph Frank

National Institutes of Health (NIH) Clinical Center, Bethesda, Maryland, United States

Background/Introduction: While stem cell (SC) therapies have shown promise, cell homing to pathological loci following systemic infusion is extremely inefficient (<1-3% injected dose). Circulating stem cells home by tethering to activated endothelium and actively transmigrating into the parenchyma in response to cytokine/chemokine and trophic factor (CCTF) gradients. pFUS treatment to skeletal muscle drives a transient and local molecular biological response, likely through mechanotransduction, which mimics transient inflammatory profiles that can attract circulating MSC. Our objectives were to further characterize, histologically and with molecular biological assays, the nondestructive nature of pFUS and whether enhanced homing permeability and retention (EHPR) of MSC and other stem cell types could be targeted by pFUS. We also investigated if the EHPR effect could be fine-tuned using pFUS (i.e. whether additional sonication/injection treatments had cumulative effects on cell homing).

Methods: Murine hamstring skeletal muscle was sonicated (1 MHz, 40 W, 5% duty cycle, 1 Hz repetition frequency) without microbubbles. For cell injections, human MSC or CD34+/CD133+ EPCs were iv injected 2 hr after pFUS. Mice were treated over the course of 3 days with combinations of pFUS and SC injections spaced 24 hrs apart. Tissues were harvested for physiological, histological, and molecular analyses.

Results and Conclusions: Mice were given single or multiple treatments (every 24 hr for 3 days) of pFUS alone (no cells). Both exposure courses were nondestructive to skeletal muscle and did not induce hemorrhage, necrosis, or apoptosis. Mast cell proliferation or degranulation was not detected and pFUS did not activate Pax7, a transcription factor necessary for muscle repair. pFUS elicited a small, predominately M2 anti-inflammatory macrophage response. However, both single and multiple pFUS treatments created short-lived local increase in several CCTFs and cell adhesion molecules (CAMs) that mediate stem cell homing. Accordingly, both MSC and EPC exhibited an EHPR effect in greater numbers following a single pFUS treatment. pFUS targeting of cells (MSC or EPC) is also tunable—when pFUS/cell treatments were repeated daily over 3 days, the EHPR effects of the SCs were significantly increased compared to muscle receiving only a single treatment of pFUS/cells (Fig 1). Furthermore, if pFUS and SC are given on the 1st day, but only iv cells on days 2 and 3 (no pFUS), additional increases in homing were not observed, suggesting additional pFUS treatments are required to achieve a compounded EHPR effect.

pFUS can noninvasively and nondestructively direct SC migration in vivo. Presumably through mechanotransduction, pFUS drives a local, transient, and generic biological response creating a "molecular zip code" that can be capitalized on to target delivery of multiple SC types to different tissues. This molecular zip code has increased CCTF and CAMs such that the number of cells homing to targeted tissue can be increased through repeated sonications coupled with SC injection. This approach of modifying local host tissue rather than the cell product creates a readily translatable approach to improve efficiency and efficacy of many cellular therapies.

Acknowledgements (Funding): This work was funded by the Intramural Research Program at the National Institutes of Health Clinical Center and National Institute of BIomedical Imaging and Bioengineering.

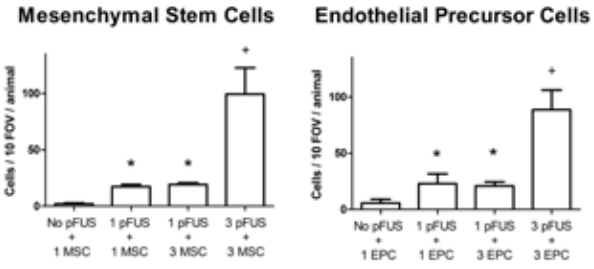

Figure 1. Human MSC and EPC were detected in pFUS-treated murine skeletal muscle by immunohistochemistry. Increased numbers of cells were observed in pFUS-treated muscle following a single course of pFUS/cell treatment. Additional increases in cell numbers were observed when pFUS/cell injections were performed daily for 3 days. However, additional cell injections after only a single pFUS treatment failed to increase cell homing to treated tissue. Statistical significance ($p < 0.05$) is denoted by * and + (n=3-4 mice per group).

P-131-EA

Tuesday
16 October 2012

Topic: Emerging Applications
Presentation Type: Poster

Reduction of Peak Acoustic Pressure and Shaping of Heated Region by Use of Multi-Foci Sonications in MR-Guided High-Intensity Focused Ultrasound Mediated Mild Hyperthermia

Ari Partanen[1], Matti Tillander[2], Pavel Yarmolenko[3], Bradford Wood[3], Matt Dreher[3], Max Köhler[2]

[1]Philips Healthcare, Bethesda, Maryland, United States
[2]Philips Healthcare, Vantaa, Finland
[3]National Institutes of Health, Bethesda, Maryland, United States

Background/Introduction: Ablative hyperthermia (>55°C) has been used as a stand-alone treatment for solid tumors, whereas mild hyperthermia (40–45°C) has been shown to be an effective adjuvant for both radiotherapy and chemotherapy. An optimal mild hyperthermia treatment is spatially accurate, with precise and homogeneous heating limited to the target region and with a low likelihood of unwanted thermal or mechanical bioeffects (tissue damage, vascular shutoff). In a mild hyperthermia setting, a sonication approach utilizing multiple concurrent foci may have the benefit of reducing acoustic pressure in the focal region (leading to reduced or no mechanical effects), while providing better control over the heating. The objective of this study was to design, implement and characterize a multi-foci sonication approach in combination with an MR-HIFU mild hyperthermia heating algorithm, and compare it to electronic sweeping of a single focus sonication method using a clinical MR-HIFU system.

Methods: Simulations (acoustic and thermal) and measurements (acoustic, with needle hydrophone) were performed. In addition, performance of multi-foci and single focus sonications was compared using a clinical MR-HIFU platform in a phantom (target diameter=4–16mm), in a rabbit thigh muscle (target diameter=8mm), and in a Vx2 tumor (target diameter=8mm). A binary control algorithm was used for real-time mild hyperthermia feedback control (target range=40.5–41°C). Data were analyzed for peak acoustic pressure and intensity, temperature accuracy (mean), homogeneity of heating (standard deviation [SD], T10 and T90), diameter and length of the heated region, and thermal dose (CEM43).

Results and Conclusions: Simulations (not shown) and hydrophone measurements (Figure-1) showed significantly lower (reduction to 33%) peak acoustic pressures within the target region with multi-foci heating compared to the single focus approach. In a rabbit Vx2 tumor, both single and multi-foci heating approaches were accurate (mean=40.82±0.12°C [single] and 40.70±0.09°C [multi]) and precise (SD=0.65±0.05°C [single] and 0.64±0.04°C [multi]), producing homogeneous heating (T10-T90=1.62°C [single] and 1.41°C [multi]) (Figures 2 and 3). Multi-foci sonications resulted in significantly shorter heated regions in beam path direction (35% reduction, $p<0.05$, Tukey). Energy efficiency was lower for the multi-foci approach. Similar results were achieved in phantom and rabbit muscle heating.

A multi-foci sonication approach was combined with a mild hyperthermia heating algorithm, and implemented on a clinical MR-HIFU platform. This approach resulted in accurate and precise heating within the targeted region with significantly lower acoustic pressures and better spatial control over heating compared to the single focus sonication method. Reduction in acoustic pressure and improvement in spatial control suggest that multi-foci heating may be beneficial in mild hyperthermia applications for clinical oncology.

Acknowledgements (Funding): The authors thank Dr. Caitlin Burke, Dr. Ashish Ranjan, Dr. Carmen Gacchina and David Woods for their support with animal studies. This research was supported by the Center for Interventional Oncology and Intramural Research Program of the National Institutes of Health, and through a Cooperative Research and Development Agreement with Philips Healthcare.

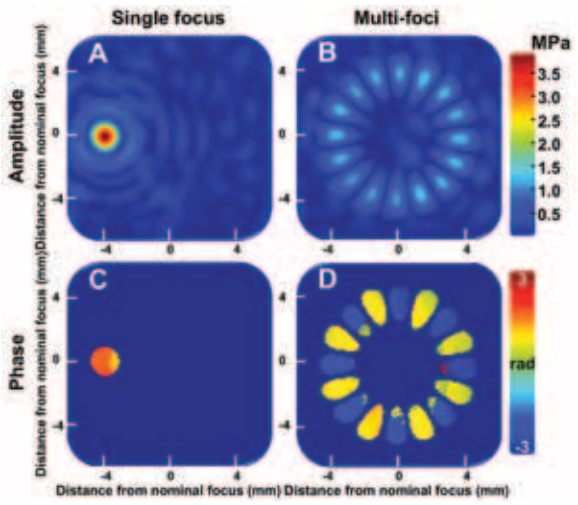

Acoustic field distributions obtained using a needle hydrophone showing the significant drop in peak pressure obtained with the multi-foci approach. A) Single focal point deflection 4 mm to the left in the image coordinates. B) Multi-foci sonication with 16 simultaneous foci spaced evenly on a circle with 8 mm diameter. C and D are the phase maps corresponding to pressure maps A and B, respectively.

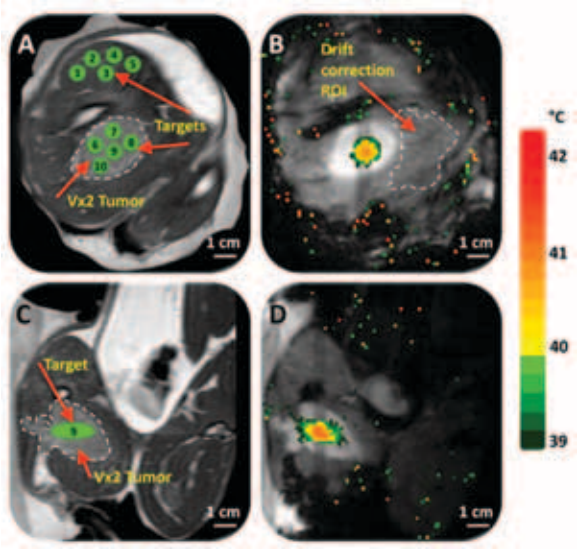

Planning and temperature mapping for mild hyperthermia using multi-foci sonication approach: A) Vx2 tumor (white dashed line) and target regions both within the tumor and normal muscle (green circles). B) Temperature map during a mild hyperthermia treatment with an 8 mm treatment cell after 3 min of heating and the ROI used for magnetic drift correction (white dashed line). C and D are corresponding sagittal images.

Sonication type	Target tissue	Mean (°C)	SD (°C)	T10 (°C)	T90 (°C)	Diameter of area ≥ 40.5°C (mm)	Volume ≥ 40.5°C length to diameter ratio	Mean thermal dose (CEM_{43})
Single-focus	Tumor	40.82 ± 0.12	0.65 ± 0.05	41.60 ± 0.09	39.98 ± 0.20	8.09 ± 0.18	1.95 ± 0.47	0.34 ± 0.04
Multi-foci	Tumor	40.70 ± 0.09	0.64 ± 0.04	41.37 ± 0.22	39.96 ± 0.14	7.99 ± 0.19	1.27 ± 0.19	0.28 ± 0.04
Single-Focus	Muscle	40.99 ± 0.10	0.74 ± 0.14	41.81 ± 0.21	40.08 ± 0.15	8.68 ± 0.30	1.95 ± 0.25	0.53 ± 0.16
Multi-foci	Muscle	40.69 ± 0.07	0.69 ± 0.06	41.51 ± 0.14	39.94 ± 0.10	8.55 ± 0.12	1.52 ± 0.27	0.35 ± 0.06

Summary of in vivo sonication results. Treatment cell size was 8 mm, and target mean temperature range was 40.5 – 41°C. All values are mean ± SD of five sonications.

P132-EA

Tuesday
16 October 2012

Topic: Emerging Applications
Presentation Type: Poster

T2 Temperature Coefficients of Adipose Tissue for MR Temperature Mapping @ 3T

Edwin Heijman[1], Jeroen Pikkemaat[2], Max Köhler[3], Jukka Tanttu[3]

[1]Philips Research, Eindhoven, Netherlands
[2]Philips Innovation Services, Eindhoven, Netherlands
[3]Philips Healthcare, Vantaa, Finland

Background/Introduction: Proton resonance frequency shift thermometry is the method commonly used for monitoring local temperature change in MR guided High Intensity Focused Ultrasound (MR-HIFU) applications as it shows a linear dependency on temperature for all aqueous tissues.[1] However, this method of thermometry is not applicable for monitoring the heating of subcutaneous fatty tissues or bone marrow due to the adipose tissue composition.[2] Without appropriate monitoring of the temperature rise in the subcutaneous fat, uterine fibroid ablations may risk causing thermal build-up in the fat layer and eventually irreversible tissue damage. Initial evidence from our collaborators seems to indicate that dynamic T2 mapping might be able to provide this temperature information. However, the T2 temperature dependency of fat may be field strength dependent, and this study was therefore performed to evaluate the T2 change as a function of temperature in bone marrow (porcine) and subcutaneous fat (human and porcine) at 3T.

Methods: Bone marrow of femur (porcine) and subcutaneous fat (human and porcine) were collected a few hours prior the T2 measurements and stored at room temperature (RT) between harvesting and experiments. Bone marrow was extracted from both the central and peripheral part of the femur. After extraction the tissues were put in small tubes (2 ml) and placed in a temperature controlled MRI phantom holder and positioned in a clinical 3T Achieva MRI scanner. The sample holder was stepwise heated from RT (~20°C) to 65°C. For each temperature step the measurement was performed when the temperature was stabilized. A single slice Turbo Spin Echo (TSE) sequence (TR=5000 ms; TE-spacing= 10 ms; 32 echoes; voxel size= 1×1×5 mm3; NSA= 2; duration= 11.5 min) was used to determine T2 as function of temperature. A dual spin-echo sequence was evaluated for fast T2 temperature mapping with: TR=1400 ms; TE1/TE2= 39/180 ms; voxel size=1×1×5 mm3; TSE- factor=30; echo-spacing=6.4 ms; NSA= 1; duration= 5.6s. The obtained T2 values not only describe the spin-spin relaxation, but also components of spin-diffusion and strong J-coupling and are here referred to as apparent T2 values.[3] Remaining tissue was used to determine the composition of the adipose tissue with high-resolution magic-angle-spinning (HR-MAS) spectroscopy using a 14T NMR spectrometer. (See Table 1, next page.)

Results and Conclusions: The HR-MAS spectra showed that all the different tissues contained mainly water and triglyceride. The fat/(water+fat) ratio was calculated from the integrals of the corresponding signals: central bone marrow= 0.82; peripheral bone marrow= 0.46; subcutaneous fat porcine = 0.88; subcutaneous fat human= 0.81. Apparent T2 values as well as apparent temperature coefficients of the adipose tissues are shown in Table 1. To investigate hysteresis, a sample with subcutaneous fat (porcine) was allowed to cool down after heating. No hysteresis was found in the values T2 or temperature coefficients obtained with the two methods.

This study shows that changes in apparent T2can potentially be used for temperature mapping of adipose tissue. However, the temperature coefficients of the bone marrow from the central and peripheral part differ significantly which may reflect differences in fat content. Moreover, the coefficients reported here were only derived from a few tissue samples. As inter-individual variation may exist, the coefficients found should be treated cautiously. Finally, due to the design of the dual echo sequence here used for rapid T2 mapping, the reported T2 values and temperature coefficients are only likely to be applicable for other sequences.

Acknowledgements (Funding): This research was supported by the Center for Translational Molecular Medicine (VOLTA).

References:

1. J. De Poorter et al., *Magn Reson Med.* 1995 Jan;33(1):74-81.
2. J. De Poorter, *Magn Reson Med.* 1995 Sep;34(3):359-67.
3. R.M. Henkelman et al., *J Magn Reson Imaging.* 1992 Sep-Oct;2(5):533-40.

Tissue	T_2 (32 echoes) [ms]	T_2 (2 echoes) [ms]	T_2 temperature coefficient [ms/°C]	apparent T_2 temperature coefficient [ms/°C]
Bone marrow (C)	70±7	82±11	5.4±0.3	6.0±0.5
Bone marrow (P)	69±7	80±10	4.1±0.3	4.2±0.3
Subc fat pig	111±4	122±7	3.5±0.2	4.1±0.3
Subc fat human	110±12	128±13	3.1±0.9	3.9±0.9

(mean±SD)

Table 1. Apparent T2 @ 20°C and T2 temperature coefficient of adipose tissue at 3T.

P-133-EA

Tuesday
16 October 2012

Topic: Emerging Applications
Presentation Type: Poster

Temporal Characterization of the Dynamic Molecular Changes in Chemoattractants Following Pulse Focused Ultrasound (pFUS) in Muscle: Implications for Cell Therapy

Pamela Tebebi[1], Scott Burks[1], Ali Ziadloo[1], L. Christine Turtzo[1], Victor Frenkel[2], Joseph Frank[1]

[1]National Institutes of Health, Bethesda, Maryland, United States
[2]The Catholic University of America, Washington, D.C., United States

Background/Introduction: Pulsed focused ultrasound (pFUS) has been used as a noninvasive nondestructive modality to enhance tissue permeability and retention in targeted drug delivery. We previously reported elevations in chemoattractants (i.e.,cytokines, chemokines and trophic factors (CCTF)) associated with minimal inflammatory changes in the targeted muscle following pFUS1. Recently we showed that pre-treatment with pFUS enhanced homing, permeability, and retention (EHPR) of human bone marrow mesenchymal stem cells in the murine kidney following local, pFUS-induced increases in CCTF in the treated tissue2. The goal of the present study was to characterize changes in these factors over time in the murine muscle in response to pFUS. Results may reveal an optimum time to administer cells based on CCTF changes, thereby maximizing EHPR effect after pFUS and ultimately translate into improved cellular therapies.

Methods: A modified Sonoblate 500 system with both a 1 MHz therapeutic transducer and an imaging transducer was used to treat the hamstrings of C3H mice. Sonications were done at 40 W (5% duty cycle, 5 Hz pulse frequency). 100 pulses per site were given in a 2 x 3 matrix (spacing = 2 mm). Treated hamstrings were harvested at various times up to 48hrs post treatment and sham mice represented untreated controls. Tissue homogenates were analyzed by ELISA for levels of CCTF's, and cell adhesion molecules (CAM) at each time point (n=6 per time point).

Results and Conclusions: Figure 1 shows significant ($p<0.05$) elevations of CCTFs in skeletal muscle at each time point post-pFUS compared to sham mice. A biphasic response to pFUS occurs as an initial increase in CCTF (30min–2hr) followed by a second peak of expression in CCTFs at 16hrs that decays through 48hrs. The overall trend was consistent with previously published studies1,2. The early elevation of chemoattactants (i.e., IL17, IL12, M-CSF, VEGF) following pFUS likely drives the expression of other CCTF detected at later time points. Increased expression of CAMs following pFUS would facilitate the EHPR effect by mediating the initial tethering of iv-administered stem cells. The major finding is that the initial effects in the muscle by pFUS result in dynamic molecular biological effects that have important implications on the ability to maximize the EHPR effect for cell therapies. The time-course of CCTF changes after pFUS indicate that the predominantly mechanical (i.e. non-thermal) effects, presumably mediated through mechanotransduction, give rise to initial molecular biological responses that are responsible for the second peak occurring at the later time points. Understanding CCTF changes following pFUS will enable appropriately timed infusions strategies of cell products and improves the implementation of cellular therapy for various diseases (i.e., ischemic disease) and in regenerative medicine.

Acknowledgements (Funding): This work was funded through the Intramural Research Program at the National Institutes of Health Clinical Center and National Institute of Biomedical Imaging and Bioengineering.

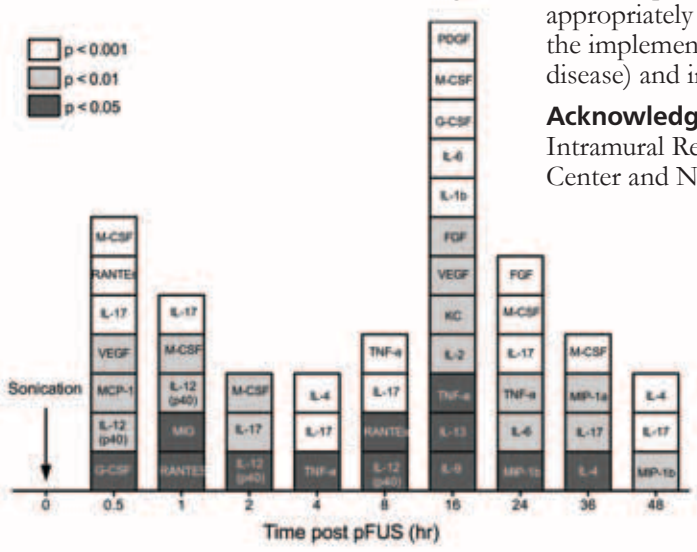

References:

1. Burks S et al *PLoS One* 2011;6:e24730
2. Ziadloo A et al *Stem Cells* 2012;30:1216-27

Time course of significantly increased chemoattractants compared to sham control following pFUS in C3H muscle ($p<0.05$). M-CSF - macrophage/monocyte colony stimulating factor, G-CSF - granulocyte colony stimulating factor, VEGF - vascular endothelial growth factor, PDGF - platelet-derived growth factor, FGF - fibroblast growth factor, MCP-1 - monocyte chemoattractant protein-1, MIP-1? - macrophage inflammatory protein-1 alpha, MIP-1? - macrophage inflammatory protein-1 beta, MIG - monokine induced by gamma, TNF-? - tumor necrosis factor-alpha, KC - keratinocyte-derived cytokine, RANTES - regulated on activation normal T-cell expressed and secreted, IL-interleukin

P-134-EA

Tuesday
16 October 2012

Topic: Emerging Applications
Presentation Type: Poster

Towards In-Vivo: Ultrasound Mediated Targeted Drug Delivery to Cancer Cells In-Vitro via a Clinical MRgFUS System

Dana Gourevich[1], Alexander Volovick[2], Osnat Dogadkin[2], Ritu Malik[1], Lijun Wang[1], Sandy Cochran[1], Andreas Melzer[1]

[1]University of Dundee, Dundee, United Kingdom
[2]InSightec, Tirat Carmel, Israel

Background/Introduction: Cancer research is one of the most investigated fields of our century. Although much progress was achieved in the understanding of the biological, chemical and physical aspects of the disease, the fundamental questions of the exact mechanism of its appearance and progression remain unclear. Currently the common cancer treatments rely on IV and oral administration of high concentration drugs combined with radiotherapy when applicable. All these methodologies work systematically on all the body tissues without differentiation between the healthy and contaminated cells, resulting in many severe side effects, which significantly harm the quality of life for cancer patients. Moreover, the lack in targeting of the anti-tumour therapy often results in an insufficient treatment that can cause reoccurrence of the disease and death. Ultrasound mediated targeted drug delivery has been in focus of many studies in the past decades and resulted in some promising results both in-vitro and in-vivo. Moreover, current possibilities of real time imaging and thermal monitoring during ultrasound application provide additional tools for better and more personal treatment. The on-going in-vivo studies of ultrasound facilitated targeted drug delivery can potentially become a first line treatment methodology for various cancer types providing both local and systematic therapy. Nonetheless, the gap in understanding of the action mechanisms of drug in conjugation with ultrasound emphasises the importance of thorough in-vitro studies. Via the in-vitro platform one can study the thermal and mechanical effects of ultrasound on a single cell model as well as on whole tissue samples under highly controlled conditions dictated by the operator. Doxorubicin (Dox) is antibiotic substance discovered over fifty years ago and is currently classified as the most potent treatment for many malignancies and especially for solid tumours. The main drawback in the treatment with Dox is the high cardio toxicity associated with the cleavage of the Dox molecule and creation of free radicals. Although many efforts were applied in order to decrease the unwanted side effect of Dox, e.g. by encapsulation into liposomes, at present there is no efficient method for delivery of Dox without the injury of the surrounding tissues. The design of a dedicated in-vitro setup for targeted drug delivery of Dox would not only provide insights into the drug penetration mechanism but also an opportunity to investigate different types of drug carriers, in order to decrease the side-effects associated with nominal Dox administration. The utilization of a clinical MRgFUS system for this purpose results not only in exceedingly controlled and monitored in-vitro protocols but also a possibility for a smoother passage to the in-vivo research platform. In the presented work the uptake of Dox within cancer cells was significantly increased by MRgFUS in the presence of microbubbles.

Methods: The application of ultrasound was achieved via the ExAblate 2000 system (InSightec, Israel) with a 0.95 MHz phased array transducer. The uptake of Dox was examined in two different types of cancer cells being breast cancer (MCF-7) and human melanoma (A375m). Moreover the viability of the cells due to the application of FUS was investigated to ensure minimal influence of the ultrasound without the drug. The viability of the cells was recorded by UV studies of the MTT assay. The addition of commercially available ultrasonic contrast agent (Sonovue, Bracco) to the drug solutions was done to serve as a cavitation nuclei. Various powers were test to define the optimal parameters for cell sonication of each individual cell line. All the results presented were achieved by a specially designed setup (Figure 1), which ensured monitored ultrasound application in the same time ensuring cell environment sterility. The penetration of Dox within the cells was quantified by fluorescence intensity measurements.

Results and Conclusions: Following the sonication of cells in the presence of microbubbles we have observed a significant increase in the cellular uptake of Dox into both cell lines as presented in Figure 2. The current setup provided the possibility of real time sub-harmonic signature recording which was then correlated to the drug uptake results, indicating that without microbubbles the appearance of cavitation is rare, while in the

treatment groups containing Sonovue both stable and transient cavitation were observed. The viability studies indicated that at the applied acoustic powers there was a relatively minor effect on the cell monolayer growth. In conclusion, the data presented here have proved the feasibility in adaption of a clinical MRgFUS system for in-vitro research on the subject of targeted drug delivery. Since the platform for FUS application on cells is now established, further optimization of the US parameters as well as application of novel carriers, drug vehicles and contrast agents conjugated polymers can be studied. The significant increase in the Dox uptake due to application of FUS in the presence of microbubbles offers a potential targeted delivery mechanism for Doxorubicin into cancer cells in-vivo. The discoveries immerging from this in-vitro cell work conducted on a commercially available MRgFUS system contributes to the greater knowledge of ultrasound mediated targeted drug delivery, allowing other groups with the same equipment to easily reproduce the results.

Acknowledgements (Funding): The research leading to these results has received funding from the European Community's Seventh Framework Programme (FP7/2007-2013) under grant agreement n° 230674 (Nanoporation project). The authors thank J. Grienfield, Y. Shafran, O. Prus and Y. Medan of InSightec Ltd. and J. Gnaim of Capsutech Ltd., for their support and assistance in this research.

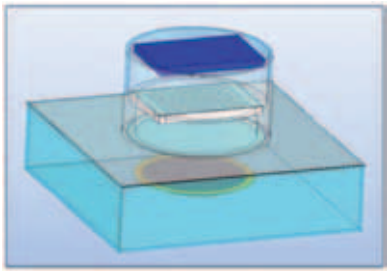

Cell Sonication Setup

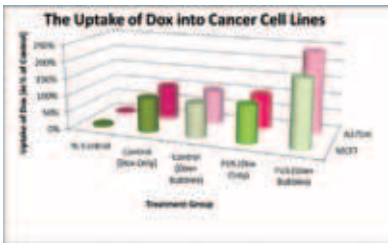

The Uptake of Dox with and without microbubbles into MCF7 and A375m cells

P-135-EA

Tuesday
16 October 2012

Topic: Emerging Applications
Presentation Type: Poster

What Are the Best Methods of Assessing Advancement in the Field of Focused Ultrasound?

Heather Huff-Simonin,Neal Kassell, Dasha Tyshlek, Arik Hananel

Focused Ultrasound Foundation, Charlottesville, Virginia, United States

Background/Introduction: The Focused Ultrasound Foundation has created a dashboard of charts and graphs (indicators) to monitor the advancement of focused ultrasound from bench to bedside. The Foundation is asking the research community to collaborate in providing the data needed to populate and regularly update these charts and graphs.

Benefits of FUS Dashboard:

- demonstrate progress to Foundation donors and prospective donors
- make it easier to secure additional funding to further advance FUS technology and treatments
- help researchers secure internal/external funding and gain administrative support to establish dedicated FUS Centers
- heighten awareness of focused ultrasound among government regulators, insurance providers and other stakeholders

P-136-LP

Tuesday
16 October 2012

Topic: Liver
Presentation Type: Poster

Acoustic and Thermal Modeling of In-Vivo Tumor Ablation With MRgHIFU

Adamos Kyriakou[1], Esra Neufeld[1], Lorena Petrusca[2], Rares Salomir[2], Niels Kuster[1],

[1]IT'IS Foundation/BIWI/ETHZ, Zurich, Switzerland
[2]Geneva University Hospital, Geneva, Geneva, Switzerland

Background/Introduction: High Intensity Focused Ultrasound (HIFU) under MR guidance is a non-invasive alternative to conventional methods of thermal ablation in which sharply delineated lesions inside the body are produced without harming the surrounding healthy tissue.

A typical HIFU transducer creates a small focal volume and lesions with dimensions in the order of millimeters. Multiple overlapping lesions are created to ablate clinically relevant volumes (order of 1cm3) either by mechanically moving a single element transducer or by using a phased array of transducer elements with individually defined amplitudes and phase delays. The latter can be used to electronically steer the focus and scan the tissue volume.

If the ablation procedure is performed improperly, viable tumor cells may survive. Such problems occur when the lesions overlap poorly, leading to insufficient coverage of the tumor area, or when ablating highly vascularized tumor regions, which are more resistant to thermal ablation. Computational acoustic and thermal modeling of the ablation procedure can help predict the treatment outcome and optimize the treatment parameters.

Methods: A software framework for numerically assessing the interaction between ultrasonic waves and biological tissue by generating 3D simulations of full wave propagation in inhomogeneous anatomical models was developed. The framework includes explicit linear and nonlinear acoustic solvers (parallelized for multi-core CPU and GPU systems). Fluid dynamic solvers for modeling acoustic streaming and thermal solvers for modeling ultrasound induced temperature increase and lesion formation were also developed and can be coupled with the acoustic solvers.

Results and Conclusions: This software framework was employed to model and simulate ablation in an ex-vivo ovine kidney surrounded by fat and muscle tissue as well as hepatic ablation in live sheep, taking into account the ribcage and all major organs in the vicinity of the liver. The anatomical models were segmented from high resolution, 3D anatomic data (VIBE) of the experimental setup. Acoustic simulations were performed. Thermal simulations using the deposited acoustic energy distribution were performed to predict the temperature increase distributions in the tissue and to calculate tissue damage while taking into account heat diffusion and (for the in-vivo case) perfusion of the tissue and the cooling effect of nearby vessels.

A novel software platform was developed to perform weakly-coupled acoustothermal simulations with spatial resolutions better than 0.1mm of a complex transducer applied to realistic anatomies. The resulting distributions were compared to in-vivo and ex-vivo measurements. The impact of anatomical features, such as bones or air-cavities, on the focus shape could be assessed.

Acknowledgements (Funding): This study was supported by the Swiss National Center of Competence in Research (NCCR) and SNFS (Grant CR32I3_125499).

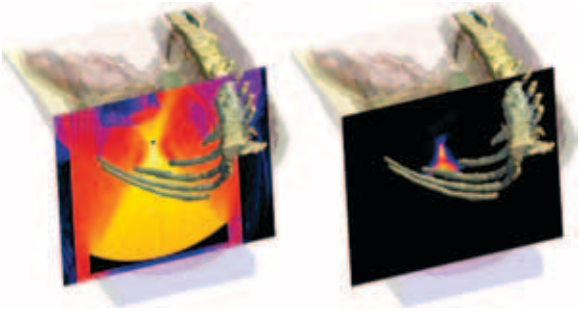

3D model of simulation replicating an experimental setup of hepatic tumor ablation in live sheep, the resulting pressure distribution (left) and temperature increase (right) on a plane through the geometric focus of the transducer (marked by a point). The effect of the ribcage, skin and air-filled cavities (like the stomach and the intestines) on the acoustic focus shape and position can be clearly seen.

P-137-LP

Tuesday
16 October 2012

Topic: Liver
Presentation Type: Poster

Efficient Computation of Optimal Treatment Plans for High Intensity Focused Ultrasound Therapy of Liver Tumors

Caroline v. Dresky[1], Joachim Georgii[1], Stefan Jakobsson[2], Alexander Scherrer[3], Daniel Demedts[1], Christian Schumann[1], Sebastian Meier[1], Tobias Preusser[1]

[1]Fraunhofer MEVIS, Bremen, Germany
[2]Fraunhofer Chalmers Center, Göteborg, Sweden
[3]Fraunhofer Institute for Industrial Mathematics (ITWM), Kaiserslautern, Germany

Background/Introduction: This work aims at the development of software assistance for the pre-operative planning of focused ultrasound therapy of liver tumors. The challenge is to create patient specific optimal treatment plans according to pre-defined therapy goals such as precise and complete tumor ablation and wide sparing of healthy tissue from overheating. Considering abdominal organs, these goals are further constrained by the shielding by the rib cage as well as the breathing motion. This motivates our detailed computer and simulation supported treatment planning. In a first step, we generate optimal treatment plans respecting ribs in the beam path, while the incorporation of motion compensation will be realized in a second step. Aiming at the generation of optimal treatment plans in reasonable time, we combine optimization methods with efficient numerical simulation techniques.

Methods: The optimization relies on the formulation of a FUS planning problem with its different therapy goals as a mathematical optimization problem. The physician can thereby approach the planning problem on the intuitive and meaningful level of therapy goals without having to consider the concrete hardware parameter settings required for achieving these goals. Based on the specified therapy goal, the problem computation is realized automatically in a top-down order by first positioning the transducer with heuristic optimization approaches, followed by the spatial alignment of the sonications and ending up with configuring the sonications in terms of times, powers, phases etc. for the electronic steering of the phased-array system using optimal control and nonlinear optimization methods.

In this step the optimization interacts with the numerical simulation of the treatment outcome for specific parameter settings. Hence, in order to allow for treatment planning in reasonable time, efficient simulation techniques are required. In order to meet these requirements, the simulation of the ultrasound propagation and resulting heat dissemination in the tissue has been effectively parallelized for execution on SIMD streaming architectures as current graphics hardware (GPU), which results in an enormous speed-up compared to conventional CPU approaches. The interaction between the GPU-based simulation and the CPU-based optimization is accelerated by running all time- and memory-consuming computational tasks related to the simulation on the GPU and just transferring the comparably small data of function values and derivatives to the CPU side.

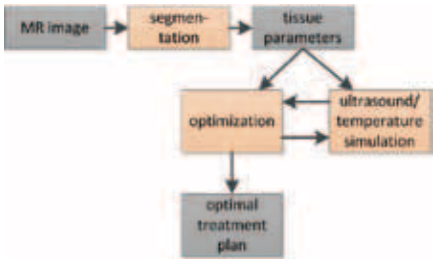

Figure 1. Schematic overview of the software assistance for treatment planning.

In order to provide clinically usable computer assistance for therapy planning, the optimization and simulation methods are integrated into a software prototype. This prototype is designed to support the entire clinical workflow beginning with the import of patient data, the segmentation of target and risk tissue and the generation of optimal treatment plans, as described above (see Figures 1 and 2).

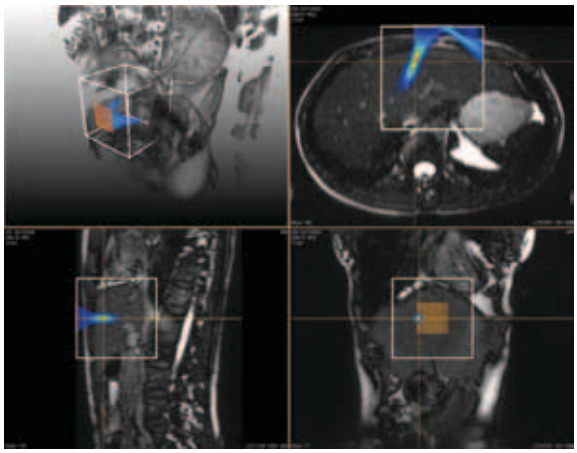

Figure 2. Screenshot of the software prototype showing the numerical simulation of a sin

Results and Conclusions: The parallel GPU implementation allows simulating a single sonication of 30s in a reasonably resolved simulation domain (2563) in 3.8s. Therefore, the numerical simulation of an entire treatment can be performed about eight times as fast as the actual treatment duration. This fact presents excellent pre-conditions for an efficient treatment planning based on the interaction of optimization and simulation methods.

Acknowledgements (Funding): This work was supported by the Fraunhofer Internal Programs under Grant No. MAVO 821 012. The project involves the Fraunhofer institutes EMI, FIRST, ITWM, MEVIS and SCAI. gle

P-138-LP

Tuesday
16 October 2012

Topic: Liver
Presentation Type: Poster

Efficient GPU Simulation of High Intensity Focused Ultrasound Therapy

Joachim Georgii, Caroline v. Dresky, Sebastian Meier, Christian Schumann, Daniel Demedts, Tobias Preusser

Fraunhofer MEVIS, Bremen, Germany

Background/Introduction: Tumor ablation using High Intensity Focused Ultrasound demands for software assistance in the planning, realization and monitoring of the treatment. In particular the consideration of abdominal organs, which are shielded by the ribs and underlie breathing motion, require physical simulation techniques in order to predict the treatment outcome. High demands on the simulation are given by the necessity to respect material inhomogeneity such as the ribs, and the requirement to perform the simulation on a region large enough to cover all risk structures. Moreover, the simulation shall support the compensation of breathing motion by plan adaption during the treatment. These facts result in enormous computational demands in terms of memory and simulation times. In the presented work, we focus on efficient methods for treatment simulation using SIMD streaming architectures such as current graphics processing units (GPUs), and specifically we address the issues arising from the rather limited local memory available on GPUs.

Methods: For the simulation of the ultrasound propagation in heterogeneous tissue, we use the hybrid angular spectrum method, while the resulting heat dissemination is computed by solving the bioheat equation by means of an explicit finite difference method. To improve the performance, both of these simulations are run on current graphics hardware. The simulation respects material inhomogeneity as well as single reflections of the ultrasound waves (see Figure1). For a simulation domain of size 5123, one requires 1 GB of memory space to only store the ultrasound pressure field in single floating point precision. In order to allow for the numerical simulation to be scalable with respect to simulation grid sizes, the implementation for the ultrasound simulation only stores the information required to compute one single slice of the hybrid angular spectrum approach in local GPU memory. The data transfer between CPU and GPU is implemented asynchronously, so that the GPU can start computations of the next slices, while the previous computed slice is downloaded to the CPU to store it.

With respect to the bioheat equation, we implemented a partitioning strategy that sweeps through all slices of the simulation domain within one single time step, similar to the angular spectrum approach. The number of slices that can be computed simultaneously is automatically determined by the available local GPU memory.

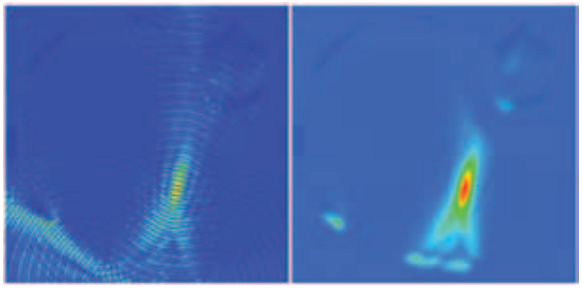

Figure 1. On the left, in the simulated pressure field the pattern of the ultrasound waves can be clearly seen. On the right, the respective heating is shown. Due to the settings of selected sonication, one can observe heating in risk structures (ribs, spine).

Results and Conclusions: We achieve simulation speed-ups between 17 and 330 compared to previous CPU simulation approaches. Since the ultrasound propagation could be implemented highly memory efficient, we can even simulate domains larger than 5123. Due to the fact that the temperature field is rather smooth, the resolution of the temperature simulation domain can be chosen coarser than the one for the ultrasound simulation. We suggest a setting, where the simulation domain is chosen such that the data fit in local GPU memory for optimal performance.

Table 1. Timing statistics of the GPU implementation using the hybrid angular spectrum approach with single reflections (rAS) and the explicit bioheat solver. Besides the times (in seconds), we state the demands on local GPU memory depending on the grid resolutions.

	NVIDIA GTX 580 (3GB)			
Pressure / Temperature Resolution	128^3 128^3	256^3 256^3	512^3 512^3	1024^3 512^3
Preprocess time	**0.314 s**	**0.314 s**	**0.314 s**	**0.314 s**
rAS time (GPU memory)	**0.466 s** (80 MB)	**2.251 s** (101 MB)	**14.50 s** (119 MB)	**122.5 s** (192 MB)
Bioheat time (GPU memory)	**0.267 s** (26 MB)	**1.425 s** (272 MB)	**21.14 s** (1664 MB)	**21.14 s** (1664 MB)

A further optimization of the simulation setup has been done by choosing different GPUs for sound propagation and heat dissemination, which results in a nearly double throughput of the system.

To conclude, the simulation framework is both amenable to deal with highly resolved grids as well as fast enough to allow for real-time treatment simulation (see Table 1).

Acknowledgements (Funding): This work was supported by the Fraunhofer Internal Programs under Grant No. MAVO 821 012. The project involves the Fraunhofer institutes EMI, FIRST, ITWM, MEVIS and SCAI.

P-139-LP

Tuesday
16 October 2012

Topic: Liver
Presentation Type: Poster

Explanted Thiel Embalmed Human Liver as a Model to Study MR-guided Focused Ultrasound Surgery

Ioannis Karakitsios[1], Timur Saliev[2], Sarfraz Ahmad[1], Helen McLeod[2], Andreas Melzer[2]

[1]IMSaT, Dundee, United Kingdom
[2]University of Dundee, Dundee, United Kingdom

Background/Introduction: MR-guided Focused Ultrasound Surgery (MRgFUS) is a useful method to ablate tumour non-invasively. Treatment of liver disease is a very demanding treatment process with high death rates. Studies on animals and human patients under general anaesthesia have reported the feasibility and accuracy of MRgFUS to coagulate tumour. Thiel embalming is used to preserve human cadavers, giving the bodies a high degree of flexibility and life-like characteristics. The focus of our study was to determine whether explanted Thiel embalmed human liver constitutes a reliable model for studying MRgFUS. For that purpose, the temperatures of the heated Thiel tissue were compared to the temperatures of fresh animal tissue.

Methods: Four explanted livers: two fresh sheep livers and two Thiel embalmed human livers were scanned with MRI (1.5 T HDxT, GE Healthcare, USA) using Fast Spoiled Gradient Echo (FSPGR) imaging with TE: Minimum, TR: 60 msec, Flip Angle: 30o and acquisition matrix 256x256. The organs were heated for 20 sec with Focused Ultrasound (FUS) (ExAblate 2000, InSightec Ltd., Israel) at various acoustic energies: 253, 506 and 709 J. Proton Resonance Frequency (PRF) MR Thermometry was applied after treatment. Post-sonication maximum temperature values (Fig. 1) of the animal liver and Thiel human liver were compared.

Results and Conclusions: Table I shows the average value of the maximum temperatures after MRgFUS treatment of fresh animal liver and Thiel embalmed human liver at various acoustic energies, and their difference.

Acoustic Energy (J) / Average value of max temperatures (oC)	253	506	709
Thiel liver temp	59	74	87
Fresh liver temp	58	73	86
Temp difference	1±0.7	1±0.93	1±0.69

Table I. Post-treatment maximum temperatures and temperature difference between Thiel and animal liver at various energies.

In conclusion, MRgFUS treatment of Thiel embalmed human liver at energies >506 J can induce tumour ablation with temperatures >56oC. There was a good correlation between temperatures achieved in the Thiel embalmed tissue and the temperatures in the fresh animal tissue. In overall, Thiel embalmed human liver constitutes a feasible, safe and reliable model to study MRgFUS treatment, ex-vivo.

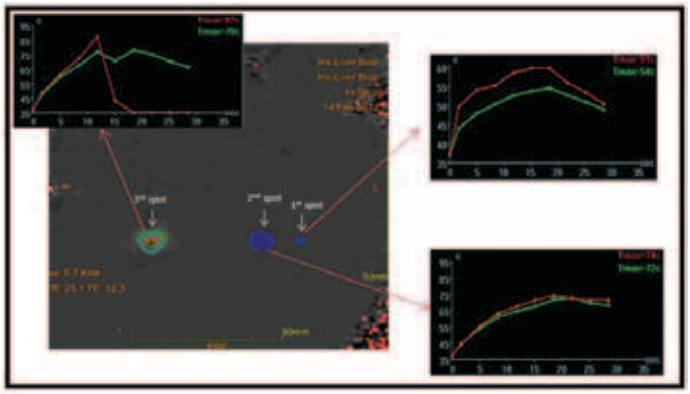

Figure 1. Post-treatment PRF images and temperature graphs of Thiel embalmed liver (a) and fresh animal liver (b) at various acoustic energies.

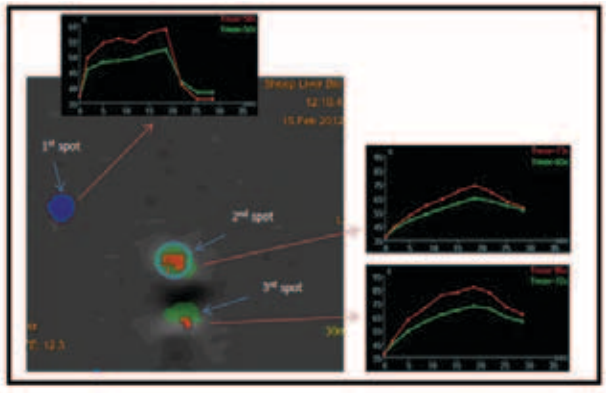

Figure 2. Post-treatment PRF images and temperature graphs of Thiel embalmed liver (a) and fresh animal liver (b) at various acoustic energies.

P-140-LP

Tuesday
16 October 2012

Topic: Liver
Presentation Type: Poster

Frequency Domain Analysis of Displacement Wave Propagation Introduced by a Transient High Intensity Focused Ultrasound Measured Using a Gradient Echo Sequence

Jiming Zhang[1], Pei-Herng Hor[1], Raja Muthupillai[2]

[1]University of Houston, Houston, Texas, United States
[2]St. Luke's Episcopal Hospital, Houston, Texas, United States

Background/Introduction: Multifrequency MR elastography (MRE) has been shown to be sensitive for early detection of subtle alterations of tissue viscoelasticity changes (1, 2). The scan time required for evaluating viscoelastic property dispersion via multiple, temporally resolved, single frequency MRE is clinically prohibitive. Here we use MR phase contrast method to measure the displacement wave emanating from a transient discharge of acoustic radiation force using a High-Intensity Focused Ultrasound (HIFU). We propose a frequency domain based analysis of the measured displacement to obtain dispersion of viscoelastic constants.

Methods: All experiments were performed on a 1.5T MR scanner equipped with a 256 channel spherical shell HIFU transducer (Sonalleve, Philips).

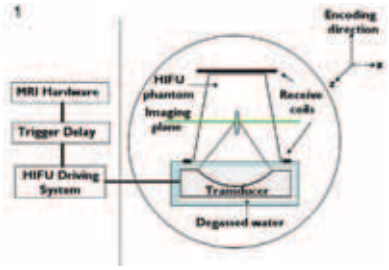

MRI Data acquisition: A phase contrast based gradient-echo pulse sequence was modified to include motion-sensitizing gradients between the excitation pulse and the spatial encoding gradients. MR acquisition parameters were: voxel size: 2.0 x 2.5 x 7 mm3; FOV: 180 x 180 mm2; TR/TE/flip angle = 40 ms/22 ms/12°; bandwidth: 110 Hz/pixel; scan time: 6.0 s. The duration and gradient strength of the symmetric bipolar motion encoding gradient (MEG) was 4 ms and 28.6mT/m. A coronal slice bisecting the plane of the HIFU focus was imaged, and the displacement encoding direction was set perpendicular to the slice-select direction (Figure 1).

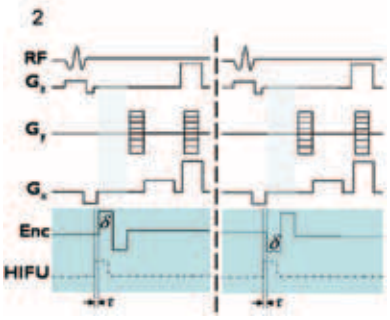

HIFU- MRI scanner Interface: The scanner triggers the HIFU device to emit a 2 ms, 400W burst of ultrasound (1.2 MHz) focusing at 6.7 cm within a gel phantom. The phase shift (tau) at 0.4 ms intervals created by HIFU burst is used to capture the displacement wave propagation by motion encoding gradient (MEG) (Figure 2).

Data Analysis: 1) A phase difference image from the two sets of raw data (acquired with opposing polarities of MEG) was reconstructed; 2) Fourier transformation of time-domain data and subsequent band-pass filtering of signal resulted in multiple single frequency images from the same data-set. 3) An inverse FT was performed on filtered frequency spectrum to capture displacement wave propagation at specific frequencies.

Results and Conclusions: Displacement maps reconstructed at four frequencies of 135Hz, 175Hz, 215Hz and 255 Hz from a single broad band excitation at two different phase shift (t) are shown in Figure 3. By measuring the distance traveled by the wave front between two delay time points, the shear wave velocity at the chosen frequency can be estimated (Figure 4).

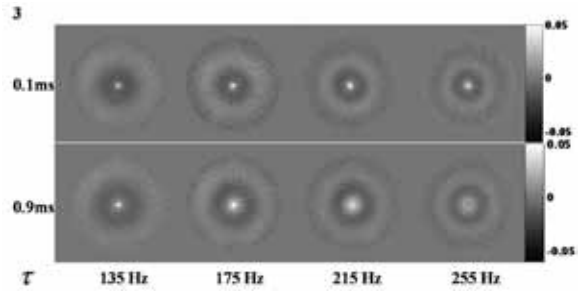

In conclusion, frequency domain analysis can be used to measure the shear wave velocity dispersion of viscoelastic tissue. It paves a way to estimate the attenuation dispersion and thus the viscoelastic tissue property.

1. Sack I et al., Neuroimage, 2009, 46(3) 625-7; 2. Wuerfel J et al. Neuroimage, 2010, 49(3)2520-5; 3. J Zhang, ISMRM, 2012, # 2922.

Acknowledgements (Funding): This study was partly funded by Ronald MacDonald fund at St. Luke's Episcopal Hospital and Texas Center for Superconductivity at University of Houston, and research support from Philips.

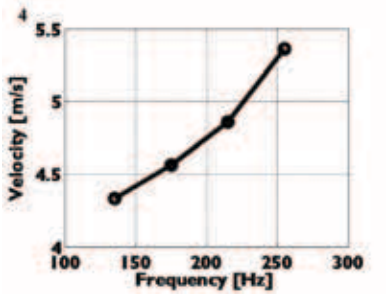

Figure 1. The MR-ARFI system setup
Figure 2. The MRI pulse sequence diagram with displacement encoding gradients
Figure 3. Displacement map of chosen frequencies 135Hz, 175Hz, 215Hz and 255Hz at trigger delay time tau of 0.1ms and 0.9ms
Figure 4. Shear wave velocity dispersion

P-141-LP

Tuesday
16 October 2012

Topic: Liver
Presentation Type: Poster

Improved Workflow With Transducer Placement Guided by Previously Acquired Data

Andrew Holbrook, Pejman Ghanouni, Kim Butts Pauly

Stanford University, Stanford, California, United States

Background/Introduction: MRgFUS treatments with extracorporeal transducers can be unnecessarily lengthened by iterative placement of the device and imaging verification of adequate placement. The motivation of this work is to improve MRgFUS workflow by introducing an image-based feedback method for transducer placement before the patient is moved into the MR system.

Methods: A ShowWX+ Pico Projector with RetroTouch technology (Microvision, Inc., Redmond, WA) was calibrated and mounted above a MR750 3T table. The projector is able to detect reflections from a sensor consisting of reflectors mounted on a mobile device attached to the FUS transducer (Figure-1). Reflector locations within its projection field are determined from these reflections and the accelerometer data. Patient fiducials can also be localized in a similar way, with a smaller reflection tool. No accelerometer is necessary if the reflectors around the fiducial are in a known scan plane. This provides registration with the previously acquired data.

Once the sensor and transducer position are known, three images from a previously acquired dataset (either CT or MR) are displayed on an in-room display right at the patient bed: two transverse and one parallel to the device face, depicted as a square overlay. The sensor is then repositioned until the images are centered on a predefined target.

In an experimental study, a target was selected on a previously acquired dataset (3D axial SPGR, TE/TR 2.1/4.5ms, 25cm FOV, 2mm slice thickness, 62.5 kHz BW, 256x128x164 matrix size, NEX 2) of a covered phantom with a single external fiducial. The FUS transducer was skipped for this demonstration and just the sensor was placed according to the methods described above. To illustrate correct placement, bright markers were placed in the location of the sensor, in the same orientation, and the phantom was imaged, and the location analyzed.

Results and Conclusions: Example images from the experiment are shown in Figure 2. The sensor was repositioned until the target area appeared to be underneath. The positioning time took under a minute, including landmarking to the fiducial. With this position, the four bright markers demonstrate that the sensor was directly over the target location.

As the phantom was covered, the only physical reference utilized was the external fiducial. Thus, patient image viewing of previously-collected volume data can potentially reduce placement time of external FUS transducers by improving the device placement success. Future work will determine the accuracy, as well as implementing this work into existing clinical trials where patients undergo a CT scan prior to FUS ablation.

Acknowledgements (Funding): We acknowledge assistance from Mark Freeman and Selvan Viswanathan from Microvision, and our funding support from NIH R01-CA121163 and P01-CA159992.

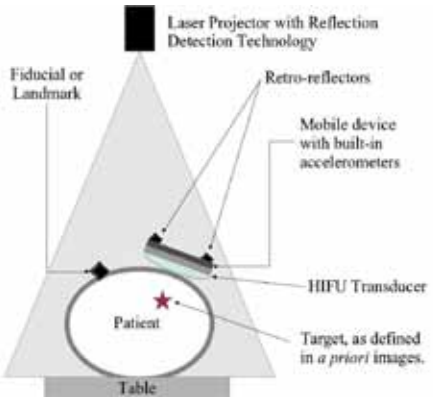

Figure 1. System schematic. A laser projector is positioned above the patient, and the projection space is landmarked to a fiducial on the patient. Retro-reflectors affixed to a device with built-in accelerometers determine the device's position with the projector space. This sensor is in turn attached to the FUS transducer, allowing for images to be displayed of the underlying anatomy.

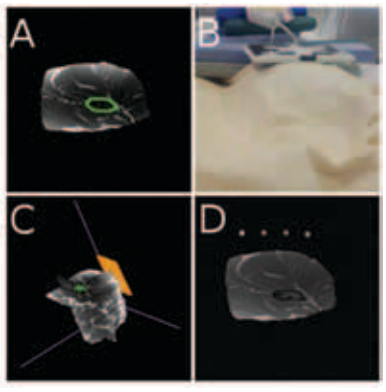

Figure 2. Image viewer work flow. A target can be painted in the a priori images (A). Next, after landmarking, the sensor can be placed inside the projection field (B). The sensor and slices directly underneath are immediately visualized on an in-room display (C). Finally, a phantom with a line of vertical markers was placed in the same location as the sensor, directly over the target and the phantom was re-imaged (D).

P-142-LP

Tuesday
16 October 2012

Topic: Liver
Presentation Type: Poster

In-Vivo Assessment of Tissue Damage During Thermal Ablations With a Multi-Pathway Mri Sequence

Chang-Sheng Mei, Renxin Chu, Lawrence Panych, Nathan McDannold, Guangyi Wang, Bruno Madore

Brigham and Women's Hospital / Harvard Medical School, Boston, Massachusetts, United States

Background/Introduction: A multi-pathway, steady-state MRI thermometry sequence is proposed for the guidance of thermal ablations. With this pulse sequence, an extra spin-echo like (PSIF) signal is acquired in addition to the usual gradient-echo like (FISP) signal, at no cost in scan time. These two independent signals can be combined to: 1) Improve the temperature-to-noise ratio (TNR) by up to 35%[1], 2) correct temperature errors due to susceptibility effects,[2] 3) help detect blood vessels for motion-tracking purposes,[3] and 4) directly assess tissue damage. While the first three advantages were reported earlier,[1-3] the main goal of the present abstract is to demonstrate the latter, i.e., the sequence's ability to capture tissue damage.

Methods: FUS heating experiments were performed in a New Zealand White rabbit model, in the thigh area (30 W for 30 s using a 1.5 MHz transducer with diameter = 100 mm and radius of curvature = 80 mm). The 2D dual-echo MR sequence shown in Figure-1 was used, and both FISP and PSIF signals were employed to calculate temperature as well as thermal dose, based on the proton-resonance frequency (PRF) shift (TEPSIF/TEFISP/TR = 2.7/6.7/10.2 ms, bandwidth = ±31.25 kHz, flip angle = 30°, FOV = 160x160 mm, matrix size = 96x128, slice thickness = 5 mm, 1 frame/s).

The present hypothesis is that our sequence might prove able to detect tissue damage directly, based on the increase in T2 that occurs at treated locations, as opposed to indirectly through temperature dose. Our T2-weighted PSIF signal should be especially-well suited for the task as a T2 increase translates into a marked signal increase. However, the T1 dependence on temperature tends to lower signal at heated locations, thus masking the T2-related signal increase we wish to detect. In the present work, the T1-related decrease was roughly compensated using as a reference voxel just outside the main lesion, such that a linear relationship between temperature and signal loss could be found. Using this linear relationship, temperature maps could be used to roughly compensate for temperature-related signal losses in the whole FOV, yielding corrected images where T2-related effects were now visible. As detailed below, tissue damage was clearly visualized in our results as a bright region, whose size was found to correlate very well with temperature-dose results.

Results and Conclusions: Temperature maps, PSIF and temperature-compensated PSIF images are shown in Figure 2 (see next page) for time points before, during, and after sonication. The thermal dose contour at 240 TEM43°C (if any) was overlaid on all images. The compensated PSIF images showed the lesion formation as a bright region that grew over time, matching very well the overlaid dose contour. The final lesion size was also validated using post-sonication T2-weighted imaging (Figure 3, next page). FISP and compensated FISP images have the similar features as the described PSIF and compensated PSIF images (data not shown), and could be combined to the PSIF results for improved SNR.

In conclusion, the proposed multi-pathway sequence can generate image contrast that helps detect thermal damage, to complement and backup measurements based on thermal dose. Thermally-damaged tissues could be seen as a bright region whose size correlated quite well with the 240 TEM43°C dose contour and with post-sonication T2-weighted data.

References:

1. Madore, et al. *MRM* 66: 658-68 (2011).
2. Madore, et al. *ISMRM* 2012, p. 1767.
3. Madore, et al. *ISMRM* 2012, p. 1638.

Acknowledgements (Funding): Support from R01CA149342 and P41RR019703 is acknowledged.

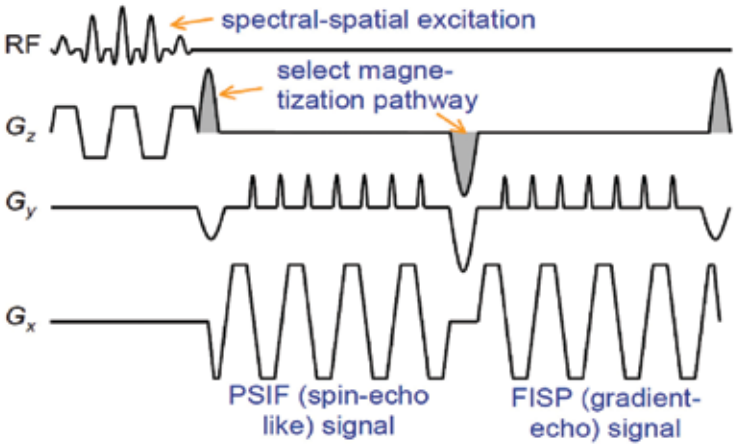

Fig 1: Our multi-shot EPI sequence acquires both a FISP and a PSIF signal [1]. For the damage-detection tests presented here, an echo train length of 1 and a sinc-shaped RF pulse were used.

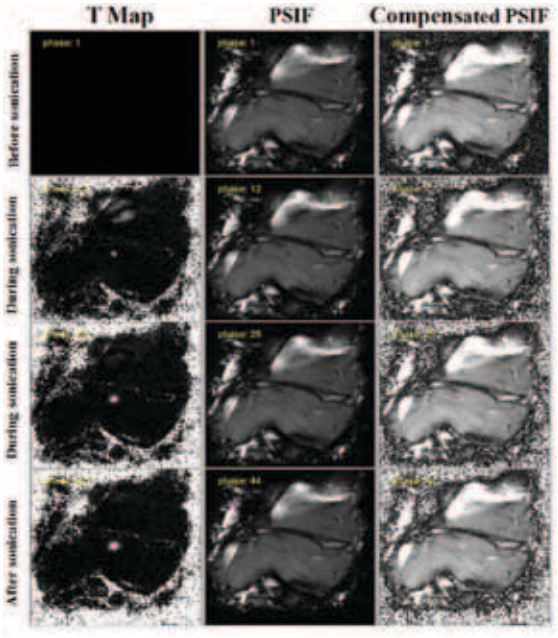

Fig 2:
Temperature maps, original PSIF images, and compensated-PSIF images are shown for different time points (before, during and after sonication). The 240 TEM43Â°C thermal dose contour is shown as an overlay. Tissue damage could be seen as a bright region in the compensated images, and its size correlated very well with the 240 TEM43Â°C dose contour

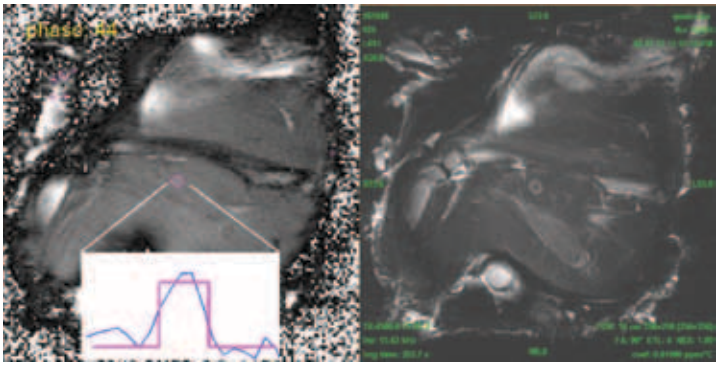

Fig 3: (Left) PSIF-based and FISP-based images were averaged in the final results, for improved SNR. The inset shows a profile of the image signal (blue) and the 240 TEM43Â°C contour (magenta) through the lesion. (Right) A T2 weighted image was acquired right after the ablation. Good agreement was found between the bright region (left), the thermal dose contour (left) and the post-sonication T2-weighted image (right).

P-143-LP

Tuesday
16 October 2012

Topic: Liver
Presentation Type: Poster

Liver Ablation by MR-guided Focused Ultrasound on Thiel Embalmed Cadaver

Timur Saliev[1], Alexander Volovick[2], Ioannis Karakitsios[1], Sarfraz Ahmad[1], Helen McLeod[1], Roos Eisma[1], Andreas Melzer[1]

[1]University of Dundee, Dundee, United Kingdom
[2]InSightec, Tirat Carmel, Israel

Background/Introduction: MRI-guided focused ultrasound surgery (MRgFUS) opens a new avenue for liver cancer therapy, particularly for treatment of common type of liver tumour such as Hepatocellular carcinoma (HCC). HCC causes around 1500 deaths per year in Great Britain (British Society of Gastroenterology, 2003). The standard approach for HCC treatment includes surgery, chemo-embolization, systemic chemotherapy, ethanol injection and ablation by microwave or radiofrequency. MRgFUS offers an alternative way for HCC management due to its more precise targeting and real-time temperature monitoring during ablation of tumour tissue, which is critical for effective therapy. Despite this, the application of MRgFUS for liver tumour ablation is complicated by factors such as the ribcage barrier, organ motion during breathing and cooling effect from natural blood flow in the organ. Secondly and more importantly, no studies for optimization MRgFUS for liver have been conducted yet. In this work an ex-vivo model was exploited for validation of MRgFUS treatment protocol for the first time. The concept of ex-vivo model is based on recent development for preservation corps from decay by using Thiel embalming technique (Thiel, W. Ann Anat 174(3): 185-195, 1992).

Thiel soft fix cadavers are an ideal model for validation and testing of medical technologies, due to their distinctive properties such as a life-like colouring, odourlessness, good muscle-joint flexibility and relative long-time preservation. In addition to the exceptional anatomical characteristics, the use of Thiel-embalmed human cadaver as a model for validation could decrease the necessity for clinical trials and pre-clinical animal studies. Present work aims to explore the feasibility of using Thiel-embalmed cadavers for MRgFUS application to liver and characterize the effect of Thiel solution on imaging / acoustic properties of the tissue.

Methods: 4 different Thiel embalmed cadavers were used for experiments. The cadaver was intubated and then connected to a ventilating system. The cadaver was then transferred to the MR suite for further MR-scanning and sonication under MR-guidance (MRI Signa HDxt 1.5 Tesla, GE Healthcare,USA). Two types of ultrasound transducers (Insightec, Israel) were used for liver ablation: portable transducer with frequency 0.5 MHz (CBS ExAblate 2100 system) and transducer incorporated into the MR-table with 1 MHz (UF ExAblate 2000 system). Planning images were acquired by using 8ch body coil (with CBS ExAblate 2100 system) and Single channel InSightec Pelvic coil (with the UF ExAblate 2000 system) (Fig.1). The temperature monitoring was based on Proton Resonance Frequency (PRF) shift of water protons provided by MR system. After establishing the respiratory motion and planning MR imaging, the liver was sonicated at two different breath holding positions: maximal inspiration and expiration.

Results and Conclusions: MRI imaging: It has been established that the Thiel solution significantly affects the imaging properties of the embalmed Thiel tissue. Different MRI protocols and sequences were applied as to optimize the visualization of organs and tissues. The optimal parameters for MR imaging of Thiel embalmed cadavers were found as the followings: Fast Spoiled Gradient Echo (FSPGR), TE=min and TR>1000 msec. It was discovered that the Bandwidth (BW) value plays a crucial role in optimization of image quality (up to 5 kHz). The short BW results in a long scanning time, which makes this technique unsuitable for application in clinical environment.

Cavitation: It has been thought that the cavitation does hinder ultrasound propagation and thereby it could impede the heating of the tissues. To reduce the cavitation, long-time sonications with minimal acoustic power were conducted. In clinical context, such long-time acquisition time is acceptable.

Liver sonication: Anatomically, a large area of the liver is covered by the rib-cage. To investigate the feasibility of treating of the liver through the ribs, the ultrasound transducers were positioned above the rib-cage (under MR-guidance). It was revealed that in terms of organ targeting and ergonomics, the positioning of portable transducer from CBS ExAblate

2100 system is more convenient, but it lacks the frequency range (0.5 MHz only). It has been demonstrated that the heating of the liver behind the rib-cage using both systems is feasible (CBS ExAblate 2100 system and UF ExAblate 2000). For the same level of acoustic power the heating produced by UF ExAblate 2000 is more effective due to its high ultrasonic frequency (1 MHz).

Rib-cage problem: The Exablate software allows closing of active piezoelectric elements of ultrasound transducer by operator's choice. The experimental data demonstrated that liver treatment through the rib-cage without closure of transducer elements causes the rib heating, which is considered as undesirable for clinical scenario. In this case the heat of the ribs by the UF ExAblate 2000 is found as more pronounced due to higher energy density applied on the ribs.

Respiratory motion: The sonication was performed for two respiratory regimes: maximum inspiration and full expiration. The acquired data indicate the importance of rib-cage movement and change of acoustic window for ultrasound propagation and tissue ablation during breathing. Data suggest that the liver was exposed more to sonication at 'maximum inspiration' phase, which results in more efficient organ heating.

In conclusion, the optimal parameters for MR scanning of Thiel embalmed cadavers were established during the experiments. The obtained MR and temperature mapping data demonstrated the effectiveness of using both types of transducers for sonication of abdominal organs in Thiel embalmed cadavers. In this model, the induced rib-cage heating and organ motion facilitated the establishment of trans-costal sonication at distinct time points within the respiratory cycle, demonstrating the feasibility of this treatment approach and the benefit of using Thiel embalmed cadavers as a model for the development of this technology.

Acknowledgements (Funding): 1) Project FUSIMO ("Patient specific modelling and simulation of focused ultrasound in moving organs"), funded under the EU's Seventh Framework Programme for Research and Technological Development. 2) Fellowship from Focused Ultrasound Surgery Foundation.

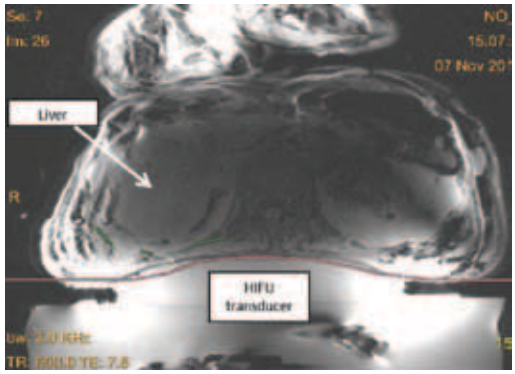

Figure 1. MRI image (Axial). Scan parameters: FSPGR, BW=2 kHz, TE=7.5msec, TR=600msec.

P-144-LP

Tuesday
16 October 2012

Topic: Liver
Presentation Type: Poster

Magnetic Resonance Guided Focused Ultrasound Ablation Surgery Accurately and Safely Targets Intra Abdominal Solid Organ Lesions in a Swine Model

Matthew McLeod, Daniel Kleiner, Amber Shada

University of Virginia, Charlottesville, Virginia, United States

Background/Introduction: High intensity focused ultrasound (HIFUS) is a noninvasive extracorporeal therapy that causes thermal injury and coagulation necrosis to targeted tissues through focalization of multiple sound waves. Incorporation of magnetic resonance (MR) anatomic guidance and MR thermal feedback allows greater precision in localizing target tissues and surrounding structures necessary for therapeutic planning and safe energy delivery in focused ultrasound surgery. Our hypothesis: MRgFUS can accurately and safely be used to target intra abdominal solid organ lesions leading to targeted tissue necrosis without collateral tissue damage.

Methods: Multiple MRgFUS sonications were performed using the ExAblate system, on a series of mock lesions in the livers and kidneys of six (9) intubated and anesthetized swine. MR thermometry using proton resonance frequency shift imaging provided location verification and thermal monitoring of targeted tissues. Each animal was euthanized immediately to inspect for collateral damage to surrounding tissues and collection of target tissues for histologic examination.

Results and Conclusions: In all segments of the liver, mock lesions demonstrated focal targeted coagulation injury on gross inspection and microscopically the lesions demonstrated increased sinusoidal hemorrhage with thermal injury and areas of coagulative necrosis with adjacent interfaces of normal tissue representing specific targeting capabilities. Major vasculature was spared with surrounding tissue necrosis. Surrounding cutaneous/subcutaneous tissues were injury free. The mock kidney lesions demonstrated gross focal ablation but less significant coagulation necrosis.

MR guided focused ultrasound surgery is a non-invasive therapy capable of delivering accurate, well visualized, and repeatable ablative thermal energy to the liver and kidney without collateral damage to surrounding tissues.

Acknowledgements (Funding): Focused Ultrasound Foundation

P-145-LP

Tuesday
16 October 2012

Topic: Pancreas
Presentation Type: Poster

MR-Guided Thermal Therapy of Pancreatic Tumors With Endogastric and Transgastric Catheter-Based Ultrasound Devices: A Feasibility Study

Punit Prakash[1], Vasant Salgaonkar[2], Serena Scott[3], Graham Sommer[4], Chris Diederich[3]

[1]Kansas State University, Manhattan, Kansas, United States
[2]University of California at San Francisco, Radiation Oncology, San Francisco, United States
[3]University of California at San Francisco, San Francicso, California, United States
[4]Stanford University, Stanford, California, United States

Background/Introduction: Image-guided thermal interventions have been proposed for palliative and potentially curative treatment of pancreatic tumors. Catheter-based ultrasound devices offer the potential for control of the 3D spatial and temporal energy deposition profile, and are under development for MR-guided thermal therapy for several disease locations. The objectives of this study were to apply theoretical and experimental techniques to investigate the feasibility of endogastric and transgastric catheter-based ultrasound for MR guided thermal therapy of pancreatic tumors.

Methods: The transgastric approach involves placement of a catheter-based ultrasound applicator (linear array of 1.5 mm OD x 10 mm L ultrasound transducers, unsectored or sectored 180°, f~7 MHz, 14g cooling catheter) inserted directly into the pancreas, either endoscopically by piercing the stomach wall or via image-guided percutaneous placement. An endogastric approach, with an ultrasound transducer assembly enclosed in a cooling balloon that is endoscopically positioned within the stomach or duodenum, can sonicate pancreatic targets from within the GI tract. Sectored tubular, planar, and lengthwise curvilinear transducers, as well as a phased array configuration, were considered for the endogastric approach. A 3D bioacoustic-thermal model was implemented using the rectangular radiator method to calculate acoustic energy distributions. A FEM solver determined the transient temperature and thermal dose profiles in tissue during heating. These models were used to determine transducer dimensions, operating frequency (3-6 MHz) and power levels, and to study the feasibility of ablating 1-3 cm diameter tumors located 2-10 mm deep in the pancreas, while thermally sparing the stomach wall. Heterogeneous acoustic and thermal properties were incorporated, including approximations for tumor desmoplasia and dynamic changes during heating. A series of anatomic models based on imaging scans of representative patients were used to investigate both approaches (Figure-1A and C). The implementation of separate cooling catheters for thermal protection of the biliary duct was investigated. Proof of concept (POC) endogastric (Figure-1B) and transgastric (Figure-1D) applicators were fabricated and experimentally evaluated in tissue mimicking phantoms under MRI thermometry. RF micro-coils were incorporated into both devices to enable active catheter-tracking and prescription of thermometry slice positions.

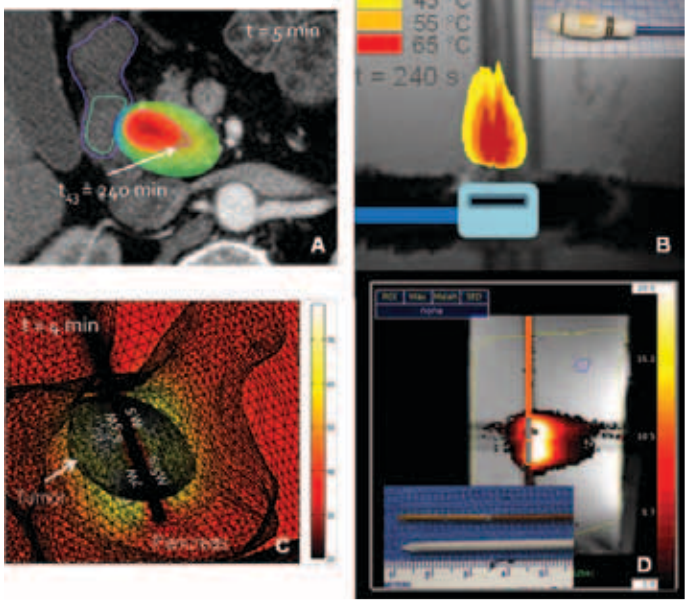

Figure 1. A) Patient-specific treatment plan for a tumor in the pancreas head ablated with an endogastric applicator, B) spatial temperature profile as measured by MR thermometry after 240 s heating with prototype endogastric ultrasound ablation device (inlet), C) temperature profile as computed by patient-specific FEM model after 240 s ablation with a multi-sectored transgastric ablation device, and D) spatial temperature profile as measured by MRT after 120 s heating with a 180° sectored transgastric applicator.

Results and Conclusions: Based on our theoretical models, unsectored and sectored interstitial ultrasound applicators could be used to ablate (t43>240min) tumors measuring 2.3-3.4 cm in diameter, when powered with 20-30 W/cm2 at 7 MHz for 5-10 mins. Endogastric applicators with planar and curvilinear transducers operating at 3-4 MHz could be used to treat tumors up to 20-25 mm away from the stomach wall within 5 min. Endogastric devices with sectored tubular transducers (10 mm OD transducer, 3-4 MHz) could ablate tumors up to a depth of 13-18 mm from the stomach wall within 5-10 mins. POC devices were fabricated and successfully integrated into the MRI environment for catheter tracking, real-time thermometry, and closed-loop feedback control. Current and future efforts will include evaluation of endoscopic device placement and targeting in an in vivo animal model.

Acknowledgements (Funding): Acknowledgements: We acknowledge support through NIH grants R21CA137472 and P01CA159992.

P-146-LP

Tuesday
16 October 2012

Topic: Pancreas
Presentation Type: Poster

MRI-Guided Focused Ultrasound Mediated Drug Delivery to Pancreatic Cancer: Safety and Efficacy

Allison Payne[1], Nick Todd[2], Christopher Dillon[2], Jill Shea[2], Roohi Gupta[3], Natalya Rapoport[2]

[1]Utah Center of Advanced Imaging Research (UCAIR), Salt lake, United States
[2]University of Utah, Salt Lake City, Utah, United States
[3]Fox Chase Cancer Center, Philadelphia, United States

Background/Introduction: Pancreatic cancer (PC) is the forth most common cause of the cancer death in the USA and presents a tough challenge for chemotherapy. PC's resistance to common chemotherapy is believed to be associated with a high content of stroma tissue in the tumor volume that prevents effective drug delivery to tumor cells. Application of tumor-directed ultrasound is expected to enhance drug diffusion in the tumor volume, drug penetration through stroma and delivery to cancerous cells. To prevent systemic drug-associated toxicities and to improve accurate drug targeting, the drug is encapsulated in an ultrasound-responsive nanocarrier (perfluorocarbon nanoemulsion). The application of MR-guided focused ultrasound (MRgFUS) both triggers drug release and enhances drug delivery to PC cells.

Methods: Red Fluorescence Protein (RFP) transfected MiaPaCa-2 tumors were subcutaneously grown in nu/nu mice. Paclitaxel (PTX)-loaded block copolymer stabilized perfluorocarbon nanodroplets were formed by perfluoro-15-crown-5-ether (PFCE) and injected systemically. The tumor was treated with MRgFUS 6 to 8 hours after the drug injection. A small animal 3-MHz HIFU device (IGT, Inc.) generated a 1 x 2 mm focal spot and all treatments were performed in a Siemens Trio 3T MRI . Spiral or grid beam trajectories were applied at four levels of continuous wave (CW) ultrasound power from 3.3 W to 13.2 W. A single treatment was given and only a fraction of the total tumor volume was treated. The temperature rise in the tumor was measured by MRI thermometry using a 2D GRE segmented EPI sequence. Five groups of animals included (1) untreated control; (2) FUS treatment without any injection; (3) FUS treatment with empty (i.e. not drug loaded) PFCE nanodroplets; (4) FUS treatment with paclitaxel (PTX) loaded PFCE nanodroplets; (5) PTX loaded nanodroplets without FUS. Cancer cell death was monitored by RFP imaging. Tumor growth/regression was monitored by RFP imaging complemented with the tumor size measurement with a caliper.

Results and Conclusions: A single combined tumor treatment with PTX-loaded nanodroplets and CW MRgFUS at 3.3 W or 6.6 W resulted in a significant delay of tumor growth and in several cases complete tumor regression. The effectiveness of the treatment appeared to depend on the ratio of a treated-to-total tumor volume. The data suggested that under ultrasound, drug was "splashed" from the sonicated volume throughout the tumor tissue. Applications of higher power levels (10 W or 13.2 W) appeared to be less effective than lower power levels; the negative effect was presumably associated with the enhanced tumor perfusion. Animals treated with MRgFUS without any injection or injected with empty droplets manifested fast tumor growth that was sometimes more accelerated than that in the untreated controls, which could result from the enhanced perfusion and/or treatment-induced inflammation. A number of animals died two to three days after the combined treatment; in these animals, MR images taken before the treatment revealed the position of the intestines in the immediate far-field of the ultrasound beam; animal death was presumably associated with the treatment-induced peritonitis.

Upon a proper ultrasound tuning, a single tumor treatment with nanodroplet-encapsulated drug and MRgFUS may result in a complete regression of the pancreatic cancer. To prevent negative effects associated with enhanced tumor perfusion, application of CW FUS at sub-ablative power levels should be always combined with the concurrent application of chemotherapeutic drugs.

Acknowledgements (Funding): FUS Foundation Grant is highly appreciated

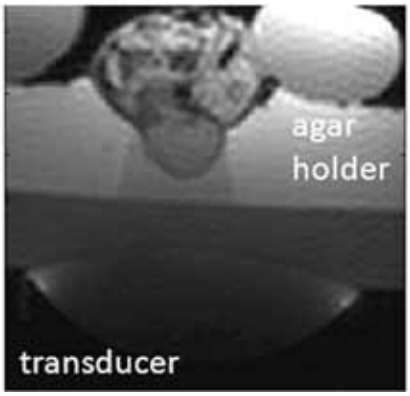

Axial image of a mouse in the experimental set.

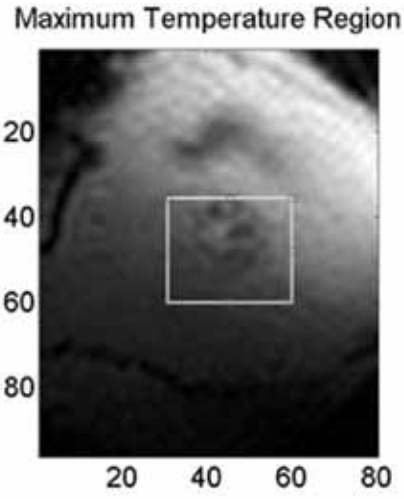

Coronal image in tumor with temperature region shown.

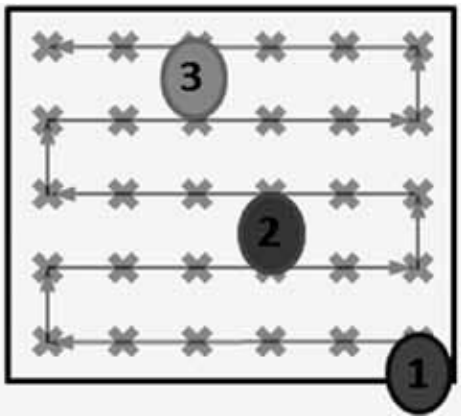

MRgHIFU treatment path with plotted voxel locations indicated.

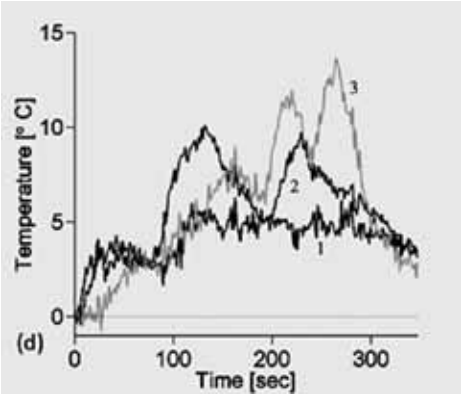

Temperature response of voxels (1); (2); and (3) as a function of time.

P-147-LP

Tuesday
16 October 2012

Topic: Liver
Presentation Type: Poster

Transfection by Plasmid DNA Following Intravenous Administration: Combination of Ultrasound and Microbubble Contrast Agent.

Jose Tlaxca[1], Alexander Klibanov[1], Balasundar Raju[2], Evgeniy Leyvi[2], William Shi[2], Shriram Sethuraman[2], Ralf Seip[2]

[1]University of Virginia, Charlottesville, Virginia, United States
[2]Philips Research North America, Briarcliff Manor, New York, United States

Background/Introduction: Gene therapy with vascular administration of naked plasmid DNA is inefficient: genetic material has to be complexed with lipid and polymer carriers, which improve intracellular transfer and result in transfection throughout the body, including non-target tissues. Ultrasound-triggered delivery of genetic material with microbubbles is now emerging as a targeted delivery technique to transfect only the insonated areas.

Transfection efficacy depends on many parameters, including ultrasound characteristics (frequency, pressure, duty cycle, focusing pattern), microbubble design and properties (concentration, circulation half-life, size, surface charge), and target model (delivery route, target location, tissue perfusion level). Optimization of the delivery and expression continues to be challenging. While novel microbubble-plasmid complex formulations are being considered, their approval for clinical use may take years. At the same time, existing clinical ultrasound contrast microbubbles co-administered with the plasmid assist transfection in the insonated tissues; this approach does not require complicated approval of a novel bubble chemical entity. We have investigated this co-administration scheme in a murine model, using lipid-shell ultrasound contrast microbubbles.

Methods: Ultrasound-assisted transfection in the liver was assessed following tail vein administration of luciferase-encoding pCMV-GL3 plasmid DNA in C57BL/6 mice, in combination with microbubbles. Focused ultrasound was provided via a Therapy Imaging Probe System (TIPS, Philips) with an 8-element annular array. Array (1mm diameter focus) was centered on the liver, and mechanically scanned in a rectangular translation pattern at 10 mm/s, repeated 6 times for the study duration (12 min). During the scan, ultrasound pulses were delivered at 1 MHz, 1 MPa peak negative acoustic pressure, 12 Hz prf. Ultrasound imaging (MI 0.1) was used to verify focal zone positioning and observe microbubble wash-in. Unfocused ultrasound was provided via a 0.75" flat transducer (A314S, Olympus, 1 MHz, 5 ms, 1 MPa, 0.033 Hz PRF, 10 min insonation). We compared intravenous bolus injection and slow infusion (co-administration) of microbubbles and plasmid. Luciferase expression was assessed with Xenogen Ivis Spectrum camera, 5 min following ip administration of luciferin.

Results and Conclusions: The dose of 50 ug plasmid did not result in a measurable luciferase expression. At 200 ug plasmid, expression was achieved, in the experiments that combined ultrasound and microbubbles. Unfocused delivery of ultrasound generated a 2.5-3.6x increase in expression vs. focused delivery. Infusion generated a 1.8-2.6x increase in expression vs. iv bolus. Ex vivo imaging of isolated organs confirmed liver transfection.

In conclusion, co-administration of clinical ultrasound contrast microbubbles and plasmid DNA may become a simple conduit towards ultrasound-triggered tissue targeted gene therapy.

Acknowledgements (Funding): Study supported by a research grant from Philips Research North America.

P-148-PR

Tuesday
16 October 2012

Topic: Prostate
Presentation Type: Poster

Development of Ultrasound Responsive- Docetaxel Encapsulated Perfluorocarbon Nanodroplets for Treatment of Prostate Cancer

Roohi Gupta[1], Xiaoming Chen[1], Dusica Cvetkovic[1], Natalya Rapoport[2], Charlie Ma[1], Lili Chen[1]

[1]Fox Chase Cancer Center, Philadelphia, Pennsylvania, United States
[2]University of Utah, Salt Lake City, Utah, United States

Background/Introduction: Treating prostate cancer remains a clinical challenge because of its heterogeneity and peculiar nature of individual cancers. Although, chemotherapy using Docetaxel (DTX) have led to improvement in survival, but these are associated with numerous drug-related toxicities and uncertainties about effective drug concentration in the tumor. One way to overcome these issues is to encapsulate DTX molecules in a shell, deliver it to the tumor and then activate its release into the tumor using focused ultrasound (FUS). In this way, DTX is delivered locally into the tumor without being toxic to healthy tissues. To achieve this goal, the present work aimed in development of ultrasound responsive DTX-loaded nanodroplets for treatment of prostate cancer.

Methods: DTX (5mg) and 20mg of biodegradable amphiphilic block copolymer {poly (ethylene oxide)-co-poly (D, L-lactide)} (PEG-PDLA) were dissolved in 1ml of tetrahydrofuran (THF). After evacuation of THF, the residual gel matrix obtained was dissolved in 1ml of phosphate buffered saline to form micelles. Perfluorocarbon (20microliters) (PFCE) was introduced in to this micellar solution and the mixture was emulsified by sonication to obtain docetaxel loaded, PFCE nanodroplets.These nanodroplets were of less than 250 nm diameter as characterized by dynamic light scattering method. To test the efficacy of the DTX loaded nanoemulsions, in vivo studies were conducted. Human prostate cancer, LNCaP cells were implanted into the prostates of male nude mice. When the tumor reached a desired size (5x5 mm), DTX nanodroplets (DTX dose - 5mg/kg) were given via i.v injections and tumors were treated with pulsed FUS (1MHz; 25W acoustic power; 10% duty cycle; 60 sec duration) using Insightec ExAblate 2000 treatment system with a 1.5 T GE MR scanner. The tumor growth was monitored with MRI and compared with the control groups.

Results and Conclusions: DTX loaded nanodroplets tend to accumulate in the tumor via enhanced permeability retention effect. When MR-guided FUS is applied to the tumor, the nanodroplets are converted into bubbles resulting in localized release of DTX in to the tumor. Our preliminary data showed effective regression of prostate tumor in mice treated with DTX nanodroplets combined with pFUS when compared to controls i.e DTX nanodroplets without pFUS and pFUS without DTX nanodroplet (work in progress).

DTX encapsulated, block copolymer stabilized PFCE nanoemulsion seems to have high potential for being effective formulations against prostate cancer when combined with image guided, focused ultrasound mediated drug delivery. Future studies will be carried out in optimizing the drug concentration in the nanodroplets for efficient ultrasound-mediated chemotherapy.

Acknowledgements (Funding): This study was supported in part by grants DOD PC073127 and DOD BC102806.

P-149-PR

Tuesday
16 October 2012

Topic: Prostate
Presentation Type: Poster

Fast and Robust Binary Temperature Controller for MRI Controlled Transurethral Ultrasound Therapy

Charles Mougenot[1], Elizabeth Ramsay[2], Mohamed Kazem[2], Rajiv Chopra[3]

[1]Philips Healthcare, Toronto, Canada
[2]Sunnybrook Health Sciences Centre, Toronto, Canada
[3]UT Southwestern, Dallas, Texas, United States

Background/Introduction: In MRI-controlled transurethral ultrasound therapy, the MR scanner plays an essential role for the guidance of thermotherapy from treatment planning, to control of the spatial heating pattern in the prostate gland during treatment. The online analysis of the deposited heat has increased in complexity as acquisition speed of the MRI has significantly increased due to higher field strength, and the introduction of larger number of receiving channels and new MRI sequences.

Simultaneously the use of a transurethral ultrasound device has the potential to reduce treatment time by sweeping the applicator over the complete prostate while sonicating simultaneously. In addition the flexibility of the device has increased with development of transducer arrays capable of sonicating at different frequencies independently for a better control of the spatial distribution of the energy emitted.

This increase of MRI data flow for real-time analysis combined with the increase of sonication parameters has led to the development of a new temperature controller with enhanced spatial and temporal accuracy, and robustness to system imperfections and tissue heterogeneities. For that purpose this study describes the evaluation of a binary controller based on a simple fuzzy logic to regulate the temperature along a target contour.

Methods: A transurethral transducer composed of 8 piezo elements of 5×4mm² operating at 4.5MHz and 14.5MHz (Sunnybrook Health Sciences Centre, Toronto, Canada) was attached to a rotational piezoelectric motor and inserted in a tissue-mimicking gel phantom. Tests were conducted inside a Philips Achieva 3T MRI to acquire every 3.7s a set of 5 contiguous transversal slices aligned with each element used by the feedback algorithm and 1 slice sagittal to get an overview of the complete treatment. The PRF thermal map resolution was 1.1×1.1×5mm³. Treatment planning and feedback controller was implemented on Sonalleve software (Philips Healthcare, Helsinki, Finland). A target volume comprised of 3 planes with a prostate-shaped target in each plane (radius ranging from 13 to 19 mm) was defined manually. When the temperature along a given contour was lower than the target temperature of 55°C, the power on the respective element was set to 4W (acoustic) and the rotation speed to 8 °/min. For all other cases, the power was turned off and the rotation speed was set to 40 °/min. The minimum rotation speed was selected across all elements to define the applicator rotation speed. As a consequence, the application was either sonicating at maximal power and rotating slowly or not sonicating and rotating at the maximal speed toward another part of the target contour.

Results and Conclusions: The thermal map on the left side of the figure (see next page) shows the maximum temperature distribution achieved since the start of the sonication for one element. The 55°C transition between the red and yellow colored voxels match with the location of the initially planned target contour. The resulting necrosis defined by the 240 CEM43 dose contour is slightly larger to ensure treatment with a positive margin. A better match between target contour and the 240 CEM43 dose contour could be achieved by using a target temperature of 52°C.

The graph on the right side of the figure illustrates the performance of the controller since the temperature at the boundary is maintained in average to 54.8°C across all elements with a standard deviation of 1.6°C. Because the sonication parameters are redefined after each set of acquired images independently of thermal history and only vary between the maximum or minimum rotation speed and power, this controller has a very fast response time. In addition this simple fuzzy logic evaluates the power and the rotation speed in only 60 ms which avoids additional system response delay.

To conclude, the use of binary controller is an effective way to control precisely the temperature over multiple slices with multiple piezo-elements without requiring prior knowledge of tissue model and fine calibrating tuning of the device.

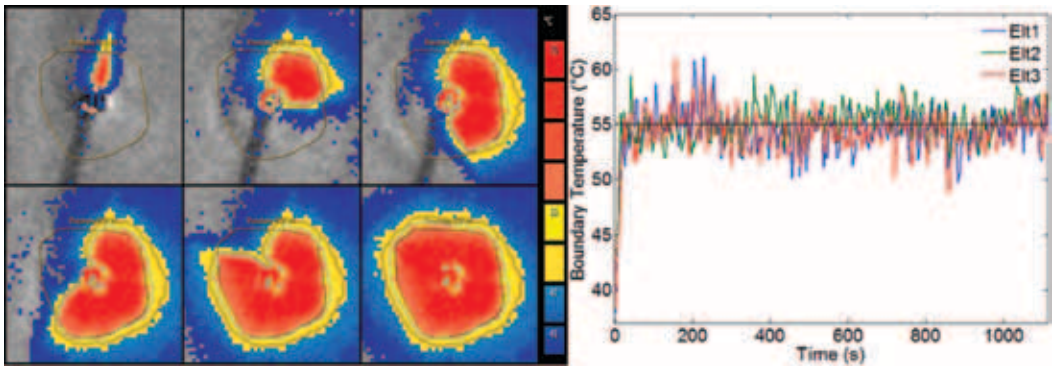

Thermal maps on the left correspond to the maximum temperature measured since the beginning of the sonication for different time point of the full treatment. The inner yellow line corresponds to the initially planned target contour. The white and orange contours correspond to the thermal dose threshold of 240 CEM43 (necrosis) and 30 CEM43 (oedema). The temporal graph on the right indicates the temperature at the target boundary for each element used (solid color lines) relatively to the target temperature of 55Â°C (dot dark line).

P-150-PR

Tuesday
16 October 2012

Topic: Prostate
Presentation Type: Poster

Non-Thermal Effect of Pulsed High-Intensity Focused Ultrasound - an in Vivo Study

Charlie Ma, Dusica Cvetkovic, Xiaoming Chen, Roohi Gupta, Lili Chen

Fox Chase Cancer Center, Philadelphia, Pennsylvania, United States

Background/Introduction: Extensive studies have been carried out on MR guided focused ultrasound (MRgFUS) for ablative therapy and drug enhancement for gene therapy and chemotherapy by many investigators and in our institution. In this work we have conducted in vivo animal experiments to explore the feasibility of pulsed high-intensity focused ultrasound (pHIFU) for non-thermal cancer therapy.

Methods: Phantom studies were first carried out to obtain suitable US parameters for non-thermal (below 42° C) sonications using an InSightec ExAblate 2000 system with a 1.5T GE MR scanner. Different combinations of acoustic powers and duty cycles were investigated, keeping the temperature below 42° C as measured by real-time MR thermometry. Nude mice with implanted (LNCaP) prostate and (MCF-7) breast cancers were treated with pHIFU (1 MHz; 5 & 25 W acoustic power, 0.1 & 0.5 duty cycle; 60 sec duration). The animals were allowed to survive for 4 weeks after the treatment. The tumor growth was monitored on a 7T MR scanner and compared with the control group.

Results and Conclusions: Significant tumor growth delay was observed in the mice treated with pHIFU. The mean tumor volume for the pHIFU treated mice was 30% and 65% smaller than that of the control mice for 5 W/0.5 duty cycle and 25 W/0.1 duty cycle treatment settings, respectively. Histology analyses performed at different time points after the pHIFU sonication indicated non-ablative cell damage together with apoptotic/mitotic cell deaths.

These in vivo experiments demonstrated that non-thermal pHIFU has a great potential for cancer therapy. Further experiments are needed to derive optimal ultrasound parameters and fractionation schemes to maximize the therapeutic effect and to investigate normal tissue toxicities.

Acknowledgements (Funding): This study was supported in part by grants DOD PC073127 and DOD BC102806. Technical support from InSightec is acknowledged.

P-151-UF

Tuesday
16 October 2012

Topic: Uterine Fibroids
Presentation Type: Poster

Magnetic Resonance Guided Focused Ultrasound Treatment of Uterine Fibroids: Comparison of the Exablate 2000 to the Exablate 2100 System

Stephen Quinn[1], John Vedelago[2], Wladislaw Gedroyc[1], Lesley Regan[1]

[1]Imperial College London, London, United Kingdom
[2]St. Mary's Hospital, London, United Kingdom

Background/Introduction: Magnetic resonance guided focused ultrasound ablation of uterine fibroids was performed using the Insightec Exablate2000 system at our institution from 2003 to January 2011.

Methods: In January 2011, a new software and transducer system, the Exablate 2100 system, was adopted. We examine the first year of using the Exablate 2100 system and compare it's safety profile and non-perfused volumes achieved to data obtained from the previous eight years, using the the Exablate 2000. We also describe differences in pre-treatment planning, patient selection and the characteristics of treated fibroids and uteri between the two groups.

Results and Conclusions: Overall, the new system has shown thus far an impeccable safety record and a significant improvement in non-perfused volumes achieved.

P-152-UF

Tuesday
16 October 2012

Topic: Uterine Fibroids
Presentation Type: Poster

MR Elastography Demonstrates Increased Stiffness of Uterine Fibroids

David Woodrum, Krzysztof Gorny, Suganti Shivaram, Joel Felmlee, Gina Hesley, Shannon Laughlin-Tommaso, Elizabeth Stewart, Richard Ehman

Mayo Clinic, Rochester, Minnesota, United States

Background/Introduction: The purpose of this study was to examine the feasibility of performing MR elastography (MRE) for uterine fibroid tissue characterization. To date, very little is known concerning how the tissue composition of the uterine fibroid may affect uterine treatments including surgery, UAE, and MR-guided focused ultrasound ablation. In this study, we use a new noninvasive technology, MR elastography, to further characterize the elastic properties of the uterine fibroids.

Methods: This study was a prospective nonrandomized single arm study with IRB approval. 55 women undergoing pelvic MRI for uterine fibroids were enrolled. MRI was performed with a 1.5-T system (Signa, GE Healthcare) with a phased-array pelvic coil. MR Elastography was performed at the end of the examination after the standard MRI fibroid protocol. A 19-cm-diameter 1.5-cm-thick cylindric passive driver developed within our institution was placed against the anterior abdominal wall over the fibroid with the center of the driver between the umbilicus and pubic bone. Continuous acoustic vibration at 60 Hz transmitted from an active driver to the passive driver through a flexible vinyl tube is used to produce propagating shear waves through the abdominal wall into the fibroid. The propagating shear waves are imaged with a modified phase contrast, gradient-echo sequence (MRE sequence) for collection of axial wave images sensitized along the through-plane direction of motion. The fibroids are identified on T2- and contrast-enhanced T1-weighted MR images, and the MRE slice is targeted to the dominant fibroid. The slice thicknesses are 6-10 mm modified according to the size of the focal lesion studied.

Results and Conclusions: Fifty-five women were enrolled with MR elastography performed during pelvic MRI. Within this group, 12 were excluded from stiffness analysis due to technical failure (5), no fibroid (4), malignant neoplasm (1), and fibroids <1cm. In this cohort of women, 45% were premenopausal, 47% were perimenopausal, and 7% were postmenopausal. Menorrhagia symptoms ranged from mild (35%), moderate (16%), to severe (49%). 31% had dysmenorrhea and 33% had urinary frequency. 35% had pelvic pain and 29% had pelvic pressure symptoms. The number of uterine fibroids ranged from 1-6 with an average of 3. Fibroid volume averaged 359 cm3 with average largest diameter of 8.15 cm. Most (83%) of the fibroids had low homogenous T2 signal and enhanced with gadolinium (95%). The dominant fibroid stiffness averaged 5.069±2.071 kPa whereas the average tissue stiffness for myometrium was significantly lower at 3.370±0.880 kPa ($P<0.05$).

Conclusion: MRE of uterine fibroids is possible and confirms increased stiffness of fibroids compared to autologous myometrium. Future work will focus on the clinical utility of MRE in diagnosis of uterine neoplasms and guidance of treatment choice and outcomes following various minimally invasive alternatives to hysterectomy.

Acknowledgements (Funding): Investigator time was funded by NIH HD RC1063312 and R01060503

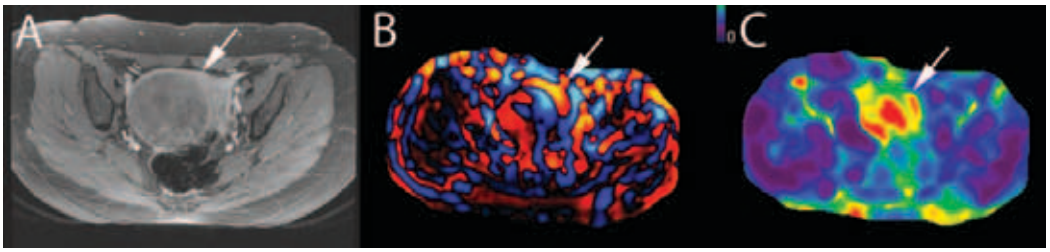

Panel A depicts T2 weighted pelvic axial image through a uterine fibroid (arrow). Panel B is phase images demonstrating shear wave propagation through the fibroid. Panel C demonstrates the calculated stiffness map showing increased stiffness (red coloration) within the fibroid.

P-153-UF

Tuesday
16 October 2012

Topic: Uterine Fibroids
Presentation Type: Poster

MRgFUS Treatment of Uterine Fibroid in a Nulliparous Woman With Acute Retention of Urine

Laveena Polina[1], Vinay Nyapathi[2]

[1]Godavari Imaging Sciences and Research Center, Rajahmundry, India
[2]GSL Medical College, Rajahmundry, India

Background/Introduction: Uterine fibroids are the most common tumors of the female reproductive tract. Treatment options for symptomatic fibroids include hysterectomy, myomectomy ,uterine artery embolization, MR-guided Focused Ultrasound (MRgFUS), and hormonal therapy. MRgFUS is a non-invasive treatment for symptomatic uterine fibroids. The following case report demonstrates successful treatment by MRgFUS of a fibroid that is hyper-intense on T2WIs with immediate alleviation of pressure symptoms on the urinary bladder.

Methods: A 44 year old unmarried, nulliparous Indian woman, BMI of 24.5 with a large uterine fibroid was referred to our center with Foley's catheterization of the urinary bladder for acute retention of urine that occurred one week prior. She also complained of heavy bleeding, passing clots, fatigue and backpain for the past 6 months and amenorrhea since 2 months. Her Symptom Severity Score (on the 0 to 100 Scale of the UFS-QoL questionnaire was 47.5 points. MRI showed a single intramural fibroid in the posterior myometrium measuring 9.0 x 5.6 x 7.2cm with a volume of 176cc on T2WI. Relative to the uterine wall, the fibroid was hyperintense and heterogeneous on T2WIs. Post-gadolinium contrast images revealed enhancement.

The treatment procedure incorporates a 1.5T MRI scanner (Signa HD, GE Healthcare, Milwaukee,WI, USA) along with a focused ultrasound system (ExAblate 2000, Insightec, Haifa, Israel). The operator uses the integrated system to deliver accurate energy pulses (termed sonications) to a location identified on anatomical T2-weighted MRI images. The heat generated during the course of these sonications is monitored using images acquired in real-time .Treatment duration was 2 hours utilizing 75 sonications with a mean energy of 2345 Joules. Post treatment contrast images showed a non-perfused volume (NPV) of 100cc achieving an NPV ratio of 54%.

Treatment was completed without complications and the patient was discharged 30 min later. The Foley's catheter was removed after 6hours.The next morning she reported that she was able to pass urine normally and was feeling well. At 3 months follow up she is asymptomatic.

Results and Conclusions: MRgFUS is a suitable treatment option for symptomatic myomas especially in patients who wish to retain future fertility.

- Even in hyperintense fibroids, MRgFUS can attain an NPV significant enough to cause symptomatic relief.
- In patients with fibroids causing acute urinary retention, MRgFUS can produce immediate symptomatic relief.

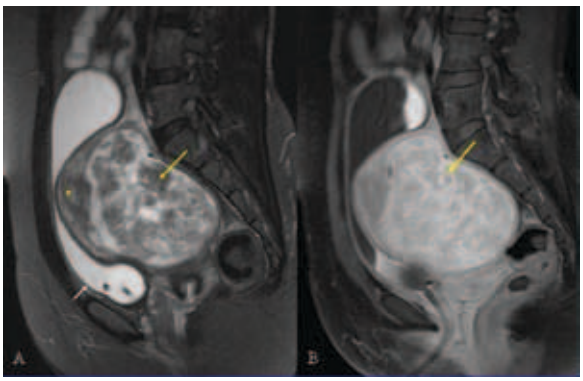

A: T2WI fat suppressed sagittal screening MR of the pelvis shows a heterogenous fibroid (yellow arrow), hyperintense relative to the uterine wall (asterix). Note the Foley's bulb in urinary bladder (white arrow).
B: Contrast enhanced SPGR sagittal screening MR of the pelvis shows enhancement of the fibroid (yellow arrow).

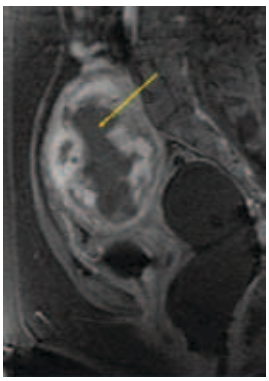

Contrast enhanced spoiled gradient recalled acquisition in the steady state (SPGR) sagittal MR of the pelvis after MRgFUS treatment shows non enhancing area (arrow) corresponding to non-perfused volume of 54%

P-154-UF

Tuesday
16 October 2012

Topic: Uterine Fibroids
Presentation Type: Poster

Noninvasive Treatment of Focal Adenomyosis With MR-guided Focused Ultrasound in Two Rural Indian Patients

Laveena Polina[1], Vinay Nyapathi[2]

[1]Godavari Imaging Sciences and Research Center, Rajahmundry, India
[2]GSL Medical College, Rajahmundry, India

Background/Introduction: Adenomyosis is a common benign gynecological disorder affecting premenopausal women and having a significant impact on a woman's health and quality of life. We present two cases of focal adenomyosis treated with MRgFUS and showing good symptomatic relief at 3 and 6 months follow-up.

Methods: Case 1 The patient was a 39-year-old nulliparous Indian woman with a body mass index (BMI) of 25.11. Her symptom severity score (SSS) was 47.5 points on the 0 to 100 scale of The Uterine Fibroid Symptom and Quality of Life UFS-QoL questionnaire. Her menstrual pain score was 10 on a scale of 0 to 10.

MRI of the pelvis showed marked thickening of the junctional zone, with 5.4 × 4.8 × 5.9 cm (volume: 91 cc) focal adenomyosis involving the posterior myometrium .Post-gadolinium contrast images revealed homogenous enhancement.

Treatment duration was 1 h 50 min (from first to last sonication), utilizing 31 sonications with a mean energy of 3516 Joules and a frequency of 1.15 MHz. The average temperature achieved was 73.4°C (min: 43°C; max: 102°C). A NPV of 40 cc and NPV ratio of 44% was achieved.

Treatment was completed without complications .At 3 months follow-up, the patient had a SSS score of 32.5 and menstrual pain score of 4. At 6 months follow-up, her SSS score had reduced to 25 points and she was totally free of the menstrual pain, with a score of 0 points.

Case 2 The patient was a 43-year-old multiparous Indian woman with a BMI of 24.2. Her SSS and menstrual pain score were 50 and 8, respectively. MRI showed marked thickening of the junctional zone, with a 4.4 × 3.4 × 5.0 cm (volume: 47 cc) focal adenomyosis involving the posterior myometrium.In addition, a 4.6 × 3.6 × 4.2 cm (volume: 35 cc) intramural fibroid, homogenously hypointense on T2W images, was noted involving the right side of the fundus of the uterus. Post-gadolinium contrast images revealed homogenous enhancement in the focal adenomyosis and heterogenous enhancement in the fibroid .

Both the fibroid and the adenomyosis were treated in 2 h 40 min, using 64 sonications with a mean energy of 1250.78 Joules and a frequency of 1.15 MHz. The average temperature achieved was 85.5°C (min: 53°C; max: 148°C). Post treatment, a nonperfused volume of 30 cc and NPV ratio of 63.8% was achieved in the focal adenomyosis. Nonperfused volume of 30 cc and NPV ratio of 85.7% was achieved in the fibroid. At 3 months follow-up, the patient had a SSS score of 40 and menstrual pain score of 5. At 6 months follow-up, her SSS score had reduced to 24 points and she was totally free of the menstrual pain, with a score of 0 points.

Results and Conclusions: Our case reports suggest that clinical improvement in symptomatic adenomyosis is achievable within a short period of time after treatment with MRgFUS. MRgFUS is a noninvasive, day-care procedure, requiring no admission and having a low complication rate. MRgFUS may be a promising alternative to hysterectomy for the patient with adenomyosis who wishes to preserve her uterus.

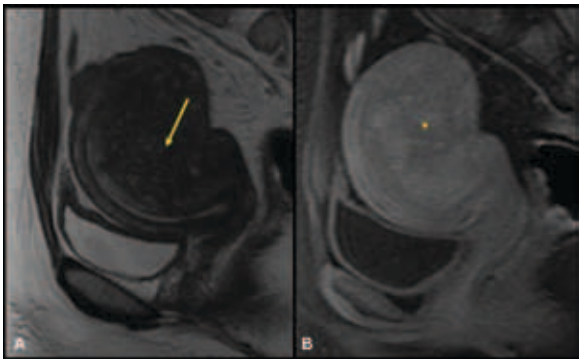

A 39-year-old nulliparous woman with focal adenomyosis. Sagittal T2W screening MRI of the pelvis (A) shows focal adenomyosis (yellow arrow) involving the posterior myometrium.

Contrast-enhanced spoiled gradient-recalled acquisition in the steady state (SPGR) (B) shows homogenous enhancement in the focal adenomyosis (asterisk).

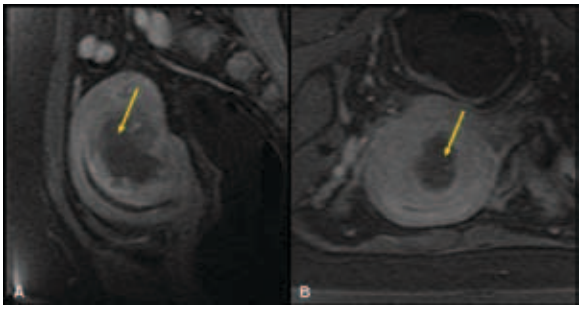

A 39-year-old nulliparous woman with focal adenomyosis. Contrast-enhanced SPGR sagittal (A) and axial (B) MR of the pelvis after MRgFUS treatment shows nonenhancing area (arrow) corresponding to nonperfused volume of 44%.

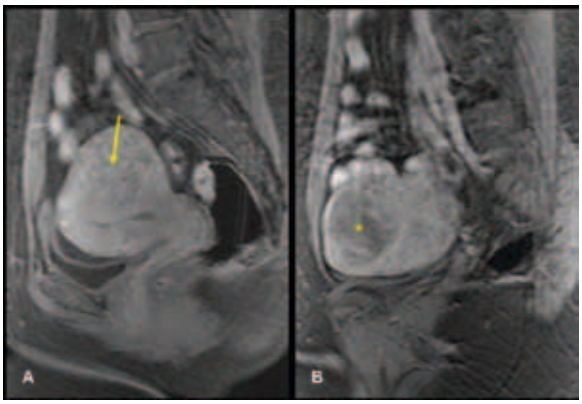

A 43-year-old multiparous woman. Contrast-enhanced SPGR sagittal screening MR of the pelvis (A, B) shows homogenous enhancement in the focal adenomyosis (arrow) and heterogenous enhancement in the fundal fibroid (asterisk).

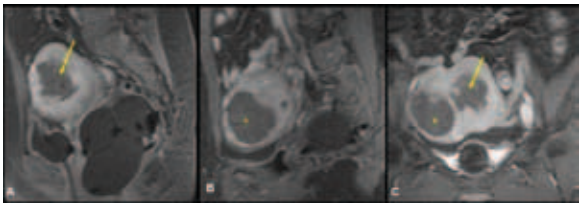

A 43-year-old multiparous woman. Contrast-enhanced SPGR sagittal (A, B) and coronal (C) MR of the pelvis after MRgFUS treatment shows nonenhancing area corresponding to nonperfused volume of 63.8% in the focal adenomyosis (arrow) and 85.7% in the fibroid (asterisk)

P-155-UF

Tuesday
16 October 2012

Topic: Uterine Fibroids
Presentation Type: Poster

Multiple Fibroid Therapy on Ablation of Single Fibroid With MR-HIFU: A Postulation Towards Enhanced Treatment Efficiency

Harsh Rastogi

Indraprastha Apollo Hospitals, New Delhi, India

Background/Introduction: Fibroids are known to be of monoclonal origin with clonal expansion and proliferation of somatically mutated cell. However, it is unclear if the same monoclonal cells seed multiple fibroids and if they carry their blood supply from parent fibroid while seeding the other parts of uterus. This study reports some interesting findings on how MR-HIFU treated symptomatic fibroids result in persistent non-perfusion of adjacent fibroids.

Methods: From our routine clinical practice with MR-HIFU treatments of fibroids, we analyzed four patients with multiple fibroids. Only the fibroids (including the largest) whose location and size correlated with the patient's symptoms were ablated with MR-HIFU therapy using volumetric ablation technique. Patient 1 presented with 10 fibroids and only two of the most inferior fibroids (measuring 7.9x7.3 cm and 4.9x6cm in coronal section) were treated. Patient 2 presented with 7 fibroids, the largest of them on anterio-superior aspect of uterus (measuring 5.4x5.6cm in coronal section) was treated. Patient 3 presented with more than 15 fibroids. Three of them including the largest left inferio-lateral (measuring 4.6x4.7cm in coronal section), and two adjacent (measuring 1.8x1.9cm and 3.5x3.6cm) were treated. Patient 4 presented with 2 fibroids (measuring 6.8x8.9cm and 7.6x4.8cm) that were divided by a septum and had a visible feeding blood vessel entering infero-laterally from the right side. Only the inferior fibroid and the septum were ablated.

Results and Conclusions: In all the four cases, non-perfused volume was observed in fibroids which were not targeted for ablation. Also, none of them had any non-perfused areas in the healthy myometrium. In patient 1: 5 of the non-treated fibroids showed non-perfusion. In addition, some of the vessels visible on T2 weighted images were seen to shrink post treatment even though they were not targeted. In patient 2, 1 additional fibroid was not perfused post treatment. In patient 3, 7 additional fibroids showed an NPV which persisted in 6 of them even on 1 month follow up of the patient. In patient 4, the superior fibroid had almost complete NPV although it was never targeted.

Conclusion: There seems to be a common thread between multiple fibroids that allows loss of blood supply to many of the non-ablated fibroids on treatment of the largest fibroid. We postulate that there appears to be a common blood vessel (or its branches) that perfuses all the fibroids that show nonperfused volume after ablation, probably linked to their monoclonal origin. More work is needed to be done, to explore and understand this mechanism and to allow a new non-invasive methodology with MR-HIFU for more efficient treatment of multiple fibroids by just targeting few of them.

P-156-UF

Tuesday
16 October 2012

Topic: Uterine Fibroids
Presentation Type: Poster

Phase 3 Clinical MRgFUS Treatment of Large Uterine Fibroids Using the Insightec ExAblate 2000: The Methodist Perspective

Howard Vo[1], Christopher Hobday[1], Denise Nebgen[2], Nam Yu[1], King Li[3]

[1]The Methodist Hospital, Houston, United States
[2]MD Anderson, Houston, United States
[3]Wake Forest School of Medicine, Winston-Salem, United States

Background/Introduction: MRgFUS is a promising non-invasive, non-radiation, point-focused therapy that has been FDA-approved for the clinical treatments of uterine fibroids. In our limited clinical study of large uterine fibroids , we shall examine procedural times and resource utilization in MRgFUS.

Methods: The Methodist Hospital (TMH) participated in a recently completed Insightec-sponsored multi-site clinical trial on uterine fibroid ablations using the Insightec ExAblate MRgFUS therapy. A total of 15 volunteers with large uterine fibroids (more than 50 mL) were chosen for the experimental treatment in accordance with both TMH's IRB and Insightec guidelines. Each treatment was scheduled for a 7-hour MRI scanner room occupancy during which other competing clinical MRI studies were deferred. For some patients, the fibroids required an additional day of treatment as allowed by the protocol and the treatment was also scheduled on a busy day.

Each treatment day was further divided into three time blocks. The first time block consisted of therapy setup and patient positioning. The second time block was allotted for ROI definition and treatment which requires manual adjustment of sonication location and its acoustic parameters. The final time block involved data viewing and setup restoration. Post-treatment MR images were taken and compared to pre-treatment MR images. The therapy setup was disassembled and the original setup restored so that the previously deferred MRI studies could now resume.

Results and Conclusions: The outcome of all the treatments was favorable. The minimum treatment coverage of each primary fibroid volume was 50%. The first time block occupied approximately 3 hours of MRgFUS time of which the majority was allocated to therapy setup with the rest of the time allocated to patient positioning. The second time block also took approximately 3 hours of MRgFUS time for treatment. The third time block took approximately 1 hour of which the majority was allocated to setup restoration. Active MRgFUS usage was about 6 hours of which about 4 hours was physician time. At least 4 personnel were present throughout each treatment.

Because MRgFUS of fibroids can be resource-intensive, it is reasonable to find ways to improve the existing procedures. Henceforth, we propose greater flexibility in hardware, software and administrative personnel scheduling which we believe will result in more efficient treatments, greater patient comfort, and less cost to both the patients and the institutions. We also believe that these benefits will have a greater appeal to both prospective patients, clinicians and researchers. Although our specific recommendations apply to the study of fibroids, they may also be useful to other MRgFUS treatments.

Acknowledgements (Funding): This work is supported by FUSF and Insightec Co.

P-157-UF

Tuesday
16 October 2012

Topic: Uterine Fibroids
Presentation Type: Poster

Pregnancy in Women Post-Treatment of Uterine Fibroids With MRgFUS

Ana Maria Ruiz Santos[1], Helena Millán Cantero[2], Emilio Gómez González[3], Jeronimo Suarez-Ramos[4]

[1]Llerena, Spain
[2]Instituto Cartuja de Tecnicas Ayanzadas en Medicina, Sevilla, Spain
[3]University of Seville, Seville, Spain
[4]Instituto Cartuja, Seville, Spain

Background/Introduction: Our objective is to analyze the results of the treatment of uterine fibroids with non invasive surgery treatment (MRgFUS) in Spain, focusing on women who wanted a pregnancy and was affected of uterine fibroid and did not want to go through conventional surgeries.

Methods: A retrospective review of all our cases, 52 women, and collected only the women who has been pregnant and studied the following data from each patient: age, type of treated fibroids and location, previous symptomatology, sterility and gravidity. From each treatment were collected duration, sonication number and non-perfused volume reached. All patients were treated under conscious sedation and were sent home an hour later. Follow up was performed by phone. We studied the results of these pregnancies too.

Results and Conclusions: The study population was reduced to six patients, between 36-41 years old (mean 37.88). 75 % of patients observed referred sterility symptomatology and failure in reproductive techniques. In our series no one mild side effects were reported. More than a half of patients (63.04 %) referred subjective improvement in another previous symptomatology three months after treatment. Five of them have delivered six healthy newborns, and we had two miscarriages in the same patients. After treatment, mean time passed between the treatment and conception was 3,6 months (range 1-7). Deliveries have been one vaginal and five cesarean sections due to vasa previa, face presentation, previous myomectomy, previous fibroid and non reassuring fetal cardiograph. No complications were recorded during pregnancy, labor or postpartum periods. All deliveries took place after 38 weeks, average 39 weeks. Newborn mean weight was 3138 gr ± 1,17(range 2700-3800).

This is the first serie of cases published in Spain. Our results seem to confirm that MRgFUS is an effective technique for the conservative treatment of uterine fibroids and it is possible to use security in women who wants a pregnancy if they are carefully selected. Our fertility results are very promising since 6 patients have conceived after MRgFUS treatment (two of them twice). Six pregnancies have been full-term, all of them older than 36 years old and 75% referring previous sterility problems.

P-158-UF

Tuesday
16 October 2012

Topic: Uterine Fibroids
Presentation Type: Poster

The Impact of Magnetic Resonance Guided Focused Ultrasound Surgery (MRgFUS) on the Quality of Life in Patients With Uterine Fibroids

Jamshid Farahati[1], György Lövey[1], Hans Christian Kolberg[1], Heike Rotter-Dier[1], Elena Gilman[2], Eberhard Heissen[2]

[1]MRgFUS Center Bottrop, Bottrop, Germany
[2]Institute of Radiology, Bottrop, Germany

Background/Introduction: Uterine fibroids are considered as one of the most important factors affecting the quality of female life. The aim of this study was to evaluate the efficacy of MRgFUS on treated patients with uterine fibroids, for symptoms relief and improving the quality of life.

Methods: 38 women were treated during 2011 with MRgFUS (Exablate 2000, Insightec Ltd.) in our MRgFUS center at Bottrop, Germany. Women were asked to participate in a questionnaire to evaluate their treatment results. All women had symptomatic uterine fibroids, and their age was between 25 to 53 years (42.34±6.33). The quality of pain and symptoms relief was recorded by a Visual Analogue Score (VAS), on a scale of 1-5 (1 representing no complaints and 5 representing severe complaints). Baseline data was collected one day before the MRgFUS treatment, and follow up was done at 3.6,9 and 12 Months post- treatment (Figure). Response to MRgFUS treatment was considered as improvement of at least 2 points in the VAS, compared to the baseline. Characteristics of responders and non-responders were compared by paired Student`s t-Test with a p value of <0.05 as the significant niveau.

Results and Conclusions: The baseline fibroids volume ranged between 9.9 and 314 ml (109±94.1), and the non-perfused volume (NPV) ratio, as measured from the post gadolinium scans, was between 24 and 93% (69.4±15.2%). Total number of sonications per treatment was between 11 and102 (43.1±22.1) with an average focal temperature of 82.6?±7.44? ranging from 65 to -90?C. Average sonication time was 140.4±61.6 minutes (20-240 min.). Two cases of complications were reported during the treatment and follow-up time; one case with a second degree skin burn and one case of reversible severe post therapy abdominal pain. Both cases were resolved within 6 days

The mean score for all recorded symptoms (VAS) declined at 3 months post- MRgFUS and revealed no significant changes up to 12 months. 30 patients (79%) were free of complaints or showed significant symptom relief after the MRgFUS treatment.

NPV ratio was the only factor differing between the responders and non-responders significantly (p=0.02), whereas age, volume of fibroids, mean sonication time and focal temperature were not significantly different between both groups.

Conclusions:

1. MRgFUS is an efficient and safe modality for treatment of uterine fibroids with improvement of quality of life in 79% of treated patients during a 12 months follow-up.

2. Improvement of symptoms after the MRgFUS treatment occurs within the 3 months follow up period.

3. NPV ratios may act as a predictive marker for the clinical outcomes in fibroid patients treated with MRgFUS.

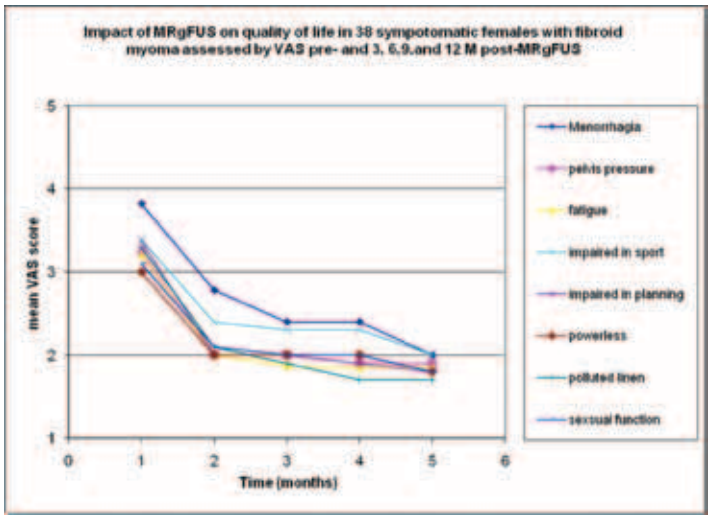

Impact of MRgFUS on quality of life in 38 sympotomatic females with fibroid myoma assessed by VAS pre- and 3, 6,9,and 12 M post-MRgFUS

P-159-YI

Tuesday
15 October 2012

Topic: Young Investigator
Presentation type: Poster

Complete or Near-complete Ablation of Symptomatic Uterine Fibroids by Volumetric MR-guided High-intensity Focused Ultrasound Therapy: Assessments of Safety and Therapeutic Efficacy

Min Jung Park

Samsung Medical Center, Seoul, Korea

This poster is based on oral presentation 20-UF.

P-160-YI

Tuesday
15 October 2012

Topic: Young Investigator
Presentation type: Poster

Cost-Effectiveness Analysis of Uterine-Preserving Procedural Treatments for Uterine Fibroids, Including Magnetic Resonance-Guided Focused Ultrasound (MRgFUS)

Anne Cain-Nielsen

University of Michigan School of Public Health, Ann Arbor, Michigan, United States

This poster is based on oral presentation 28-UF.

P-161-YI

Tuesday
15 October 2012

Topic: Young Investigator
Presentation type: Poster

Effects of HIFU Ablation on Bone Metastases: From MRI, SPECT/CT and MicroCT Point of View

Sin Yuin Yeo

Eindhoven University of Technology, Eindhoven, Netherlands

This poster is based on oral presentation 62-BM.

P-162-YI

Tuesday
15 October 2012

Topic: Young Investigator
Presentation type: Poster

Enhanced delivery of liposomal doxorubicin via permeabilization of the blood-brain/blood-tumor barriers using focused ultrasound and microbubbles significantly improves survival in a rat glioma model after multiple treatments

Muna Aryal

Boston College/Brigham and Women's Hospital, Boston, Massachusetts, United States

This poster is based on oral presentation 12-BR.

P-163-YI

Tuesday
15 October 2012

Topic: Young Investigator
Presentation type: Poser

Enhanced MR-guided HIFU Ablation of Rabbit VX2 Tumors In Vivo using Phase-Shift Nanoemulsions

Jonathan Kopechek

Boston University, Boston, Massachusetts, United States

This poster is based on oral presentation 12-BR.

P-164-YI

Tuesday
16 October 2012

Topic: Young Investigator
Presentation Type: Poster

Localisation of Prostate Cancer Foci With Transrectal Quantitative Shear Wave Elastography - A Step Towards Focal Therapy for Prostate Cancer

Sarfraz Ahmad, Omar Aboumarzouk, Ghulam Nabi

Ninewells Hospital / University of Dundee, Dundee, United Kingdom

Background/Introduction: Standard grey scale transrectal ultrasound (TRUS) is based on increased brightness in relation to the strength of the echo, intrinsically falls short of making a reliable differentiation between cancer and normal hyperplasia of the prostate gland. Shear wave elastography (SSI) is a new method of obtaining quantitative tissue elasticity data during TRUS biopsies of Prostate. The aims of this study were;

1- to determine the whether SSI can help in picking up extra cancer foci to the current 12 core biopsies technique.

2 - to compare quantitative SSI for benign/malignant classification.

Methods: A prospective protocol driven study with prior ethical and institutional approval was designed to assess the feasibility of SSI in the detection of Prostate cancer (PCa). Using the Aixplorer® ultrasound system (SuperSonic Imagine, Aix en Provence, France), patients with suspected PCa underwent transrectal 12- core systematic biopsies. Additional biopsies were directed using shear wave mode of the machine, if the lesions appeared to be outside the biopsied area. Two orthogonal elastography images were obtained of each region of the biopsied areas. Elastsography measurements were correlated with histology results. Prior to recruitment of patients for the study, a custom made commercially available prostate phantom model 066 (CIRS, Tissue simulation & Phantom technology, Virginia, USA) was used for training, optimisation of the prostate gland sonographic technique and assessment of inter-observer variations.

Results and Conclusions: The phantom studies showed the abnormal foci within the phantom models were visible only with SSI (Figure 1 a-b). Fifty (50) patients were recruited into the study. The data was divided into two groups: patients with PSA ≤ 20µg/L (n = 39) and patients with PSA > 20 µg/L (n=11). SSI detected abnormal areas which were not visible with grey scale ultrasound (Figure 2). Of all the patients, thirty three (33/50; 66%) were diagnosed with PCa while additional 4 (8%) patients had PIN or atypia. Thirteen (13/50; 26%) patients had benign biopsies. PCa had higher stiffness as compared to benign tissues; Benign vs PCa (PSA≤ 20) - p = 0.008. Benign vs PCa (PSA>20) - p = 0.0007. PCa (PSA ≤ 20) vs PCa (PSA>20) - p = 0.003. Additionally, It was observed that the mean Young modulus (kPa) was higher in prostate cores with a Gleason score of 7 (163 kPa ±63) than in those with a Gleason score of 6 (95 kPa ± 28.5) [p = 0.007]. The mean Young modulus of Gleason 8 cores was 113 kPa (±20), however this was not statistically different (p > 0.05) from Gleason score 6 and 7 cores.

Conclusions: The SSI provides quantitative information about the prostatic tissue and in our preliminary observation can accurately direct biopsies to the cancer foci within the prostate. This has huge potential for focal treatment and future prostate biopsies protocols.

Acknowledgements (Funding): The authors thank Super Sonic Imagine (Super Sonic Imagine, Aix en Provence, France) for an equipment grant to support this work.

The abnormal nodules (representative of the cancerous tissues) within the prostate phantom were only visible with SWE (shown as yellow colour nodules).

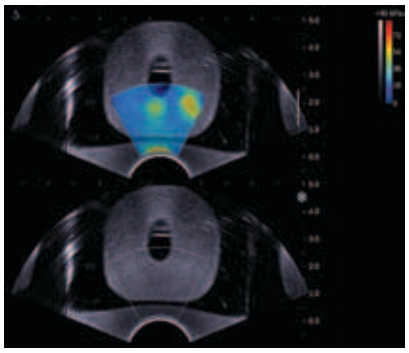

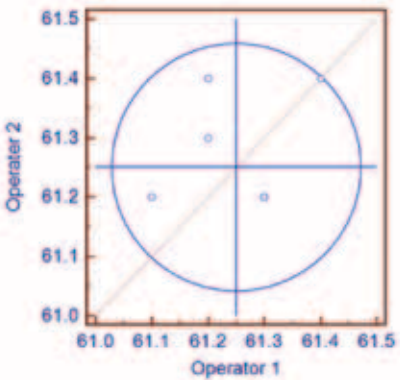

The correlation between measurement by two observers of the mean stiffness on each pair of elastography images acquired by two different operators with an intraclass correlation coefficient of 0.93 (95% CI 0.62 to 0.99).

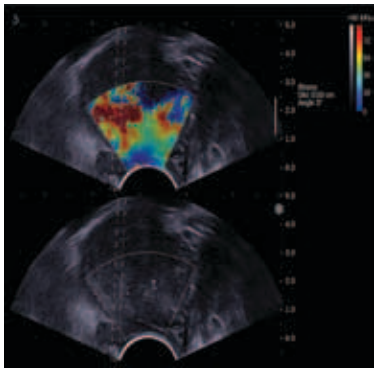

Comparison of grey scale TRUS (B-mode; bottom row) and overlaid SSI images (top row) - representative images, showing abnormal area (red - high stiffness) detected only by SSI.

P-165-YI

Tuesday
15 October 2012

Topic: Young Investigator
Presentation type: Poster

Medium term outcomes following primary focal therapy using HIFU for localised prostate cancer

Louise Dickinson

University College Hospital, London, United Kingdom

This poster is based on oral presentation 49-PR.

P-166-YI

Tuesday
15 October 2012

Topic: Young Investigator
Presentation type: Poster

Optimizing MR thermometry for clinical phase I breast tumor ablation study

Roel Deckers

University Medical Center Utrecht, Utrecht, Netherlands

This poster is based on oral presentation 42-BT.

P-167-YI

Tuesday
15 October 2012

Topic: Young Investigator
Presentation type: Poster

Osteoid Osteoma: preliminary results of a non-invasive treatment using Magnetic Resonance guided Focused Ultrasound

Beatrice Cavallo Marincola

University of Rome — Sapienza, Rome, Italy

This poster is based on oral presentation 63-BN.

P-168-YI

Tuesday
16 October 2012

Topic: Young Investigator
Presentation Type: Poster

Patterns of Magnetic Resonance Imaging Change After Transcranial Magnetic Resonance Guided High Intensity Focused Ultrasound Treatment for Essential Tremor: Result From ET001K, ET002K

Ji Hee Kim

Yonsei University College of Medicine, Seoul, South Korea

Background/Introduction: Transcranial magnetic resonance-guided high intensity focused ultrasound (tcMRgFUS) is a novel, noninvasive, and precise neurosurgical treatment strategies against a variety of brain disease. A Phase I clinical study was initiated to treat patients with essential tremor with tcMRgFUS.

The purpose of this study is to investigate the patterns of magnetic resonance imaging (MRI) change after tcMRgFUS for essential tremor.

Methods: Two patients with essential tremor underwent tcMRgFUS treatment. The treatment were performed using the ExAblate 4000 device (Insightec), which consists of a 30cm diameter hemispherical 1024 elements phased array transducer operating at 650 kHz. The system was integrated with a clinical 3.0T MRI unit (GE, Sgina). On completion of the treatment phase, MRI scans were acquired to assess the effect of tcMRgFUS treatment on the target and adjacent brain regions. Also, follow-up MRI scans were conducted at 1 day, 7 days, 1 month, and 3 months post-sonication.

Results and Conclusions: MRI of the sonication lesion immediately following the sonication revealed a mostly hyperintense ellipsoid lesion on T2-weighted imaging. It was consist of isointense to slightly hypointense center surrounded by a strongly hyperintense ring. It was irregularly demarcated by a hypointense area of perifocal cytotoxic edema, which completely receded over a month. This lesion immediately following the sonication showed slightly hypointense lesion on T1-weighted imaging, with a strong ring enhancement of about 1 to 2 mm thickness on the contrast-enhanced T1-weighted imaging. This enhancement represents disruption of BBB. An MRI scan acquired 1 day after the sonication revealed BBB restoration manifested as resolution of enhancement of the sonication lesion. This lesion 1 month after the sonication showed new enhancement, indicative of surgical change, but no evidence of enhancement at 3 months follow-up. The hypointense lesion immediately following the sonication was changed hyperintense lesion on T1-weighted imaging at 3 months after the sonication, which was suspected to the area of necrotic tissue containing debris with high protein content. Also, we found hemorrhagic change in the lesion on gradient echo imaging. We are planning to document in detail additional findings of our ongoing clinical phase I study on ten patients.

P-169-YI

Tuesday
15 October 2012

Topic: Young Investigator
Presentation type: Poser

Pulsed Focused Ultrasound (pFUS) Induces Targeted Homing of Therapeutic Mesenchymal Stem cells (MSC) to Kidneys during Acute Tubular Necrosis and Leads to Improved Renal Function

Scott Burks

National Institutes of Health Clinical Center, Bethesda, Maryland, United States

This poster is based on oral presentation 35-EA.

P-170-YI

Tuesday
16 October 2012

Topic: Young Investigator
Presentation Type: Poster

Radio Frequency Coil Design for Magnetic Resonance Guided Focused Ultrasound in the Brain

Emilee Minalga[1], Nick Todd[2], Robb Merrill[1], Allison Payne[1], Dennis Parker[2], J Hadley[1]

[1]Utah Center of Advanced Imaging Research, Salt Lake City, Utah, United States
[2]University of Utah, Salt Lake City, Utah, United States

Background/Introduction: The purpose of this work was to design a coil that allows for open ultrasound access to the cranium for interventional MRI, provides high SNR in the brain, and keeps the majority of the coil circuitry away from the top of the head. This coil could ultimately be used in transcranial MRI guided focused ultrasound (MRgHIFU) systems.

Methods: Two coil designs were investigated. Both had coil elements that were non-overlapped and capacitively decoupled in a common leg. The first design was a triangular-shaped, three-channel phased array that fit on top of the head like a cap. The second design had 6 rectangular elements that wrapped around the back of the head. Both designs were integrated with a stereotactic head frame.

Three experiments were performed in a Siemens TIM Trio 3T MRI scanner (Erlangen, Germany). Comparisons were done with the following four coils: Body coil (BC), 12-channel (12ch) commercial head coil, 3-channel (3ch) brain coil, and 6-channel (6ch) brain coil.

Exp.1) Signal to Noise Ratio (SNR) maps were obtained using a standard gradient echo pulse sequence

Exp.2) To compare the relative temperature measurement performance of the coils, the 3D GRE sequence was repeated 19 times on a single human volunteer using the BC, 3ch and the 6ch coils. The standard deviation of the calculated temperature through time was calculated for each pixel in the image.

Exp.3) Finally, To assess the ultrasound transparency of a single coil rung of the 3ch coil, MRI temperatures were made while a single point and circular HIFU heating trajectories were performed in a homogeneous phantom with and without a single copper/k

Results and Conclusions: Exp.1) The SNR plots showed that in the central brain the 3ch/6ch coils had a 245%/332% increase compared to the BC, 34.5%41.2% increase compared to the 12ch commercial head coil.

Exp.2) The standard deviation of the temperature measurements over time showed that there is improved accuracy using the MRgHIFU brain coil. The average temperature error for a small ROI in the middle of the brain at a depth of 3 cm (9 cm) from the top of the head was: 1.8 °C (1.6 °C) for the BC, 0.67 °C (0.98 °C) for the 3ch. For the 6ch the temperature error 9cm from the top of the head was 0.69°C.

Exp.3) Phantom temperature measurements made with and without the copper/ kapton coil rung in place showed no significant difference in the heating patterns for the single point and circular trajectories.

Both the 3ch and 6ch coil can be combined with a small amount of coil coupling. Where the most coupling between the 3ch and 6 ch coil has -13.1 dB isolation.

Discussion

Both coils gave better SNR results in the central brain region than the body coil and the 12ch coil. The 3ch coil gave better SNR at the cranium surface and the 6ch gave better SNR in the deep central portion of the brain. If combined together great coverage of the entire head region of interest could be obtained. Both coils are designed to fit around and operate with the stereotactic head device and to not interfere with the ultrasound beam unlike many clinically available RF head coils. Both coils are a good trade off between design simplicity, compatibility with the stereotactic frame, and improved SNR in the brain. Patient treatment should be improved with the high SNR and better MR anatomy images provided by either coil. Both coils will also provide improved temperature monitoring for transcranial MRgFUS treatments.

Acknowledgements (Funding): This work is supported by NIH grants R01 CA134599 and R01 EB013433, the Ben B. and Iris M. Margolis Foundation, The Mark H. Huntsman chair, and the Focused Ultrasound Surgery Foundation, Siemens Healthcare.

P-171-YI

Tuesday
15 October 2012

Topic: Young Investigator
Presentation type: Poser

Role of Magnetic Resonance Guided Focused Ultrasound Surgery (MRgFUS) in Treatment of Patients with Lumbar Facetal Arthropathy

Abhijit Patil

Jaslok Hospital and Research Centre, Mumbai, India

This poster is based on oral presentation 64-BN.

P-172-YI

Tuesday
16 October 2012

Topic: Young Investigator
Presentation Type: Poster

Targeted Hyperthermia in Prostate With an MR-Guided Endorectal Ultrasound Phased Array: Patient Specific Modeling and Preliminary Experiments

Vasant Salgaonkar[1], Punit Prakash[2], Viola Rieke[1], I-Chow Hsu[1], John Kurhanewicz[1], Chris Diederich[1]

[1]University of California at San Francisco, San Francisco, California, United States
[2]Kansas State University, Lawrence, Kansas, United States

Background/Introduction: Mild hyperthermia (40-44 oC) can augment radiotherapy and improve drug delivery in deep seated tumor sites. Feasibility of producing targeted hyperthermia in prostate with a commercially available MR-guided endorectal ultrasound (ERUS) phased array ablation system was explored in the simulation study and preliminary experiments presented herein.

Methods: Simulations incorporated the Pennes biothermal model implemented using 3D finite element methods. Model geometry was obtained by contouring pelvic anatomy from representative patient MRI and CT scans (n=6) to identify a range of focal cancer targets in prostate, critical organs and potential ERUS applicator position. Acoustic energy distributions were computed by rectangular radiator method for a device similar to Insightec ExAblate ERUS applicator (2.3 MHz, 990 elements, 2.3×4.0 cm2). Several array beamforming strategies were evaluated for selectively heating contiguous tumor volumes (>41 oC), while limiting temperatures in the surrounding anatomy. Hardware and software constraints of the ExAblate system pertaining to power densities, sonication durations and switching speeds were incorporated in the model to investigate continuous (as opposed to pulsed) targeted hyperthermia for 15-30 min. These energy delivery techniques were implemented during preliminary experiments in tissue mimicking phantom material. The experiments were conducted under real time MRI-based temperature monitoring at 3T (GRE TE=7.2 ms, TR=15 ms, BW 10.5 kHz, FOV=20 cm, matrix 256x128, flip angle=40º).

Results and Conclusions: T>41 oC was computed in 10-20 cm3 volume with planar (iso-phase) or diverging (Figure-A) sonications at 1.2–1.7 W/cm2. These may be useful in treating a posterior quadrant (Figure-B), or entire posterior half of the prostate. T>41 oC was calculated in 3-9 cm3 volume at 1.3–3.3 W/cm2 acoustic intensity during multifocal or curvilinear sonications, which may be useful in selectively treating focal disease confined to one lateral side of posterior prostate. Beamforming techniques may be employed to deliver conformable hyperthermia by tailoring acoustic energy deposition along both the array length (Figure-C) and angular expanse. Electronic and mechanical scanning may be used in whole prostate hyperthermia under MR-temperature control to more carefully tailor heating. MR-temperature distributions were measured in a phantom sonicated at 1.3 W/cm2 by the Exablate applicator for several beamforming configurations. 4-8 oC temperature rises could be successfully induced in the phantom, consistent with calculated values and lower power settings. MRg ERUS systems, already in clinical trials for ablation, may be controlled to deliver 15-30 minutes of continuous hyperthermia in prostate. It may be effectively utilized as an adjuvant to hypofractionated radiotherapy and existing thermally mediated or conventional chemotherapeutic agents.

Acknowledgements (Funding): This research is supported by NIH R01 122276, 111981.

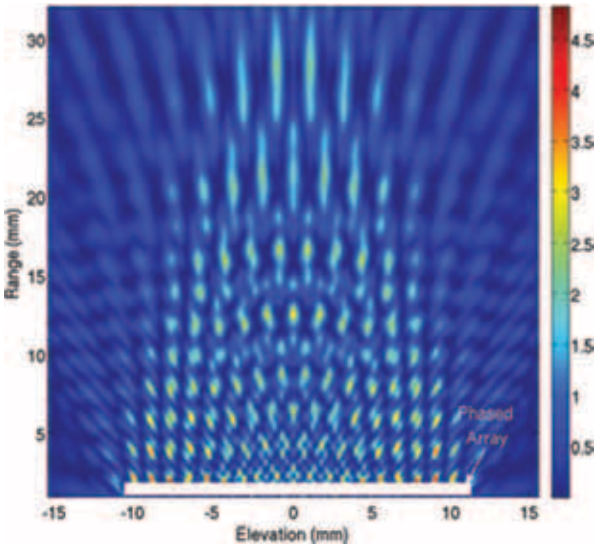

(A) Simulated diverging acoustic intensity (W/cm2) pattern from ERUS array.

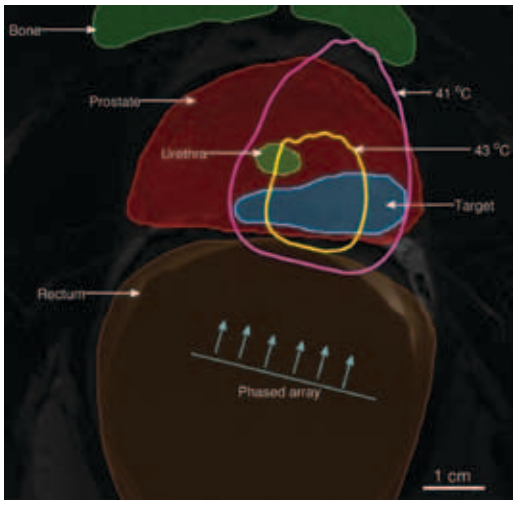

(B) Axial view of a patient-specific biothermal model showing hyperthermia to a target volume in posterior quadrant of the prostate heated by diverging beam pattern at 2.2 W/cm2.

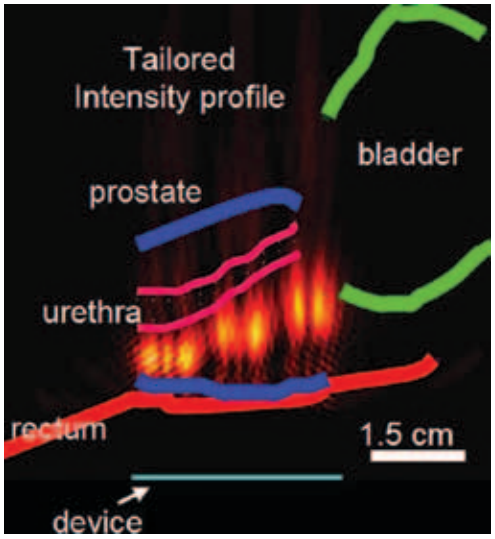

(C) Sagittal view showing acoustic energy deposition tailored along the array length with respect to power input and focal depth to conform to prostate shape.

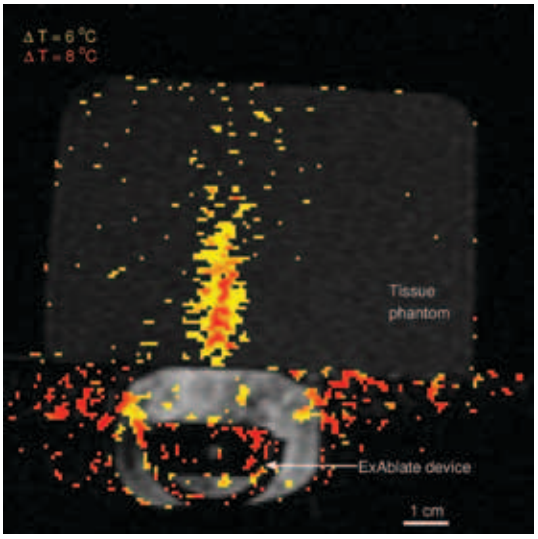

(D) Axial slice of MR-temperature monitoring in a phantom sonicated by Insightec ExAblate ERUS device curvilinearly focused at 25 mm depth along the array length.

P-173-YI

Tuesday
15 October 2012

Topic: Young Investigator
Presentation type: Poser

Transcranial MR Guided Focused Ultrasound Treatment of ICH

Stephen Monteith

University of Virginia, Charlottesville, Virginia, United States

This poster is based on oral presentation 11-BR.

Poster Map

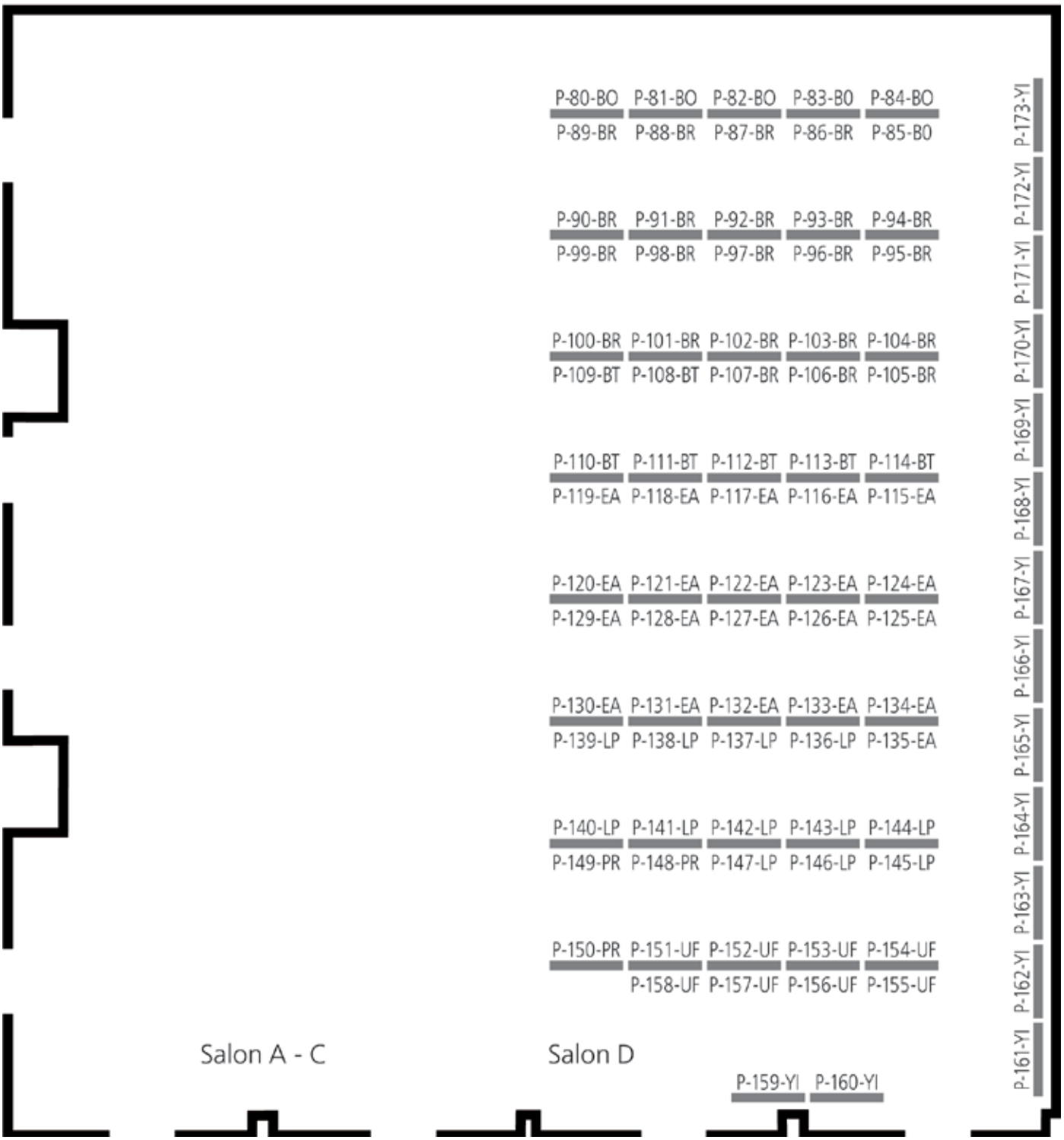
P-80-BO P-81-BO P-82-BO P-83-BO P-84-BO
P-89-BR P-88-BR P-87-BR P-86-BR P-85-BO
P-90-BR P-91-BR P-92-BR P-93-BR P-94-BR
P-99-BR P-98-BR P-97-BR P-96-BR P-95-BR
P-100-BR P-101-BR P-102-BR P-103-BR P-104-BR
P-109-BT P-108-BT P-107-BR P-106-BR P-105-BR
P-110-BT P-111-BT P-112-BT P-113-BT P-114-BT
P-119-EA P-118-EA P-117-EA P-116-EA P-115-EA
P-120-EA P-121-EA P-122-EA P-123-EA P-124-EA
P-129-EA P-128-EA P-127-EA P-126-EA P-125-EA
P-130-EA P-131-EA P-132-EA P-133-EA P-134-EA
P-139-LP P-138-LP P-137-LP P-136-LP P-135-EA
P-140-LP P-141-LP P-142-LP P-143-LP P-144-LP
P-149-PR P-148-PR P-147-LP P-146-LP P-145-LP
P-150-PR P-151-UF P-152-UF P-153-UF P-154-UF
P-158-UF P-157-UF P-156-UF P-155-UF
P-173-YI P-172-YI P-171-YI P-170-YI P-169-YI P-168-YI P-167-YI P-166-YI P-165-YI P-164-YI P-163-YI P-162-YI P-161-YI
Salon A - C
Salon D
P-159-YI P-160-YI

Author Index by Name

Author Index by Name (continued)

Author Index by Name (continued)

Author Index by Name (continued)

Author Index by Organization

Author Index by Organization (continued)

Author Index by Organization (continued)

Author Index by Organization (continued)

Author Index by Organization (continued)

Notes

Young Investigator Award Program

The Focused Ultrasound Foundation established the Young Investigator Award Program to encourage quality research by clinicians and scientists-in-training and to support their presentation of meritorious scientific papers at major venues such as the 3rd International Symposium on Focused Ultrasound.

Graduate students, research fellows, clinical fellows and junior faculty members are eligible to apply for the awards, which provide up to $2,000 in reimbursement for symposium registration, travel and lodging expenses. The 2012 Young Investigator Awards are funded in part by a $19,000 grant from the National Cancer Institute (R13CA171719). The funding comes from the National Institutes of Health (NIH) Conference Grant Program which supports high quality conferences that are relevant to the scientific mission of the NIH and to public health.

Fifteen Young Investigators are participating in the 3rd International Symposium on Focused Ultrasound and being acknowledged in several ways:

Pre-symposium Publicity: To emphasize the significance of the Young Investigator Awards, the Foundation is using several communications channels – a press release, e-blast and newsletter article – to announce the selection of our 2012 recipients.

Name Badges and Announcement: Award recipients will receive unique name badges that indicate their status as Young Investigators. They will be acknowledged at the Symposium opening session, and senior investigators will be encouraged to interact with them throughout the conference.

Evening Reception and Poster Session: Young Investigators will have a designated section of the Poster Hall. On Tuesday, 16 October 2012, during the Evening Reception and Poster Session, they will have an opportunity to showcase and present their work to the larger focused ultrasound community.

Young Investigator Award Review Committee

Selection of the 2012 Young Investigator Award recipients was based on peer-review scoring of each applicant's abstract by the Symposium Scientific Committee. The final roster of recipients was determined by the Young Investigator Award Review Committee:

Gail ter Haar, PhD
Joint Department of Physics, Institute of Cancer Research
Royal Marsden Hospital, Sutton, UK

Arik Hananel, MD
Medical Director, Focused Ultrasound Foundation

John Snell, PhD
Brain Program Technical Director, Focused Ultrasound Foundation

2012 Young Investigator Award Recipients

Sarfraz Ahmad, PhD

SpR Urology and Clinical Research Fellow
Urology
Ninewells Hospital, University of Dundee
Dundee, United Kingdom

Awarded for: Localisation of Prostate Cancer foci with Transrectal Quantitative Shear Wave Elastography - a step towards focal therapy for Prostate Cancer [P164-YI]

Additional Presentations: P-139-LV, P-143-LV

Muna Aryal, PhD

Student
Physics Department
Boston College
Radiology Department
Brigham and Women's Hospital
Boston, Massachusetts, United States

Awarded for: Enhanced delivery of liposomal doxorubicin via permeabilization of the blood-brain/blood-tumor barriers using focused ultrasound and microbubbles significantly improves survival in a rat glioma model after multiple treatments [12-BR/P-162-YI]

Additional Presentation: P-98-BR

Scott Burks

Postdoctoral Fellow
Radiology and Imaging Sciences
National Institutes of Health Clinical Center
Bethesda, Maryland, United States

Awarded for: Pulsed focused ultrasound (pFUS) induces targeted homing of therapeutic mesenchymal stem cells (MSC) to kidneys during acute tubular necrosis and leads to improved renal function [35-EA/P-169-YI]

Additional Presentations: P-130-EA, P-133-EA

Anne Cain-Nielsen

Student (MS Candidate)
Biostatistics
University of Michigan School of Public Health
Ann Arbor, Michigan, United States

Awarded for: Cost-Effectiveness Analysis of Uterine-Preserving Procedural Treatments for Uterine Fibroids, Including Magnetic Resonance-Guided Focused Ultrasound (MRgFUS) [28-UF/P-160-YI]

2012 Young Investigator Awards (continued)

Beatrice Cavallo Marincola, MD

PhD Student
Radiological, Oncological and Pathological Sciences
University of Rome —Sapienza
Rome, Italy

Awarded for: Osteoid Osteoma: preliminary results of a non-invasive treatment using Magnetic Resonance guided Focused Ultrasound [63-BN/P-167-YI]

Additional Presentations: 58-BM, 69-LV, P-83-BN

Roel Deckers, PhD

Postdoctoral researcher
Image Sciences Institute
University Medical Center Utrecht
Utrecht, The Netherlands

Awarded for: Optimizing MR thermometry for clinical phase I breast tumor ablation study [42-BT/P-166-YI]

Additional Presentations: 39-BT, 60-BM, 75-LV

Louise Dickinson, MD

Academic Clinical Fellow in Urology
University College Hospital
London, United Kingdom

Awarded for: Medium term outcomes following primary focal therapy using HIFU for localised prostate cancer [49-PR/P-165-YI]

Additional Presentations: 53-PR, 54-PR, 55-PR

Ji Hee Kim, MD

Clinical Fellow
Department of Neurosurgery
Yonsei University College of Medicine
Seoul, Korea

Awarded for: Patterns of Magnetic Resonance Imaging Change After Transcranial Magnetic Resonance Guided High Intensity Focused Ultrasound Treatment for Essential Tremor: Result From ET001K, ET002K [P-168-YI]

2012 Young Investigator Awards (continued)

Jonathan Kopechek, PhD

Postdoctoral Fellow
Mechanical Engineering
Boston University
Boston, Massachusetts, United States

Awarded for: Enhanced MR-guided HIFU Ablation of Rabbit VX2 Tumors In Vivo using Phase-Shift Nanoemulsions [34-EA/P-163-YI]

Additional Presentations:

Emilee Minalga, PhD

Graduate Research Assistant
Radiology Department
University of Utah
Salt Lake City, Utah, United States

Awarded for: Radio Frequency Coil Design for Magnetic Resonance Guided Focused Ultrasound in the Brain [P-170-YI]

Additional Presentations: P-96-BR, P-108-BT

Stephen Monteith, MD

Neuro-Endovascular Fellow
Department of Neurosurgery
Thomas Jefferson University
Philadelphia, Pennsylvania, United States

Awarded for: Transcranial MR Guided Focused Ultrasound Treatment of ICH [11-BR/P-173-YI]

Additional Presentations P-102-BR

Min Jung Park

Fellow
Radiology
Samsung Medical Center
Seoul, Korea

Awarded for: Complete or Near-complete Ablation of Symptomatic Uterine Fibroids by Volumetric MR-guided High-intensity Focused Ultrasound Therapy: Assessments of Safety and Therapeutic Efficacy [20-UF/P-159-YI]

Additional Presentation: P-120-EA

2012 Young Investigator Awards (continued)

Abhijit Patil, MD, DNB

Clinical and Research Associate
Department of CT, MRI and MRgFUS
Jaslok Hospital and Research Centre
Mumbai, India

Awarded for: Role of Magnetic Resonance Guided Focused Ultrasound Surgery (MRgFUS) in treatment of patients with Lumbar Facetal Arthropathy [64-BN/P-171-YI]

Additional Presentation: 44-LD

Vasant Salgaonkar, PhD

Research Specialist
Radiation Oncology
University of California, San Francisco
San Francisco, California, United States

Awarded for: Targeted hyperthermia in prostate with an MR-guided endorectal ultrasound phased array: patient specific modeling and preliminary experiments [P-172-YI]

Additional Presentations: 53-PR, 54-PR, P-145-LV

Sin Yuin Yeo, MSc

Doctoral Student
Biomedical Engineering
Eindhoven University of Technology
Eindhoven, The Netherlands

Awarded for: Effects of HIFU Ablation on Bone Metastases: From MRI, SPECT/CT and MicroCT Point of View [62-BM/P-161-YI]

Additional Presentation: P-84-BN

Research Funding in Focused Ultrasound

Research Awards | Awards of up to $100k for one-year projects

The FUSF Research Awards Program provides funding to support investigator-initiated projects through two tracks: a Clinical Track geared towards preclinical and pilot clinical studies that promise to lead to the development of a reimbursable clinical indication for focused ultrasound within the next five to seven years and a High Risk Track, which supports early-stage, proof-of-concept projects that are unlikely to receive funding from other sources but could have a profound impact on the advancement of the field of focused ultrasound. Researchers in all stages of their careers are encouraged to apply. Applications are accepted on a rolling basis with quarterly funding decisions based on expert external review.

For more information | Visit "Programs > Research" on the Foundation website at http://www.fusfoundation.org or contact Matt Eames, Director of Extramural Research, at meames@fusfoundation.org.

FOCUSED ULTRASOUND FOUNDATION

Notes

Sponsors

Platinum Sponsors

Gold Sponsor

Bronze Sponsor

Friends

Foundation

ExAblate®

The Operating Room of the Future

InSightec welcomes participants to

The 3rd International Focused Ultrasound Symposium

Excellence backed by Experience

- The only FDA approved MRgFUS system
- Thousands of patients successfully treated
- Continuous technological evolution based on clinical experience
- Several applications under development

InSightec

Bringing therapy into focus

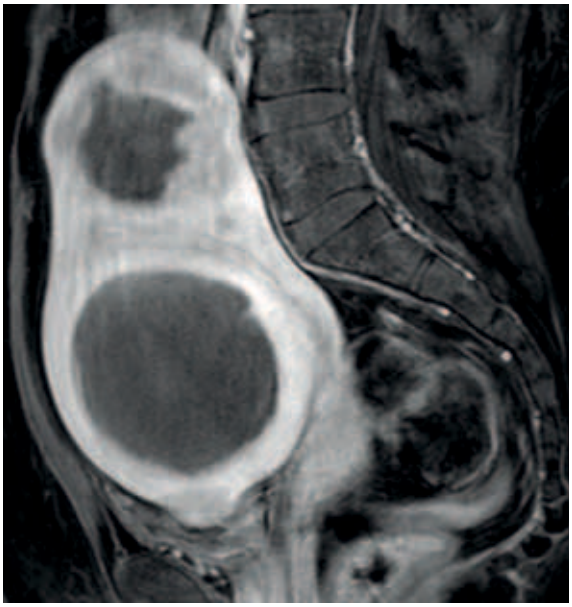

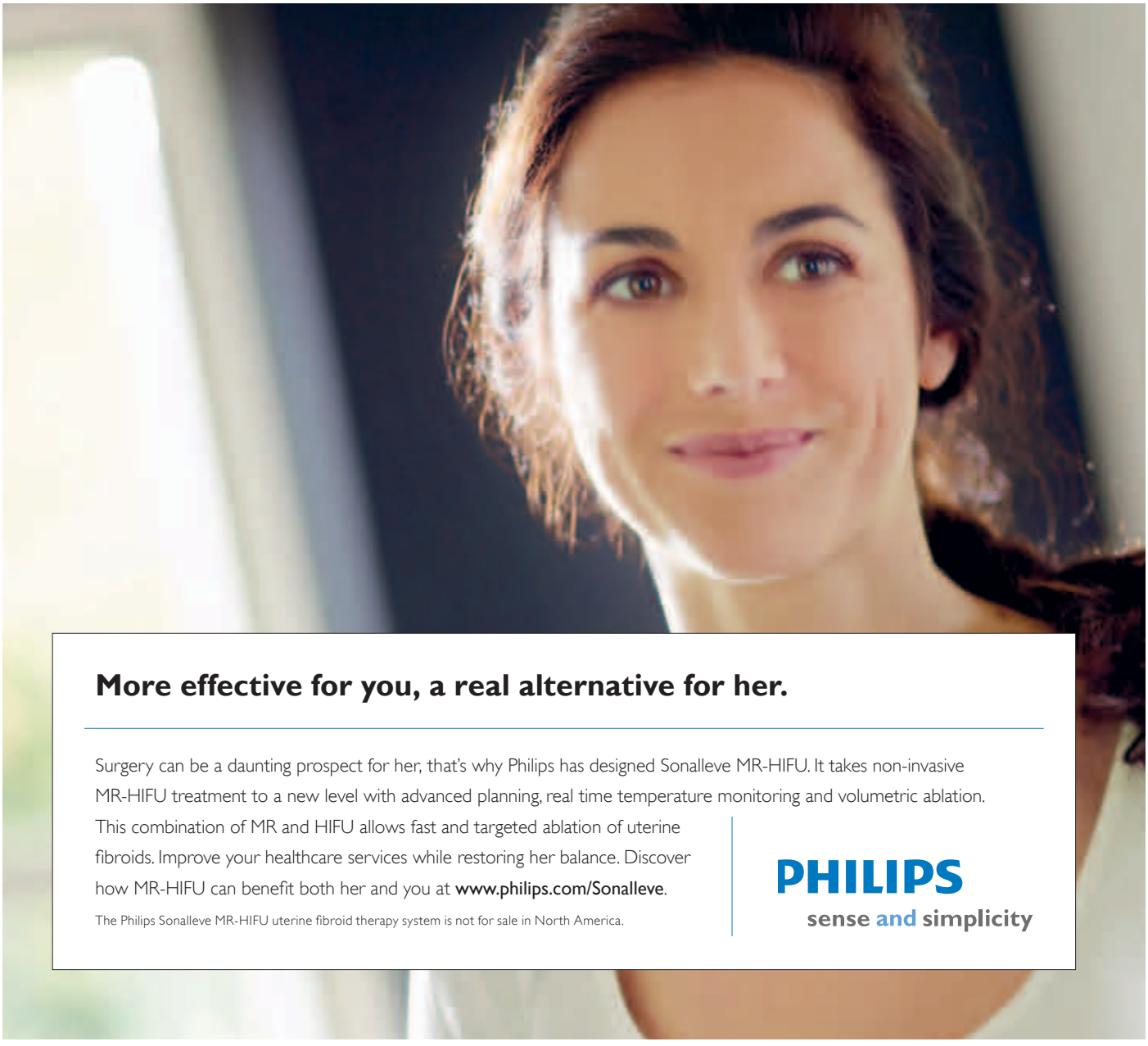

More effective for you, a real alternative for her.

Surgery can be a daunting prospect for her, that's why Philips has designed Sonalleve MR-HIFU. It takes non-invasive MR-HIFU treatment to a new level with advanced planning, real time temperature monitoring and volumetric ablation. This combination of MR and HIFU allows fast and targeted ablation of uterine fibroids. Improve your healthcare services while restoring her balance. Discover how MR-HIFU can benefit both her and you at **www.philips.com/Sonalleve**.

The Philips Sonalleve MR-HIFU uterine fibroid therapy system is not for sale in North America.

PHILIPS

sense and simplicity

FUS Instruments

Preclinical Focused Ultrasound Solutions

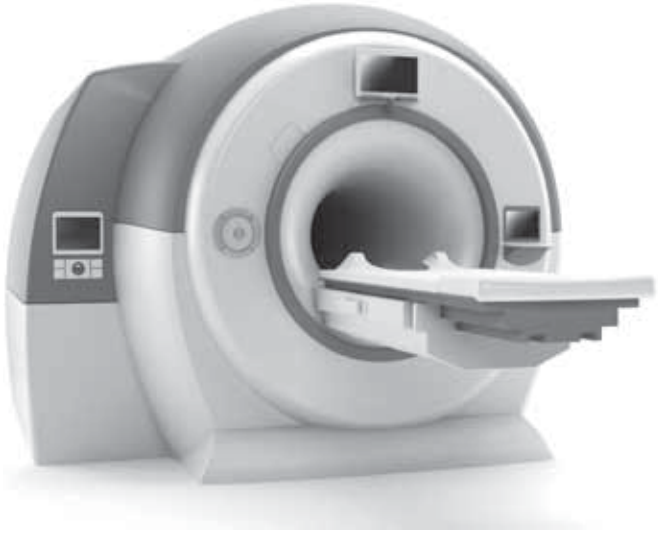

VIFU-2000

PRE-CLINICAL HIFU SYSTEM

Fit-for-your Lab with Great Efficiency

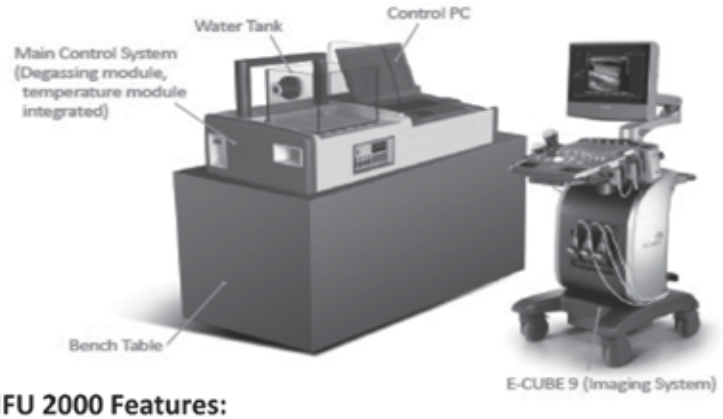

VIFU 2000 Features:

- Turn key system: an ultrasound-guided HIFU system
- Real-time US-imaging during HIFU treatment with automatic target alignment
- Smart workflow to increase research productivity and efficiency
- Built-in water treatment system, including degassing and temperature control capability
- 3-axis motorized positioning system for precise delivery of ultrasound energy to the target
- Flexible RF driving system: capable to deliver various treatment protocols
- Available in Wet and/or Dry type (Dry type available end of 2012)
- PCD module and contrast imaging will be available 2013

Serving the Research Community with Dedication

"We are ultrasound professionals."

ALPINION MEDICAL SYSTEMS

Imagine treating cancer, Parkinson's disease, epilepsy and brain tumors without surgery, radiation or the side effects of chemotherapy.

FOCUSED ULTRASOUND FOUNDATION

With further research and development, these achievements may be possible through Focused Ultrasound, an early-stage, noninvasive therapeutic technology.

Unfortunately, it takes decades for a major medical technology like Focused Ultrasound to become mainstream. Every year we shave off that process equates to reduced death and suffering for countless people, including our family, our friends and maybe ourselves.

HELP US ACHIEVE OUR GOAL TO IMPROVE THE LIVES OF MILLIONS WORLDWIDE BY MAKING FOCUSED ULTRASOUND AVAILABLE IN THE SHORTEST TIME POSSIBLE.

It's All About Patients

SAVING TIME = SAVING LIVES

Focused Ultrasound Foundation www.fusfoundation.org | Charlottesville, VA | T 434.220.4993

Focused Ultrasound Foundation www.fusfoundation.org | Charlottesville, VA | T 434.220.4993